

**Mechanisms of 1,25-Dihydroxyvitamin D Resistance in Cancer Cells:
Examination of VDR/RXR/Coactivator Localization, Interaction and Intra-
nuclear Kinetics by Fluorescence Imaging Techniques**

By

Sylvester Jusu

A thesis submitted to the faculty of Graduate Studies and Research in partial fulfillment of the requirements for the degree of Doctor of philosophy

© Sylvester Jusu, 2015

August 2015

Department of Medicine
Division of Experimental Medicine
McGill University
Montreal Quebec
Canada

ABSTRACT

1,25-Dihydroxyvitamin D₃ (1,25(OH)₂D₃), the biologically active metabolite of vitamin D₃, is a pleiotropic fat-soluble hormone which regulates calcium homeostasis via the transcriptional activation of target genes through the nuclear vitamin D receptor (nVDR). More recently, non-classical potent actions of vitamin D including pro-differentiation, anti-proliferation through growth arrest and apoptosis have been recognized in a variety of normal and cancer cells.

The currently known major regulator of the biological activity of 1,25(OH)₂D₃ is the nuclear VDR (nVDR) complexed with its heterodimer, the retinoid X receptor (RXR). Binding of the 1,25(OH)₂D₃ to VDR enhances VDR/RXR heterodimerization and allows for the association with specific DNA sequences named vitamin D response elements (VDREs). The complex consisting of VDR/RXR and 1,25(OH)₂D₃ binds to the VDREs and acts as a ligand-dependent transcription factor. This activated complex then recruits a coactivator complex, known as vitamin D receptor-interacting protein complex (DRIP) and other proteins including histone acetyltransferase. Acetylated histones relax chromatin structure to make DNA accessible and permit initiation of transcription of the target genes. Several cancer cells derived from a variety of tissues have been shown to be resistant to the antiproliferative action of 1,25(OH)₂D₃.

In previous work, we showed that in a normal keratinocyte cell line HPK1A, the growth inhibitory action of 1,25(OH)₂D₃ is enhanced and more cells are arrested in Go/G1 phase of the cell cycle. However, in the ras-transformed keratinocytes, HPK1A_{ras}, achieving comparable inhibition of cell growth and cell cycle arrest requires 10-100 fold higher concentrations.

Though the two cell lines express VDR and RXR α similarly, phosphorylation of RXR α at serine 260 through the Ras-Raf-MAP kinase pathways is responsible for

the very weak growth inhibitory action and partial resistance observed in HPK1Aras cell lines.

We show, through transfection of green fluorescent protein (GFP) hVDR and hRXR α tagged constructs, that both hVDR and hRXR α are localized in the nucleus in $1\alpha,25(\text{OH})_2\text{D}_3$ - treated HPK1A and in HPK1Aras cells treated with UO126 (1,4-diamino-2,3-dicyano-1,4-bis[2-aminophenylthio]) or following transfection of the non- phosphorylatable hRXR α ala260 mutant. Also, we demonstrate using Fluorescence Resonance Energy Transfer (FRET) that hVDR and hRXR α interact in the absence of the ligand in both HPK1A and HPK1Aras cell lines. However, ligand addition increases their interaction in HPK1A cell but only in HPK1Aras cells treated with either UO126 or transfected with the non- phosphorylatable hRXR α ala260 mutant. This clearly demonstrates that heterodimerization of the hVDR / hRXR α complex and interaction in HPK1Aras cells can be improved and possibly reversed with the use of a non-phosphorylatable hRXR α ala260 mutant which completely abolishes hRXR α phosphorylation and restores the function of $1\alpha,25(\text{OH})_2\text{D}_3$.

Furthermore, we demonstrate using Fluorescence Recovery After Photobleaching (FRAP) and Fluorescence Loss in Photobleaching (FLIP) using (GFP)-tagged hRXR α wildtype or the non-phosphorylatable hRXR α ala260 mutant transfected into HPK1A and HPK1Aras cell lines and treated with $1,25(\text{OH})_2\text{D}_3$ that the residence time and immobile fractions of hRXR α wt in the nucleus of HPK1Aras cells decreased compared to the non-transformed HPK1A cells. In contrast, treatment with a map –extracellular kinase (MEK1/2) inhibitor UO126 or expression of the non-phosphorylatable hRXR α ala260 mutant reversed the effect on residence time and immobility. This was further confirmed by subcellular colocalization/ partitioning studies of hVDR/hRXR α wildtype and hVDR /hRXR α mut respectively. Next we showed that hVDR/hRXR α wt complex binding

to DNA was impaired in the HPK1Aras cells but could be improved upon pre-treatment with UO126 or transfection of the non-phosphorylatable hRXR α ala260 mutant. Lastly, using FRET we showed that in the ras-transformed cells, DRIP205 co-activator recruitment was impaired with the VDR but completely abolished with the RXR.

In summary, blocking the MAPK phosphorylation of hRXR α in the ras-transformed keratinocytes either by using the MEK inhibitor UO126 or transfection of the non-phosphorylatable hRXR α ala260 mutant could restore the function of 1,25(OH) $_2$ D $_3$ on VDR/RXR α binding and co-activator recruitment. We conclude that inhibition of RXR phosphorylation and the restoration of its original function might be an effective strategy for controlling cancer cell growth in a variety of human malignancies.

RESUMÉ

La 1,25-Dihydroxyvitamin D₃ (1,25(OH)₂D₃), la forme biologiquement active de la vitamine D, est une hormone pleiotropique liposoluble qui régule l'homéostasie du calcium via l'activation transcriptionnelle de gènes par l'intermédiaire du récepteur à la vitamine D (RVD). Plus récemment, des actions nouvelles et puissantes ont été découvertes incluant des effets cellulaires pro-différentiateurs, antiprolifératifs par arrêt de la croissance et induction de l'apoptose dans un grand nombre de cellules normales et cancéreuses.

Le régulateur majeur connu de l'activité biologique de la 1,25(OH)₂D₃ est le RVD nucléaire (n RVD) complexé à son hétérodimère le récepteur rétinol X (RRX). La liaison de la 1,25(OH)₂D₃ au RVD augmente l'hétérodimerisation du complexe RVD/RRX et permet son association avec des séquences d'ADN appelées éléments de réponse à la vitamine D (ERVD). Le complexe comprenant le RVD/RRX et la 1,25(OH)₂D₃ se lie aux ERVDs et agit comme un facteur de transcription dépendant du ligand. Le complexe actif recrute alors un complexe de co-activation appelé complexe d'interaction avec le RVD ou CIRVD ainsi que d'autres protéines telles l'histone acétylase. Les histones acétylées permettent la relaxation de la structure chromatinienne permettant l'accessibilité à l'ADN et l'initiation de la transcription des gènes cibles. Plusieurs cellules cancéreuses dérivées d'une variété de tissus sont résistants à l'action antiproliférative de la 1,25(OH)₂D₃.

Nos travaux antérieurs ont montré que dans une lignée de keratinocytes normaux appelée HPK1A l'action antiproliférative de la 1,25(OH)₂D₃ est présente comme dans les keratinocytes normaux et que les cellules sont bloquées dans la phase G₀/G₁ du cycle cellulaire. En revanche, dans la lignée de keratinocytes humains transformée HPK1A ras, un tel effet n'est observé qu'à des concentrations de 1,25(OH)₂D₃ 10 à 100 fois supérieures.

Bien que ces deux lignées expriment de façon similaire le RVD et le RRX, la phosphorylation du RRX sur la serine 260 à travers le circuit Ras-Raf-MAP kinase est responsable de l'effet diminué de la $1,25(\text{OH})_2\text{D}_3$ et donc de la résistance observée dans les cellules HPK1A ras.

Nous avons montré dans l'étude présente en utilisant des transfections des récepteurs RVD et RRX liée à la protéine fluorescente verte(PFV) que le RVD et le RRX sont localisés dans le noyau cellulaire dans les cellules HPK1A traitées à la $1,25(\text{OH})_2\text{D}_3$.et dans les cellules HPK1A ras prétraitées avec le UO126 ou transfectées avec le mutant non-phosphorylable RRX ala 260.

Par ailleurs, nous avons démontré en utilisant le Transfert par Énergie de Résonance Fluorescente(TERF) que le n RVD et le h RXR interagissent en l'absence de ligand à la fois dans les cellules HPK1A et HPK1A ras. Cependant l'addition de ligand augmente leur interaction dans les cellules HPK1A mais seulement dans les cellules HPK1A ras après traitement avec l'UO126 ou la transfection avec le mutant non-phosphorylable RRX ala 260.

Ceci démontre clairement que l'hétérodimerization du complexe RVD/RRX et son interaction dans les cellules HPK1A ras peuvent être améliorées et possiblement rétablies avec l'utilisation du mutant non-phosphorylable RRX ala 260 qui abolit complètement la phosphorylation du RRX et restore la fonction de la $1\alpha,25(\text{OH})_2\text{D}_3$.

De plus, nous avons démontré en utilisant les méthodes de Récupération de la Fluorescence Après Photo blanchissage(RFAP) et la Perte de Fluorescence Après Photo blanchissage(PFAP) et la transfection des RRX et RRXala260 mutants liés au PFV puis traitées à la $1\alpha, 25(\text{OH})_2\text{D}_3$ montrent une diminution des temps de résidence ainsi que de la fraction immobile du RRX dans les cellules HPK1A ras en comparaison aux cellules HPK1A. En revanche le traitement avec l'inhibiteur de

la kinase extracellulaire map (MEK1/2) UO126 (1,4-diamino-2,3-dicyano-1,4-bis [2-aminophenylthio] ou l'expression du mutant non-phosphorylable RRX ala 260 rétablissent l'effet normal sur le temps de résidence et l'immobilité. Ceci fut confirmé en utilisant des études de partition/colocalization compartementales cellulaires du h RVD/h RRX et du h RVD/h RRX mutant respectivement. Nous avons ensuite démontré que la liaison du complexe h RVD/ h RRX à l'ADN était compromise dans les cellules HPK1A ras mais pouvait être améliorée par un prétraitement avec le UO126 ou la transfection avec le mutant RRX non-phosphorylable ala260.

Finalement en utilisant la méthode TERF nous avons démontré que dans les cellules transformées HPK1A ras, le recrutement du coactivateur CIRVD 205 avec le RVD était altéré mais qu'il était complètement aboli avec le RRX.

En résumé, en bloquant la phosphorylation induite par la MAPK du RRX dans les cellules transformées HPK1A ras en utilisant l'inhibiteur du MEK le UO126 ou la transfection du mutant RRX non-phosphorylable, nous avons pu rétablir la fonction de la $1\alpha,25(\text{OH})_2\text{D}_3$ sur la liaison du complexe RVD/RRX ainsi que le recrutement de son coactivateur.

Nous concluons que l'inhibition de la phosphorylation du RRX et le rétablissement de sa fonction originelle pourrait être une stratégie efficace pour contrôler la croissance cellulaire dans un bon nombre de cancer humains.

Foreword

The Guidelines Concerning Thesis Preparation issued by the Faculty of Graduate Studies and Research at McGill University reads as follow: "As an alternative to the traditional thesis format, **the dissertation can consist of a collection of papers of which the student is an author or co-author.** These papers must have a cohesive, unitary character making them a report of a single program of research. The structure for the manuscript-based thesis must conform to the following:

1. Candidates have the option of including, as part of the thesis, the text of one or more papers submitted, or to be submitted, for publication, or **the clearly-duplicated text (not the reprints) of one or more published papers.** These texts must conform to the "Guidelines for Thesis Preparation" with respect to font size, line spacing and margin sizes and must be bound together as an integral part of the thesis.
2. The thesis must be more than a collection of manuscripts. All components must be integrated into a cohesive unit with a logical progression from one chapter to the next. In order to ensure that the thesis has continuity, **connecting texts that provide logical bridges preceding and following each manuscript are mandatory.** In general, when co-authored papers are included in a thesis the candidate must have made a substantial contribution to all papers included in the thesis. In addition, the candidate is required to make an explicit statement in the thesis as to who contributed to such work and to what extent. This statement should appear in a single section entitled "Contributions of Authors" as a preface to the thesis."

I have chosen to write my thesis with two papers that will be published, one manuscript that is currently being reviewed by my supervisor and

co-supervisor and one that has been submitted for publication. This thesis is divided in 6 chapters. Chapter 1 is a general introduction and review of the literature. Chapters 2 and 3 are in the form of original papers, each with its own abstract, introduction, experimental procedures, results, discussion and references. Chapter 4 discusses my work and its implication in cancer treatment. Chapter 5 discusses the conclusion with special reference to an updated model regarding resistance of HPK1Aras cells to $1,25(\text{OH})_2\text{D}_3$ growth inhibition. Also, it discusses the current structure of VDR/RXR complex binding to coactivator. Chapter 6 lists the claims to original research.

Publications arising from this thesis and contributions made by co-authors

Publication arising from the thesis

Chapter 2:

Jusu S., Presley J., Kremer R (2015). Phosphorylation of human Retinoid X receptor α at serine 260 impairs subcellular localization, receptor interaction, nuclear mobility and $1\alpha, 25$ dihydroxyvitamin D_3 – dependent DNA binding in ras –transformed keratinocytes.

Manuscript submitted to The Journal of Biological Chemistry

Chapter 3:

Jusu S., Presley J., Kremer R (2015). Examination of VDR/RXR/DRIP205 interaction, intranuclear kinetic and DNA binding in ras-transformed keratinocytes and its implication for designing optimal vitamin D therapy in cancer.

Manuscript awaiting submission

Contribution of Authors

Chapter 2: Cloning of fluorescently tagged VDR, RXR α wt, RXR α mut and DRIP205 and its LXXLL chimeras were performed with Dr. Benoit Ochiatti. All other experiments including cell viability, cell proliferation, cell cycle, transfection, protein expression, Fluorescent Resonance Energy Transfer,

Fluorescent Loss in Photobleaching, live cell imaging, DNA binding studies were performed by the candidate. The LSM 510 and LSM780 confocal microscope settings were supervised by Drs. John Presley and Min Fu. Dr. Richard Kremer supervised and Dr. John Presley advised on the experimental work, data analysis and reviewed the manuscript with the candidate.

Chapter 3: All experiments were designed by the candidate. Furthermore, all the experiments including single transfection, co-transfection, intra-nuclear binding, and coactivator recruitment, data gathering and data analysis were also carried out by the candidate. Dr. Richard Kremer supervised and Dr. John Presley advised and reviewed both the data and manuscript written by the candidate

Acknowledgements

First, I want to express my gratitude to my supervisor Dr. Richard Kremer for being extremely supportive from the first day I started working in his lab to my final day of submission of this thesis. Dr. Kremer gave me the freedom and all the support needed to carry out graduate research at a PhD level. I would also want to thank Dr. John Presley for mentoring me and giving me all the guidance needed. Dr. Presley was tremendously helpful in guiding me on live and fixed cell fluorescence imaging techniques. He not only recommended a lot of references which became very useful in my experimental work but also spent a lot of hours with me in the early days when I was acquiring live cell imaging data. I will forever be grateful. Furthermore, I would also like to thank Dr. Loan Nguyen for recommending Dr. Presley as the “go to person” for my work and being my first “tutor” at the Calcium Lab. Loan answered most of the technical questions regarding my experiments. Her generosity and willingness to explain to me the simplest techniques during my early days at the research lab made a tremendous impact on me. Thanks also to my friend Dr. Min Fu, for providing many technical tips on fluorescent imaging techniques. Dr. Min Fu helped me a lot in making reservations for use of the confocal microscope and gathering good quality imaging data. Many thanks to Dr. Benoit Ochiatti for helping me with the design and cloning of my GFP-tagged plasmids needed for the work.

My gratitude is also extended to my academic advisor Dr. Hendy for his exigency to me to produce a very good PhD and to the other members of my thesis committee, Drs. Monzur Murshed and Hugh Bennett for their constructive criticisms regarding my work progress. I would like to thank my partners at the Calcium Lab, Aimee-lee Luco, Dr. Jiarong Li, Mrs. Isabel Bolivar, Mrs. Miren Gratton, Yofi Cohen and Mrs. Jing Liang. They were always available when I needed them for general advice, technical assistance and to Mrs. Patricia Hales for her invaluable secretarial assistance. Furthermore, many thanks to the staff at Experimental Medicine for all the assistance rendered to me. Also, I extend my most sincere thanks to the Fonds de la Recherche en Sante du Quebec and the Canadian Institute of Health Research for their financial support during my training. Finally, I would like to thank the many friends I made in other labs, my family for their understanding, unconditional love and support during and throughout the whole process.

TABLE OF CONTENTS

| | |
|--|----|
| Abstract | 02 |
| Resume | 05 |
| Forward | 08 |
| Manuscripts Awaiting Publication | 10 |
| Contribution of Authors | 10 |
| Acknowledgement | 12 |
| Table of Contents | 24 |
| List of Figures | 22 |
| List of Tables | 25 |
| List of Abbreviations | 26 |
| CHAPTER 1: Introduction | 29 |
| 1.1 The Vitamin D Endocrine System | 30 |
| 1.2 Sources of Vitamin D | 30 |
| 1.3 Synthesis and Metabolism of 1,25(OH)₂D₃ | 32 |

| | |
|---|----|
| 1.3.1 Synthesis of 1,25(OH)₂D₃ | 33 |
| 1.3.2 Metabolism of 1,25(OH)₂D₃ | 34 |
| 1.4 The Vitamin D Binding Protein | 35 |
| 1.5 Biological Effects of 1,25(OH)₂D₃ | 36 |
| 1.5.1 1,25(OH)₂D₃ Non-Genomic Effects | 37 |
| 1.5.2 1,25(OH)₂D₃ Genomic Effects | 38 |
| 1.5.3 1,25(OH)₂D₃ Dual Regulation of Gene Expression by Genomic and Non-Genomic Pathways | 38 |
| 1.6 Biological Implications of 1,25(OH)₂D₃ Action | 39 |
| 1.7 Vitamin D Analogues and Therapeutic Agents | 42 |
| 1.8. The Nuclear Receptor Superfamily | 48 |
| 1.8.1 Classification of The Nuclear Receptor Superfamily | 49 |
| 1.8.2 Structure and Function of Nuclear Receptors | 52 |
| 1.9 The Vitamin D Receptor | 54 |

| | |
|---|----|
| 1.9.1 Coregulators of Vitamin D Receptor Action | 57 |
| 1.9.2 VDR Mutations and 1,25(OH)₂D₃ Resistance | 58 |
| 1.9.3 VDR Polymorphisms and 1,25(OH)₂D₃ Resistance | 62 |
| 1.9.4 VDR Knockout Mice and 1,25(OH)₂D₃ Resistance | 64 |
| 1.9.5 Epigenetic Mechanisms and 1,25(OH)₂D₃ Resistance | 66 |
| 1.10 The Retinoid X Receptor | 68 |
| 1.11 Nuclear Receptor Phosphorylation | 72 |
| 1.11.1 VDR Phosphorylation | 73 |
| 1.11.2 RXR Phosphorylation | 74 |
| 1.11.3 MAPK-dependent Phosphorylation | 75 |
| 1.11.4 Glucocorticoid Receptor (GR) | 76 |
| 1.11.5 Progesterone Receptor (PR) | 76 |

| | |
|--|------------|
| 1.11.6 Estrogen Receptor (ER)..... | 76 |
| 1.12 Interaction between Retinoid and Vitamin D Signaling Pathways..... | 78 |
| 1.13 Carcinogenesis..... | 80 |
| 1.13.1 Keratinocyte Carcinogenesis..... | 80 |
| 1.13.2 Ras Oncogene and Carcinogenesis..... | 81 |
| 1.13.3 Ras Signaling Pathway..... | 83 |
| 1.13.4 Therapeutic Approaches to Interrupting Ras Signaling | 86 |
| 1.13.5 Clinical Trials Targeting RAS/RAF/MEK/ERK Pathway..... | 104 |
| 1.14 Nucleocytoplasmic Trafficking of VDR/RXR Complex..... | 108 |
| 1.15 Rationale, Hypothesis and Specific Aims..... | 110 |
| 1.15.1 Rationale..... | 110 |
| 1.15.2 Hypothesis..... | 114 |
| 1.15.3 Specific Aims..... | 115 |

| | |
|--|------------|
| CHAPTER 2: Phosphorylation of Human Retinoid X Receptor-α at Serine 260 Impairs Subcellular Localization, Nuclear Mobility and $1\alpha, 25$-dihydroxyvitamin D₃- Dependent Signal Transduction in Ras-transformed Keratinocytes..... | 117 |
| 2.1 Abstract..... | 118 |
| 2.2 Introduction..... | 120 |
| 2.3 Experimental Procedures..... | 121 |
| 2.4 Results..... | 132 |
| 2.5 Discussion..... | 141 |
| 2.6 Acknowledgement..... | 148 |
| | |
| CHAPTER 3: Examination of VDR/RXR/DRIP205 Interaction, Intranuclear Kinetics and DNA Binding in Ras-transformed Keratinocytes and Its Implication for Designing Optimal Vitamin D Therapy in Cancer..... | 169 |
| 3.1 Abstract..... | 171 |
| 3.2 Introduction..... | 172 |
| 3.3 Experimental Procedures..... | 175 |

| | |
|---|-----|
| 3.4 Results | 185 |
| 3.5 Discussion | 194 |
| 3.6 Acknowledgement | 199 |
| CHAPTER 4: General Discussion | 214 |
| 4.1 Mechanisms of 1,25(OH)₂D₃ Resistance through RXR | 215 |
| 4.2 Nucleocytoplasmic transport of VDR and RXR | 221 |
| 4.3 RXR as Target for Chemoprevention and Cancer Treatment | 224 |
| 4.3.1 RXR/RAR as a Target | 227 |
| 4.3.2 RXR/PPAR as a Target | 230 |
| 4.3.3 Inhibition of Phosphorylation of RXR with Acyclic Retinoids | 231 |
| 4.3.4 Combination of Cancer Chemoprevention with Acyclic Retinoids | 236 |
| CHAPTER 5: Conclusion | 240 |
| CHAPTER 6: Claims and Originality | 252 |

| | |
|---|-----|
| References | 254 |
| Appendix | 304 |
| Abstracts Submitted/Presented at Conferences | 305 |

List of Figures

| | | |
|---------------------|--|----|
| Figure 1.1: | Schematic diagram of Vitamin D metabolism..... | 31 |
| Figure 1.2: | Schematic diagram of potential mechanism of action of vitamin D..... | 36 |
| Figure 1.3: | Schematic diagram of studies done with vitamin analogues..... | 47 |
| Figure 1.4: | Structural and functional organization of nuclear receptors..... | 54 |
| Figure 1.5: | Functional domains in human VDR..... | 55 |
| Figure 1.6: | Proposed mechanisms of gene induction and repression by human VDR..... | 56 |
| Figure 1.7: | Mutations in VDR that cause HVDRR..... | 61 |
| Figure 1.8: | Schematic drawing of different conformational states of nuclear receptor LBD..... | 69 |
| Figure 1.9: | Structural view on how the binding of various ligands can induce different nuclear receptor conformations, thereby modulating their transcriptional activity | 71 |
| Figure 1.10: | Intracellular signaling through the ERK1/2 MAP kinase pathway signaling pathway | 84 |
| Figure 1.11: | Past and ongoing approaches to develop inhibitors of mutationally activated RAS | 87 |
| Figure 1.12: | Compounds developed to target mutationally | |

| | | |
|---------------------|---|-----|
| | activated RAS..... | 99 |
| Figure 1.13: | Inhibitors of RAS effector signalling under clinical evaluation..... | 103 |
| Figure 1.4: | Crystal structure of RXR showing serine 260 phosphorylation site by RAS/RAF/MAPK cascade..... | 111 |
| Figure 2.1: | Effects of 1,25(OH) ₂ D ₃ and UO126 on cell growth and cell viability..... | 150 |
| Figure 2.2: | Effects of 1,25(OH) ₂ D ₃ on VDR and RXR α subcellular localization in HPK1A and HPK1Aras cells | 153 |
| Figure 2.3: | Effects of 9 cis-RA on RXR α subcellular localization in HPK1A and HPK1Aras cells..... | 156 |
| Figure 2.4: | Effects of RXR α phosphorylation on VDR/hRXR α co-localization in HPK1A and HPK1Aras cells..... | 159 |
| Figure 2.5: | Effects of RXR α phosphorylation on VDR and RXR interaction In HPK1A and HPK1Aras cells..... | 161 |
| Figure 2.6: | Effects of RXR phosphorylation on intra-nuclear kinetics of RXR in HPK1A and HPK1Aras cells..... | 163 |
| Figure 2.7: | Determination of receptor-DNA interaction..... | 165 |
| Figure 2.8: | Proposed model for nuclear import of VDR, RXR and VDR:RXR interaction and DNA binding in non-transformed and ras-transformed cells..... | 168 |
| Figure 3.1: | Effects of RXR α phosphorylation on intra-nuclear mobility and binding of RXR α by FRAP..... | 200 |
| Figure 3.2: | Effects of RXR α phosphorylation on VDR and DRIP205 | |

| | | |
|--------------------|---|-----|
| | intranuclear colocalization in HPK1A and HPK1Aras cells..... | 202 |
| Figure 3.3: | Effects of RXR α phosphorylation on RXR α and DRIP205 intranuclear colocalization in HPK1A and HPK1Aras cells..... | 204 |
| Figure 3.4: | Effects of RXR α phosphorylation on VDR/DRIP205 coactivator and VDR/LXXLL motif interaction in HPK1A and HPK1Aras cells..... | 206 |
| Figure 3.5: | Effects of RXR α phosphorylation on RXR α /DRIP205 coactivator and RXR α /LXXLL motif interaction in HPK1A and HPK1Aras cells..... | 208 |
| Figure 3.6: | Effects of RXR α phosphorylation on VDR/DRIP205 complex binding to DNA in HPK1A and HPK1Aras cells..... | 210 |
| Figure 3.7: | Effects of RXR α phosphorylation on RXR α /DRIP205 complex binding to DNA in HPK1A and HPK1Aras cells..... | 212 |
| Figure 4.1: | Schematic representation of VDR and RXR nuclear Import domain..... | 223 |
| Figure 4.2: | A schematic representation of RXR α phosphorylation in HCC cells..... | 228 |
| Figure 4.3: | Schematic diagram of studies done with vitamin D analogues..... | 230 |
| Figure 4.4: | Retinoid refractories due to RXR α phosphorylation and its restoration in ACR liver carcinogenesis..... | 233 |
| Figure 4.5: | Concept of clonal deletion and inhibition therapy in | |

| | | |
|--------------------|--|-----|
| | HCC by ACR..... | 238 |
| Figure 5.1: | Reviewed model for 1, 25(OH) ₂ D ₃ resistance in ras-transformed cells through conformational change of VDR/RXR α and impaired coactivator interaction, DNA binding | 243 |
| Figure 5.2: | VDR shows similarity to canonical NR structural organization..... | 244 |
| Figure 5.3: | The overall architecture of the DBD complex of RXR-VDR On canonical DR3 element..... | 245 |
| Figure 5.4: | The interaction of coactivator peptides with VDR..... | 247 |
| Figure 5.5: | The full length RXR-VDR structural model derived from SAXS and cryo-EM experiments..... | 249 |

List of Tables

| | | |
|-------------------|---|-----|
| Table 1.1: | VDR polymorphisms associated with cancer..... | 63 |
| Table 2.1: | Effects of RXR α phosphorylation on cell cycle in HPK1A and HPK1Ara cells..... | 149 |

List of Abbreviations

| | |
|--|--|
| 1,25(OH) ₂ D ₃ : | 1,25-Dihydroxyvitamin D ₃ : |
| 25-OHD: | 25-Hydroxyvitamin D |
| 1α-OHase: | 1α-hydroxylase enzyme |
| 24-OHase: | Vitamin D ₍₃₎ 24-hydroxylase |
| AF(1)(2): | Activation function(1)(2) |
| ANOVA: | Analysis of variance |
| ATRA: | All-trans retinoic acid |
| C-terminal: | Carboxyl terminal |
| CYP24: | 1,25-dihydroxyvitamin D ₃ 24-hydroxylase |
| CYP27B1: | 25-Hydroxyvitamin D ₃ 1-alpha-hydroxylase |
| DBP: | Vitamin D binding protein |
| DBD: | DNA binding domain |
| DR: | Direct repeat |
| DMEM: | Dubelcco's modified eagle's medium |
| DNA: | Deoxyribonucleic acid |
| DRIP: | Vitamin D receptor-interacting protein |
| ER: | Estrogen receptor |
| ERK: | Extracellular –signal regular kinase |

| | |
|----------------------------------|---|
| GR: | Glucocorticoid receptor |
| HAT: | Histone acetyltransferase |
| HCC: | Hepatocellular carcinoma |
| HPV: | Human papilloma virus |
| HRE: | Hormone response element |
| HVDRR: | Human vitamin D resistant rickets |
| E2: | Estrogens (Estradiol) |
| FBS: | Fetal Bovine Serum |
| KDa: | Kilodalton |
| MAPK: | Mitogen activated protein kinase |
| MEK: | MAP or ERK kinase |
| NSCLC: | Non-small cell lung cancer |
| PBS: | Phosphate buffered saline |
| PPAR γ : | Peroxisome proliferator-activator receptor gamma |
| PR: | Progesterone receptor |
| PTH: | Parathyroid Hormone |
| RANK: | Receptor activator of nuclear factor kappa B |
| RANK-L | Receptor activator of nuclear factor kappa B ligand |
| RAR (α, β, γ): | Retinoic acid receptor (α, β, γ) |

| | |
|----------------------------------|---|
| RARE: | Retinoic acid response element |
| RIP140: | Receptor interacting protein 140 |
| RXR (α, β, γ): | Retinoid X receptor (α, β, γ) |
| SEM: | Standard error of mean |
| SRC: | Steroid receptor activator |
| TR: | Thyroid receptor |
| VDR: | Vitamin D receptor |
| VDRE: | Vitamin D response element |

CHAPTER 1: Introduction

1.1 The Vitamin D Endocrine System

In the early 20th century groundbreaking research on vitamin D elucidated its essential role in calcium and phosphate homeostasis, bone mineralization. Clinical and molecular genetic data generated by dedicated scientists not only provided unequivocal evidence for the obligatory role of the nuclear vitamin D receptor (VDR) in mediating the actions of vitamin D but also enabled major public health advances. The biologically active form of vitamin D₃ which came to attention by virtue of its antirachitic properties is made in the kidney thus generating the fat-soluble secosteroid 1,25(OH)₂D₃ (Norman, 1979; DeLuca, 2004; Hendy, 2005).

1.2 Sources of Vitamin D

Vitamin D is a secosteroid (has a similar molecular structure to other steroids however, the bond between C-9 and C-10 of the B-ring carbon atoms is not joined) and is classified into five major classes: ergosterol (D₂), cholecalciferol (D₃), 22,23 dihydroergocalciferol (D₄), sitosterol (D₅) and stigmasteroid (D₆). The active form of vitamin D, 1 α ,25-dihydroxyvitamin D₃ (1,25(OH)₂D₃ or 1,25D₃) is derived by the metabolic hydroxylation of cholecalciferol (D₃) (Norman et al., 2000, 2002; Byford et al., 2002; Molnar, 2015). When we discuss vitamin D, we generally refer to two molecules, vitamin D₂ and D₃. The same metabolic pathway applies to vitamin D₂. Vitamin D₃ can be obtained from fortified foods, fatty fish or fish liver oil while vitamin D₂ (ergocalciferol) is the form obtained from plants through the photolysis of plant steroid ergosterol. However, the majority of vitamin D₃ is synthesized subcutaneously (Deeb et al., 2007). Thus the skin is the principal source of vitamin D (Fig. 1.1, Deeb et al., 2007; Holick, 2009)

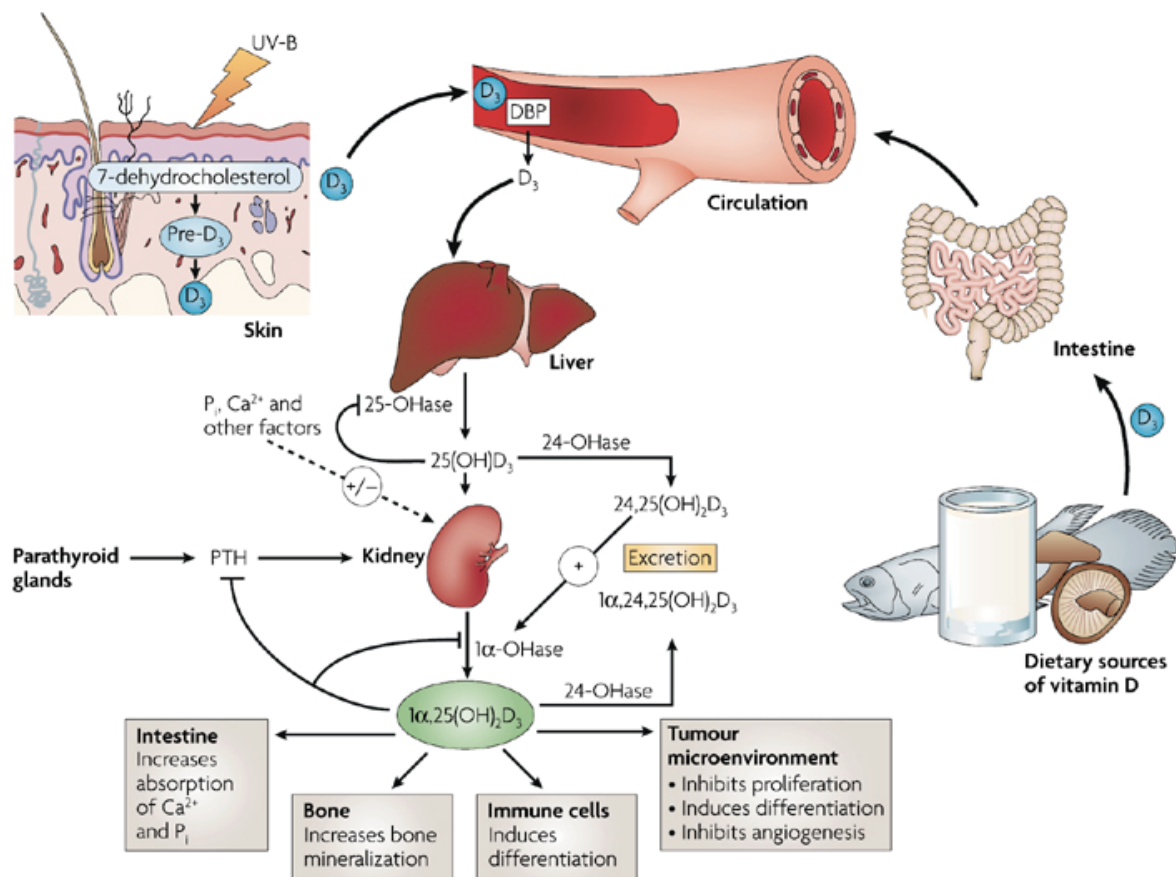


Figure 1.1: Vitamin D Endocrine System. Photochemical synthesis of vitamin D₃ (cholecalciferol, D₃) occurs cutaneously where pro-vitamin D₃ (7-dehydrocholesterol) is converted to pre-vitamin D₃ (pre-D₃) in response to ultraviolet B (sunlight) exposure. Vitamin D₃, obtained from the isomerization of pre-vitamin D₃ in the epidermal basal layers or intestinal absorption of natural and fortified foods and supplements, binds to vitamin D-binding protein (DBP) in the bloodstream, and is transported to the liver. D₃ is hydroxylated by liver 25-hydroxylases (25-OHase). The resultant 25-hydroxycholecalciferol (25(OH)D₃) is 1-hydroxylated in the kidney by 25-hydroxyvitamin D₃-1-hydroxylase (1-OHase).

This yields the active secosteroid 1,25(OH)₂D₃ (calcitriol), which has different effects on various target tissues. The synthesis of 1,25(OH)₂D₃ from 25(OH)D₃ is stimulated by parathyroid hormone (PTH) and suppressed by Ca²⁺, Pi and 1,25(OH)₂D₃ itself. The rate-limiting step in catabolism is the degradation of 25(OH)D₃ and 1,25(OH)₂D₃ to 24,25(OH)D₃ and 1,24,25(OH)₂D₃, respectively, which occurs through 24-hydroxylation by 25-hydroxyvitamin D 24-hydroxylase (24-OHase), encoded by the CYP24A1 gene. 24,25(OH)D₃ and 1,24,25(OH)₂D₃ are consequently excreted. The main effects of 1,25(OH)₂D₃ on various target tissues are highlighted above (Adapted from Deeb et al., 2007).

Important developments have increased our understanding of this hormone; it is now believed that 1,25(OH)₂D₃ is produced by the kidneys and locally by activated macrophages and keratinocytes to act as an endocrine, paracrine and an autocrine factor (Reichel et al., 1989). The formulation of the concept of a vitamin D endocrine system was dependent both on the key role of the kidney in producing 1,25(OH)₂D₃ in a carefully regulated fashion (DeLuca et al., 2001; DeLuca, 2004) and also the discovery of the vitamin D receptor in the intestine (Norman, 1974). The nearly ubiquitous presence of VDR, the extrarenal production of vitamin D metabolites, the regulation of multiple genes not involved in calcium metabolism and analysis of the phenotypes of VDR-deficient mice and men broadened the scope of spectrum of its biological activities than the originally regulatory mechanism of calcium homeostasis (Bouillon et al., 1976, 1995).

1.3 Synthesis and Metabolism of 1,25(OH)₂D₃

1.3.1 Synthesis of 1,25(OH)₂D₃

Vitamin D can be derived from nutritional origins in the diet or it can also be synthesized endogenously from cholesterol in the skin through the action of sunlight or ultraviolet light. The synthesis is a purely photochemical reaction and no enzymes are involved. However, the reaction is a highly regulated multistep process requiring a sufficiently large concentration of 7-dehydrocholesterol (7DHC) and UV-B light at 290-315 nm. In the epidermis, sunlight exposure causes the breakage of the bond between C-9 and C-10 of the B-ring (photochemical ring opening) to form previtamin D₃ (Bouillon et al., 1995; Norman et al., 2000). It has been demonstrated *in vitro* that vitamin D₃ is biologically inert. Administration to vitamin D deficient animals causes a physiological response after a 6-12 hr lag period (Solomon et al., 1999). The delay reflects the time required to activate vitamin D₃ by a series of hydroxylation reactions (Bouillon et al., 1995). Vitamin D₃ obtained from the isomerization of previtamin D₃ in the epidermal basal layers then binds to vitamin D binding protein (DBP) also called transcalfiferin in the blood stream (Bouillon et al., 2000) where it is either taken up immediately by the adipose tissue for storage or is then transported to the liver for metabolism (Bouillon et al., 1995).

Hepatic 25 –hydroxylation: The previtamin D₃ is then converted to 25-hydroxyvitamin D₃ (25(OH)D₃) by liver microsomal enzyme 25 –hydroxylase (25-OHase). 25(OH)D₃ is the most abundant metabolite of vitamin D₃ and its levels fluctuate with seasons. The highest fluctuation is observed during the summer months (Bouillon et al., 1995, 2008).

Renal 1 α -hydroxylation: In the kidneys, 25(OH)D₃ is 1 α - hydroxylated by the enzyme 1 α -hydroxylase (1 α -OHase). This yields the biologically active secosteroid

$1\alpha, 25(\text{OH})_2\text{D}_3$ which have various effects on target tissues (see fig. 1.1). Though it was previously believed that this hydroxylation reaction occurs exclusively in the mitochondria of renal proximal tubule cells by cytochrome P-450 enzyme 1α -hydroxylase, a number of tissue and cell types (extra-renal sites) such as activated macrophages and keratinocytes are now known to be capable of accomplishing the final activation step of $1,25(\text{OH})_2\text{D}$ (Reichel et al, 1989). Furthermore, major synthetic approaches have been used in recent years to synthesize the hormone $1,25(\text{OH})_2\text{D}_3$ and its various analogs. These analogs not only have varying degree of biological potency but also can preferentially stimulate vitamin D over all others (Bouillon et al., 1995, 2008). Other vitamin D metabolites include 25,26-dihydroxyvitamin D_3 , $25(\text{OH})\text{D}_3$ -26,23-lactone and 23-oxo- $1,25(\text{OH})_2\text{D}_3$ (De Luca, 2004). The physiological role of these metabolites remains to be determined.

1.3.2 Metabolism of $1,25(\text{OH})_2\text{D}_3$

$1,25(\text{OH})_2\text{D}_3$ is actively metabolized by the enzyme 24-hydroxylase (CYP24-OHase) encoded by the CYP24A1 gene at C-24 producing $1,24,25(\text{OH})_2\text{D}_3$, $1,24(\text{OH})_3\text{D}_3$ metabolites respectively. The second most abundant circulating metabolite of vitamin D_3 is $24, 25(\text{OH})_2\text{D}_3$. However, in humans under normal circumstances, its concentration in serum is ten fold less than $25(\text{OH})\text{D}$ (Jones et al., 1998). The 25-hydroxyvitamin D_3 - 1α -hydroxylase and 24-hydroxylase are very tightly and reciprocally regulated by $1,25(\text{OH})_2\text{D}_3$ itself and parathyroid hormone (PTH) (Tanaka and De Luca, 1981). CYP24-OHase was originally believed to be exclusively located in the kidney and to be involved only in the metabolism of $25(\text{OH})\text{D}_3$ to $24,25$ -dihydroxyvitamin D_3 . It has however, been subsequently shown to be present in vitamin D target tissues including enterocytes,

osteoblasts, keratinocytes and parathyroid cells. CYP24-OHase is now known to use and prefer $1,25(\text{OH})_2\text{D}_3$ as a substrate to $25(\text{OH})\text{D}_3$ (Jones et al., 1998). CYP24-OHase catalyzes the degradation of $1,25(\text{OH})_2\text{D}_3$ to the biliary excretory form calcitroic acid via a 5-step pathway collectively known as C24-oxidation pathway (Jones et al., 1998). It has been shown that human breast cancers had amplified CYP24-OHase levels which will increase degradation of $1,25(\text{OH})_2\text{D}_3$ within the tumor and as a consequence diminish its local activity (Jones et al., 1998).

1.4 The Vitamin D Binding Protein (DBP)

The DBP is a 55 kDa α -globulin transcalferrin protein that it synthesized in the liver. This transport protein has a single, high affinity site that binds vitamin D and all of its metabolites. The affinity for $25(\text{OH})\text{D}_3$ and $24,25(\text{OH})_2\text{D}_3$ are however higher than $1,25(\text{OH})_2\text{D}_3$ (Belsey et al., 1974). In circulation, vitamin D is complexed with transcalferrin and $25(\text{OH})\text{D}_3$ is the most abundant circulating form of the vitamin. This is due to the fact that there is a strong affinity for the DBP protein in the blood (Cooke et al., 1997). The advantage of this selectivity is the access of the biologically active $1,25(\text{OH})_2\text{D}_3$ into target cells (Deeb et al., 2007). Normally, only 0.04% of $25(\text{OH})\text{D}_3$ and 0.4% of $1\alpha,25-(\text{OH})_2\text{D}_3$ are free in plasma, the remainder being tightly bound to either a DBP (85–88%; high affinity; dissociation constant [Kd] ~ 1 nM) (Arnaud and Constans, 1993) or albumin (12–15%; low affinity) (Bikle et al., 1986). Only free unbound vitamin D sterols are considered to be biologically active, since only the free form and not DBP-bound $1\alpha,25-(\text{OH})_2\text{D}_3$ induces metabolic responses in target cells (Bikle 2014, Bikle et

al., 2015). The DBP also functions to maintain stable serum stores of vitamin D metabolites, modulate bioavailability and influence responsiveness of some end-organs (Safadi et al., 1999).

Megalyn and cubulin are two proteins that have been recognized as responsible for the uptake of the DBP. Megalyn acts to uptake the DBP to other tissues; cubulin binds the complexes differently and is internalized by megalyn (Haussler et al., 2011).

1.5 Biological Effects of 1,25(OH)₂D₃

Extensive evidence supports the view that 1,25(OH)₂D₃ generates biological responses by genomic and non-genomic pathways (Fig. 1.2, Haussler et al., 2011; Bikle et al., 2015).

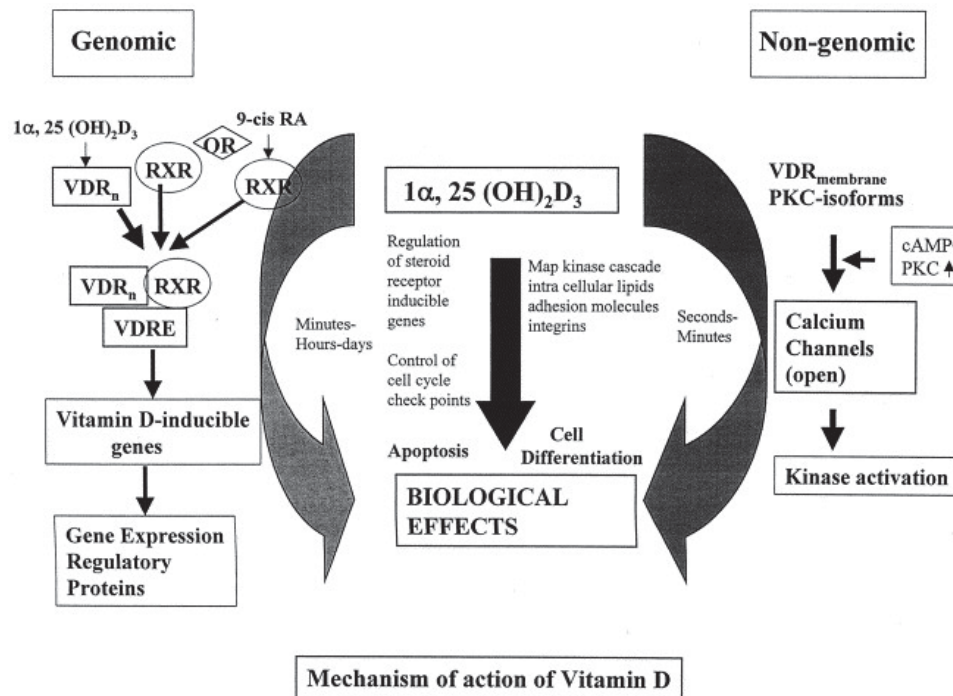


Figure 1.2: Schematic diagram of potential mechanism of action of vitamin D. Vitamin D functions both via genomic and non-genomic pathways. Possible pathways of both of these mediations of vitamin D action are shown in this diagram (Adapted from Mehta and Mehta, 2002).

1.5.1 1,25(OH)₂D₃ Non-Genomic Effects:

Non genomic actions of 1,25(OH)₂D₃ are rapid and transcription independent (Deeb et al., 2007). However, non-genomic signaling pathway may indirectly affect transcription through cross-talk with other signaling pathways (Deeb et al., 2007). Data suggests that non-genomic effects begin at the plasma membrane involving a non-classical membrane receptor (memVDR) and a 1,25(OH)₂D₃ - membrane associated rapid response steroid binding receptor (1,25D₃-MARRS also called ERp57/GRp58/PDIA3). The 1,25D₃-MARRS receptor is an endoplasmic reticulum (ER) thiol-disulphide oxidoreductase that was originally identified as the chaperone ERp57 (Nemere et al., 2012). More recently it has been identified as a protein disulfide isomerase, family A member 3 (PDIA3). In the caveolae where PDIA3 exists, interaction with phospholipase A2 (PLA2) activating protein (PLAA) and caveolin-1 initiate the non-genomic rapid signaling of 1,25(OH)₂D₃ via PLA2, phospholipase C (PLC), PKC and ultimately the ERK1/2 family of mitogen activated protein kinases (MAPK) (Boyan et al., 2012). The most well documented non-genomic effect is the rapid intestinal absorption of calcium ions. Binding of 1,25(OH)₂D₃ to the proposed membrane receptor stimulates calcium influx through voltage sensitive calcium (Ca²⁺) channels, release of calcium from intracellular stores, activation of phosphorylation cascades and phospholipid turnover leading to release of calcium to colon and skeletal

muscle cells. A hormone is said to have non-genomic effects if the physiological response is rapid and can be observed within seconds following administration of the hormone. This action contrasts genomic effects which are normally mediated by nuclear hormone receptors and are slow taking hours or days (Deeb et al., 2007). Non-genomic mechanisms of action have already been ascribed to several other steroid responsive systems (human sperm, neuronal membranes, endometrial cells), including glucocorticoids, estrogens, and progesterone (Jones, et al., 1998; Deeb et al., 2007).

1.5.2 1,25(OH)₂D₃ -Genomic Effects

Most of the biological actions induced by 1,25(OH)₂D₃ are mediated through the nuclear VDR (nVDR) which binds to VDREs in the regulatory regions of 1,25(OH)₂D₃ target genes (see section below). The genomic pathway is activated after the binding of 1,25(OH)₂D₃ to its nuclear receptor leading to the target gene transcription. Most genomic effects are on cell growth, cell differentiation, immune-modulation (Bouillon, 1995; Jones et al., 1998; Quack and Carlsberg, 2000; Deeb et al., 2007).

1.5.3 1,25(OH)₂D₃ Dual Regulation of Gene Expression by Genomic and Non-genomic Pathways.

Though the structural requirements of the ligands which bind to their membrane receptor and induce rapid non-genomic actions differ from those involved in genomic actions (Normal et al., 2000), there is compelling evidence that the non-

genomic and non-genomic activities of nuclear receptor ligands, including $1,25(\text{OH})_2\text{D}_3$ may complement each other to activate VDR and amplify its genomic activity (Norman et al., 2000; De Luca, 2004). For example, while the $1,25(\text{OH})_2\text{D}_3$ -liganded VDR selectively recognizes VDREs in the promoter regions of osteopontin (OPN) and osteocalcin (OCN) genes, $1,25(\text{OH})_2\text{D}_3$ can also employ rapid non-genomic pathways to modulate the steady state levels of OPN and OCN mRNA (Campbell et al., 2010). Furthermore, antagonism of the non-genomic pathway blocks $1,25(\text{OH})_2\text{D}_3$ -mediated OCN expression (Baran et al., 1992). Also, rapid activation of cytosolic kinases by $1,25(\text{OH})_2\text{D}_3$ may phosphorylate critical coactivators resulting in modulation of VDR-dependent gene transcription (Barletta et al., 2002). Using the non-genomic pathways, $1,25(\text{OH})_2\text{D}_3$ can modulate a repertoire of cytosolic kinases and second messenger systems that show some level of cell- or tissue-specificity e.g. activation of phospholipase A2 in chondrocytes and protein kinase A in enterocytes (Norman et al., 2002).

1.6 Biological Implications of $1,25(\text{OH})_2\text{D}_3$ Action

The traditional role of $1,25(\text{OH})_2\text{D}_3$ in the regulation of calcium and phosphate transport and bone mineralization are well known and extensively studied (Bouillon et al., 1995; Deeb et al., 2007). The $1,25(\text{OH})_2\text{D}_3$ endocrine system maintains mineral homeostasis and bone metabolism by the appropriate transcriptional activation or repression of target genes in cells that are involved in these processes. In humans, the concentration of calcium in serum is tightly controlled at 2.0 – 2.5 mmol/L total calcium (Rasmussen et al., 1963).

$1,25(\text{OH})_2\text{D}_3$ stimulates intestinal calcium and phosphate absorption, bone calcium and phosphate resorption and renal and phosphate absorption. In bone, actions of

1,25(OH)₂D₃ together with parathyroid hormone increases the re-absorption of calcium by activating the proteins involved in calcium and phosphorus absorption (De Luca et al., 2001). The plasma concentration of calcium and phosphorus increase due to the activated proteins thus providing conditions necessary to support bone mineralization (DeLuca et al., 2001). In periods of little dietary calcium intake, 1,25(OH)₂D₃ helps the mobilization of calcium by interacting with osteoblasts. In osteoblasts 1,25(OH)₂D₃ induce receptor activator nuclear factor-κB ligand (RANKL) which further activates osteoclastogenesis causing bone resorption (DeLuca, 2004).

More recent studies show that 1,25(OH)₂D₃ has many additional effects which include regulation of cell proliferation, pro-differentiation and immune modulation in multiple tissues (Reichrath et al., 2007; Bikle 2014; Bikle et al., 2015). These tissues include keratinocytes, breast epithelial cells and prostate cells. Gniadecki and co-workers (1996) showed that in keratinocytes cultures, low concentrations of 1,25(OH)₂D₃ stimulate proliferation *in vitro* while high concentrations inhibits proliferation. Similarly, Bonjour and co-workers (2007) found that addition of 1,25(OH)₂D₃ to prostate cancer cells resulted in the inhibition of proliferation and invasiveness and tumor progression in animal models of prostate cancer. The mechanism involves alteration of the transcription of genes involved in proliferation. Such results support the notion 1,25(OH)₂D₃ has an anti-cancer properties. Furthermore, 1,25(OH)₂D₃ has been found to play a role in immune modulation. It inhibits maturation of dendrites (the branched projections of a neuron that act to propagate the electrochemical stimulation received from other neural cells to the soma or cell body of the neuron from which the dendrites project), suppresses the stimulation of the major histocompatibility complex II

molecules (Reichrath et al., 2007) and regulates the proliferation and differentiation of B cells (Chen et al., 2007). Cantorna (2006) reported that $1,25(\text{OH})_2\text{D}_3$ affects immune function by increasing the production of regulatory T-cells and decreasing the activation of $\text{T}_\text{H}1$ -cells hence allowing for the maintenance of a crucial T-cell balance. The over-activation of $\text{T}_\text{H}1$ -cells has been implicated in autoimmune diseases such as multiple sclerosis. Current research is now focusing on the mechanisms by which $1,25(\text{OH})_2\text{D}_3$ reduces inflammation associated with progression and the severity of autoimmune diseases. Cohen-Lahav et al., (2006) investigated the molecular pathways involved in the anti-inflammatory action of $1,25(\text{OH})_2\text{D}_3$ using animal models and cell based studies respectively. The group found that $1,25(\text{OH})_2\text{D}_3$ decreases NF κ B, a transcription factor that plays an important role in the initiation of the transcription of inflammatory genes including chemokines and inducible nitric oxide synthase (iNOS) as well as inhibiting apoptosis. They also reported that the overexpression of the tumor necrosis factor (TNF α), an immune system modulator is found in a number of inflammatory diseases and that decreasing TNF α could provide an anti-inflammatory therapy. Recently, Hansdottir et al., (2010) using human tracheobronchial epithelial cells (hTBC) showed that $1,25(\text{OH})_2\text{D}_3$ decreases the respiratory syncytial virus induction of NF κ B –linked chemokines and cytokines in the airway epithelium while still maintaining antiviral properties. Finally, $1,25(\text{OH})_2\text{D}_3$ has been shown to regulate the central nervous system development (its neuroprotective effect is associated with its influence on neurotrophin production and release, neuromediator synthesis, intracellular calcium homeostasis, and prevention of oxidative damage to nervous tissue), reproduction (it controls several genes involved in embryo implantation, affects semen quality,

testosterone concentrations and fertility outcomes) and to play a protective role against other types of cancer (Welsh et al., 2003; Chen et al., 2007; Holick, 2009; Narvaez et al., 2014).

1.7 Vitamin D Analogues and Therapeutic Agents

Accumulating evidence for correction of bone abnormalities, pro-differentiating, anti-proliferating and photo-protective effects of $1,25(\text{OH})_2\text{D}_3$ from *in vitro*, *in vivo* and epidemiologic studies have increased interest in the use of vitamin D as a therapeutic agent in a variety of clinical situations such as cancer treatment, autoimmune disease, organ transplantation and infection (Deeb et al., 2007; Bouillon, 2008; Bikle, 2014) (Fig. 1.3). However, the therapeutic potential of this hormone has been limited by severe hypercalcemic effects and its degradation by vitamin D-24-hydroxylase (24-OHase) in 24-hydroxylated products (Campbell, 2010). To improve the clinical potential and minimize the current side effects, the development of vitamin D analogues with more specific action has been in progress. These synthesized analogues of vitamin D will either retain or enhance the efficacy of vitamin D activity while reducing or eliminating its associated toxicity (Bouillon et al., 2008).

More than 1000 analogues have been synthesised by various groups modifying the side chain of the molecule, as well as introducing changes in the A and B rings. Changes in the C and D rings are not very common due to the rigidity of the structure (Guyton et al., 2001; Deeb et al., 2007; Bikle, 2014). Although many of these analogues have been evaluated in cell culture models for their antiproliferative activity, only a few have shown reduced toxicity and increased

efficacy in *in vivo* mammary carcinogenesis models. These analogues include EB1089, KH1060, Calcipotriol, RO24–5531, 22-oxa-calcitriol and 1 α -24-ethyl-cholecalciferol (1 α (OH)D₅) (Mehta and Mehta, 2002; Banerjee and Chatterjee, 2003; Deeb et al., 2007). Another class of vitamin D analogues, with two side chains also termed Gemini compounds, has received considerable attention since they are very active at very low concentrations (Norman et al., 2008), although no *in vivo* chemoprevention studies have been reported. The analogues can activate or block the specific genomic effects of 1,25(OH)₂D₃ and at the same time cause fewer undesirable side effects like hypercalcemia or hypercalciuria (Farach-Carson et al., 1993).

Calcipotriol (MC903) has been marketed and used as a topical treatment for psoriatic plaques (Kragballe et al., 1991). It blocks hyperproliferation of keratinocytes and stimulates their differentiation. Interestingly, it is rapidly metabolized by the skin cells thus preventing systemic effects on calcium homeostasis. In animal studies, analog 22-oxocalcitol (OCT) has been reported to be a potent downregulator of PTH. It is therefore used in clinical trials in the treatment of secondary hyperparathyroidism (Colston et al., 1992). A third analog EB1089 has been reported to induce differentiation and inhibit proliferation without causing hypercalcemia. The potency of EB1089 on growth inhibition in human keratinocytes has been reported to be 10-100 fold higher than 1,25(OH)₂D₃ (Yu et al., 1995). Furthermore, EB1089 has been shown to block parathyroid related peptide (PTHrP) production, reverse hypercalcemia and reduce the development of bone metastasis in animal model of human breast cancer (El Abdaimi et al., 1999, 1999b). Although clinical trials for the treatment of breast cancer have been conducted, this has not translated into approved therapeutic

applications for the treatment of breast cancer (Jones et al., 1998; Carlsberg et al., 2001; Bikle 2012b, 2014).

Gulliford et al., (1998) reported a Phase I clinical trial that was conducted between May 1993 and June 1995. Thirty-six patients with advanced breast and colorectal cancer (histologically proven metastatic or locally advanced breast and colon carcinoma) were given the vitamin D analog EB1089 in a controlled trial protocol or compassionate treatment. In the protocol treatment, eleven patients were given a single day's dosing of EB1089 at a dose of 0.15-0.6 $\mu\text{g m}^{-2}$. This was followed by a 5-day repeated dosing period. Similarly, twenty-five patients received only the 5-day repeated dosing at dose levels of 0.9-17 $\mu\text{g m}^{-2}$. The results showed a similarity in the location of positive disease sites, tumour sizes and distribution.

In the compassionate treatment, twenty-one patients received treatment between 10 and 234 days (mean 90 ± 62 days). For comparative purposes, similar EB1089 dose levels were administered as that used in the per protocol phase however the dosage could be reduced if hypercalcaemia developed in either phase. Patients who became hypercalcaemic had EB1089 treatment stopped allowing serum calcium to return to normal before resuming treatment. No complete or partial responses were observed but six patients on treatment for more than 90 days showed stabilization of disease.

In both treatment scenarios, data failed to show any observable anti-tumour effects. A possible explanation was that since all patients had received anti-cancer therapy, EB1089 may not have any measurable effect/benefit above and beyond standard chemotherapy in advanced cancer. EB1089 may be more likely to be beneficial in

the earlier stages of disease or in patients with minimal disease (Gulliford et al., 1998).

Evans and co-workers (2002) conducted a phase II clinical trial with EB1089 in thirty-six patients with advanced inoperable cancer of the exocrine pancreas. Patients were given EB1089 at a starting dose of 20 µg once daily prior to the evening meal. The dosage was increased every 2 weeks until a dose that resulted in hypercalcaemia was achieved. (Hypercalcemia was defined as fasting albumin-corrected serum calcium greater than 2.80 mmol l⁻¹ or non-fasting albumin-corrected serum calcium greater than 3.0 mmol l⁻¹). When hypercalcemia occurred, treatment was discontinued for 1 week and then resumed at the dose level immediately below the one causing hypercalcaemia. Following this, no further dose adjustment was performed unless further episodes of hypercalcaemia were apparent. Dose levels of 5, 10, 15, 20, 30, 40 and 60 µg daily were allowed. Before completing 8 weeks of treatment, twenty-two patients were withdrawn from original thirty-two patients that were recruited for the clinical trial. The withdrawal of 20 of the twenty-two patients was due to clinical deterioration as a result of disease progression. Only fourteen patients completed at least 8 weeks of treatment and were evaluated for EB1089 efficacy. While five of the 14 patients showed no further disease progression during a period of 88-532 days (median= 168 days), no objective response was observed. The median survival was about 100 days and although, EB1089 was well tolerated in this cohort of pancreatic cancer patients, objective anti-tumour effect in this advanced disease stage setting was not found.

In summary, preclinical studies have shown promising therapeutic potential of 1,25(OH)₂D₃ and its analogs but the therapeutic efficacy of these agents has not

translated in therapeutic benefits in the few trials so far conducted. However, these preliminary observations have reinforced the possibility that less hypercalcemic analogues of vitamin D, with modified chemical structures that make them less prone to degradation by 24-OHase must be developed if the therapeutic advantage of vitamin D is to be realized (Deeb et al., 2007). Such approach has been developed by Genzyme with a novel compound which effectively blocks 24-OHase thus effectively preventing the degradation of $1,25(\text{OH})_2\text{D}_3$ into calcitroic acid or its analogues (Ferla et al., 2014a, 2014b). Therefore, combination of such inhibitors of 24-OHase with D analogue may provide the best therapeutic combination (Fig.1.3).

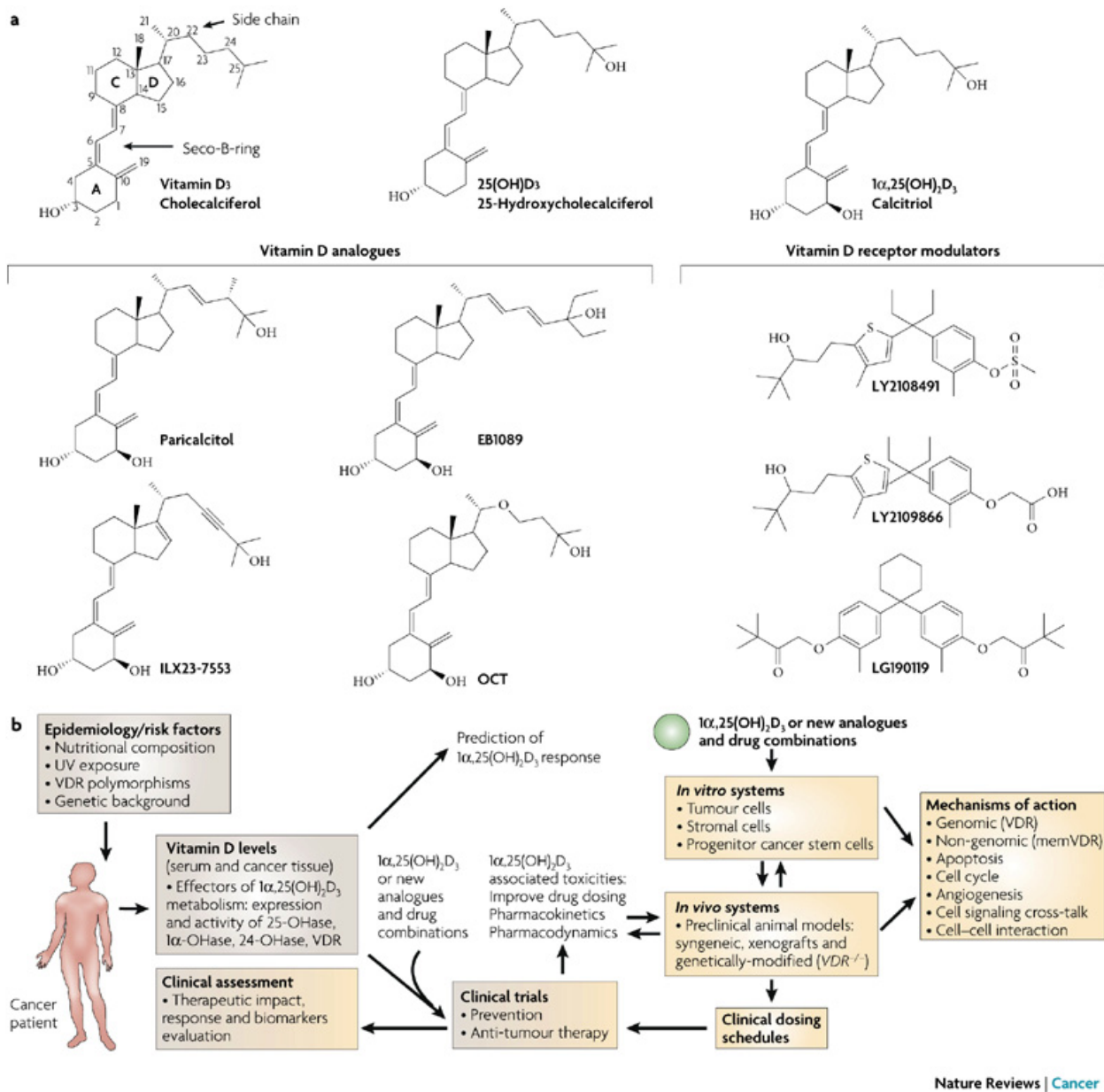


Figure 1.3: Studies done with vitamin D analogues. (a) Cholecalciferol (vitamin D₃) is 25-hydroxylated at C-25 (denoted by carbon atom systems on the structure of cholecalciferol) to form 25-hydroxycholecalciferol (25(OH)D₃). This is 1-hydroxylated at C-1 by 1-OHase to yield 1,25(OH)₂D₃ (calcitriol). 1,25(OH)₂D₃ is a secosteroid that is similar in structure to steroids but with a 'broken' B-ring

(denoted seco-B-ring) where two of the carbon atoms (C-9 and C-10) of the four steroid rings are not joined. Many vitamin D analogues (left) retain the secosteroid structure with modified side chain structures around the C-24 position, which makes them less hypercalcemic and less prone to degradation by 24-OHase. Several structures of vitamin D analogues referred to in the text are shown: paricalcitol (19-nor-1(OH)₂D₂), ILX23-7553 (16-ene-23-yne-1,25(OH)₂D₃), OCT (Maxacalcitol, 22-oxa-1,25(OH)₂D₃) and EB1089 (Seocalcitol, 1-dihydroxy-22,24-diene-24,26,27-trihomo-vitamin D₃). Vitamin D receptor modulators (VDRMs, right) are non-secosteroidal in structure. Some of the representative compounds described are LY2108491, LY2109866 and LG190119. (b) Paradigm for development and clinical translation of 1,25(OH)₂D₃ as an anticancer agent. Establishment of *in vitro* and *in vivo* experimental systems is crucial to developing 1,25(OH)₂D₃ or vitamin D analogues that target vitamin D metabolism and signalling. These systems allow the mechanisms of action of 1,25(OH)₂D₃ to be studied along with novel analogues (also in combination with cytotoxic drugs) in multiple transformed cell types and their biological effects (tumour and normal tissues) in animals. Importantly, studies on the pharmacokinetics and pharmacodynamics of drug action will enable the development of better designed clinical dosing schedules for clinical trials that will mirror the exposures active in preclinical models where optimal biological effects of 1,25(OH)₂D₃ are demonstrated and are achievable in human tumours in clinical therapy (Adapted from Deeb et al., 2007).

1.8 The Nuclear Receptor (NR) Super Family

The NR superfamily consists of 48 homologous transcription factors that function as molecular sensors for a diverse set of lipophilic hormones, vitamins and dietary lipids (Rochette –Egly et al., 2003; Berrabah et al., 2011). The members share overlapping and distinct tissue expression patterns resulting in coordinated regulation of transcriptional programs that control reproduction, development, differentiation and physiological responses to lipophilic hormones as well as the metabolic requirement of the organism. The family includes proteins that recognize steroid hormones (estrogens, progestins, and androgens), fatty acid, bile acids, oxysterols, vitamins A and D and thyroid hormones (Rochette-Egly et al., 2003). The hormones easily traverse the cell membranes and bind to their specific intracellular nuclear receptors which function by recognizing specific DNA sequences in the promoter regions or response elements of the target gene. Activation of these NR target genes requires binding of the receptor to specific DNA response elements (Glass et al., 2000). Analysis of the nuclear receptor core motif reveals that the response elements consist of a six base pair recognition sequence or half site that is arranged into direct or inverted repeats (Glass et al., 2000). The expression of numerous genes is regulated by nuclear receptors. Many of these genes are associated with disease explaining why nuclear receptors are molecular targets for approximately 13 % of FDA approved drugs (Francis et al., 2003).

1.8.1 Classification of Nuclear Receptor Superfamily

The NR superfamily is divided into four classes based on DNA binding and dimerization properties. Class I nuclear receptors include the steroid hormone receptors, estrogen receptors (ER), glucocorticoid receptors (GR),

mineralocorticoid receptors (MR), progesterone receptor (PR) and androgen receptors (AR). These receptors are generally found in the cytoplasm associated with chaperone protein in the absence of a ligand. In the presence of a ligand, they form homodimers and translocate into the nucleus where they recognize and bind to the inverted repeats of the hormone response elements. Some of the class I receptors such as ER which are found primarily in the nucleus are capable of binding DNA in the absence of a ligand (Mangelsdorf et al., 1995). The ER was first used to demonstrate their homodimeric binding property using an electrophoretic mobility shift assay (EMSA). Cells were transfected with vectors encoding either the full length ER or an ER mutant lacking the N-terminal (A/B) domain. The cell extracts were then incubated with a radioactively labeled, double-stranded oligonucleotide having the sequence of an estrogen response element. Three different protein-DNA complexes were analyzed by EMSA; a slow moving migrating complex formed by homodimers of the full-length ER, a fast migrating complex indicating the formation of homodimers of the truncated ER and a complex of intermediate mobility formed by heterodimers of both the full-length and truncated ER (Kumar et al., 1988). The intermediate band confirmed that two molecules of the receptor bind to a single DNA response element (Kumar et al., 1988).

The class II nuclear receptors include the non steroid binding nuclear receptors such as vitamin D receptor (VDR), retinoic acid receptor (RAR), thyroid hormone receptor (TR), and peroxisome proliferator-activated receptor (PPAR) (Mangelsdorf et al., 1995). These class II receptors are found constitutively in the nucleus and bind DNA in a ligand-independent manner. They form heterodimers with retinoid X receptors (RXR) and bind to direct repeat hormone response

elements containing the sequence AGGTCA. In this class, binding specificity depends on the number of nucleotides between repeats known as direct repeats. For example, PPAR binds a single nucleotide spacer (DR1), while TR binds with four nucleotide spacers (DR4) and RXR binds with five nucleotide spacers (DR5). The subtle differences in the nucleotide consensus half sites and the spacing between the half sites confers response element discrimination (Mangelsdorf et al., 1995). In the absence of ligand, the nuclear receptors bind to hormone response elements and actively repress transcription by recruiting corepressor proteins. In the presence of a ligand, there is ligand- receptor interaction which further stabilizes DNA binding leading to the release of the corepressors and the recruitment of coactivators to DNA (Chen and Evans, 1995; Glass, et al., 2000)

The class III and class IV nuclear receptors are often collectively called orphan receptors because they have no known ligand. They are the most abundant class of the nuclear receptor superfamily. The class III receptors will bind direct repeat hormone response elements as monomers whereas the class IV will bind half sites as monomers or dimers (Mangelsdorf et al., 1995). They have been classified into several categories. The first category which binds DNA as homodimers includes the hepatocyte factor 4 (HNF4) and chicken ovalbumin upstream promoter-transcription factor (COUP-TF). The response elements of these receptors are diverse including both direct and inverted repeats (Connely et al., 1994). HNF4 binds to the direct repeat 1 (DR1) elements as a homodimer and mediates strong transactivation while COUP-TF is a potent transrepressor thought to be mediated by the strong C-terminal repressor domain (Connely et al., 1994). Forman and coworkers (1995) showed that COUP-TF can form heterodimers with RXR in addition to its homodimerizing capacity.

The second category includes the liver X receptor (LXR), nerve growth factor IB-like receptor (NGF-IB) and farnesoid X receptor (FXR). Members of this category heterodimerize with RXR. Much like the VDR, heterodimerization with RXR is essential for these receptors to bind with high affinity to their response elements. Orphan receptors which are heterocomplexed with RXR have the potential to respond to 9-cis retinoic acid, a high affinity RXR ligand or to a novel orphan ligand (Leblanc et al., 1995). For example, NGFI-B formation of a heterodimer with RXR creates a complex that is 9-cis retinoic acid responsive (Forman et al., 1995).

The third category is composed of receptors that bind to DNA as monomers. This includes the steroidogenic factor-1 (SF-1) a nuclear orphan receptor involved in the production of steroid synthesis for the nuclear receptors (Lala et al., 1992). Binding of these receptors to DNA involves interaction with an extended half site where the nucleotide flanking the 5'-region of the consensus sequence are important for increasing the number of specific base pair contacts and augmenting the affinity of the monomeric receptor for the core recognition motif (Wilson et al., 1992). It has been reported that the action of some of the orphan receptors may not require binding of the ligand and may therefore function as ligand-independent transcription factors (Mangelsdorf et al., 1995).

1.8.2 Structure and Function of Nuclear Receptors

The nuclear receptors are a large family of evolutionarily conserved transcription factors. They share a homologous modular structure and functional organization generally consisting of six conserved domains (A-F) (Gronemeyer and Bourguet,

2009; le Maire et al., 2010; Rastinejad et al., 2014). Each domain possesses a distinct biochemical function. The A and B domains are located in the amino-terminal region and contain the activation function (AF-1) domain which activates transcription independent of ligand binding (Gigore et al., 1986). Domain C contains two highly conserved type II zinc fingers which together constitute the nuclear receptor DNA binding domain. The central DNA binding domain allows the nuclear receptors to interact with sequence specific DNA elements. Located in the first zinc finger is a P box which makes direct contact with the major groove nucleotides and mediates sequence specific recognition and binding of the nuclear receptor to hormone response elements (Umesono and Evans, 1989). The hinge region found in region D confers conformational flexibility and contains the nuclear localization signal (Tsai and O'Malley, 1994). The ligand binding domain also known as region E is the largest domain and contains the second activation function (AF-2). Unlike AF-1, activation by AF-2 is ligand dependent. This region plays an important role in ligand recognition and binding, receptor dimerization, coactivator interaction and ligand-dependent transcriptional regulation (Bourguet et al., 2000; Egea et al., 2000; Orlov et al., 2012). The ligand binding domain contains hydrophobic pockets which bind ligands causing structural alteration resulting from the movement of the α -helix 12 that is located within the C-terminus of the ligand binding domain. The function of the F region at the C-terminus has yet to be determined (Wahli et al., 1991, Fig. 1.4).

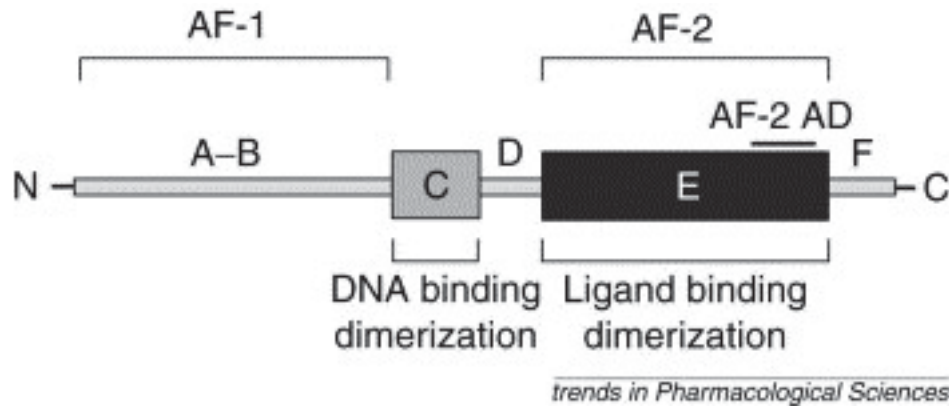


Fig.1.4. Structural and functional organization of nuclear receptors. Nuclear receptors consist of six domains (A–F) based on regions of conserved sequence and function. The DNA-binding domain (DBD; region C) is the most highly conserved domain and encodes two zinc finger modules. The ligand binding domain (LBD; region E) is less conserved and mediates ligand binding, dimerization and a ligand-dependent transactivation function, termed AF-2. Within the AF-2, the integrity of a conserved amphipathic α -helix termed AF-2 activation domain (AD) has been shown to be required for ligand-dependent transactivation. The N-terminal A–B region contains a cell- and promoter specific transactivation function termed AF-1. The region D is considered as a hinge domain. The F region is not present in all receptors and its function is poorly understood (Adapted from Bourguet et al., 2000).

1.9 The Vitamin D Receptor

The human VDR gene which encodes the VDR is found on chromosome 12q. The gene is composed of a promoter and regulatory regions and exons which encode the six A-F domains of the full length VDR protein (Deeb et al., 2007, Fig.1.5).

The human VDR is a 427 amino acid protein with molecular mass of 50 kDa organized in a similar manner like other members of the nuclear receptor superfamily (Baker et al., 1988; Normal et al., 2002). The length of the A/B domain of the VDR is 20 amino acids long. The function of this domain has yet to be defined. The DNA binding or C domain which is composed of 66 amino acids and contains two zinc fingers is located between amino acids 20 and 90. The C terminus or E or ligand binding domain is between amino acids 130 and 423. This domain is responsible for high affinity ligand binding and, coactivator interaction, dimerization and transactivation (Fig. 1.6). To effectively bind to DNA and activate gene transcription, VDR requires heterodimerization with RXR (Barsony et al., 1997; Sone et al., 1999). Heterodimerization is made possible because the E domain of the VDR contains nine hydrophobic heptad repeats (Forman et al., 1990). Mutation in the VDR heptad repeats has been shown to abrogate VDR-RXR complex formation (Hausler et al., 2011).

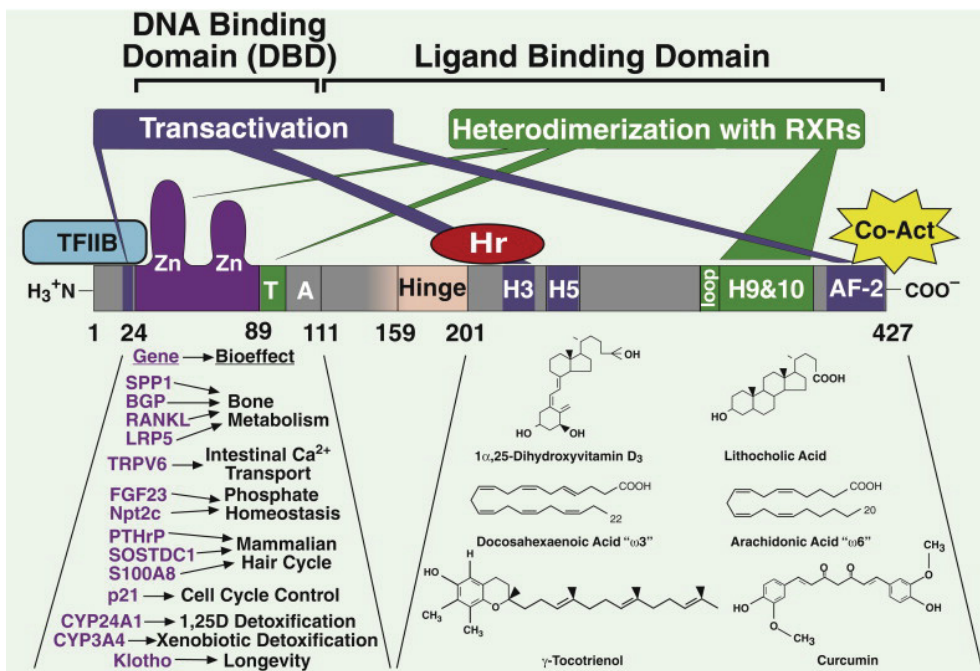


Figure. 1.5: Functional domains in human VDR. Highlighted at the left is the human VDR zinc finger DNA-binding domain which, in cooperation with the corresponding domain in the RXR heteropartner, mediates direct association with the target genes listed at the lower left, leading to the indicated physiological effects. The official gene symbol for BGP is BGLAP, for RANKL is TNFSF11, for Npt2c is SLC34A3, for PTHrP is PTHLH, and for klotho is KL. Below the ligand-binding domain (at the right) are illustrated selected VDR ligands, including several novel ligands (Adapted from Haussler et al., 2011).

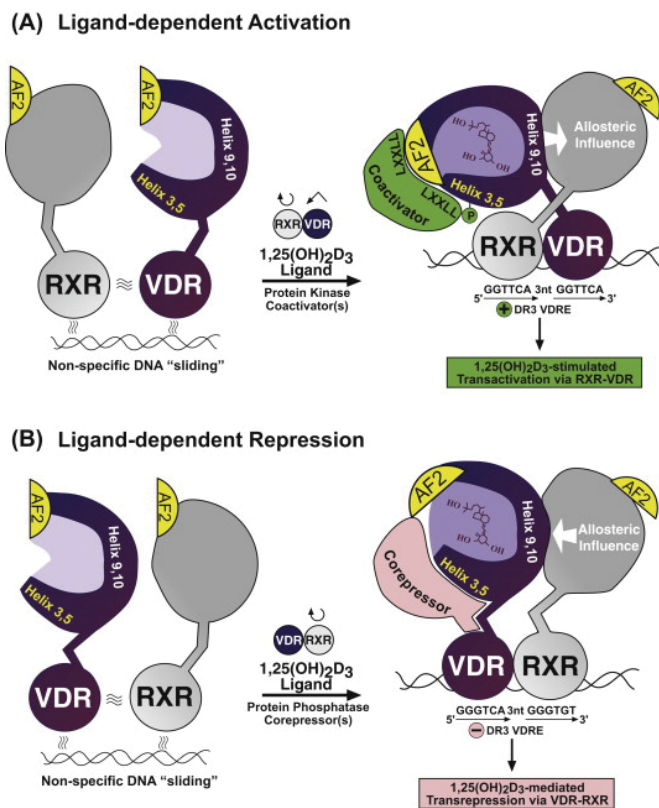


Figure 1.6. Proposed mechanisms of gene induction and repression by VDR. (A) Allosteric model of RXR-VDR activation after binding 1,25(OH)₂D₃ and

coactivator, phosphorylation, and docking on a high-affinity positive VDRE (mouse osteopontin). See text for explanation. (B) Allosteric model for VDR-RXR inactivation after binding $1,25(\text{OH})_2\text{D}_3$ and corepressor, dephosphorylation, and docking in reverse polarity on a high-affinity negative VDRE (chicken PTH) (Adapted from Haussler et al., 2011)

1.9.1 Coregulators of Vitamin D Receptor Action

Nuclear receptors including VDR require a number of coregulators for ligand-dependent transcriptional activation or repression. The coregulators are divided into coactivators and corepressors.

The Vitamin D interacting protein (DRIP) complex (also known as TRAP/SMCC, PBP, ARC or human mediator) is one of the best characterized coactivators. The DRIP complex is a large multimeric group of novel proteins and a subset of proteins homologous to the yeast mediator (Fondell et al., 1996; Rachez et al., 1998, 2000). DRIP does not have intrinsic histone acetyl-transferase (HAT) activity. Thus, activation of gene transcription requires the recruitment of more potent HATs and other cofactors possessing HAT activity. One subset of the DRIP complex that mediates direct interaction with the VDR is DRIP205 (also known as TRAP220). DRIP205 binds to the AF-2 domain of the VDR and other nuclear receptors through its nuclear interaction domain (NID) called LXXLL motif (also called NR boxes). Studies using isolated wild type and reconstituted DRIP205 complexes containing mutations in the LXXLL motifs have shown that the LXXLL motifs are essential in mediating strong ligand –dependent interaction.

Furthermore, they are critical components in nuclear receptor mediated transcription (Ren et al., 2000; Rachez et al., 2000; Burakov et al., 2000).

A second group of coactivators is the p160/steroid receptor coactivator (SRC) family of coactivators. Members of this family of proteins include SRC-1/NCoA-1, TIF2/GRIP1, and pCIP/RAC3/AIB-1/ACTR/TRAM-1 (Rachez et al., 2000; Burakov et al., 2000). The p160/SRC family binds to VDR via their own LXXLL motifs. A second characteristic of the p160 coactivators is the possession of an intrinsic HAT activity and the ability to recruit other coactivators such as CREB binding protein (CPB), its homolog p300 and pCAF proteins. The recruitment of the other coactivators likely facilitates ligand-dependent transcription through their HAT activity (Burakov et al., 2000). Bikle and coworkers (2007) showed that both DRIP205 and SRC participate in vitamin D-dependent keratinocyte differentiation in distinct ways.

In contrast to the coactivators, the corepressors actively repress target gene activation. The group includes NR corepressor (NCoR), silencing of retinoid acid and thyroid hormone (SMRT) and receptor interacting protein 140 (RIP140). In the unliganded state, both NCoR and SMRT are reported to associate with nuclear receptors including VDR and recruit histone-modifying enzymes such histone deacetylase (HDAC) complexes to NR target gene promoters thereby repressing transcription. RIP140 however, directly interact with the C-terminal binding proteins (CtBPs). This interaction results in the recruitment of HDACs followed by transcriptional repression (Perissi and Rosenfeld, 2005; Perissi et al., 2010).

1.9.2 VDR Mutations and 1,25(OH)₂D₃ Resistance

Mutations in the VDR result in target organ resistance to $1,25(\text{OH})_2\text{D}_3$ and cause hereditary $1,25(\text{OH})_2\text{D}_3$ D resistant rickets (HVDRR) disease also known as vitamin D-dependent ricket type II (Malloy et al., 2014). It is a loss of function mutations in the gene encoding the VDR. It produces a defective VDR protein which results in an impaired ability of the VDR to signal and to regulate target genes even in the presence of elevated $1,25(\text{OH})_2\text{D}_3$ concentrations. This interferes with some aspect of $1,25(\text{OH})_2\text{D}_3$ binding or VDR signaling which include (1) completely abolishing $1,25(\text{OH})_2\text{D}_3$ binding, (2) reduction in VDR affinity for $1,25(\text{OH})_2\text{D}_3$ binding, (3) disruption of RXR α heterodimerization or (4) interference with coactivator interactions (Malloy et al., 1997, 2011; Malloy and Feldman 1998, 2010, 2011; Feldman et al., 2013). Also, mutations in the VDR DBD interfere with VDR binding to vitamin D response elements (VDREs) in target genes preventing the VDR/ $1,25(\text{OH})_2\text{D}_3$ complex from signaling target genes. Premature stop mutations prevent the formation of adequate VDR protein or in fact result in no detectable VDR at all (Feldman et al., 2013).

The disease is an autosomal recessive disease affecting both males and females equally. The heterozygous parents (normally carriers of the genetic trait) are usually asymptomatic to the disease and have normal bone development. Malloy et al., (2011) in a recently published study, showed that a child harboring a heterozygotic mutation in the gene encoding the VDR (Glu420Ala) developed clinically severe HVDRR due to dominant negative suppression of the wild-type allele. Children who are affected may also exhibit alopecia of the scalp and total body. They usually fail to respond to treatment with calcitriol even though they often have very elevated endogenous levels of calcitriol. Successful treatment

requires reversal of hypocalcemia and secondary hyperparathyroidism. This is usually accomplished by the administration of high doses of calcium given either intravenously or sometimes orally to bypass the intestinal defect in VDR signaling (Feldman et al., 2013).

HVDRR is different from vitamin D-dependent rickets type 1 (VDDR-I) or pseudovitamin D deficiency rickets (PDDR) in which the critical enzyme 25-hydroxyvitamin D-1 α -hydroxylase (1 α -hydroxylase or CYP27B1) which synthesises 1,25(OH) $_2$ D $_3$ from 25(OH)D becomes defective also due to various loss of function mutations. Both diseases are rare autosomal recessive disorders characterized by hypocalcemia, secondary hyperparathyroidism and early-onset rickets (Feldman and Malloy, 2014).

Recent reviews have discussed 45 unique mutations identified in the VDR gene as the cause of HVDRR. These mutations in the DBD prevent the VDR from binding to DNA, causing total resistance to 1,25(OH) $_2$ D $_3$ even though 1,25(OH) $_2$ D $_3$ binding to the VDR is normal (Malloy and Feldman 1998, 2010, 2011; Malloy et al., 1999, 2011; Feldman et al., 2013; Feldman and Malloy, 2014). Other mutations that have been identified in the VDR as a cause for 1,25(OH) $_2$ D resistance include nonsense mutations, insertions/substitutions, insertions/duplications, deletions and splice site mutations. In a study investigating the cause of HVDRR, Feldman and Malloy (2014) identified eleven missense mutations in the VDR. Lastly, VDR mutations in the LBD may disrupt ligand binding or heterodimerization with RXR α , or prevent coactivators from binding to the VDR and cause partial or total hormone resistance (Fig, 1.7; Malloy et al., 2002).

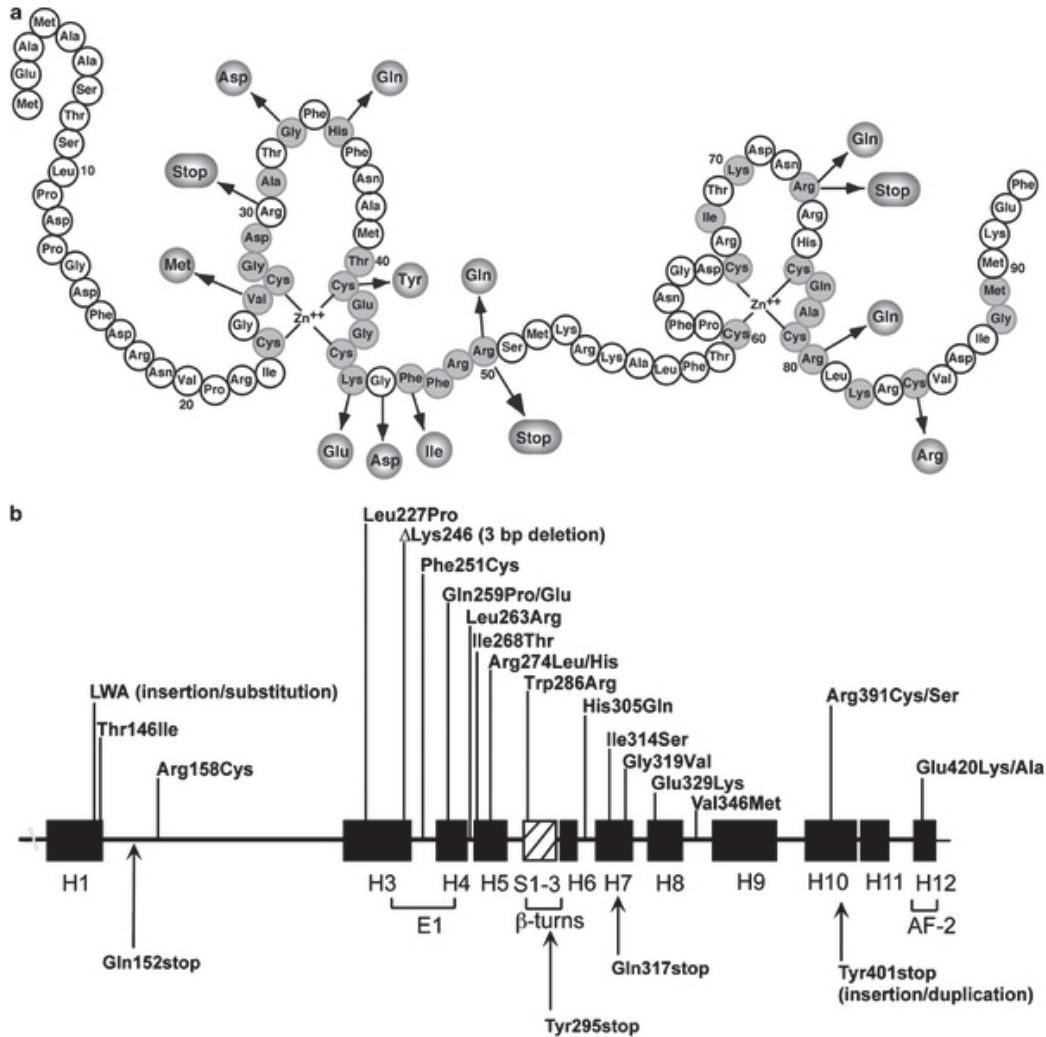


Fig 1.7: Mutations in the VDR that cause HVDRR. (a) Location of mutations in the DNA-binding domain (DBD). Conserved amino acids are shaded. (b) Location of mutations in the ligand-binding domain (LBD). The α -helices are shown as black boxes and the β -turns as hatched box. Missense mutations are on top and nonsense mutations on bottom. E1 and AF-2 (activation function 2) represent helices important for transactivation. (Adapted from Feldman et al., 2013).

Several other mutations have been identified in the VDR that affect VDR:RXR α heterodimerization thereby causing HVDRR. These include, Gln259Pro and Phe251Cys (Cockerill et al., 1997; Malloy et al., 2001), Gln259Glu (Macedo et al., 2008) and Val346Met (Arita et al., 2008). All of the patients with defects in VDR:RXR α heterodimerization had alopecia. In the VDR LBD, Arg391 mutation to Arg391Cys had no effect on ligand binding but reduced its transactivation activity. Arg391 is located in helix H10 where the RXR α dimerization interface is formed from helix H9 and helix H10 and the interhelical loops between H7–H8 and H8–H9 in VDR. Arg391 was also mutated to serine (Arg391Ser) (Nguyen et al., 2006). Malloy and coworkers (2002) reported that a Glu420Lys mutation located in helix H12 of VDR caused no defect in multiple steps in VDR gene regulation including ligand binding, VDR:RXR α heterodimerization or DNA binding. However, the Glu420Lys mutation abolished VDR binding to the coactivators SRC-1 and DRIP205 (Feldman and Malloy, 2014).

1.9.3 VDR Polymorphism and 1,25(OH) $_2$ D $_3$ Resistance

Previous studies have revealed that the loss of VDR during de-differentiation of colon cancer cells, the presence of mutations in the VDR and VDR polymorphisms as some of the mechanism imparting vitamin D resistance (Matusiak et al., 2005). A polymorphism is a genetic variant that occurs in non-coding parts of the gene (introns) so they would not be seen in the protein product (Valdivieso and Fernandez, 2006). However, in the regulatory parts of the gene, these changes affect both the degree of expression of the gene and the level of expression of the protein. For instance, changes in the 5' (five prime)-promoter of the VDR gene can affect mRNA expression patterns and levels and alterations in the 3' (three prime)

untranslated region (UTR) sequence variations can affect mRNA stability and protein translation efficiency. The changes can also occur in exonic parts of the DNA leading to altered protein sequences. When DNAs are digested with restriction enzymes and separated by agarose gel electrophoresis, DNA fragments of different lengths are produced because DNA sequence polymorphisms display different migration profiles from wild-type fragment when run on the agarose gel. Such polymorphisms that displays various lengths which are different from the wild-type sequence following restriction digestion are called Restriction Fragment Length Polymorphisms (RFLPs) (Valdivieso and Fernandez, 2006).

Recent meta-analyses have detailed very strong associations between certain cancers and the genetic polymorphisms (see table 1.1).

| Cancer | VDR polymorphisms |
|---------------|----------------------------------|
| Prostate | Fok1, Bsml, Taq, Apal, poly (A) |
| Breast | Fok1, Bsml, Taql, Apal, poly (A) |
| Melanoma | Fok1, Bsml, |
| Colorectal | Fok1, Bsml, |
| Thyroid | Fok1, Bsml, Taql, |

Table 1.1: VDR polymorphisms associated with cancer (Adapted from Vuolo et al., 2012).

For example, in melanoma with Bsml and FokI; prostate cancer with Bsml, FokI, Apal; breast cancer with Bsml, FokI, and TaqI (Chen et al., 2009; Kostner et al.,

2009; Raimondi et al., 2009, Vuolo et al., 2012). In prostate cancer, haplotype analysis showed that the allelic variants BsmI(B)–APAI(A)–TaqI (t) were associated with a higher Gleason score (a parameter used to help evaluate the prognosis of men with prostate cancer using samples from a prostate biopsy) than allelic variants BsmI (b)–APAI (a)–TaqI (T). Cancers with a higher Gleason score are more aggressive and have a worse prognosis. Lowe and coworkers (2005) also reported that risk of developing breast cancer was six times higher for women with low levels of 25(OH)D (<20 ng/ml) associated with the BsmI bb genotype than women with sufficient levels of 25(OH)D (>20 ng/ml) and BB or Bb genotype (Chen et al., 2009). Penna-Martinez et al., (2009) however found that while the AA and FF alleles of the VDR polymorphism ApaI and FokI VDR polymorphisms and the haplotype tABF conferred protection from follicular carcinoma, the haplotype Tabf appeared to be associated with an increased follicular thyroid carcinoma risk. Others researchers have reported the effects of protein polymorphisms and single nucleotide polymorphisms in the 5' UTR of the VDR prostate cancer risk and a higher colorectal cancer risk in patients with the VDR polymorphism FokI, PolyA, TaqI, Cdx2, and ApaI (McCullough et al., 2009; Touvier et al., 2011; table1.1). Thus the importance of the VDR and the action of 1,25(OH)₂D₃ in cancer progression are supported by a wide array of basic and pre-clinical data but still lack clear clinical evidence from randomized clinical.

1.9.4 VDR Knockout Mice and 1,25(OH)₂D₃ Resistance

The development of VDR knockout and knockdown mice by Li and coworkers (1997), Yoshizawa et al., (1997) and several other groups have further increased

our understanding of $1,25(\text{OH})_2\text{D}_3$ resistance via mutations in the VDR gene. The DBD domain of VDR has been the region to create the knockdown. The VDR-null mice (VDRKO) recapitulate the findings in the children with HVDRR. The VDR-null mice appear normal at birth and become hypocalcemic and their PTH levels rise sometime after weaning. Bone mineralization is severely impaired and signs of rickets develop over time. The VDR-null mice have normal hair at birth but develop progressive alopecia, thickened skin, enlarged sebaceous glands and epidermal cysts. Li and coworkers (1997), Yoshizawa et al., (1997) showed that while the heterozygote mice appeared phenotypically normal, the homozygotes manifested symptoms similar to patients with HVDRR. About 90 % of these mice died within 15 weeks following birth. Other symptoms acquired by the homozygous mice included hypocalcemia, low bone mass, hypophosphatemia, alopecia and hyperparathyroidism (Yoshizawa et al., 1997). The mice also had about ten fold elevated levels of $1,25(\text{OH})_2\text{D}_3$ and low circulating levels of $24,25(\text{OH})_2\text{D}_3$. Yoshigawa et al., (1997) suggested that the similarities observed in the VDR null mice and the HVDRR patients were further proof that the bone mineral homeostatic function of $1,25(\text{OH})_2\text{D}_3$ was mediated by the vitamin D receptor through the regulation of calcium and phosphate absorption in the intestine. Interestingly, the abnormalities observed in the VDR knock out mice could be reversed by feeding the animals with a “rescue diet” containing high levels of calcium and phosphate (Li et al., 1997). The rescue diet normalized parathyroid hormone (PTH) levels and improved bone mineralization. A similar effect was also observed in HVDRR patients on calcium infusion therapy (Balsan et al., 1986). While the rescue diet corrected defects in bone mineralization, it had no effects on alopecia implying that these two functions of VDR are independent.

In other words, many of the abnormalities resulting from the hypocalcemia and are not directly caused by the absence of a functional VDR (Malloy and Feldman 1998, 2010, 2011, Malloy et al., 1999, 2011). These findings provide evidence that mutant VDRs that were unable to mediate classic genomic activity leading to 1,25(OH)₂D₃ resistance. This evidence provides strong support for the hypothesis that the VDR is required and involved in its signaling.

1.9.5 Epigenetic Mechanisms and 1,25(OH)₂D₃ Resistance

Epigenetic mechanisms play an important role in regulating VDR gene expression (Fetahu et al., 2014). Enzymes acting in the nucleus can carry out a complex interplay of epigenetic mechanisms involving DNA methylation and covalent modifications of histones by methylation, acetylation, phosphorylation, or ubiquitination. The enzymes include DNA methyltransferases (DNMTs), which carry out the DNA modification and histone acetyltransferases (HATs), histone deacetylases (HDACs), histone methyltransferases (HMTs) and histone demethylases (HDMs), which regulate covalent histone modifications. Epigenetic impairment of VDR signaling is suggested to be one of the mechanisms that leads to reduced responsiveness to 1,25(OH)₂D₃ actions. It is reported that vitamin D interacts with the epigenome at various levels (Marik et al., 2010, Fetahu et al., 2014). Also, the promoter regions of critical genes coding for VDR and CYP27B1, CYP24A1 and 25-hydroxylase (CYP2R1) possess large CPG islands. They can therefore be silenced by DNA methylation (Fetahu et al., 2014). Marik et al., (2010) reported that in breast tumors, the methylation of the VDR gene at exon 1a was significantly higher with 65% of CpGs methylated compared to 15% of CpGs

methylated in the normal breast tissue. The group showed that *in vitro*, three hypermethylated regions in exon 1a of breast cancer cell lines, became demethylated following treatment with the DNMT1 inhibitor 5-aza-2'-deoxycytidine (DAC). However, treatment with 1,25(OH)₂D₃ had no effect on methylation of these regions.

Furthermore, the hypermethylation of CPG islands (CGIs) in epigenetically silenced genes is often associated with loss of acetylation on histone 3 and 4 (H3 and H4), loss of methylation of lysine (K) 4 on H3 (H3K4), and gain of methylation of K9 and K27 on H3 (H3K9 and H3K27) (Esteller, 2008).

In cancer, expression of CYP27B1 is often downregulated. Murayama et al., (2004) reported that the promoter region of CYP27B1 contains a negative VDRE (nVDRE) located at around 500 bp. This region consists of two E-box like motifs and is responsible for 1,25(OH)₂D₃-dependent transrepression. This seems to be achieved through recruitment of both HDACs and DNMTs by VDR/RXR to the promoter region of CYP27B1 (Takeyama and Kato, 2011). Thus there is an increased methylation of the CPG island located within CYP27B1. In the MBA-MB-231 breast cancer cells, CYP27B1 hypermethylation resulted in gene silencing. However, this effect was reversed by treatment with deoxy C (Shi et al., 2002).

Also, the physical interaction of VDR with coactivators and the chromatin remodelers or modifiers such as HATs, HDACs, HMTs can result in epigenetic changes. Gene activity throughout the genome is dictated by the chromatin environment; post-translational modifications of the N-terminal tails of histone proteins can thus allow nucleosomes to shift the chromatin to a relaxed state

resulting in gene activation (Meyer et al., 2013). In malignant prostate primary cell cultures, elevated expression of the NCoR2/SMRT co-repressor mRNA was correlated with reduced 1,25(OH)₂D₃ antiproliferative response. This suggested that the VDR/ co-repressor ratio may be critical in determining responsiveness of cancer cells to 1,25(OH)₂D₃ (Campbell and Adorni, 2006). In a parallel study involving ER α negative breast cancer cell lines and primary cultures, elevated levels of NCoR1 mRNA was associated with 1,25(OH)₂D₃ insensitivity. The authors found that targeting the epigenetic lesion by co-treatment with 1,25(OH)₂D₃ and a HDAC inhibitor trichostatin A restored the cells to 1,25(OH)₂D₃ sensitivity. Yoneda et al., (1984) showed earlier that the histone acetyltransferase inhibitor butyrate augments 1,25(OH)₂D₃ actions.

1.10 The Retinoid X Receptor

Retinoids are natural and synthetic derivatives of vitamin A, which regulate development (Tanaka et al., 2004), cell proliferation (Lotan et al., 1990) and differentiation (DeLuca et al., 2001, 2004). Also, they act as preventive agents of cancer. Because of these roles, they are presently being used in treatment of certain types of cancer including hepatocellular carcinoma and acute promyelocytic cancer. Furthermore, they have also been tested in diverse clinical trials to prevent solid tumors including oral, head and neck, non-melanoma skin cancers, breast, cervical dysplasia and xeroderma pigmentosum (Shilkaiti et al., 2015; diMasi et al., 2015). Many studies have shown their effectiveness on inhibition of cancer cell growth *in vivo* and *in vitro* (diMasi et al., 2015). However, the clinical use of retinoids is limited by the large dosage required to reach therapeutic potency

(Tanaka et al., 2004). Two distinct nuclear receptor families mediate the physiological actions of retinoids (Evans, 1988; Mangelsdorf et al., 1995). These include retinoid acid receptor (RAR) which consist of three subtypes (RAR α , RAR β and RAR γ) and the retinoid X receptor (RXR) also consisting of three subtypes (RXR α , RXR β and RXR γ). Each of the RAR binds both the ligands all-trans-retinoic acid (ATRA) and 9-cis-retinoic acid (9-cis-RA). The RXR preferentially bind 9-cis-RA (Fig. 1.8; Tanaka et al., 2004).

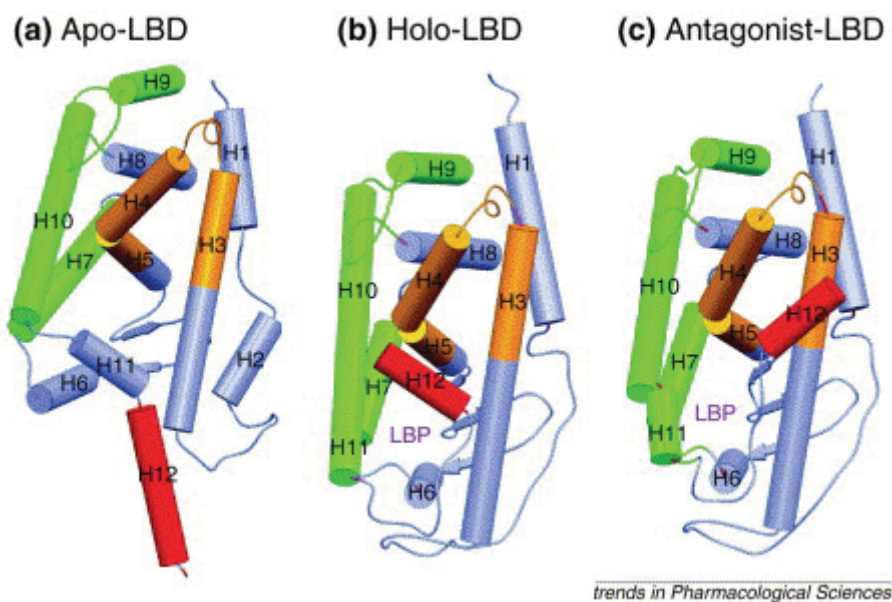


Fig. 1.8: Schematic drawing of three different conformational states of nuclear receptor ligand-binding domains (LBDs). (a) The unliganded (apo) retinoid X receptor (RXR) LBD. (b) The agonist-bound (holo) retinoic acid receptor (RAR) LBD. (c) The antagonist-bound RAR LBD. The α -helices (H1–H12) are depicted as rods whereas broad arrows represent the β -turn. The various regions of the LBD are coloured depending on their function: the dimerization surface is shown in

green, the co-activator and co-repressor binding site, which also encompasses the nuclear receptor LBD signature motif is shown in orange and the activation helix H12 that harbours the residues of the core activation function 2 (AF-2) activation domain (AD) is shown in red; other structural elements are shown in mauve. Abbreviation: LBP, ligand-binding pocket (Adapted from Bourguet et al., 2000).

The retinoid X receptor (RXR) is a ligand-inducible transcription factor that belongs to a group of nuclear receptors including receptors for small hydrophobic hormones such as steroids, retinoic acid, vitamin D, thyroid hormone and metabolites of long-chain fatty acids that associate with specific DNA response elements (REs) in the promoter region of target genes and act either to activate or to repress transcription (Mangelsdorf et al., 1995; Long et al., 2015). The REs are usually comprised of two repeats of the hexameric sequence PuG(G/T)TCA arranged in direct, inverted, or everted repeats. The repeats are usually variable in the number of base pairs between the two half-sites (Mangelsdorf et al., 1995; Castelein et al., 1997; Li et al., 2002). As suggested by the repeat structure of their response elements, most nuclear receptors bind to cognate DNA as dimers. RXR, which is activated by the 9-cis isomer of retinoic acid, can bind to cognate DNA with a high affinity and regulate transcription as a homodimer (DeLuca et al., 1995; Li et al., 2002). In contrast, tight binding of some other receptors, e.g., RAR, VDR, TR, and the PPAR to cognate DNA usually requires that they heterodimerize with RXR, and their transcriptional activities seem to be exerted mainly via these heterodimers. RXR thus plays a central role in regulating a number of signaling pathways (Li et al., 2002).

The molecular mechanisms by which hydrophobic hormones regulate the transcriptional activities of their respective receptors are not completely understood as yet, but available information suggests that ligand binding serves to modulate protein-protein interactions of nuclear receptors with multiple targets (Fig, 1.9). For example, binding of ligands to several receptors including RAR, TR and RXR, allows them to interact with coactivator proteins that, presumably link them with the general transcription machinery. Ligand binding by RAR and TR also induces the release of a corepressor that associates with these receptors in the absence of ligands. The corepressor interacts with RXR only weakly and in a ligand-independent fashion, suggesting that the activity of this receptor might be regulated by a different mechanism (Fig, 1.9; Bouillon et al., 2008; Norman, 2008; Haussler et al., 2011).

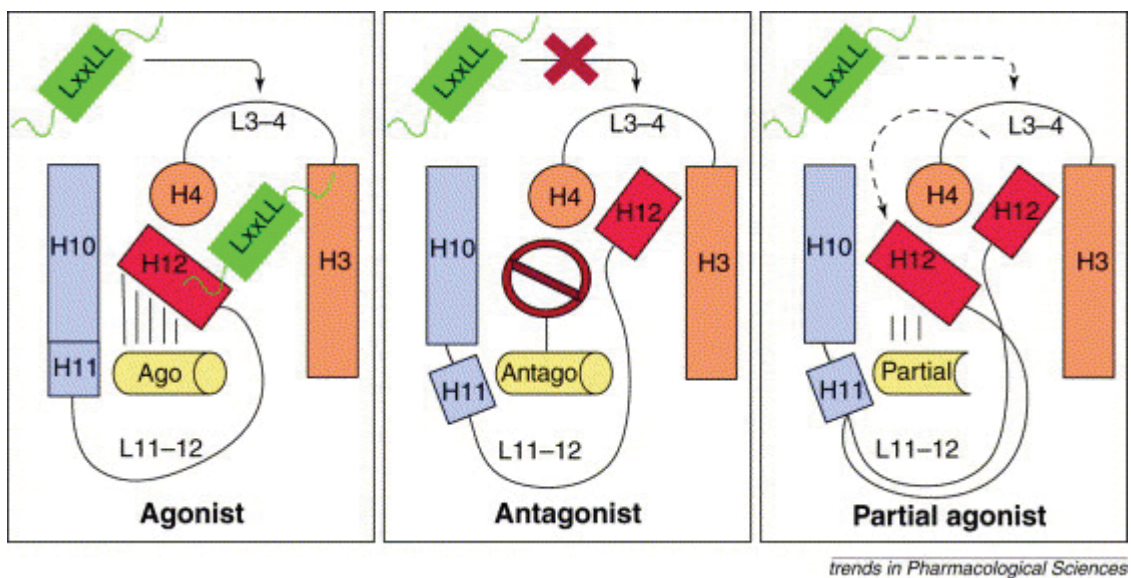


Fig.1.9. Structural view on how the binding of various ligands can induce different nuclear receptor conformations, thereby modulating their transcriptional activity.

Agonist ligands (left) induce a conformation of nuclear receptor ligand-binding domains (LBDs) in which the holo-position of helix H12 is firmly stabilized (note that the black lines between the ligand and H12 indicate that the overall holo-LBD conformation is strongly stabilized by the ligand, which does not necessarily have to directly interact with H12). This active conformation provides a surface to which co-activators can bind via their nuclear receptor boxes that contain LxxLL motifs. By contrast, antagonists with bulky substitutions (centre panel) prevent the proper positioning of H12 in its agonistic site and therefore destabilize the interaction surface. The antagonist-induced unwinding of the C-terminal part of helix H11 allows helix H12 to bind to the static part of the co-activator binding site. In the presence of partial AF-2 agonists–antagonists (right), the holo-form is poorly stabilized (black lines). However, the agonist position of H12 is not precluded by a steric hindrance of the ligand and the active conformation might, at least transiently, be adopted. Consequently, the biological activity of such ligands might be highly dependent on the cellular concentration of co-activators and co-repressors. Abbreviations: Ago, agonist; Ant, antagonist (Adapted from Bourguet et al., 2000).

1.11 Nuclear Receptor Phosphorylation (NR)

Nuclear receptors are mostly phosphoproteins that orchestrate the transcription of specific gene networks in response to binding of their cognate ligands.

Prophorylation has been implicated in an array of activities namely, DNA binding, transcriptional activation interaction with other proteins and stability of the NR. NR-phosphorylated residues lie mainly within the N-terminal A/B region.

The phosphorylation site or residues ranges from one or two sites as in RARs or PPARs to at least thirteen sites in PR. VDR is an exception, as this region is not phosphorylated, probably due to its very short length (Rochette-Egly, 2003). The sites located in the N-terminal A/B region of NRs mostly contain serine residues that are surrounded by prolines and therefore correspond to consensus sites for proline-dependent kinases, which include cyclin-dependent kinases (CDKs) (Morgan, 1994, 1997) and MAP kinase (Chang and Karin, 2001). Phosphorylation can either act to enhance, inhibit or terminate the activity of the receptor through the induction of DNA dissociation or nuclear receptor degradation or through decreasing the ligand affinity (Rochette-Egly, 2003).

1.11.1 VDR Phosphorylation

The VDR is a phosphoprotein which becomes phosphorylated after $1,25(\text{OH})_2\text{D}_3$ administration. Pike and Slator (1986) demonstrated that VDR present in mouse 3T6 cells is hyperphosphorylated in response to physiologic concentrations of $1,25(\text{OH})_2\text{D}_3$. Brown et al., (1991) showed that phosphorylation is an early event in the mechanism of $1,25(\text{OH})_2\text{D}_3$ action. The rapid onset of this response to $1,25(\text{OH})_2\text{D}_3$ may play an initiating event in the transcriptional process mediated by VDR. Studies with ROS/2.8 cells revealed that the main phosphorylation domain of hVDR resided between methionine (Met197) and valine (Val234) (Jones et al., 1991). Within this domain is a cluster of serine (S) residues many of which resemble consensus sites for casein kinase II. Jurutka et al., (1993) used site directed mutagenesis to define serine (Ser208) as the site on VDR phosphorylated by casein kinase II in vitro and in vivo. While phosphorylation of VDR by casein

kinase II enhances transactivation, alteration of Ser208 to alanine (Ala208) or Gly208 has no effect on VDR transactivation (Jurutka et al., 1996).

Hsieh et al., (1993) further showed that a second major phosphorylated site on VDR was Ser51 which resides between the two zinc fingers binding modules in the DBD of VDR. It is a consensus site for protein kinase C (PKC) and is selectively phosphorylated by PKC β isoform *in vitro* and *in vivo*. However, phosphorylation at Ser51 interferes with VDR binding to DNA thus suggesting a negative feedback loop of VDR-activated transcription mediated by PKC phosphorylation of Ser51 (Hsieh et al., 1991, 1993). Mutation of Ser51 to Asp51, a residue that mimics a phosphorylated serine produces a receptor that cannot bind VDR to DNA or be phosphorylated by purified PKC. There are currently four known sites of serine phosphorylation on the human VDR.

(<http://www.phosphosite.org/proteinAction.action?id=5051&showAllSites=true>).

These include Ser51 (Hsieh et al., 1991; 1993; Barletta et al., 2004), Ser172 (Nakajima et al., 2000), Ser182 (Hsieh et al., 2004) and Ser208 (Jurutka et al., 1996; Arriagada et al., 2007). Only Ser208 is a substrate for casein kinase II. Serine 51 is a substrate for protein kinase C and Ser172 and Ser182 are both substrates for protein kinase A (Jurutka et al., 1996; Nakajima et al., 2000). Thus phosphorylation of VDR may alter its interaction with nuclear receptor comodulatory proteins that play a critical role in the transcriptional response (Rochette-Egly, 2003).

1.11.2 RXR Phosphorylation

A total of eight phosphorylated sites have been identified on RXR. These include AF-1 domain at residues S360 by PKA, S22 by Cdk/cyclin, S161, S75 and S87 by JNKs. At the AF-2 domain RXR is phosphorylated at residue S265 by JNKs and Y248 and Y397 by MKK4 (Rochette-Egly, 2003). It has recently been shown that phosphorylation negatively modulates the activity of nonsteroidal NRs such as RXR and their heterodimerization partner. MAPK-mediated hyperphosphorylation of the RXR α LBD impairs the transcriptional activity of RAR/RXR and VDR/RXR heterodimers (Taneja et al., 1997; Lee et al., 2000; Matsushima-Nishiwaki et al., 2007).

According to three-dimensional structural studies of nuclear receptors (NRs), it has been proposed that phosphorylation of the serine residue located in the omega loop between helices H1 and H3 and close to helix 12 would create conformational changes within the LBD, disrupting the interactions with coregulators (Bourguet et al., 2003). Furthermore, phosphorylated RXR α would also be more resistant to proteolytic degradation, resulting in the accumulation of the inactive receptor. This would create a dominant negative and the inhibition of the target genes (Figs. 1.8 and 1.9, Adachi et al., 2002).

Our laboratory previously reported that the human RXR α is phosphorylated by MAPK at serine 260 similar to serine 265 in mouse (Solomon et al., 1999, 2000). The effects of this phosphorylation on 1,25(OH) $_2$ D $_3$ and VDR signaling on VDR/RXR interaction and kinetics will be the focus of this study.

1.11.3 MAPK- Dependent Phosphorylation

1.11.4 *Glucocorticoid Receptor (GR)*

Mason and Housley (1993) identified seven phosphorylation sites on GR. Phosphorylation of GR at Ser246 by MAP kinase was reported to inhibit ligand-dependent transactivation. However, GR phosphorylation at Ser224 and Ser230 by cyclin –dependent kinase was found to enhance the ligand –dependent transactivation suggesting that the activity of GR is differentially altered in response to various signaling pathways (Krstic et al., 1997).

1.11.5 *Progesterone Receptor (PR)*

The chicken PR is phosphorylated at nine different sites on PR. Five of these sites are phosphorylated in basal conditions but enhanced in the presence of progesterone. The other four are only phosphorylated when the hormone is present (Weigel et al., 1995; Beck et al., 1996). The human PR has three human PR isoforms (hPRA, hPRB and hPRC) transcribed from the same gene, containing distal and proximal promoters. In general, PRs act as heavily phosphorylated transcription factor for mitogenic protein kinases that are often elevated and/or constitutively activated in invasive breast cancers (Hagan et al., 2011, 2012). MAPK activation can lead to phosphorylation of PR, transcriptional coactivators, and/or activation of downstream MAPK target genes (i.e. Cyclin D1). MAPK signaling modulates PR activity directly by phosphorylating the receptor on consensus site of serine residues Ser294 and Ser345 (Faivre et al., 2008; Lange et al., 2000). These distinctly regulated phosphorylation events have unique functional consequences for PR that ultimately regulate cell fate (Hagan et al., 2011).

1.11.6 *Estrogen Receptor (ER)*

ER contains two isoforms ER α and ER β , which can undergo multiple post-translational modifications including, phosphorylation, acetylation, ubiquitylation, and sumoylation (Weigel and Zhang, 1998; Ward and Weigel, 2009). Numerous phosphorylation sites on multiple amino acid residues have been located throughout the whole ER α protein and within all major structural domains: These include, the N-terminal A/B domain, i.e. serine 46 (S46), serine 47 (S47), tyrosine 52 (Y52), serine 102 (S102), serine 104 (S104), serine 106 (S106), serine 118 (S118), serine 154 (S154) and serine 167 (S167); the DNA-binding or C domain, tyrosine 219 (Y219), serine 236 (S236) (Chen et al., 1999, 2013), the hinge or D domain, serine 305 (S305) (Michalides et al., 2004), and the ligand-binding domain or E domain, threonine 311 (T311) (Lee and Bai, 2002) and tyrosine 537 (Y537) (Arnold et al., 1995*b*). At the N-terminal AF-1 region, serine residues S102, S104 and S106 at the N-terminal AF-1 region are phosphorylated by extracellular signal-regulated kinases 1 and 2 (ERK1/2) and mitogen-activated protein kinase (MAPK) (=MEK1/2) pathways and by glycogen synthase kinase-3 (GSK-3). These modifications result in ligand-independent transcription by ER α and to an agonistic activity of tamoxifen. Serine 118 (S118) is a notable phosphorylation site on ER α that is targeted by a number of kinase pathways including MAPK, GSK-3, IKK α , CDK7, and mTOR/p70S6K. S118 phosphorylation by MAPK increases binding of coactivator SRC3 and renders ER α hypersensitive to estradiol (Likhite et al., 2006). Phosphorylated S118 decreases ER α affinity for tamoxifen and reduces binding to DNA when ER α is tamoxifen bound (Likhite et al., 2006). Vendrell et al., (2005) reported that tamoxifen-resistant cell lines exposed to prolonged tamoxifen exposure were found

to have elevated MAPK activity and increased S118-phosphorylation. Also, the Ras/MAPK pathway can be activated upstream by IGF. This results in the phosphorylation of ER α S118 leading to ER α activation and enhanced response to estradiol. Estrogen-dependent phosphorylation of S118-P can occur not only through the ERK1/2 MAPK pathway, but also by IKK α and CDK7.

1.12 Interaction between Retinoids and Vitamin D Signaling Pathways

Retinoids and vitamin D differ in the specificity of the respective receptors for the response elements. The actions of both retinoids and VDRs have been identified to be mediated by two signaling pathways including RXR-dependent and RXR-independent mechanisms (Schrader et al., 1993). To define the sequences necessary and sufficient for 1,25(OH) $_2$ D $_3$ response, Schrader and co workers (1993) used mutagenesis to convert the retinoid specific response element of the human RAR β promoter into the 1,25(OH) $_2$ D $_3$ /RARE of the human osteocalcin promoter. They found that VDR homodimers only bind to the motif RGGTGA. The extended osteocalcin element also contains an imperfect direct repeat based on the motif RGGTGA spaced by three nucleotides, which is bound by RXR homodimers and activated by 9-cis-RA. Furthermore, the group reported that responsiveness of the osteocalcin element to ATRA was mediated neither by RAR homodimers nor by RAR-RXR heterodimers. In addition, VDR-RAR heterodimer bound to the osteocalcin response element and mediated activation by ATRA. Also, the VDR-RXR heterodimer bound to pure RAREs but it does not mediate activation by vitamin D alone. In combination with ATRA, however, 1,25(OH) $_2$ D $_3$ was reported to enhance VDR-RAR heterodimer-mediated gene expression. Their finding suggests a direct interaction between nuclear signaling by retinoic acid and

1,25(OH)₂D₃ increasing the combinatorial possibilities for gene regulation by the nuclear receptors involved (Schrader et al., 1993)

RXR functions both as a homodimer and also heterodimerizes with multiple members of the nuclear receptor superfamily. Thus permissive heterodimers of RXR (RXR/PPAR, RXR/LXR, RXR/NGF1-B) allow RXR signaling whereas non-permissive heterodimers of RXR (RXR/RAR, RXR/TR) inhibit RXR signaling (Perez et al., 2012). Studies combining 9-cis-RA and 1,25(OH)₂D₃ have shown that the effects can be antagonistic, additive or synergistic. MacDonald and co-workers (1993) showed that 9-cis-RA not only inhibited DNA binding of the VDR/RXR heterodimer but also transcription from a vitamin D response element containing a reporter construct. Haussler et al., (1997) suggested that in the rat osteocalcin system, the mechanism of 9-cis-RA antagonism involved the diversion of RXR favoring the formation of retinoid-occupied RXR homodimers. However, it has been demonstrated in human pancreatic cells and colon carcinoma cells that 9-cis-RA enhances the growth inhibitory action of 1,25(OH)₂D₃ (Kane et al., 1996; Zugmaier et al., 1996). Furthermore, the combination of these ligands was demonstrated to synergistically enhance accumulation of 24-hydroxylase mRNA in human skin (Kang et al., 1997), as well as the growth inhibition of LNCaP prostate cancer cells (Blutt et al., 1997). The mechanism of 9-cis-RA action on 1,25(OH)₂D₃ -stimulated transcription has been postulated to first involve an interaction between 1,25(OH)₂D₃ ligand and the VDR in the nucleus of target cells. Such an interaction will promote heterodimer formation with RXR and subsequent binding to DNA. According to this model, occupation of the heterodimer by 1,25(OH)₂D₃ renders the RXR incapable of interacting with 9-cis-RA resulting in the silencing of the retinoid signal transduction. A second postulate is that 9-cis-

RA is capable of inducing the dissociation of RXR from the VDR/RXR heterodimer funneling the RXR into the formation of homodimers. This process is made possible because RXR is in a 9-cis-RA-receptive state regardless of its dimerization status (Hausler et al., 1997). In the unliganded TR, it was shown that 9-cis-RA inhibits TR signal transduction (Lehmann et al., 1993). Similarly, Forman and co-workers (1995) reported that in the presence of thyroid hormone, 9-cis-RA does not bind to the RXR partner.

1.13 Carcinogenesis

Carcinogenesis is the process where a normal healthy cell progresses to a quasi-normal, hyperplastic variant and finally to a neoplastic, invasive cancer (Leigh et al., 1990). It is a complex process involving the interplay between genetics, environmental exposure and other factors combined to create conditions more or less favorable for the development and dissemination of cancer. For cancer cells to develop and thrive, they must acquire a variety of specific capabilities: growing inappropriately, avoiding elimination by defense mechanisms, stimulating their microenvironment, providing needed support and spreading to new locations within the body. The processes that regulate these acquired abilities include gene expression as controlled by chromatin structure, signal transduction events in response to cell-cell interactions, hormone exposure and fatty acid metabolism and DNA damage and repair responses (Leigh et al., 1990; Popp et al., 2000).

1.13.1 Keratinocyte Carcinogenesis

The process of carcinogenesis occurs frequently in the skin and in North America, one-third of all cancers are attributed to non-melanoma skin cancers (Leigh et al.,

1990). The most reported skin cancers are basal cell carcinomas followed by squamous cell carcinomas. Non-melanoma skin cancers are said to be caused by factors including exposure to ultraviolet light (sunburns), chemical carcinogens, long outdoor/ wind exposure, cigarette smoke and human papilloma virus (HPV) infections (Leigh et al., 1990). In the classical mouse skin cancer model, application of a chemical carcinogen to the skin initiates the formation of benign growths (papillomas) (Sexton et al., 1993). This initiating event is often followed by the induction of an activating point mutation in the mouse cellular Harvey-ras proto-oncogene (Brown et al., 1993b; Sexton et al., 1993). Most of the human squamous cell carcinoma samples analyzed have shown a high proportion of ras mutation and growth suppression of p53 (Daya-Grosjean et al., 1995).

1.13.2 The Ras Oncogene and Carcinogenesis

The *ras* family genes are among the most well studied and frequently detected genes participating in oncogenesis of human tumors. In the mammalian genome, three *ras* proto-oncogenes have been identified: these include H-*ras*, K-*ras* and N-*ras* (Barbacid, 1987; Cox et al., 2014). All of them encode similar GTP-binding proteins of the same molecular weight (21KDa), termed p21 proteins. These cellular components are associated with the inner face of the plasma membrane, thus playing a major role in the transduction of exogenous signals that are essential for the regulation of vital cell functions (Lowy et al., 1991). The interchange of the p21 proteins between “on” (GTP-bound) and “off” (GDP-bound) position allows them to operate as switches in the cytoplasmic relay of external growth and differentiation signals (Hwang and Cohen, 1997). Interaction of p21 with the raf oncoprotein results in activation of a cascade of serine/threonine kinases. The

intensity and duration of this event strongly contributes to the regulation of cell differentiation and division (Avruch et al., 1994). Mutated *ras* genes were first recognized for their transforming ability when transfected into NIH/3T3 cells which acquired anchorage independent growth (Stacey et al., 1984). Transgenic mice expressing activated *ras* oncogenes driven by keratinocyte keratin (K10) specific promoters have been shown to be highly susceptible to developing squamous cell carcinomas (Bailleul et al., 1990). Single point mutations were discovered in codons 12, 13, 59 and 61 of the *ras* gene which activated and increased the transforming potential of *ras* (Barbacid, 1987). These activating mutations are resistant to GTPase-activating protein mediated GTPase action and are therefore locked in the active GTP-bound state (Trahey et al., 1987). Durst and co-workers (1989) reported the induction of immortalized cultured keratinocytes to express a more malignant phenotype after transfection with an activated *ras* oncogene. The doubling time of these cells were shorter than their non-*ras* transfected controls. Recently, it has been shown that *ras* and its downstream effectors are modulators of key players of cell cycle progression (Adjei, 2001; Cox et al., 2014).

The incidence of *ras* mutations in carcinomas of the lung (30 %), myeloid leukemia (30 %), colon (50 %) and thyroid tumours (50 %) are high (Bos, 1989). However, pancreatic adenocarcinomas contain a mutated *K-ras* gene in 90 % of tumors accounting for the highest incidence of *ras* mutations among the various human tumours (Cox et al., 2014). In some human tumours such as in the breast, a mutant *ras* gene is identified only occasionally (5%). In addition to point mutations, *ras* genes can also acquire transforming properties through quantitative

mechanisms. Expression of abnormally high levels of *ras* via gene amplification or problems with its regulatory sequences contributes to malignancy (Cox et al., 2014).

1.13.3 The Ras Signaling Pathway

The ras protein is involved in an interrelated complex of signaling proteins including, raf, rac, rho and PI3K (Repaksky et al., 2004). The Ras/Raf/mitogen-activated protein kinase kinase (MEK)/extracellular signal-regulated kinase (ERK) cascade regulates proliferation, differentiation, survival, motility, and tissue formation (Cox et al., 2014). Ras is a GTP/GDP binding protein; it has intrinsic GTPase activity and is involved in multiple signal transduction pathways (Adjei, 2001; figure 1.10).

The mitogen activated protein (MAP) kinases and their subordinates are recruited by direct interaction of the Ras p21 protein with the Raf oncoprotein. The mitogenic signals thus initiated by the membrane receptors with tyrosine kinase activity are then converted by p21 into a cascade of serine/threonine kinases. The signal that results in cell division or differentiation however, depends on the intensity, duration and the intracellular conditions. (Avruch et al, 1994).

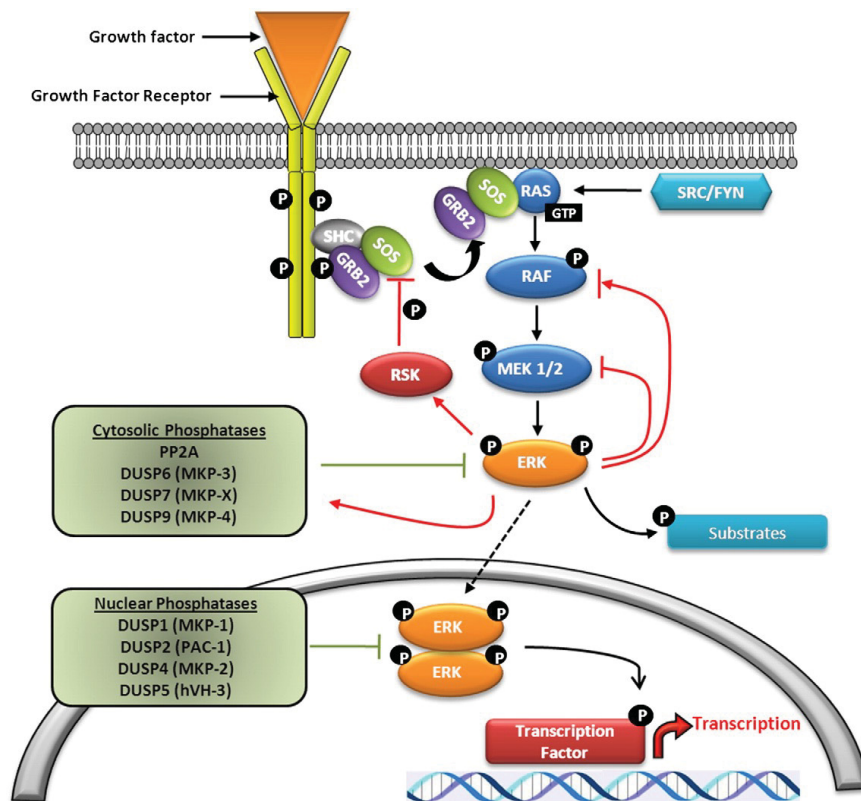


Figure. 1.10: Intracellular signaling through the ERK1/2 MAPKinase pathway (example of a growth factor receptor). The SHC/GRB2/SOS complex is recruited by the phosphorylated tyrosines of the intracellular domain of the receptor. Then SOS activates RAS and RAS/GTP recruits RAF which initiates the MAPKinase cascade leading to the phosphorylation of ERK1/2 by MEK1/2. Several inhibitory pathways are activated which are indicated in red lines. DUSP: dual specificity protein phosphatase; GRB2: growth factor receptor-bound protein 2; MKP: MAPK phosphatase; SHC: SRC homology 2 domain containing transforming protein 1; SOS: son of sevenless (Adapted from Zassadoski et al., 2012).

Ras mutation activating MEKs and ERKs occurs in a relatively large number of human tumors (Cox et al., 2014). Raf or Ras mutations predict sensitivity to MEK

inhibitors and the pharmacologic MEK inhibition counteracts growth of Raf or Ras mutant xenografts and are currently being investigated as anticancer drugs in combined therapies (Cox et al., 2014). The ras gene family is frequently implicated in human tumors by four different mechanisms: mutation of ras proto-oncogenes (Bos, 1989), gene amplification, insertion of retroviral sequences and alterations in regulation of transcription. With the exception of mutations, all other mechanisms result in activating the transforming properties of ras genes by quantitative mechanisms. Overexpression of the mutant T24 H-ras oncogene may cause oncogenic transformation of early passage rodent cells and in the presence of strong enhancer sequences, elevated expression of even the normal protooncogene can rescue the cells from senescence. In addition, H-ras overexpression correlates with metastatic potential of cells in tissue culture (Zachos and Spandios, 1997; Cox et al., 2014) and increased levels of p21 have been detected in a variety of human cancers (Zachos and Spandios, 1997).

Ras has also been reported to associate with and constitutively activate the phosphatidylinositol 3-kinase PI3K-AKT pathway. Specifically, GTP-bound ras can activate the catalytic subunit of the PI3K enzyme by binding to it. The PI3K contains SH2 and SH3 domains that are normally recognized by growth factor receptors. Activation of PI3K leads to phosphorylation of inositol diphosphate into the second messenger inositol triphosphate (IP3). IP3 can directly activate protein kinase C which is a key player in mitogenic signaling (Cox et al., 2014). The interchange of the ras proteins between GTP-bound (on) and GDP-bound (off) position allows them to operate as switches in the cytoplasmic relay of external growth and differentiation signals (Hwang and Cohen, 1997). Thus termination of

ras signals involves hydrolysis of the bound GTP to GDP but this reaction is catalyzed slowly by ras. Interestingly, this reaction can be accelerated by association of ras with a GTPase –activating protein (P120GAP) (Bollag et al., 1992)

1.13.4 Therapeutic Approaches to Interrupting Ras Signaling.

Due to the high percentage of human tumors harboring oncogenic ras mutations, interrupting the ras-signaling pathway has been a major focus of new-drug-development efforts (Barbacid, 1987; Cox et al., 2014). The concern however, is that the deregulation of any component of the ras pathway that renders it constitutively active may also induce malignant transformation. Thus, in tumors that possess a mutated ras protein, the approach is to directly block the activity of ras itself. This can be accomplished through the prevention of ras association with the plasma membrane, which is critical for its transforming ability (Gibbs et al., 1991). The major approaches taken are as follows: (1) the inhibition of ras protein expression through the use of small interfering RNAs (RNA silencing) or oligonucleotides and ribozymes (2) the prevention of membrane localization of ras and (3) the inhibition of downstream effectors of ras function (Adjie 2001; Cox et al., 2014; Fig. 1.11).

Antisense therapeutics have been used in the development of novel anticancer therapy. Antisense agents are valuable because they can inhibit the expression of a target gene in a sequence-specific manner. Three types of antisense strategies can be distinguished. These include (1) RNA interference induced by small interfering RNA molecules; (2) ribozymes, that trigger RNA cleavage through catalytically

active oligonucleotides and (3) the use of single stranded antisense oligonucleotides (Tolcher, 2005; Kim et al., 2007).

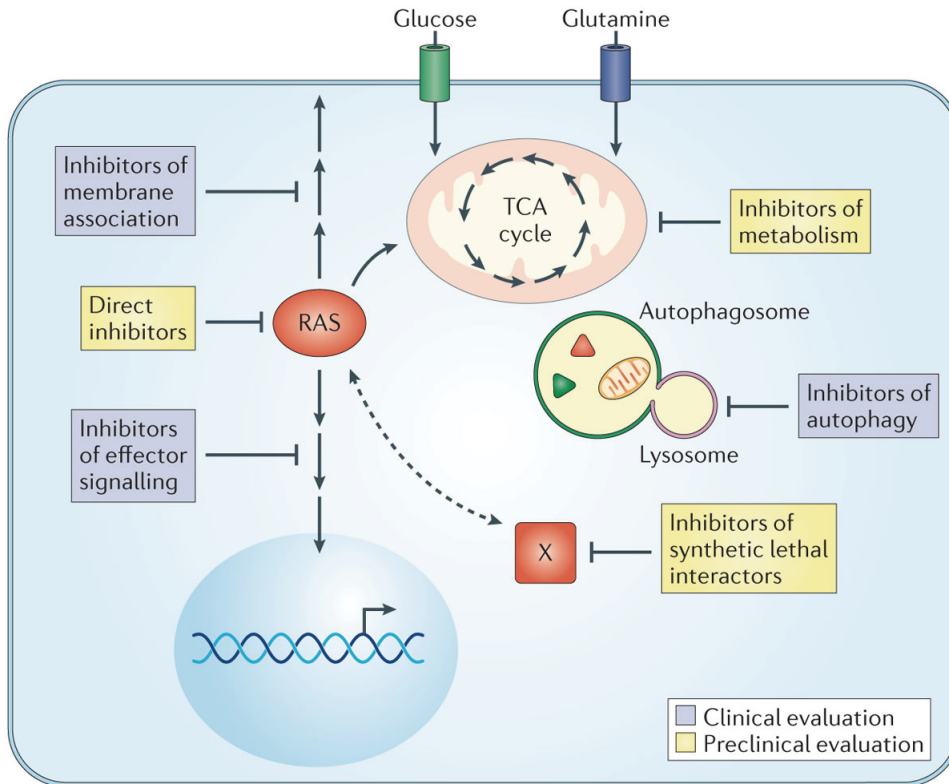


Figure 1.11: Past and ongoing approaches to develop inhibitors of mutationally activated RAS include RAS-binding small molecules that disrupt key functions of RAS, inhibition of the CAAX motif-targeted enzymes that promote RAS membrane association, inhibitors of effector signalling function, unbiased RNA interference, genetic or chemical screens for synthetic lethal interactors and inhibitors of RAS-mediated changes in metabolism. Inhibiting autophagy could leave RAS-transformed cells with insufficient macromolecules to sustain growth. TCA, tricarboxylic acid (Adapted from Cox et al., 2014).

RNA interference (RNAi) provides an alternative therapeutic approach to small molecule and antibody-based therapeutics for inhibiting ras protein expression and function. In principle, the method can be applied to reversibly silence any target gene. This increases the druggable landscape from 10% to virtually 100% of the genome. Several different types of RNAi are currently being used to inhibit expression of the target gene. These include: short-interfering RNA (siRNA), short-hairpin RNA (shRNA) and micro RNA (miRNA). The siRNA and shRNA are generally 20–22 nt in length, but they can be up to 30nt. These were designed to overcome issues with immune system stimulation and complete translation arrest observed when longer RNA sequences were used for RNAi, and to optimize the silencing effects (Elbashir et al., 2001). Guillermet-Guibert and co-workers (2009) used sphingosine kinase-1-targeted siRNA to increase gemcitabine sensitivity in pancreatic cancer cells. Li and co-workers (2009) similarly showed that ShRNA silencing of zinc transporter ZIP4 could inhibit tumor growth and extend the survival of nude mice with pancreatic cancer xenografts. Another interesting strategy to deliver suicide genes to tumor cells which encode for drug-activating enzymes and re-expressing tumor suppressor genes. Several siRNA molecules have already been evaluated in human clinical trials. These include a siRNA targeting IL-10 for treatment of preeclampsia, VEGF and VEGFR-1 for macular degeneration, and BCR-ABL for CML (de Fougerolles et al., 2007; www.clinicaltrials.gov).

Gene therapy is another alternative therapeutic approach using different mechanism. Here, the approach involves strategies to increase the expression of the normal (wildtype) gene products (Sadelain et al., 2003; Robbins et al., 2004;

palmer et al., 2008). The most common strategies utilize viral vectors including adenoviruses, adeno-associated viruses, retroviruses or pox viruses contained in nanoparticles to deliver the gene of interest (Markt et al., 2003; Brentjens et al., 2007; Palmer et al., 2008). In theory, gene therapy can be used for any gene with a known sequence. The approach is especially attractive for genetic disorders such as cystic fibrosis, severe combined immunodeficiency (SCID) and muscular dystrophy (Robbins et al., 2004; Palmer et al., 2008). This is because the disorders are well characterized, the mutations responsible for most cases of the disease are known, and there are no existing effective treatments. In the cancer field, the clinical potential of gene therapy has also been examined extensively as a treatment modality for the effective and safe approach to selectively target Ras-mutated tumor cells. Lisiansky and co-workers (2012) used this approach to selectively eliminate Ras-transformed cells by overexpressing the pro-apoptotic protein, p53 upregulated modulator of apoptosis (PUMA) under the control of a Ras-responsive promoter in a K-Ras transformed R1 rat enterocyte cell line harboring K-Ras mutations. They constructed adenoviral vectors containing the PUMA gene downstream of the ras responsive elements (Ad-PY4-PUMA). Infection of the cells with the adenoviral vector markedly inhibited cell growth by 40-50 %. While apoptosis was activated in all cells with high Ras activity, normal rat enterocytes remained unaffected. A follow-up *in vivo* study was conducted in athymic mice and results showed that infection with Ad-PY4-PUMA inhibited the growth of established tumors by 35 % compared with (Ad-SV40-PUMA control vector). Hence, selective overexpression of PUMA efficiently inhibited the growth of Ras-transformed cells while sparing the normal ones.

Johnson et al., (2009) carried out a phase II gene therapy clinical trial on thirty-six patients with metastatic melanoma using genetically engineered lymphocytes. The genes encoding the T-cell receptors (TCRs- which are highly reactive to melanoma/melanocyte antigens) were engineered into retroviral vectors and used to transduce autologous peripheral lymphocytes administered to the 36 patients with metastatic melanoma. Results show that the cells of the engineered gene persisted at high levels in the blood of all the patients 30 days following treatment. Furthermore, the blood of all the patients that responded showed higher *ex vivo* antitumor reactivity compared to non-responders. Lastly, all the patients who received either the human or mouse TCR showed regression of their cancers by 30% and 19% respectively. While the use of T cells expressing highly reactive TCRs were able to mediate cancer regression in the patients and target rare cognate–antigen-containing cells throughout the body, one needs carefully examine toxicities that might result from the expression of tumor-associated antigens on normal tissues. In the above clinical trial, patients also exhibited destruction of normal melanocytes in the skin, eye, and ear. In some cases, local steroid administration was required to treat inflammations of the eye and the hearing loss.

Ribozymes are another therapeutic approach used to target ras signaling. They are ribonucleic acid (RNA) enzymes found in the ribosomes where they join amino acids together to form protein chains. Ribozymes catalyzes specific reactions in a similar way to that of protein enzymes. Though the naturally occurring ribozymes are self-splicing, they also play a role in other vital reactions such as RNA splicing, transfer RNA biosynthesis, and viral replication. As such, modifications of

ribozymes have yielded catalytic oligonucleotides that can cleave a targeted RNA sequence or revise the mRNA to generate correct sequences that can be translated into normal proteins. Hence ribozymes can be targeted to a variety of molecules, and have been developed as experimental therapeutics for cancer and other human diseases (Sullenger and Cech, 1994; Grassi et al., 2004; Bartolome et al., 2004). A phase II clinical trial for the treatment of cancer patients with a ribozyme (Angiozyme) was recently underway in the USA. The study involved examining the effectiveness of RPI.4610 in treating 40 patients with metastatic kidney cancer (www.clinicaltrials.gov- NCT00021021) but its results have not yet been published and the FDA has not approved ribozymes treatments at the time of our writing.

In the antisense approach specific RNA sequences are targeted to block the translation of the RNA message into protein. Synthetic oligonucleotides are developed and these bind to RNAs encoding proteins, thereby preventing RNA translation. Thus the antisense oligonucleotides (AONs) exert their inhibitory effects on mRNA function, which in turn inhibits the synthesis of the particular protein. Designing an AON compound to specifically inhibit a member of a multigene family is relatively easy due to the degeneracy of the genetic code. Hence AONs can inhibit gene expression by targeting virtually any region within the RNA transcript (Adams and Cory, 2002; Klasa et al., 2002; Redell and Tweardy, 2005; Tolcher, 2005; Kim et al., 2007; Leonetti and Zupi, 2007).

Antisense oligonucleotides directed against the activated ras oncogene have been in development. These oligonucleotides hybridize to complementary mRNA

sequences and decrease ras protein expression through multiple mechanisms, including RNase H-mediated cleavage of hybridized ras mRNA. K-ras antisense approaches have utilized large constructs incorporated into plasmids or viral vectors (Adjie, 2001). Giannini et al., (1999) used this method to generate K-ras antisense RNA that reduced K-ras protein levels and also inhibited the growth of the H460A non-small cell lung cancer (NSCLC) cell line in culture. When the K-ras viral construct was administered intratracheally to nude mice bearing implanted human lung cancers, 87% of treated mice were reported to be tumor free compared with 10 % of control mice. The antisense oligonucleotide ISIS-2503 was previously used in clinical trials to inhibit the translation of H-ras mRNA in the treatment of NSCLC, breast and colorectal cancers. It has also been used in combination with gemcitabine against locally advanced and metastatic pancreatic adenocarcinoma (Geary et al., 1997; Alberts et al., 2004).

Major challenges regarding the use of antisense oligonucleotides include efficacy, off-target effects, delivery and side effects. Early Phase I clinical trials with most antisense oligonucleotides were focused solely on their toxicity following demonstration of therapeutic activity in animal models. These trials did not evaluate the expression of the target gene in patients. Phase II/III clinical trials have thus failed due to a lack of observed efficacy (Kelland, 2005). Consequently, monitoring the expression of the target gene during Phase I trials would provide critical information on whether the oligonucleotide is reaching the target tissue in human patients and ultimately causing the desired inhibitory effect (Kelland, 2005).

One of the first and widely used modifications introduced in therapeutic antisense oligonucleotides is phosphorothioate (PS) modification. The advantage of this modification in clinical settings is to improve the oligonucleotide therapeutic potential by increasing resistance to degradation and extending circulation times after systemic administration (Kibler-Herzog et al., 1991). Since the protein binding is not specific, it can potentially lead to associated toxicities or cellular effects that are not entirely sequence specific. These effects include complement activation, increased coagulation times and unwanted immune activation (Mou et al., 2001; Krieg et al., 2003; Senn et al., 2005). Another challenge is the efficiency and targeted delivery of nucleic acid (plasmid DNA, siRNA and AONs) therapeutics. Specific features influence the cellular uptake and delivery vector development. For example, AONs are usually single-stranded, have short chain size and very low charge density. The aromatic bases are usually not buried inside a double helix but exposed. This confers a slight hydrophobic character to the molecule. These factors enable some level of interaction with the cell membrane oligonucleotides. Therefore, they are internalized poorly by cells whether or not they are negatively charge and become inefficient (Stein et al., 1993; Watts and Corey, 2012). They tend to localize in endosomes/lysosomes, where they are unavailable for antisense purposes. Furthermore, numerous studies have shown that “naked” AONs *in vivo* have a wider tissue distribution. They tend to preferentially accumulate in the liver and kidney and to a lesser extent in spleen, lymph nodes and bone marrow (Graham et al., 1998; Geary, 2009; Straarup et al., 2010).

To enhance cellular uptake and oligonucleotide spatial and temporal activity, a range of techniques and carriers/transporters have been developed. The techniques improve interactions of different carrier formulations with the AONs or nanoconjugates. Cationic lipids and polymers are used as carrier formulations for delivery of different nucleic acids. The carrier systems thus (1) protect the nucleic-acid from extracellular and intracellular degradation, until it reaches its target, (2) achieve a prolonged circulation time in order to be accumulated in the location of interest, (3) efficiently interact with the cellular membrane to promote uptake (generally through endocytosis processes), (4) promote escape from endocytic vesicles and finally (5) dissociate from the active nucleic-acid to carry out its function (Juliano et al., 2012; Yin et al., 2014).

Farnesyl protein transferase and its inhibitors (FTIs) were previously developed to target Ras signaling (Adjie, 2001; Dinsmore and Bell., 2003). They are currently being used to inhibit Ras membrane localization (Kelland, 2003; Morgan et al., 2003; Antonio et al., 2011). In mammals, farnesyl transferases (FTpase) are prenylation zinc metalloenzymes that recognizes proteins with a COOH terminus CAAX motif and catalyzes the transfer of a 15-carbon farnesyl group from a farnesyl pyrophosphate to the C-terminal cysteine. FTase exists as an $\alpha\beta$ heterodimer in which the 48-KD α subunit is shared with another prenylation enzyme, the geranylgeranyltransferase I (GGT-1; GGTase-1), whereas the 45-KD β subunit (which contains the binding site) is responsible for substrate specificity. The CAAX motif plays an important role in the recognition of peptide substrates. Association of Ras at the membrane requires the addition of a 15- carbon farnesyl isoprenoid by the FTPase (Kohl et al., 1993). This modification occurs at the

consensus CAAX sequence (C = cysteine; A = an aliphatic amine acid; and X = any amino acid) contained at the C-terminus of all ras proteins. Results from kinetic assays and analysis of lipidated CAAX proteins derived from eukaryotic cells have shown that FTpase have a preference for methionine, serine, glutamine, or alanine while GGTase-I have a preference for leucine or phenylalanine in the X position (Lane and Beese, 2006). Ras mutants with mutation of the cysteine in the CAAX sequence cannot be farnesylated and are unable to associate with the plasma membrane or transform mammalian cells in culture (Willumsen et al., 1984). The farnesyl transferase inhibitors (FTIs) fall into three main classes: (1) the CAAX competitive inhibitors, such as L731735, L744832, Lornafarnib (SCH66336) and Tipifarnib (R115777) that compete with the CAAX portion of ras for farnesyl transferase; (2) the FPP competitive inhibitors, such as PD 169451 and RPR 130401 that compete with the substrate FPP for binding to farnesyl transferase; and 3) the bisubstrate inhibitors, such as BMS-186511 which are combinations of (1) and (2) (Liu et al., 1998; Norgaard et al., 1998).

The numerous chemically diverse FTIs developed have been tested in early clinical trials and inhibition of farnesyl transferase by these compounds in normal patient tissues and tumor cells has been documented (Adjei et al., 2000; Ryan et al., 2000; Caponigro et al., 2003; Dinsmore and Bell, 2003; Kelland, 2003; Morgan et al., 2003). FTIs showed impressive anti-H-Ras and anti proliferative activity in preclinical cell cultures, a large variety of cancer cell lines and leukemia. Also they appear to have anti-tumor activity in solid tumors and mouse models. In particular an H-Ras-driven mammary tumor model (James et al., 1993; Kohl et al., 1993; Dinsmore and Bell, 2003; Antonio et al., 2011). Also, their toxic effects appear to be manageable. Furthermore, drugs that inhibit the action of FTPase may also be

useful in inhibiting neoplastic transformation by mutations that affect upstream components of the pathway that mediate their effects through ras (Adjie, 2001). These impressive observations resulted in Phase I studies in 1999 followed by a progression to Phase III clinical trials in 2002 (Dinsmore and Bell, 2003; Kelland, 2003; Morgan et al., 2003; Antonio et al., 2011). Results showed that though FTIs effectively blocked H-Ras farnesylation and membrane association, and transformation they did not effectively block N-Ras and K-Ras protein prenylation, membrane association and transforming activity. This was due to the biochemical difference among the three Ras proteins (Antonio et al., 2011).

Other therapeutic intervention used in interrupting ras signaling include the interruption of signaling pathways downstream of ras by the use of raf kinase and MEK inhibitors. It is documented that c-raf kinase acts downstream of ras in the MAP kinase pathway. C-raf may also be activated by other mechanisms such as bcl-2 (wang et al., 1996). Dominant inhibitory mutants of raf have been reported to inhibit proliferation and reverse transformation in K-ras transformed NIH/3T3 cells (Kolch et al., 1991). A previously developed 20-mer-phosphothiorate antisense oligonucleotide inhibitor called ISIS 5132 was reported to inhibit c-raf kinase. In the initial proof-of-principle studies, its antiproliferative effects was demonstrated in cultured human cell lines with concomitant reduction in c-raf kinase mRNA (Monia et al., 1996). Phase II non-randomized clinical trial was previously conducted to study the efficacy of ISIS 5132 in 22 patients with recurrent epithelia ovarian cancer. In the study design, a dose of 4 mg/kg/day was administered by continuous venous infusion to each patient over a period of 21 to 28 days. Nineteen patients were evaluated for toxicity; sixteen for response and three patients were

ineligible. Results showed that the drug was well tolerated with no episodes of Grade 3 or 4 hematologic or biochemical toxicity. However, four of the patients treated showed six episodes of grade 3 non-hematologic toxicity including lethargy (2 patients); anorexia (1 patient); abdominal pain (2 patients) and shortness of breath (1 patient). Overall, the results did not show any beneficial effects of ISIS 5132 at 4 mg/kg/day when used as a single agent in recurrent ovarian cancer. Twelve of the patients had documented progression of the disease; sixteen showed no response and four of the patients had stable disease for a median of 3.8 months (Oza et al., 2003).

As previously described, the ras protein is involved in an interrelated complex of signaling proteins including raf, rac, rho and PI3K (Repaksky et al., 2004; Taber et al., 2009). The sequential activation of MAPK kinase (MAPKK or MEK1) and MAP kinase (ERK1/2) occurs downstream of ras. MAP kinase, in turn, phosphorylates downstream substrates involved in cellular responses, such as cytoskeletal changes and gene transcription, proliferation, differentiation, survival, motility, and tissue formation (Wellbrock et al., 2004; Murphy and Blenis, 2006). The activation of MAP kinase is also important in gene regulation promoting G1 cell cycle progression before DNA replication and spindle assembly during both meiotic and mitotic cell division. Inappropriate activation of the MAP kinase pathway through mutations introduced via oncogenes, is a feature of many neoplasms. Such single-point mutations of the ras gene can lead to its constitutive activation of ras protein. These mutated forms of ras have impaired GTPase activity. Although they still bind GTPase –activating protein (GAP) there is no “off” switch, since GTPase is no longer activated. This results in continuous

stimulation of cellular proliferation (Adjie, 2001). Molecules, such as MEK are therefore potential targets for cancer therapy. Sebolt-Leopold and co-workers (2008) have reported the discovery of PD184352, a highly potent and selective inhibitor of the upstream kinase MEK, which is orally active. This MEK inhibitor was reported to inhibit tumor growth by as much as 80% in mice implanted with col 26 and HT 29 colon carcinomas. Also, the efficacy was achieved with a wide range of doses with no signs of toxicity and correlated with a reduction in the levels of activated MAP kinase in excised tumors. The results presented indicate that MEK inhibitors represent a promising, non-cytotoxic approach to the interruption of the ras/MAP kinase pathway for cancer therapy (Sebolt-Leopold et al., 2008).

Direct targeting of RAS has been thought to be very challenging even after thirty years. New potential binding sites have been identified using computational approaches. However, deep hydrophobic pockets on the surface of K-RAS that would allow tight binding of small molecules have been lacking (Cox et al., 2014). Several attempts to discover small molecules that bind directly to RAS have been reported (Fig 1.12).

Furthermore, new classes of compounds have been developed and are currently under clinical investigation (Fig. 1.12, Cox et al., 2014). These range from low affinity inhibitors, GEF inhibitors, inhibitors of C-RAF binding, mutant specific inhibitors, inhibitors of ras converting enzyme (CAAX), and isoprenylcysteine carboxylmethyltransferase (ICMT; also known as protein-*S*-isoprenylcysteine *O*-

methyltransferase), inhibitors of palmitoylation and depalmitoylation and inhibitors of post-translational modification.

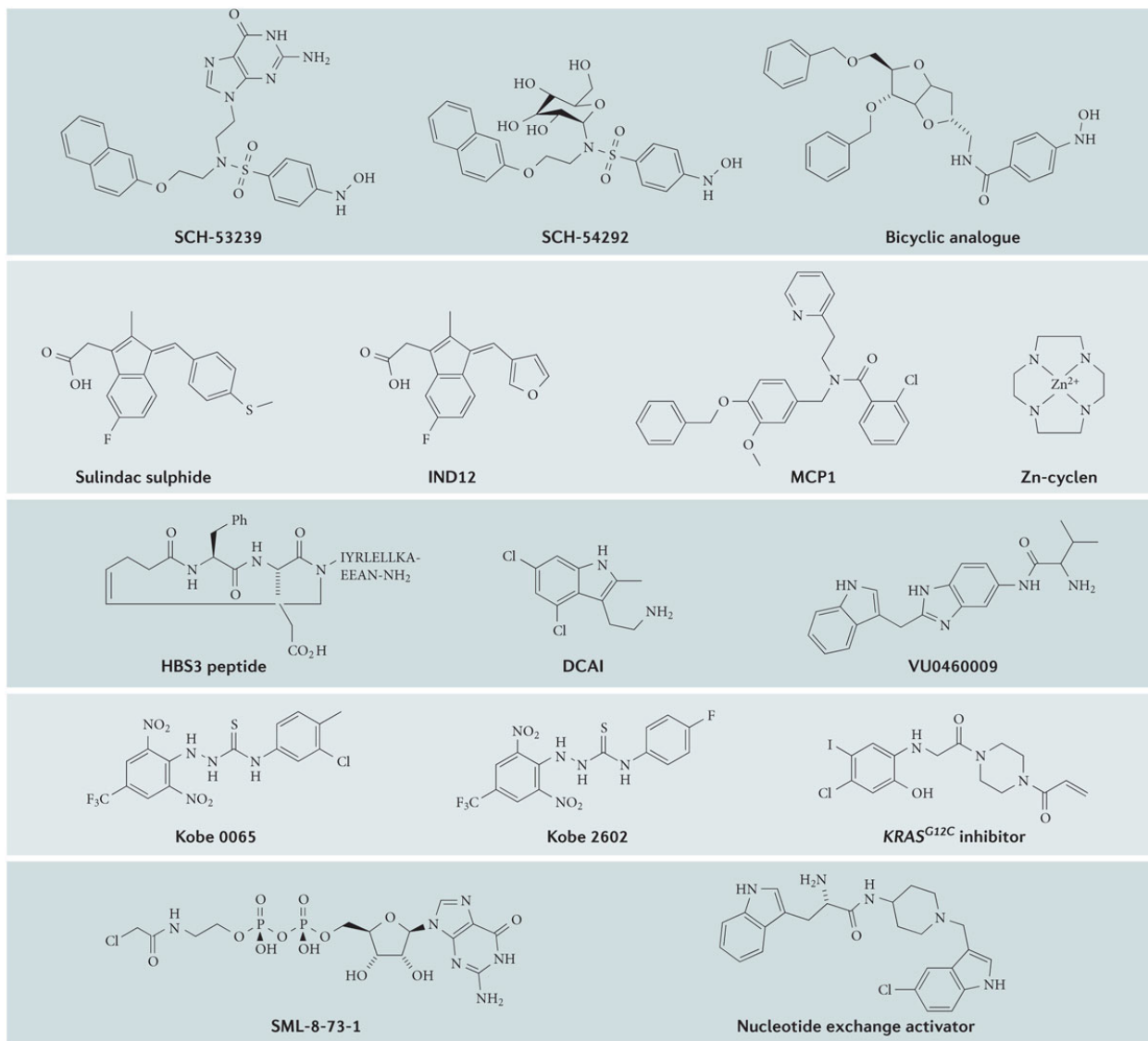


Figure 1.12. Compounds development to target mutationally activated RAS SCH-53239 was designed to inhibit guanine nucleotide exchange Structure–activity relationship studies led to the development of a derivative with greater water solubility, SCH-54292. Subsequently, another group used molecular modelling to

design a series of sugar-derived bicyclic analogues. On the basis of earlier observations that the non-steroidal anti-inflammatory sulindac showed antitumour activity in *Hras*-mutant rat mammary carcinomas, the active metabolite sulindac sulphide was evaluated and found to bind to H-RAS. IND12 is a sulindac derivative that blocks the growth of RAS-transformed cells. MCP1 was identified in a yeast two-hybrid screen for inhibitors of H-RAS binding to full-length C-RAF. Zinc-cyclen selectively binds to and stabilizes the conformational state of RAS that has weak effector-binding affinity. The HBS3 peptide is a mimic of the SOS1 α H helix that interacts with H-RAS. DCAI and were identified in fragment-based library screens for K-RAS4B-binding molecules. Kobe 0065 was identified in a computer docking screen of a virtual compound library and was selected for its ability to inhibit H-RAS–GTP binding to RAF–RAS-binding domains (RBDs). Kobe 2602 was identified in a subsequent computer-assisted similarity search of 160,000 compounds. A K-RAS^{G12C} inhibitor (the Shokat compound) was identified using a disulphide-fragment-based screening approach with GDP-bound K-RAS-G12C. SML-8-73-1 covalently binds to K-RAS-G12C and occupies the nucleotide-binding site. The nucleotide exchange activator (compound 4) stimulates RAS–GTP formation, but disrupts extracellular signal-regulated kinase (ERK) and phosphoinositide 3-kinase (PI3K) signaling (Adapted from Cox et al., 2014).

K-Ras has especially proved challenging to inhibit as it exerts its tumorigenic actions by activating primarily three effector proteins, Raf kinases, phosphatidylinositol 3-kinases (PI3K), and Ral guanine nucleotide exchange factors. PI3K, or its principal target AKT kinases have been reported to maintain

xenograft tumor growth upon silencing oncogenic Ras (Lim and Counter, 2005). This means that certain cancers including pancreatic cancers become addicted to PI3K-AKT signaling. Though families of PI3K and AKT proteins are druggable and components of the pathway represent attractive targets, their proteins are highly related and are also involved in a series of normal physiological processes. Furthermore, general inhibitors of these kinases can be toxic (Liu et al., 2009). However, a new target is the substrate endothelial Nitric Oxide Synthase (ENOS or NOS III)-catalysed nitrosylation. ENOS belongs to the NOS family, which generate nitric oxide. The family also includes neuronal NOS (nNOS or NOS I) and inducible NOS (iNOS or NOS II) (Alderton et al., 2001). Unlike AKT, ENOS plays a limited role in normal physiology, mainly in vasorelaxation (Dudzinski et al., 2006) and *eNOS*^{-/-} mice are viable (Shesely et al., 1996). Evidence suggests that inhibition of ENOS has anti-tumor effects. Gratton and co-workers (2003) reported that in hepatocarcinoma and lung carcinoma xenograft models, peptide-mediated inhibition of ENOS decreases tumor vascular permeability and tumor growth. Also, shRNA knockdown of ENOS reduced tumor growth of two pancreatic cancer cell lines with highly phosphorylated ENOS (Lim et al., 2008). Hence, inhibiting ENOS may be a way to indirectly exploit the reliance of cancer cells on oncogenic KRas for tumorigenesis. The NOS inhibitor N^G-nitro-L-arginine methyl ester (L-NAME) was previously developed and clinically evaluated in ten patients with hematologic malignancies and severe septic shock pathological conditions. In the study, L-NAME modulated the hemodynamics and showed a dose-dependent increase in systemic vascular resistance and blood pressure in a patient with septic shock (Kiehl et al., 1997). The results thus demonstrated that L-NAME plays a beneficial role in inhibiting nitric oxide synthase in leucocytopenic patients with

severe septic shock conditions. L-NAME is moderately selective for eNOS and nNOS over iNOS (Alderton et al., 2001).

In a pancreatic cancer mouse model, Lampson et al., (2012) showed that loss of ENOS by genetic ablation resulted in a decrease in the development of pre-invasive pancreatic lesions and an increase in lifespan in mice with advanced pancreatic cancer. These effects were similarly observed following the oral administration of the clinically evaluated L-NAME. However, nitric oxide can both inhibit and enhance tumorigenesis (Fukumura et al., 2006). Activation of wild-type ras proteins has been reported following the post-translational modification at C118. This activation is reported to promote activities that are required for cancer growth driven by mutant K-RAS (Cox et al., 2014).

Furthermore, L-NAME is relatively benign when compared to other conventional cytotoxic chemotherapy. Lastly, the major side effect of chronic administration of L-NAME is hypertension (Baylis et al., 1992).

RAF/MEK/ERK inhibitors are also been investigated. MEK1 and MEK2 (which have 80% identity) are the only well validated substrates of Raf and the only well-validated MEK1 and MEK2 substrates are the highly related ERK1 and ERK2 serine/threonine kinases (which have 86% identity). These findings indicate that the signaling cascade once though as a simple, linear and unidirectional is much more complex. The current view is that the RAF/MEK/ERK cascade is at the centre of a complex signalling network that has multiple inputs and outputs, feed-forward and feedback mechanisms, and multiple scaffold proteins that dynamically regulate signalling and ERK activity. More than 200 substrates have now been identified for ERK1 and ERK2. Developing new methods to inhibit multiple

pathways will be needed in future. This view has prompted combining inhibitors of components of the RAF and/or PI3K effector networks. Both preclinical and clinical evaluations are underway (Cox et al., 2014; Fig. 1.13).

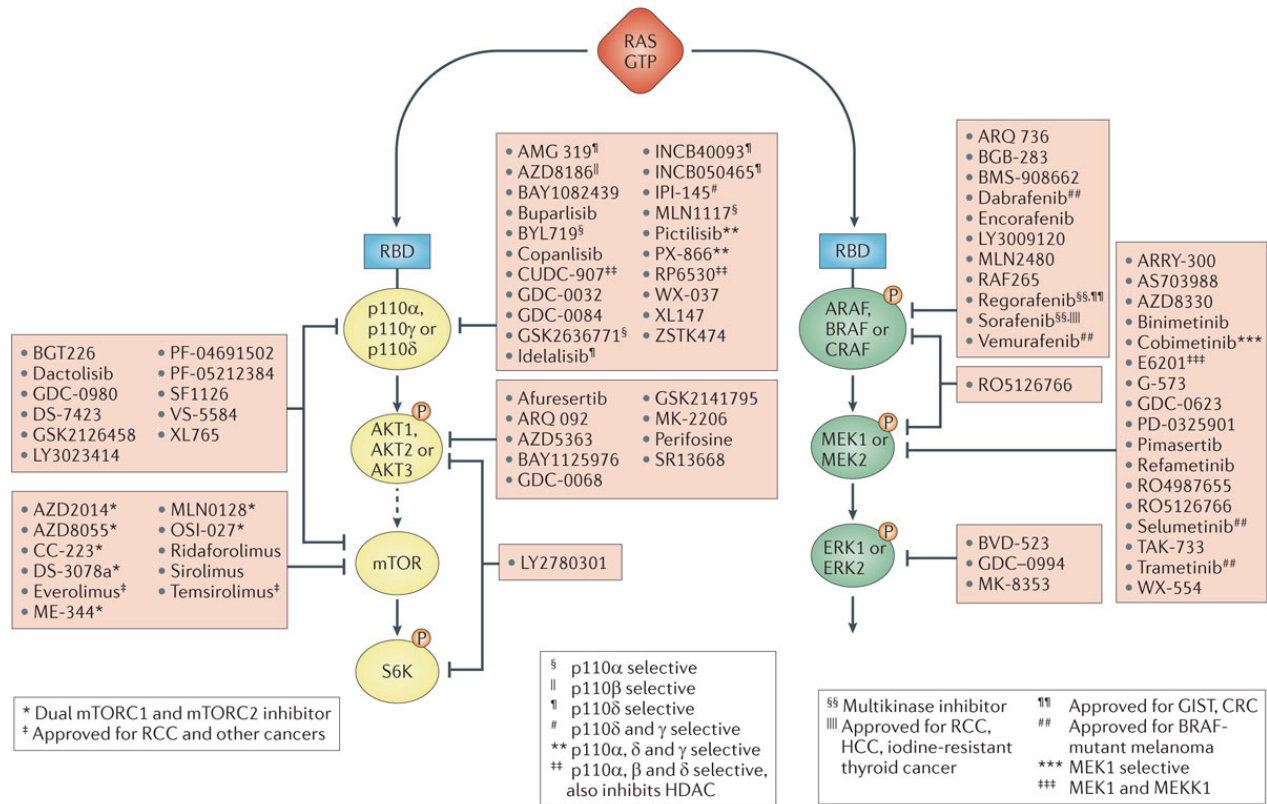


Figure 1.13. Inhibitors of RAS effector signalling under clinical evaluation. RAS proteins bind to the RAS-binding domain (RBD) of the p110 catalytic α -, γ - and δ -subunit of class I phosphoinositide 3-kinases (PI3Ks). Unless otherwise indicated, PI3K inhibitors are pan-class I. RAS binds to the RBD of A-RAF, B-RAF and C-RAF. Mammalian target of rapamycin (mTOR) exists as two distinct complexes, mTOR complex 1 (mTORC1; which contains the regulatory-associated protein of TOR1 (RAPTOR)) and mTORC2 (which contains the rapamycin-insensitive companion of mTOR (RICTOR)). Rapamycin and its analogues (also known as

rapalogues, which include everolimus, ridaforolimus and temsirolimus) are selective for mTORC1, forming a complex with mTOR and FKBP12. Second-generation mTOR inhibitors are ATP-competitive inhibitors of mTOR kinase activity. Data compiled from ClinicalTrials.gov. CRC, colorectal cancer; ERK, extracellular signal-regulated kinase; GIST, gastrointestinal stromal tumour; HCC, hepatocellular carcinoma; MEK, MAPK–ERK kinase; MEKK, MEK kinase; RCC, renal cell carcinoma (Adapted from Cox et al., 2014).

1.13.5 Clinical Trials Targeting RAS/RAF/MEK/ERK Pathway

A number of reports have demonstrated the preclinical efficacy both *in vitro* and *in vivo* of targeting Ras/Raf/Mek/Erk pathway. However, efficacy data obtained from clinical studies are currently limited. Other studies are now using Ras inhibitors in combination with other chemotherapeutic agents to increase efficacy (<http://clinicaltrials.gov>). Adjei and co-workers (2008) carried out a Phase I pharmacokinetic and pharmacodynamic study of AZD6244 (ARRY-142886; AstraZeneca/Array Biopharma), a potent and selective, adenosine triphosphate–uncompetitive inhibitor of MEK1/2 in patients with advanced melanoma, breast, colorectal and other types of cancers for which there was no curative or life-prolonging therapy. Results showed that the safety and tolerability of AZD6244 was manageable and suitable when administered at an oral dose of 100 mg orally, twice daily continuously. Though in humans, *in vivo* target inhibition was achieved with AZD6244, it was not sufficient for antineoplastic activity. The most common side effects of AZD6244 were rash. The results supported clinical development of AZD6244, and Phase II studies.

Lucas and co-workers (2010) in a multi-institutional Phase II study evaluated the efficacy of AZD6244 in the treatment of iodine-131 refractory papillary thyroid carcinoma (IRPTC) and papillary thyroid carcinoma (PTC) in 32 evaluable patients. AZD6244 was administered as an oral suspension at a dose of 100 mg twice daily for 28-day cycles. Results showed that 10 patients had progression of the disease; 21 with stable disease and only 1 patient showed a partial response. The mean progression free survival (PFS) was 53.6 weeks. Rash was the most common side effect of AZD6244 with 18% of subjects developing grade 3/4 rash. The conclusion from this study is that the response rates and progression free survival were inadequate surrogates to prove clinical benefit of AZD6244.

In another study, Infante and co-workers (2013) carried out a Phase Ib study of trametinib, (GSK1120212; another oral MEK inhibitor) in combination with gemcitabine in advanced solid tumours and a Phase II randomised, double-blind, placebo-controlled trial for patients with untreated metastatic adenocarcinoma of the pancreas (Infante et al., 2014). Results in both studies showed that the addition of trametinib to gemcitabine neither improved overall survival nor progression-free survival in patients with previously untreated metastatic pancreas cancer.

In a similar Phase II study carried out by Blumenschein and co-workers (2015), one hundred and twenty-nine patients with K-RAS-mutant NSCLC were randomly assigned to the treatment with either trametinib (GSK1120212) or docetaxel as second-line chemotherapy. The primary endpoint was progression free survival (PSF). Results showed that the median PSF was 12 weeks and it was not statistically different between the treatment groups. Furthermore, the partial responses in both the trametinib and docetaxel arms were similar (12%). The most

frequent adverse events in patients using trametinib were rash, diarrhea, nausea, vomiting, and fatigue.

Two inhibitors of Raf including sorafenib and PLX4032 (Plexxikon; RG7204, Roche Pharmaceuticals) have also undergone significant clinical evaluation. Sorafenib (BAY 43-9006) has been shown to be a potent inhibitor of both wild type and mutant B-Raf kinases *in vitro*. It binds to the ATP-binding pocket and prevents kinase activation, thereby preventing substrate binding and phosphorylation. Also, it has been reported to inhibit multiple cell surface receptors involved in tumor angiogenesis. These receptors include VEGFR-2, VEGFR-3, PDGFR- β , Flt-3, c-Kit and FGFR-1. It was approved in 2005 for the treatment of advanced renal cell carcinomas (RCC) and in 2007 for unresectable hepatocellular carcinoma (HCC) (Flaherty et al., 2010).

PLX4032 (now known as Vemurafenib/RO5185426) is a potent and selective inhibitor of mutant B-Raf. *In vitro* analysis has shown it to be a highly selective inhibitor of B-Raf kinase activity, with an IC_{50} of 44 nM against V600E-mutant B-Raf (Sala et al., 2008). Furthermore, it has been reported to inhibit cell proliferation and MEK activation in melanoma and thyroid carcinoma cell lines harboring mutant B-Raf. However, other cell culture and mouse model studies conducted with PLX4032 showed that while it was effective against *B-RAF* mutant tumor cell lines, it led to Raf activation in *RAS* mutant cell lines (Rajakulendran et al., 2009; Heidorn et al., 2010; Hatzivassiliou et al., 2010). These findings thus raised serious questions about using Raf inhibitors in *RAS* mutant tumors.

Consistent with previous preclinical findings regarding the anti-tumor activity of PLX4032 in mutant B-RAF melanomas, Flaherty and co-workers (2010) carried out a Phase I/II clinical trial to assess the efficacy, toxicity and pharmacokinetics of PLX4032. Fifty-five patients (49 with melanoma) in a dose-escalation phase and an additional 32 patients with metastatic melanoma were selected for the study. The dose escalation phase was a trial phase open to patients with any type of tumor. Groups of three to six patients received a daily dose of 200 mg of PLX4032 orally. Subsequently, groups received the drug at higher doses up to 1600 mg twice daily until dose-limiting side effects including rash, fatigue, arthralgia (joint pain) were observed. A recommended dose with fewer or no side effects was then determined. All 32 patients with metastatic melanoma in the extension phase were then treated with the recommended dose. Eligibility to this phase was restricted to patients with melanomas harboring a V600E B-RAF mutation, as determined by a polymerase-chain-reaction assay (PCR- TaqMan). All of the patients received continuous treatment with PLX4032 until unacceptable side effects or disease progression occurred. Analyses were conducted at baseline, day 1, day 8, day 15, day 29, and every 4 weeks thereafter.

Results showed that in the dose escalation phase, 10 of the 16 patients with melanoma and tumors carrying the V600E B-RAF mutation had a partial response and 1 had a complete response to PLX4032. These patients were receiving 240 mg or more of PLX4032 twice daily. In the extension phase where 32 patients were originally recruited, 24 patients had a partial response and 2 had a complete response. The overall median progression-free survival among patients was more than 7 months. However, patients with B-RAF mutation who responded to

PLX4032 quickly developed drug resistance between 2-18 months and the average duration of response was only 6.2 months. Eighty- nine percent of commonly observed side effects included arthralgia, rash, nausea, photosensitivity, fatigue, cutaneous squamous-cell carcinoma, pruritus, and palmar–plantar dysesthesia. These results demonstrated that in patients carrying tumors containing activating V600E B-RAF mutations, targeting tumors with PLX4032 can induce a partial tumor regression in most cases and complete regression in some cases. Furthermore, the dramatic initial tumor regression observed was far greater than the one observed using the standard of care drug (dasatinib). An ongoing Phase III clinical trial (Baines et al., 2011) is currently underway to determine the benefit of PLZ4032 on overall survival.

1.14 Nucleocytoplasmic Trafficking and the VDR/RXR Complex

The steroid receptors are a group of nuclear receptors which translocate into the nucleus in response to binding to their cognate ligands. Once inside the nucleus, they bind to the hormone response elements DNA and recruit other factors necessary for gene transcription or repression. It is now known that the import and export cycle or nucleocytoplasmic shuttling of the steroid receptors is a mechanism through which they carry out genomic and non-genomic signaling events (Chahine and Pierce, 2009).

The cells of eukaryotes are known to be surrounded by plasma membrane with elaborate organelles and a complex endomembrane system (Hung and Link, 2011). These organelles provide distinct compartments for different metabolic activities. Within these compartments are the nucleus and the cytosol where protein translation is confined. For proteins to exert their functions in different organelles,

the translocation is very important. Up to 50 % of the proteins manufactured by a cell have to be transported across at least one cellular membrane to reach their functional destination (Chacinska et al., 2009). Thus for the normal functioning of a cell, the protein transport machinery does not only accomplish the movement of information and material within and across a cell, but also ensures that the right amount of protein is present at the right time and place (Ellenberg et al., 1997; Hung and Link, 2011).

Protein transport and subcellular localization are therefore essential to the functioning of protein and has been suggested as a means to not only achieve functional diversity but also ensures access of proteins to other interacting partners leading to a functional biological network (Butler and Overall, 2009).

Dysregulation of the protein trafficking machinery and aberrant protein localization caused by mutation, altered expression of cargo proteins or transport receptors have been linked to human diseases as diverse as cancer, kidney diseases and Alzheimer's (Kau et al., 2004; Robben et al., 2006; Nair and Rost, 2008; Zhang et al., 2008; Cordeddu et al., 2009; Hung and Link, 2011). Thus the movement of proteins from the cell cytoplasm into and out of the nucleus is now appreciated as an important paradigm in biology.

Previous nucleocytoplasmic studies show that binding of $1,25(\text{OH})_2\text{D}_3$ to VDR in the cytoplasm of cells stimulates heterodimerization of the VDR-RXR complex and redistribution to the nucleus (Barsony et al., 1990; Barsony and McKoy, 1997; Barsony, 1999; Michigamy et al., 1999; Klopot et al., 2007). Furthermore, nucleocytoplasmic trafficking of the VDR/RXR complex has been shown to be an active process that is enhanced in the presence of $1,25(\text{OH})_2\text{D}_3$ treatment.

However, it is dependent on the presence of intact nuclear localization sequences

and various importins (Prufer et al., 2000; Yasmin et al., 2005). A thorough discussion of its implication will be presented in chapter 4.

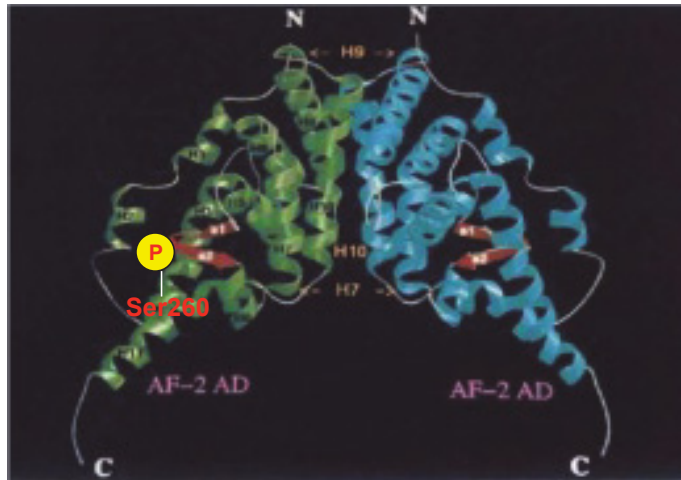
1.15 Rationale, Hypothesis and Specific Aims

1.15.1 Rationale

Although, *in vitro* 1,25(OH)₂D₃ has been shown to promote differentiation in myeloid cells, inhibit proliferation in breast, prostatic and colon carcinoma cells and *in vivo* inhibit tumor growth in prostate, breast and colon cells it is now becoming apparent that several cancer cell lines are resistant to the growth inhibitory action of 1,25(OH)₂D₃. These cell lines including human breast carcinoma cells, pancreatic cells and squamous cell carcinomas don't respond well to 1,25(OH)₂D₃ treatment (Narayanan et al., 2004; Klopot et al., 2007). Thus an understanding of the mechanism of resistance could pave the way to better therapeutic approach leading to controlling the deregulated growth of these cells.

Previous works in Dr. Richard Kremer's laboratory indicate that in ras transformed keratinocytes, hRXR α is phosphorylated at serine 260, a MAPK consensus site located in the omega loop –AF-2 interacting domain of RXR α . As a result both attenuation of ligand- dependent transactivation by VDR/ RXR α complex and reduced physiological response to growth inhibition and antiproliferative effects to vitamin D, a retinoic acid receptor ligand LG1069 and all trans retinoic acid (ATRA) are observed (Solomon et al., 1998, 1999, 2001; Macorrito et al., 2008; figure 1.14). Importantly, the phosphorylation at serine 260 also impairs the recruitment of DRIP205 and other coactivators to the VDR/ RXR α complex (Solomon et al., 1999; Macorrito et al, 2008).

Crystal structure of nuclear receptor RXR α showing phosphorylation site where serine 260 is localized



Three dimensional point of contact in the activation function, AF-2 (H11) Domain & omega loop between H1 and H3 where ser260 is localized on hRXR α

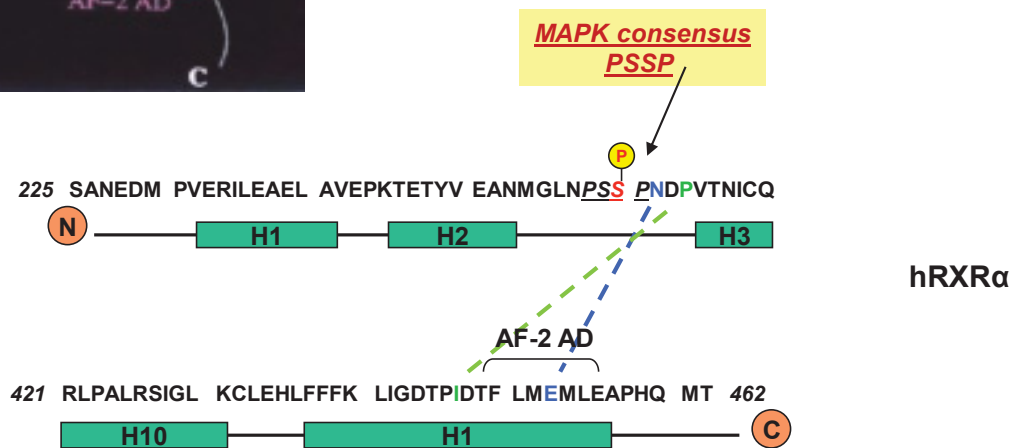


Figure 1.14: Crystal structure of nuclear receptor RXR showing phosphorylation site where serine 260 is located (Adapted from Bourguet et al., 1995).

This therefore raises the possibility that hRXR phosphorylation at serine 260 might induce a conformational change of the VDR/RXR complex as it is located at a critical site in the omega loop between H1 and H3 helices of the hRXR α ligand binding domain. Thus hRXR α phosphorylation at serine 260 may play an important role in the malignant transformation of ras cells by releasing cells from vitamin D – dependent growth suppression (Matsushima- Nishiwaki et al., 2001).

Also, since serine 260 is in a region of close spatial proximity to regions of potential coactivators and corepressors, phosphorylation may affect other signaling pathways involving the recruitment of partners other than vitamin D receptor (Solomon et al., 1999; Macorrito et al., 2008; Fig. 1.14).

Furthermore, Lu and co-workers (2012) demonstrated that phosphorylation of hRXR α at serine 260 interferes with its function and delays its degradation in cultured human hepatocellular carcinoma (HCC), leading to enhanced cellular proliferation. They showed that hRXR α is not phosphorylated and highly ubiquitinated in normal liver and in nonproliferating hepatocyte cultures rendering it sensitive to proteasome-mediated degradation. However, in both human HCC tissues and a human HCC cell line, HuH7, phosphoserine 260 hRXR α (phosphorylated hRXR α) is resistant to ubiquitination and proteasome-mediated degradation. In these tissues and cells, serine 260 is phosphorylated by MAP kinase. Also they found that full-length RXR α resides in the nucleus whereas truncated hRXR α was more cytoplasmic. They concluded that switching of the ubiquitin/proteasome-dependent degradation of hRXR α by phosphorylation at serine 260 may be responsible for the aberrant growth of HCC and its suppression by retinoids (Lu et al., 2012).

Studies examining nucleocytoplasmic trafficking of VDR and RXR have mostly been conducted in COS-7 kidney cells which are characterized by low expression of endogenous VDR (Pruffer et al., 2000; 2002; Pruffer and Barsony, 2002) and more recently Caco2 cells (intestinal cell line that spontaneously differentiates and recapitulates many of the features of the absorptive epithelial cell of the small intestine including vitamin D regulated intestinal calcium absorption) (Fleet et al., 1994,1999,2002; Fleet, 2006; Klopot et al., 2007). The impact of $1\alpha,25(\text{OH})_2\text{D}_3$

treatment on VDR and RXR distribution and nucleocytoplasmic trafficking in non-malignant human keratinocytes (HPK1A cells) has not been examined in ras transformed malignant human keratinocytes (HPK1Aras cells). To better understand and compare the biology of cancer cells to their normal counterparts, we previously used human keratinocytes (HPK1A) cell line that was established by stable transfection of human papillomavirus type 16 in normal human keratinocytes (NHK). These (immortalized but non-malignant) cells have an indefinite life span but retain differentiation properties characteristic of normal human keratinocytes and are non-tumorigenic when injected into nude mice. HPK1A cells were further transformed into the malignant HPK1Aras cell line following transfection with a plasmid carrying an activated Ha-ras oncogene. HPK1Aras cells form colonies in soft agar and produce invasive tumors when transplanted into nude mice a hallmark of their malignant phenotype. Ha-ras has been shown to induce transformation by binding key cellular proteins and altering their activities. Moreover, the ras-transformed cell line continue to express the ras-oncogene and stably display the hallmarks of transformation through many generations. The development of these cell lines allowed us to characterize the events leading to vitamin D resistance during tumor progression (Sebag et al., 1992) by directly comparing the properties of transformed cells to the parental culture from which they were derived. Importantly, endogenous expression of both VDR and RXR in the non-transformed HPK1A and ras-transformed HPK1Aras cell lines were similar (Macorrito et al., 2008).

Following a series of well designed and carefully documented experiments that propose to monitor using novel imaging techniques, the properties of non-cancerous HPK1A cells treated with vitamin D to the tumorigenic ras-transformed

HPK1Aras cells. We posit that careful examination of HPK1A and HPK1Aras keratinocytes are better suited model systems to study vitamin D action in cancers as compared to COS7 cells.

Consequently, in the present study we aimed to examine the consequences of hRXR α phosphorylation at serine 260 on nucleocytoplasmic trafficking of the VDR/RXR complex in both HPK1A and HPK1Aras cells.

We anticipate that the nucleocytoplasmic trafficking of VDR/RXR complex and coactivator recruitment in HPK1Aras cells is disrupted. Furthermore, we hypothesize that intra-nuclear kinetics will also be altered in HPK1Aras cells compared to normal non-malignant HPK1A cells suggesting a critical role played by RXR α phosphorylation at serine 260 in inducing hormone resistance to the growth inhibitory action of vitamin D. We think that the partial resistance to the growth inhibitory action to the ligand can be reversed through the restoration of the right conformational change in VDR/RXR complex formation and coactivator recruitment. This could be achieved by inhibiting MAPK activity using a MAPK inhibitor UO126 or by overexpression of a non-phosphorylatable mutant at serine 260 to alanine (hRXR α mutS260A, hRXR α S260A). We will carefully examine our hypothesis using subcellular localization studies, FRET, FRAP, FLIP and confocal microscopy.

1.15.2 Hypothesis

Our hypothesis is that: *hRXR phosphorylation at ser260 is a central regulator of vitamin D action in cancer cells.* The specific hypothesis is that hRXR α at serine

260 plays a critical role in both VDR/RXR interaction and nucleocytoplasmic trafficking of the receptor complex.

Our plan is to carry out *in vitro* assays on fixed and live cells using imaging techniques to understand the mechanisms of resistance and how phosphorylation at serine 260 could be reversed. These studies should provide fundamental information on the molecular basis of vitamin D resistance in cancer cells and help develop therapeutic strategies to overcome this resistance. Furthermore, since RXR heterodimerizes with several nuclear receptors other than the VDR, the implications of these studies are very broad for the treatment of malignancies and other diseases.

1.15.3 Specific Aims:

1. Use biochemical approach to investigate the effects of hRXR α phosphorylation at serine 260 on proliferation, cell viability and cell cycle in a non- transformed HPK1A and ras- transformed HPK1A_{ras} cell lines.
2. Use Green Fluorescent Protein (GFP) tagged constructs of VDR and RXR to assess the effects of RXR phosphorylation on subcellular localization of VDR and RXR in both non-transformed and ras-transformed cell lines.
3. Use fluorescently tagged constructs of VDR and RXR and Fluorescent Resonance Energy Transfer (FRET) and confocal microscopy to determine the effects of hRXR α phosphorylation at Serine 260 on hVDR/hRXR α heterodimer interaction.

4. Use confocal microscopy and Fluorescence Loss In Photobleaching (FLIP) to investigate the effects of hRXR α phosphorylation at serine 260 on intranuclear kinetics of hRXR α in cells transfected RXR α wt-GFP or RXR α mut-GFP -GFP and treated with 1,25 (OH) $_2$ D $_3$.
5. Use confocal microscopy and Fluorescence Recovery After Photobleaching (FRAP) to investigate the effects of hRXR α phosphorylation at serine 260 on intranuclear kinetics of hRXR α in cells transfected RXR α wt-GFP or RXR α mut-GFP -GFP and treated with 1,25 (OH) $_2$ D $_3$.
6. Determine effects of RXR α phosphorylation at serine 260 on DRIP205 coactivator and DRIP205 LXXLL motif interaction with VDR and RXR α in both non-transformed HPK1A and ras-transformed HPK1Aras cells.
7. Propose a model on the mechanisms of resistance in the ras-transformed HPK1Aras cells and how phosphorylation on serine 260 can be inactivated.

Chapter 2

Phosphorylation of Human Retinoid X Receptor α at Serine 260 Impairs Subcellular Localization, Receptor Interaction, Nuclear Mobility and $1\alpha, 25$ dihydroxyvitamin D_3 – Dependent DNA Binding in Ras –transformed Keratinocytes.

Sylvester Jusu¹, John F. Presley² and Richard Kremer¹

¹Department of Medicine and Calcium Research Laboratory, McGill University Health Center, 1001 Decarie Boulevard, Montreal, Quebec H4A 3S1

²Department of Anatomy and Cell Biology, McGill University, 3640 Rue University Montreal, Quebec H3A 0C7

*Running title: RXR α phosphorylation on serine 260 impairs $1, 25$ dihydroxyvitamin D_3 dependent signal transduction in ras-transformed cells

To whom correspondence should be addressed: Richard Kremer, Department of Medicine and Calcium Research Laboratory, McGill University Health Center, 687 Pine Avenue W. Montreal, Quebec H3A 1A1. Canada Tel.: (1)-514 784-2770; Fax (1-514-933-8784). E-mail: richard.kremer@mcgill.ca

The contents of this chapter has been submitted to the Journal of Biological Chemistry

Abstract

Human retinoid X receptor alpha (hRXR α) plays a critical role in DNA binding and transcriptional activity through its heterodimeric association with several members of the nuclear receptor superfamily including the hVDR. In malignant HPK1Aras cells, the relative resistance to the growth inhibitory effects of 1 α ,25(OH) $_2$ D $_3$, is observed. We previously showed that hRXR α phosphorylation at serine 260 through the Ras-Raf-MAP Kinase activation is responsible for this resistance. In this report, we investigated further the mechanisms of this resistance by assessing the effects of RXR α phosphorylation on receptor subcellular localization, hVDR/ hRXR α interaction, intra-nuclear mobility and DNA binding of GFP-tagged hVDR or hRXR α wild type or the non-phosphorylatable hRXR α -S260A mutant in the presence of either 1 α ,25(OH) $_2$ D $_3$, 9-*cis*-Retinoic Acid, the MEK inhibitor UO126 or a combination of UO126 and 1 α ,25(OH) $_2$ D $_3$. We show through transfection of hVDR and hRXR α tagged constructs and different fluorescence imaging techniques of fixed and live cells that the nuclear localization, heterodimer interaction and binding of hVDR/ hRXR α complex to DNA are impaired in HPK1Aras cells when compared to the non-malignant normal HPK1A cells. However, transfection of HPK1Aras cells with the non-phosphorylatable hRXR α -S260A mutant or combined treatment with 1 α ,25(OH) $_2$ D $_3$ and UO126 reverses the effects. This suggests that in HPK1Aras cells, hRXR α phosphorylation significantly disrupts nuclear localization, intra-nuclear trafficking and binding to chromatin of the hVDR/hRXR complex.

Abbreviations: MEK, Mitogen Extracellular Kinase; FRET, Fluorescence Resonance Energy Transfer; FLIP, Fluorescence Loss in Photobleaching; UO126,

(1,4-diamino-2,3-dicyano-1,4-bis[2-aminophenylthio] butadiene); MAPK; Mitogen activated protein kinase; HPK1Aras, malignant ras- transformed keratinocytes; hVDR, human vitamin D receptor; hRXR α , Human retinoid X receptor alpha; GFP, green fluorescent protein; hRXR α -S260A, non-phosphorylatable hRXR α ala260 mutant;

Introduction

$1\alpha, 25$ - dihydroxyvitamin D ($1\alpha,25(\text{OH})_2\text{D}$), the hormonally active metabolite of vitamin D, besides its effect on bone and mineral homeostasis (Evans, 1988; Barsony et al., 1990, 1997; Michigami et al., 1999; Tavera-Mendoza et al., 2006) is known to affect immuno-modulation (Yu et al., 1995; Ingraham et al., 2008; Verstuyf et al., 2010), promotes cellular differentiation and inhibits cell proliferation (Bikle, 2012). The majority of the actions of $1\alpha,25(\text{OH})_2\text{D}$ are mediated through vitamin D receptor (VDR), a member of the nuclear receptor steroid/thyroid superfamily of transcriptional regulators. $1\alpha,25(\text{OH})_2\text{D}$ directly modulates the transcription of several target genes by binding to the VDR. The ligand bound activated complex functions as a heterodimer by interaction with the retinoid X receptor (RXR). This heterodimer (VDR/RXR) is capable of binding to the vitamin D response elements in the promoter regions of target genes resulting in activation or repression of transcription via interaction with transcriptional cofactors and the basal transcriptional machinery (Barsony et al., 1990; Dong and Noy, 1998; Bourguet et al., 2000; Egea et al., 2000; Bettoun et al., 2003; Narayanan et al., 2004; Pike and Meyer, 2010; Haussler et al., 2011; Orlov et al., 2012; Bikle, 2014; Olmos-Ortiz et al., 2015).

Although, *in vitro* studies have shown that $1\alpha,25(\text{OH})_2\text{D}_3$ promotes differentiation of myeloid cells (Suda et al., 1986) and inhibits proliferation of breast (Colston and Hansen, 2002), colon (Kane et al., 1996), prostatic (Getzenberg et al., 1997; Polek and Weigel, 2002) and other cancer cells (Colston et al., 1981; Yu et al., 1995; Fujioka et al., 1998) it is now apparent that several human cancer cell lines are resistant to the growth inhibitory action of $1\alpha,25(\text{OH})_2\text{D}_3$ (Sebag et al., 1992; Yu

et al., 1995; Solomon et al., 1999). Attempts to treat cancer patients using vitamin D and its analogs have not yet translated into effective and approved therapies (Suda et al., 1986; Solomon et al., 1999; Bikle, 2014). Thus an understanding of the mechanism of that resistance could pave the way to improve the efficacy of vitamin D therapies in cancer.

Studies in our laboratory indicate that phosphorylation of the hRXR α is an important mechanism underlying the resistance to the growth inhibitory action of vitamin D in malignant keratinocytes. The resistance to the growth inhibitory action of vitamin D was secondary to hRXR α phosphorylation at serine 260, a critical site located in close spatial proximity to regions of potential coactivators and corepressors interactions with the RXR (Solomon et al., 1998, 2001; Macoritto et al., 2008). These earlier studies demonstrated that phosphorylation of hRXR α not only disrupts its VDR/RXR interaction but also coactivator recruitment perhaps by altering the conformation of the VDR/RXR/comodulator complex and its biological activity. We therefore hypothesize that RXR phosphorylation at ser260 is a central regulator of $1\alpha,25(\text{OH})_2\text{D}_3$ action in cancer cells that could be targeted therapeutically. In the present studies, we use *in vitro* imaging techniques including, Fluorescent Resonance Energy Transfer (FRET) and Fluorescence Loss In Photobleaching (FLIP) to better understand the mechanisms of this resistance and how phosphorylation on serine 260 could be inactivated.

EXPERIMENTAL PROCEDURES

Reagents

1 α ,25(OH)₂D₃ and 9-*cis*-RA were purchased from Sigma Aldrich (St. Louis, MO, USA) and stock solutions were prepared in ethanol. The mitogen-activated and extracellular regulated kinase kinase (MEK1/2) inhibitor UO126 (1,4-diamino-2,3-dicyano-1,4 bis[2-aminophenylthio] butadiene) was purchased from Promega (Madison, WI, USA) and stock solutions was prepared in DMSO. Human vitamin D receptor (hVDR) (C-20) and human retinoid X receptor α (hRXR α) (D-20) antibodies were obtained from Santa Cruz Biotechnology (Santa Cruz, CA, USA).

Cell lines and Culture

The HPK1A cell line was previously established by stably transfecting normal human keratinocytes with human papillomavirus type 16 (Sebag et al., 1992). In culture, these cells have an indefinite life span but retain differentiation properties characteristic of normal keratinocytes and are non-tumorigenic when injected into nude mice. These immortalized cells were then transformed into the malignant HPK1Aras cell line after transfection with a plasmid carrying an activated Ha-ras oncogene (Sebag et al., 1992). HPK1Aras are malignant cells which form colonies in soft agar and also produce invasive tumors when transplanted into nude mice. The cells were grown in Dulbecco's Modified Eagle's Medium (DMEM) (Gibco, Buffalo, NY, USA) supplemented with 2 mM of glutamine, 100 IU/ml of penicillin, 100 μ g/ml of streptomycin and 10% of fetal bovine serum (FBS) and passaged twice weekly in six, twenty four or ninety- six well Falcon plates (Corning, NY, USA).

Proliferation Assay

For assessment of cell proliferation, HPK1A and HPK1Aras cells were seeded in 24 well plates at a density of 1×10^4 cells/well and were grown in DMEM supplemented with 2 mM of glutamine, 100 IU/ml of penicillin, 100 μ g/ml of streptomycin and 10% fetal bovine serum (FBS). After 24 hr, the medium was replaced with serum free DMEM overnight to synchronize the cells. At the start of the experiment, the medium was replaced with DMEM containing 5 % charcoal stripped FBS and $1\alpha,25(\text{OH})_2\text{D}_3$ (10^{-9} M to 10^{-7} M concentration) as a single agent or in combination with the MEK1 inhibitor UO126 (10^{-6} M concentration). Control cells were treated with vehicle alone (ethanol 0.1% and DMSO 0.1 % v/v). Treatment was continued for 72 hours. At the end of the experiment, cells were washed with phosphate buffered saline (PBS), trypsinized and counted with a Coulter counter.

Alamar Blue Cell Viability Assay

Cells were seeded in 96 well plates at a density of 5×10^3 cells/well and the experiment carried out as above in the proliferation assay. At the end of each experiment, 50 μ l of Alamar Blue (Invitrogen, Grand Island, NY, USA) was added to each well and the plate was further incubated at 37°C for 4 hrs, and then transferred to a plate reader and absorbance at 550 nm was determined as per manufacturer's instruction.

Cell Cycle Analysis with Propidium Iodide (PI) Staining

HPK1A and HPK1Aras cells were seeded into six-well plates at a density of 5.0×10^5 cells/plate for 24 hrs grown as described above in the proliferation assay and treated with 10^{-7} M $1,25(\text{OH})_2\text{D}_3$ alone or in combination with 10^{-6} M UO126. The

cells were trypsinized, washed in PBS and fixed in 70 % ethanol at 4°C overnight. 1×10^5 cells were then resuspended in 40 µg/ml PI solution with 1 mg/ml RNase and incubated in the dark at 37°C for 30 min. DNA content and cell cycle analysis was carried out using a FACScan flow cytometer (BD Biosciences, Maryland, USA). Different phases of the cell cycle were assessed by collecting the signal at channel FL2-A. The percentage of the cell population at a particular phase was estimated by the BD CellQuest software.

Cloning of Fluorescently tagged (plasmids) constructs.

Subcloning of VDR plasmids

VDR/pSG5 was a kind gift from Dr. John White's laboratory (McGill University, Montreal, Canada). The expression vector was originally constructed by inserting a 2.1-kilobase EcoRI fragment containing the entire coding region of the human VDR into the EcoRI site of pSG5 (Ferara et al., 1994). VDR-CFP, VDR-GFP, VDR-YFP and VDR-mCherry plasmids were constructed by PCR amplification of hVDR sequence using hVDRpSG5 as a template and forward GGTTAC CTCGAG ATG GAG GCA ATG GCG GCC AGC ACT TCC CTG and reverse GTTAC CCG CGG AGA GGA GAT CTC ATT GCC AAA CAC TTC G primers were designed with an XhoI and SacII restriction sites. The hVDR PCR product was ligated to the GFP variants a generous gift from Dr. Stephan Laporte (McGill University, Montreal, Canada) and mCherry (Clontech, (Mountain View, CA, USA).

Subcloning of RXR α Plasmids

The hRXR α wild type (WT) and ala260 hRXR α mutant were a kind gift from Dr. Ronald Evans laboratory (The Salk Institute of Biological Science, La Jolla California, USA; Solomon et al., 2001) The hRXR α wt and the hRXR α ser260 ala mutant fluorescent GFP variants (ie GFP, CFP, YFP and mCherry) were constructed by PCR amplification of hRXRwt and the hRXR α ser260 ala mutant (hRXR α S260A) sequences using hRXR α wt and the hRXR α ser260 ala mutant as templates and forward GGTTAC CTCGAG ATG GAC ACC AAA CAT TTC CTG C and reverse GTTAC CCG CGG AGA AGT CAT TTG GTG CGG CGC CTC CAG C primers were designed to creat new XhoI and SacII restriction sites. The resulting amplified PCR products were ligated to mCherry and the GFP variants respectively.

Transfection

HPK1A and HPK1Aras cells were maintained in DMEM containing 10% FBS. For experimentation, cells were plated overnight in six well plates on # 1 coverslips (Fisher Scientific, Pittsburgh, PA) for fixed cell or 35 mm MatTek glass bottom dishes (MatTek Corporation, Ashland, MA, USA) for live cell experiments. Cells were plated at 8×10^4 cells/ well (HPK1A) and 6×10^4 cells/ well (HPK1Aras) in DMEM containing 10% FBS. The next day the medium was changed to serum free DMEM for an hour prior to initiating the experiment. Transfection was carried out in serum free DMEM FuGENE HD at a FuGENE HD/ DNA transfection ratio of 6 μ l:2 μ g DNA as per manufacturer's protocol. (Roche Applied Science, Indianapolis, IN). The cells were transfected with vectors encoding hRXR α -YFP, hRXR α -GFP (2.0 μ g) or hVDR-CFP, hVDR-GFP (3.0 μ g). In co-transfection studies, a total of 5 μ g of the co-transfected vectors was used per well. After 4 hr of

incubation, the medium was supplemented with 10 % FBS (by adding 200 ul of FBS/well). Following a 30 hr incubation, the medium was changed to DMEM containing 5 % FBS and incubated overnight. The next day, the cells were treated with vehicle (Ethanol+ DMSO 0.1 % v/v) or 1,25(OH)₂D₃ (10⁻⁷ M), 9 *cis*-RA (10⁻⁷ M), UO126 (10⁻⁶ M) alone or a combination of UO126 and with 1,25(OH)₂D₃ for 4 hr. For real time live cell microscopy, the transfected cells were first transferred on to a heated stage at 37 °C for drug treatments and data acquisition. For fixed cell experiments, the cells were washed with PBS after the treatment and fixed for 15 mins in 4 % paraformaldehyde at 37 °C. Following fixation, cells were re-washed in PBS and mounted using Shandon immu-Mount mounting medium (Fisher Scientific, Pittsburgh, PA, USA). For subcellular localization studies, following fixation and re-washing cells, were stained with either DAPI or Hoechst 33342 dye (Invitrogen, Grand Island, NY, USA) for 10 minutes and then mounted using Shandon immu-Mount mounting medium (Fisher Scientific, Pittsburgh, PA, USA). Imaging was carried out the next day using a Zeiss LSM 510 or LSM 780 confocal microscope (Jena, Germany).

Fluorescence Microscopy, Time-Lapse Imaging, and Image Processing

HPK1A and HPK1Aras cells were grown on 35-mm glass-bottom dishes (MatTek Corporation, Ashland, MA, USA) (live cells) or 22 mm no.1 glass slides (fixed cells). Time lapse imaging was performed using a confocal laser scanning microscope (model LSM 510, Carl Zeiss, Inc., Jena, Germany) equipped with a motorized triple line Kr/Ar laser, a 100× 1.4 NA Planapochromat oil immersion objective, a 63× 1.3 NA Planapochromat oil immersion objective, a 40× 1.3 NA Neofluar oil immersion objective, a 25× 0.8 NA Neofluar immersion corrected

objective and a temperature and CO₂ controlled stage. Time-lapse sequences were recorded using the time-series function of the Zeiss LSM software.

Receptor Expression and Subcellular Distribution using Confocal Microscopy

GFP vector alone, hVDR-GFP, hRXR α wt-GFP and hRXR α mut-GFP expression vectors were monitored by viewing and counting fluorescing cells using a Plan-Neofluor 40 x/ 1.3 oil objective, 488 nm excitation and 515-565 nm emission filters (Carl Zeiss Inc.). To monitor subcellular distribution of the receptors, at least ten healthy cells were observed at random from at least 10 fields of view (FOV) (on average one per FOV). Repeated experiments were done using the same parameters. Z-stacks of double-labeled images were collected to account for total cellular fluorescence.

Morphometric Analysis of Subcellular Localization

For evaluation of nuclear/cytoplasmic signal distribution, confocal images were taken of each fluorescing cell. A single optical slice was taken of each cell with focus set to maximize the circumference of the nucleus. At least ten cells were evaluated for each experimental condition. Cells that showed clear morphological changes due to protein overexpression were excluded from statistical analysis. Image analysis was performed using the ImageJ 1.41 public domain software (U.S. National Institutes of Health, Bethesda, MD, USA) to determine the nuclear (Fn) cytoplasmic (Fc) and background (Fb) fluorescence. Briefly, a mean density measurement of pixel numbers was made on a nonsaturated region of interest (ROI) consisting of the total nucleus, the whole cell (nucleus and cytoplasmic compartments combined) and a background region outside of the cell. The ratio of

nuclear to cytoplasmic fluorescence (F_n/c) was then determined according to the formula $F_n/c = (F_n - F_b)/(F_c - F_b)$. Data are presented as mean \pm S.E. (Racz and Barsony, 1999; Kuuisto et al., 2012)

Fixed Cell Imaging and Fluorescence Resonance Energy Transfer (FRET)

Microscopy

HPK1A and HPK1A_{ras} cells were grown on 22mm no.1 coverslips and cotransfected with either VDR-CFP/hRXR_{wt}-YFP or VDR-CFP/hRXR_{mut}-YFP respectively. Transfected cells were next treated with either vehicle control (Ethanol + DMSO 0.1 % v/v), 1,25(OH)₂D₃ (10^{-7} M) alone or a combination of UO126 (10^{-6} M) and 1,25(OH)₂D₃. Treatments were carried out for 4 hr before fixing, mounting and FRET data acquisition using a Zeiss LSM 510 confocal microscope with a Zeiss 40 \times NA 1.4 Neo-fluor oil objective and a chamber to maintain a temperature of 37 °C and 5% CO₂. To assay dequenching of donor after photobleaching, a series of eight images of the CFP channel were taken. YFP within the nucleus was bleached after image 4 by scanning with the 514 nm laser line at maximum intensity. CFP intensities inside the nucleus were compared between the immediately prebleach image (image 4) and the postbleach image (image 5). Dequenching was defined as nuclear CFP intensity in image 4 divided by nuclear CFP intensity in image 5. The remainder of the image sequence served as a control for focus stability. At least ten cells per treatment were photobleached for each experiment. Experiments were repeated twice.

To calculate FRET percentage, the fluorescence intensities of three regions of interests (ROIs)- a region in close proximity to the cell (background), a region in

the nucleus that was photobleached (bleached region) and a region of the nucleus that was not bleached (unbleached region) was selected and data acquired for both YFP and CFP. The fluorescent intensities of CFP immediately before the bleach and immediately after the bleach were next background corrected by subtracting fluorescence intensity of the background region in the CFP channel of the same image. The prebleach and postbleach CFP corrected intensities were then used to calculate the percent dequenching, which is a measure of FRET in this experimental design. A total of ten images were analyzed per experimental condition. Percent dequenching was calculated as follows: Dequenching % = (CFP_corrected postbleach / CFP_corrected prebleach) X 100. In this measure, 100% represents a baseline with no change in fluorescence, indicative of no significant FRET, while values greater than 100% are consistent with FRET prior to dequenching.

Live Cell Imaging using Fluorescent Loss In Photobleaching (FLIP)

Microscopy

Fluorescent Loss In Photobleaching (FLIP) (Cole et al., 1996, Houtsmuller et al., 1999) was used to assess real-time intra-nuclear mobility of GFP-tagged proteins in the presence or absence of ligand. HPK1A and HPK1A_{ras} cells were transfected with GFP tagged hRXR α wt or hRXR α mut respectively. After 30 hr transfection, the media was changed to one containing 5 % charcoal stripped FBS and the cells were treated with vehicle control (Ethanol +DMSO 0.1%v/v) or 1,25(OH) $_2$ D $_3$ (10 $^{-7}$ M) as above. All photobleach image series were obtained on a 37 °C heated stage using a 40 \times /1.3 NA oil immersion lens. Fluorescence in a narrow strip (4 μ m) spanning one-fourth the width of the nucleus was bleached using repeated (50-200)

scans of 488 nm illumination with 100 % laser transmission. Bleaching alternated with image acquisition at 5% laser transmission. Cells were scanned 0.8 to 3 sec per image with two –to- eight line averaging. Fluorescence intensity in an ROI on the opposite side of the nucleus and outside of the bleach ROI was quantitated at each time point and normalized to the fluorescence intensity before bleaching. A neighboring unbleached cell served as a control for focus drift and photobleaching during image acquisition. Normalization was done to the prebleach data point (Farla et al., 2004). At least ten cells were collected per treatment condition.

The Zeiss LSM software package was used to define regions of interests (ROIs), collect mean fluorescence intensities of the background, whole nucleus and the whole cell for each data set measured under the same experimental condition. Images were background subtracted and data normalized and exported into Microsoft Excel before quantitation and processing. The analyzed data were used to plot curves, calculate mobile fraction, diffusion constants and half time of recovery. The mobile fraction M_f was calculated using the equation: $M_f = (F_{pre} - F_{end}) / (F_{pre})$ (Lippincott-Schwartz et al., 2001; Snapp et al., 2002) where F_{pre} is the average fluorescence in the ROI before bleaching and F_{end} is the fluorescence immediately after the bleach. The immobile fraction was calculated as $I_f = 1 - M_f$ or $I_f = 100 - M_f$ where the normalized data was converted to percentages. Decay rates were calculated by fitting a one phase exponential decay curve $Y = Span * \exp(-K * X) + Plateau$ in GraphPad Prism. The half-time of fluorescence loss ($t^{1/2}$) is the time required for the fluorescent intensity in the bleach ROI to reduce by 50 % (Snapp et al., 2002). ($t^{1/2}$) was calculated as $0.69/K$, which assumes pseudo-first-order kinetics. To determine a model-independent half-life of fluorescence loss, the

fluorescent intensity data was transformed using a 0 % to 100 % scale and the time at which fluorescence intensity fell to 50% of full intensity defined as the $t_{1/2}$. At least ten cells were selected at random for each experimental condition. Statistical analysis using ANOVA and t-test were carried out in GraphPad Prism.

Binding of Receptor DNA to Hoechst Dye

HPK1A and HPK1A_{ras} cells were seeded on 22 mm (MatTek Corporation, Ashland, MA, USA) glass slides at a concentration of 1×10^5 cells/ well for 24 hrs in DMEM containing 10 % FBS. The next day, the cells were transfected with hVDR-GFP, hRXR α wt-GFP or hRXR α mut-GFP using FuGENE HD at a DNA/Fugene ratio of 2 μ g:6 μ l as described in transfection protocol above and cells treated with the drugs for (as previously done) 2hr prior to fixation. The cells were next washed with PBS, and fixed in 4 % paraformaldehyde for 15 minutes. Cells were re-washed with PBS and stained with Hoechst 33342 dye (1 μ g/ml) for ten minutes at room temperature. Finally, cells were re-washed with PBS and slides mounted with immuno-mount medium. Imaging was carried out the next day using both the 488 nm and 405 nm lasers to compare colocalization of the GFP and Hoechst dye in the cells. Image analysis was carried out by selecting the nuclei in the images and determining the mean fluorescence intensity of all the GFP and Hoechst dye pixels selected using the Zeiss LSM 780 Image Examiner. The built-in-Pearson's correlation coefficient function was used to compare colocalization of Hoechst dye (a DNA marker) to GFP within the nucleus. The data obtained was further evaluated for statistical significance using the Graphpad prism software.

Statistical Analysis

We used analysis of variance (ANOVA) and t-test in GraphPad Prism software. Results are presented as mean \pm standard error of at least eight independent measurements. Data was analyzed statistically by one-way analysis of variance followed by a post- hoc test and student t-test. Means were considered significantly different when P values were below 0.05

Results

Inhibition of Mitogen Activated Protein (MAP) Kinase activity enhances ras-transformed HPK1Aras cells' response to $1\alpha,25(\text{OH})_2\text{D}_3$ on cell growth and cell cycle.

Effects on cell growth

To test whether the non-transformed HPK1A and the ras-transformed (HPK1Aras) cells were sensitive to the growth inhibitory action of $1\alpha,25(\text{OH})_2\text{D}_3$, we treated both cell lines with various concentration of $1\alpha,25(\text{OH})_2\text{D}_3$ alone or in combination with UO126. In HPK1A cells we observed a dose dependent growth inhibition with $1\alpha,25(\text{OH})_2\text{D}_3$ but no further growth inhibition when UO126 was added (Fig.2.1A, $p < 0.05$). In contrast HPK1Aras transformed cells were less responsive to treatment with $1\alpha,25(\text{OH})_2\text{D}_3$ alone (Fig. 2.1B, $p > 0.05$), but pre-treatment for 30 minutes with the MEK inhibitor UO126, restored $1\alpha,25(\text{OH})_2\text{D}_3$ response ($p < 0.05$). Similar effects were observed on cell viability in both cell lines using the Alamar blue assay (Fig. 2.1C and 2.1D).

Effects on Cell cycle

We used flow cytometry to determine the effects of $1\alpha,25(\text{OH})_2\text{D}_3$ on cell cycle. HPK1A and HPK1Aras cells were treated with either vehicle, $1\alpha,25(\text{OH})_2\text{D}_3$ alone or in combination with UO126 for 72 hr before flow cytometric analysis. In HPK1A cells, $1\alpha,25(\text{OH})_2\text{D}_3$ addition or pre-treatment with MEK inhibitor UO126 significantly increased percentage of cells in G0/G1 phase from 70.6 % to 81.2 % when compared to vehicle control ($p < 0.05$). Although UO126 significantly increased the percentage of cells in G0/G1 when added alone, it did not enhance $1\alpha,25(\text{OH})_2\text{D}_3$ effects (Table 2.1, $p > 0.05$). In HPK1Aras cells, treatment with $1\alpha,25(\text{OH})_2\text{D}_3$ slightly increased the percentage of cells in G0/G1 phase (64.9 % to 69.2 %) when compared to vehicle ($p < 0.05$). However, pre-treatment with the MEK inhibitor UO126 followed by addition of $1\alpha,25(\text{OH})_2\text{D}_3$ significantly increased the percentage of cells in G0/G1 phase (69.2 % to 81.0 %) as compared to $1\alpha,25(\text{OH})_2\text{D}_3$ treatment alone ($p < 0.05$). (Table 2.1).

Effects of $1\alpha,25(\text{OH})_2\text{D}_3$ treatment on subcellular localization of hVDR and hRXR α in non-transformed HPK1A and ras-transformed HPK1Aras cells

In HPK1A cells, hVDR fluorescence distribution of the whole cell was both cytoplasmic and nuclear in the absence of a ligand. The nuclear/total cell hVDR fluorescence ratio was (0.56 ± 0.02). However, ligand addition significantly increased the nuclear localization of hVDR (nuclear/total cell hVDR ratio was 0.91 ± 0.02) (Fig.2.2A and 2.2F, $p < 0.001$). Similarly in the absence of the ligand, hRXR α was both cytoplasmic and nuclear (0.66 ± 0.04) but nuclear translocation increased after ligand addition (0.91 ± 0.02) (Fig.2.2B and 2.2G, $p < 0.05$). To determine the involvement of hRXR α phosphorylation on VDR localization in HPK1Aras cells, we similarly transfected the cells with VDR-GFP. VDR was

found to be both cytoplasmic and nuclear in vehicle treated cells (0.37 ± 0.05). Addition of $1\alpha,25(\text{OH})_2\text{D}_3$ alone or a combination of the MEK inhibitor UO126 and $1\alpha,25(\text{OH})_2\text{D}_3$ significantly increased VDR accumulation in the nucleus compared to control (0.51 ± 0.02) (Fig. 2.2C and 2.2H, $p < 0.05$). However, addition of the MEK inhibitor UO126 alone did not increase the nuclear accumulation of VDR when compared to control (0.31 ± 0.05). The combination of UO126 and $1\alpha,25(\text{OH})_2\text{D}_3$ increased nuclear accumulation of VDR by more than 1.5 fold compared to control and about 2 fold compared to $1\alpha,25(\text{OH})_2\text{D}_3$ or UO126 treatment alone (0.60 ± 0.01) (fig. 2.2C and 2.2H, $p < 0.005$).

We also assessed the effects of phosphorylation on hRXR α subcellular localization. Similar to the protocol above, we transfected the cells with either RXR α wt-GFP or RXR α mut-GFP plasmids. In HPK1Aras cells transfected with RXR α wt-GFP plasmids, RXR α was found to be predominantly nuclear without treatment (vehicle) (0.40 ± 0.04). Treatment with $1\alpha,25(\text{OH})_2\text{D}_3$ (0.40 ± 0.05) or MEK inhibitor UO126 (0.41 ± 0.04) alone did not increase nuclear accumulation of RXR α compared to control (0.40 ± 0.04) (Fig. 2.2D and 2.2I, $p > 0.05$). However, a combination of UO126 and $1\alpha,25(\text{OH})_2\text{D}_3$ (0.53 ± 0.05 vs 0.40 ± 0.04 $p < 0.05$) increased the nuclear accumulation of RXR α compared to vehicle, $1\alpha,25(\text{OH})_2\text{D}_3$ and UO126 alone treated cells (Fig. 2.2D and 2.2I, $p < 0.05$). In cells transfected with RXR α mut-GFP plasmids, $1\alpha,25(\text{OH})_2\text{D}_3$ (0.70 ± 0.05) or a combination of UO126 and $1\alpha,25(\text{OH})_2\text{D}_3$ (0.68 ± 0.14) significantly increased nuclear accumulation of RXR α compared to vehicle (0.43 ± 0.01) or MEK inhibitor UO126 alone (0.47 ± 0.03 , Fig. 2.2E and 2.2J, $p < 0.05$). Furthermore treatment with MEK UO126 alone (0.47 ± 0.03) did not increase nuclear accumulation of RXR α compared to vehicle (0.43 ± 0.01).

Effects of 9-cis-Retinoic Acid treatment on subcellular localization of RXR α in non-transformed HPK1A and ras-transformed HPK1A_{ras} cells

The intensity of RXR α wt-GFP was quantitated using confocal microscopy. There was significant increase of RXR α in the nucleus following 9-*cis*-RA (0.76 ± 0.02) treatment when compared to control (0.65 ± 0.06 , Fig 2.3A and 2.3D, $p < 0.05$). In HPK1A_{ras} cells transfected with RXR α wt-GFP plasmids, treatment with 9-*cis*-RA alone did not increase nuclear accumulation of RXR α (0.57 ± 0.027) compared to control (0.56 ± 0.065) ($p > 0.05$). However, pre-treatment with the MEK inhibitor UO126 followed by treatment with 9-*cis*-RA significantly increased the nuclear accumulation of RXR α compared to vehicle or 9-*cis*-RA alone treated cells (0.72 ± 0.014) (Fig. 2.3B and 2.3E, $p < 0.05$). In cells transfected with RXR α mut-GFP plasmids, 9-*cis*-RA treatment alone (0.84 ± 0.01) or a combination of UO126 and 9-*cis*-RA (0.86 ± 0.02) significantly increased nuclear accumulation of RXR α compared to vehicle (0.57 ± 0.02 , $p < 0.05$). Furthermore, treatment with the MEK inhibitor UO126 alone (0.67 ± 0.03) did not significantly increase nuclear accumulation of RXR α compared to vehicle (0.57 ± 0.02) (Fig. 2.3C and 2.3F, $p > 0.05$).

Effects of RXR α phosphorylation on VDR/ hRXR α nuclear colocalization in non-transformed HPK1A and ras-transformed HPK1A_{ras} cells

We used Pearson correlation coefficient to compare VDR/ RXR α colocalization in the nuclear compartment of the non-transformed and ras-transformed cells. In HPK1A cells co-transfected with VDR-mCherry/RXR α wt-GFP, treatment with $1\alpha,25(\text{OH})_2\text{D}_3$ (0.81 ± 0.01) significantly increased nuclear VDR/ hRXR α wt colocalization when compared to vehicle (0.41 ± 0.05 , Fig.2.4A and 2.4B,

$p < 0.0001$). The effect observed is similar to the one seen when RXR and VDR were transfected separately.

In HPK1Aras cells co-transfected with VDR-mCherry/RXR α wt-GFP, treatment with $1\alpha,25(\text{OH})_2\text{D}_3$ alone (0.46 ± 0.06) did not increase VDR/ hRXR α wt colocalization when compared to vehicle (0.40 ± 0.13 , Fig.2.4C, $p > 0.05$,).

However, treatment with UO126 alone (0.60 ± 0.05) or a combination of UO126 and $1\alpha,25(\text{OH})_2\text{D}_3$ (0.81 ± 0.02) significantly increased VDR /hRXR α nuclear colocalization when compared to control (Fig.2.4C, $p < 0.05$). When the cells were co-transfected with VDR-mCherry/RXR α mut-GFP, treatment with $1\alpha,25(\text{OH})_2\text{D}_3$ alone (0.81 ± 0.01) significantly increased VDR/ hRXR α mut colocalization when compared to vehicle (0.41 ± 0.05 , Fig.2.4D , $p < 0.05$). Similarly, treatment with UO126 alone (0.65 ± 0.02) or a combination of UO126 and $1\alpha,25(\text{OH})_2\text{D}_3$ (0.80 ± 0.01) significantly increased VDR /hRXR α nuclear colocalization when compared to control (Fig.2.4D, $p < 0.05$).

Effects of RXR α phosphorylation on VDR and hRXR α interaction in living cells using FRET

We used Fluorescence Resonance Energy Transfer (FRET) to investigate interaction between VDR and RXR α after ligand binding in both cell lines. We assayed FRET between our YFP and CFP-tagged proteins and compared it with cotransfected CFP and YFP probes which served as negative controls (Fig 2.5A). As expected our results showed VDR/RXR heterodimeric interaction indicating that our FRET pairs were competent to form heterodimers. No FRET signal was observed with the negative control CFP/YFP probes in both cell lines (Fig. 2.5B).

Next, we tested for VDR and RXR α interaction in both cell lines using the VDR-CFP and RXR α wt-YFP or RXR α mut-YFP FRET pairs. Results show that VDR form heterodimers with RXR α in the absence of ligand in both cell lines. In HPK1A cells co-transfected with VDR-CFP/RXR α wt-YFP, treatment with 1 α ,25(OH) $_2$ D $_3$ alone (10 ± 1.9 %) or a combination of UO126 and 1 α ,25(OH) $_2$ D $_3$ (5.5 ± 0.74 %) increased interaction between VDR and RXR α compared to vehicle (3.4 ± 0.62 %) or UO126 (3.2 ± 0.39 %) (Fig. 2.5C, $p < 0.05$). In cells co-transfected with VDR-CFP/RXR α mut-YFP, treatment with 1 α ,25(OH) $_2$ D $_3$ also increased FRET efficiency. However, treatment with UO126 or a combination of UO126 and 1 α ,25(OH) $_2$ D $_3$ had similar effects and did not increase FRET efficiency when compared to vehicle alone ($p > 0.05$). Efficiency increased only with 1 α ,25(OH) $_2$ D $_3$ treatment ($p < 0.005$, data not shown).

In HPK1Aras cells, co-transfection with VDR-CFP/RXR α wt-GFP and treatment with either 1 α ,25(OH) $_2$ D $_3$ (5.2 ± 0.56 %) or UO126 (4.7 ± 0.54 %) alone did not increase FRET efficiency compared to vehicle (4.6 ± 0.55 %, Fig. 2.5D, $p > 0.05$). However combined treatment of UO126 and 1 α ,25(OH) $_2$ D $_3$ significantly increased VDR/RXR α interaction compared to vehicle or 1 α ,25(OH) $_2$ D $_3$ treatment alone (7.0 ± 0.66 % ; Fig. 2.5D, $p < 0.05$). When the cells were co-transfected with VDR-CFP/RXR α mut-YFP, VDR and RXR α interaction significantly increased on treatment with 1 α ,25(OH) $_2$ D $_3$ (11.37 ± 0.46 %) when compared to vehicle (5.68 ± 0.57 %) (Fig. 2.5E, $p < 0.05$). Furthermore, combined treatment with UO126 and 1 α ,25(OH) $_2$ D $_3$ significantly increased VDR/RXR α interaction (12.73 ± 1.17 %) when compared to control (5.68 ± 0.57 %) (Fig. 2.5E, $p < 0.0001$). Taken together, these data suggests that VDR/RXR α interaction and heterodimerization is

enhanced when RXR α phosphorylation is blocked or abolished in the ras – transformed cells.

Effects of RXR α phosphorylation at serine 260 on intra-nuclear mobility of RXR α using FLIP

To test whether the receptors could be immobilized by binding to DNA, we used Fluorescence Loss In Photobleaching (FLIP) to investigate the intra-nuclear movement of RXR α . In these experiments, a living cell is repeatedly photobleached in the same spot using high laser power and the cell is imaged before each new round of photobleaching. If the GFP-labelled molecules are shuttling between the bleaching and reporting points, then the fluorescence will decrease at both points. Relatively immobile proteins in contrast will be bleached effectively at the bleaching point, but not at the reporting point. The rate of loss of fluorescence from the region of interest contains information on the rate of dissociation of the protein from the particular compartment (Fig. 2.6A-E) (Green et al., 1988). Thus by measuring the dissociation kinetics of RXR α within the nuclear compartments we could determine how mobile the protein is within the nuclear compartment and whether a fraction of it is immobile example by binding to chromatin. HPK1A cells were transfected with either RXR α wt-GFP or RXR α mut-GFP and treated with or without 1 α ,25(OH) $_2$ D $_3$. A nuclear area of 16 μm^2 (4 μm width) was next selected as the region of interest and repeatedly photobleached at 1 s interval for the duration of the experiments. Multiple data points gathered over time were fitted to a one phase dissociation curve. By repeatedly photobleaching an area within the nucleus (nucleoplasmic area) our results showed that more than

70 % of the RXR α -GFP nuclear pool was mobile in both cell lines. Furthermore, this observation showed that in the nuclear compartment, the nucleolus-associated pool of RXR α is continuously and rapidly exchanged with the nucleoplasmic pool. Consistent with this interpretation, repeated bleaching of a nucleus resulted in the complete loss of RXR α -GFP signal in the entire nucleus and also the cytoplasm. Thus, this experiment provided a direct demonstration of intra-nuclear mobility. Based on these, we calculated decay constant, half-time and the immobile fraction as described in methods. In HPK1A cells transfected with RXR α wt-GFP, the rate of dissociation of the receptor from the unbleached portion of the nucleus in 1 α ,25(OH) $_2$ D $_3$ treated cells was not significantly different from the vehicle control (data not shown, $p > 0.05$). The half time of dissociation of the RXR α wt-GFP in the nuclear compartment after 1 α ,25(OH) $_2$ D $_3$ treatment (112.02 ± 13.5 s) was longer than the vehicle control (98.11 ± 11.2 s data not shown, $p > 0.05$). FLIP experiments demonstrated that in the non-transformed HPK1A cells, RXR α rapidly exchanges between the bleached and unbleached portions of the nuclear compartment at a similar rate. Interestingly, RXR α was found to be stably anchored (28.0 ± 2.5 % bound) to other nuclear proteins within the nuclear compartment on treatment with 1 α ,25(OH) $_2$ D $_3$. This immobile fraction was significantly larger when compared to vehicle treated cells (10 ± 1.6 % bound, Fig. 2.6F, $p < 0.05$). Taken together, the results indicate that ligand addition in the non-transformed cells increases the half time of dissociation and bound fraction of the receptor in the unbleached portion of the nuclear compartment.

In the ras-transformed cells transfected with RXR α wt-GFP, treatment with 1 α ,25(OH) $_2$ D $_3$ significantly increased the decay rate compared to vehicle (data not shown). However there was no significant difference in the residence time of

RXR α in the nucleus of both 1 α ,25(OH) $_2$ D $_3$ or vehicle treated cells (data not shown, $p > 0.05$). Also, the percentage of immobile fraction was comparable but not significantly different between 1 α ,25(OH) $_2$ D $_3$ and (8.06 \pm 1.49 %) vehicle treatment (7.32 \pm 0.76 %, Fig.2.6G, $p > 0.05$). Interestingly, treatment with UO126 alone (14.81 \pm 2.0 %) or pre- treatment with UO126 followed by 1 α ,25(OH) $_2$ D $_3$ treatment (20.17 \pm 3.30 %) significantly increased the percentage of immobile fraction compared to control (Fig.2.6G, $p < 0.05$).

In HPK1Aras cells transfected with RXR α mutant-GFP, treatment with 1 α ,25(OH) $_2$ D $_3$ significantly decreased the decay rate when compared to vehicle (data not shown). The residence time of RXR α in the nuclear compartment in 1 α ,25(OH) $_2$ D $_3$ treated cells significantly increased when compared to vehicle control (data not shown, $p < 0.005$). Furthermore, the percentage of immobile fraction in 1 α ,25(OH) $_2$ D $_3$ treated cells was significantly higher (22.12 \pm 2.02 %) compared to vehicle (11.74 \pm 1.23 %, Fig.2.6H, $p < 0.05$). The effect observed was probably due to slowly exchanging receptor pools and binding to nucleoplasmic components. Furthermore, treatment with UO126 alone (16.00 \pm 1.674 %) or combined treatment with UO126 followed by 1 α ,25(OH) $_2$ D $_3$ treatment (23.46 \pm 2.67 %) significantly increased the percentage of immobile fraction compared to control (Fig.2.6H, $p < 0.05$).

Effects of 1 α ,25(OH) $_2$ D $_3$ on VDR/RXR α complex binding to DNA in non-transformed HPK1A and ras-transformed HPK1Aras cells

We first assessed the effects of RXR α phosphorylation on VDR/RXR complex binding to DNA in HPK1A cells (Fig. 2.7 A and B). HPK1A cells transfected with

VDR-GFP (Fig. 2.7A) or RXR α wt-GFP (Fig. 2.7 D) and treated with vehicle or 1 α ,25(OH) $_2$ D $_3$ were fixed and stained with Hoechst 33342, a widely used DNA-specific dye, which emits blue fluorescence under ultraviolet (UV) illumination when bound to DNA. Hoechst has a preference to bind to A/T-rich DNA sequences and highlight a subset of the genome. Colocalization of RXR α wt-GFP or VDR-GFP and DNA (Hoechst 33342) was compared using Pearson's correlation coefficient. Results showed that the VDR/RXR complex bound more to DNA in cells treated with 1,25(OH) $_2$ D $_3$ compared to vehicle (Fig, 2.7A-2.7E, $p < 0.001$). We next compared VDR/RXR complex binding to DNA in HPK1Aras cells transfected with either VDR-GFP or RXR α wt-GFP. We found no significant difference in 1,25(OH) $_2$ D $_3$ compared to vehicle treated cells (Fig, 2.7F and 2.7G, $p > 0.05$). However, when cells were pre-treated with UO126 followed by 1,25(OH) $_2$ D $_3$ treatment, binding to DNA significantly increased compared to vehicle or 1,25(OH) $_2$ D $_3$ treatment alone (Fig. 2.7F and 2.7G, $p < 0.05$). Similarly, in HPK1Aras cells transfected with RXR α mut-GFP and treated with 1,25(OH) $_2$ D $_3$, a significant increase in the VDR/RXR complex binding to DNA was observed when compared to vehicle (Fig. 2.7H, $p < 0.05$). Pre-treatment with UO126 followed by 1,25(OH) $_2$ D $_3$ increased binding to DNA when compared to vehicle treatment alone. However, there was no significant difference in levels compared to treatment with 1,25(OH) $_2$ D $_3$ alone (Fig 2.7H, $p < 0.05$).

DISCUSSION

The effects of 1 α ,25(OH) $_2$ D $_3$ on keratinocytes and other cancer cells have been reported to include growth inhibition, cell cycle arrest, induction of differentiation and apoptosis (Sebag et al., 1992; Colston et al., 1994; Lee et al., 1995; Simboli-

Campbell et al., 1997; Wu et al., 1997; Colston and Hansen, 2002; Hager et al., 2004; Alagbala et al. 2007; Welsh, 2007; Lianjun et al., 2008;). In our earlier studies (Sebag et al., 1992; Solomon et al., 2001; Macoritto et al., 2008), we found that the immortalized non-transformed (HPK1A) cells were more sensitive to the growth inhibitory action of $1\alpha,25(\text{OH})_2\text{D}_3$ compared to the neoplastic, ras-transformed (HPK1Aras) keratinocytes. However, pre-treatment of HPK1Aras cells with MEK inhibitors partially restored the sensitivity of the ras-transformed cells to $1\alpha,25(\text{OH})_2\text{D}_3$ (Macoritto et al., 2008). In the present study the effect on growth inhibition were further corroborated with cell cycle distribution data which showed a shift following MEK inhibitor UO126 and $1\alpha,25(\text{OH})_2\text{D}_3$ treatment with more than 80 % of cells arrested in G0/G1 phase and a reduction in percentage of S-phase entry cells. However, in the ras-transformed cells, the effects of $1\alpha,25(\text{OH})_2\text{D}_3$ on cell cycle distribution was only observed after pre-treatment with UO126. To further explain the mechanisms by which hRXR α phosphorylation at serine 260 impairs vitamin D signaling in ras-transformed cell lines (Sebag et al., 1992; Macoritto et al., 2008), we examined changes in subcellular localization, VDR/ RXR α interaction and DNA binding. Investigating the subcellular localization of both VDR and RXR α in non-transformed and ras-transformed cell lines, we found that although VDR can partition from the cytoplasm to the nucleus as a single entity, its nuclear accumulation is increased when it forms a complex with RXR α . Also, transfection of the ras-transformed cells with a non-phosphorylatable mutant increased the nuclear accumulation of RXR α from 45 to 60 %. The results thus suggest that VDR and RXR α can both reside in the cytoplasm and nucleus in the absence of ligand. While ligand binding increases the nuclear localization of both VDR and RXR α in the non-transformed cells,

significant further nuclear accumulation of both receptors with ligand is only observed in ras-transformed cells following transfection with either the non-phosphorylatable RXR α -mutant or pre-treatment with the MEK inhibitor UO126. Our findings on both VDR and RXR α distribution in the non-transformed cells is not only supported by other reports (Barsony et al., 1990; Jakob et al. 1992; Reichrath et al., 1997; Sugawara et al., 1997; Prufer et al., 2000; Narayanan et al., 2004) but it also reveals new and interesting features of the distribution of both VDR following 1 α ,25(OH) $_2$ D $_3$ treatment and RXR α following either 1 α ,25(OH) $_2$ D $_3$ or 9-cis-RA treatment in the non-transformed and ras-transformed cells.

These data clearly suggest that phosphorylation of RXR α retains a fraction of RXR α in the cytoplasm and this fraction is induced to undergo nuclear localization upon blocking phosphorylation (Yasmin et al., 2005). In the current study, the heterodimer experiments carried out with cyan and yellow fluorescent chimeras of VDR, RXR α wt and a non-phosphorylatable RXR α -mutant using FRET microscopy thus confirmed that compared to non-transformed HPK1A cells, VDR/RXR α heterodimer interaction in ras-transformed cells was compromised and that blocking phosphorylation either by pre-treatment with the MEK inhibitor UO126 or the non-phosphorylatable RXR α -mutant improves VDR/ RXR α interaction. The validity of FRET studies showing that tagged constructs are competent to form heterodimers are well supported by previous work on the impact of dimerization on subcellular trafficking using FRET (Prufer et al., 2000). Our results are also supported by previous reports showing that the nuclear import of VDR is enhanced in the presence of RXR thus suggesting that this process

involves VDR-RXR heterodimers formation (Prufer et al., 2000, 2002; Yasmin et al., 2005).

Our current study further support the view that heterodimerization may influence the subcellular localization of the VDR/RXR α heterodimers. Our confocal imaging studies using confocal microscopy clearly showed that dimerizing RXR α with VDR facilitates nuclear accumulation of VDR. Furthermore, our FRET data gave a mechanistic support to these subcellular localization imaging studies. While our observation supports a novel mechanism by which the RXR heterodimerization partner dominates the activity of the heterodimers, it differs from reports from Yasmin and co-workers (2005) suggesting that nuclear accumulation of RXR-VDR heterodimers is mediated predominantly by the VDR. Our results are more consistent with the predominant role played by RXR α at least in this cancer model.

Previous research had demonstrated that steroid receptors are in constant rapid motion within the nucleus and that they accumulate in discrete nuclear foci after hormone binding (McNally et al., 2000; Tyagi et al., 2000; Stenoien et al., 2001).

Previous FRET studies in living cells using RXR α and vitamin D receptor (VDR) fluorescent chimeras have led to the conclusion that RXR α does not only dynamically shuttle between nucleus and cytoplasm but it also heterodimerizes with VDR in the cytoplasm regardless of calcitriol ($1\alpha,25(\text{OH})_2\text{D}_3$) binding status (Barsony et al., 1997; McNally et al., 2000; Dawson and Xia., 2012). Also, photobleaching studies with VDR and RXR tagged fluorescent chimeras have revealed that they also move rapidly within the nucleus and accumulate in foci upon agonist treatment (Racz and Barsony, 1999; Prufer et al., 2000, 2002).

Pruffer et al., (2000, 2002) reported that VDR, RXR heterodimerization can occur in the cytoplasm without ligand addition. Although, we did not measure RXR/VDR heterodimerization in the cytoplasm, we showed by colocalization studies and FRET that the VDR/RXR heterodimerizes in the nucleus without ligand addition and that ligand addition increases heterodimerization and interaction.

Our results on intra-nuclear binding of RXR α as assayed by FLIP in live cells showed that phosphorylation decreased binding of hRXR α to chromatin in the nuclear compartment of ras-transformed cells and that ligand addition blunted this interaction. These live cells studies confirm and expand our previous data demonstrating that blocking phosphorylation with a non-phosphorylatable RXR α mutant in the ras-transformed HPK1Aras cells increased RXR α binding to DNA and subsequently restored vitamin D function (Macorrito et al., 2008). However, our data indicate that within the nuclear compartment, movement of RXR α is not restricted to particular nuclear domains. We recorded two distinct kinetic pools of RXR α -GFP in the nucleus; a large mobile pool, which represents the continuously exchanging molecules within the nucleoplasmic compartment responsible for the fluorescence signal loss and a smaller, less mobile (bound) fraction which does not contribute to the fluorescence loss over the time scale of the experiment. We hypothesize that this immobile fraction could represent receptor bound to DNA or to chromatin.

We tested the hypothesis by quantifying colocalization of GFP-tagged receptor with Hoechst dye on chromatin structure at the level of individual pixels using the Pearson correlation coefficient. Our results are in accordance with the FLIP results showing that binding is affected in the ras-transformed keratinocytes. Since

$1\alpha,25(\text{OH})_2\text{D}_3$ does not bind to $\text{RXR}\alpha$, it is possible that the non-phosphorylatable $\text{RXR}\alpha_{\text{mut}}\text{-GFP}$ induced a conformational change allowing VDR to bind DNA upon ligand addition and resulting in docking of new factors or the recruitment of cofactors to the VDR- $\text{RXR}\alpha$ receptor complex. The increase in residence time after ligand addition as shown by FLIP might also reflect the strengthening of the interaction with slowly or non-diffusing nuclear components such as chromatin. Furthermore, the increased interaction could result from either an increased affinity or from stabilization of interaction leading to longer binding events (Misteli et al., 2000; Feige et al., 2005). In the ras transformed cells, protein phosphorylation which is known to alter DNA interaction could inhibit immobilization of receptors on chromatin leading to inhibition of vitamin D signaling in the cancer cells (Lu et al., 1995; Dou et al., 1999). Solomon and co workers (1999) previously proposed that in ras-transformed cells, $\text{RXR}\alpha$ phosphorylation at serine 260 would result in conformational changes within the LBD, disrupting the interactions with co-regulators and therefore decreasing transcriptional activities ultimately resulting in resistance to the growth inhibitory action of vitamin D. More recently we reported that phosphorylation at Serine 260 impairs recruitment of DRIP205 and other co-activators to the VDR- $\text{RXR}\alpha$ heterodimer (Macoritto et al., 2008) whereas other groups reported that it also delayed nuclear export and $\text{RXR}\alpha$ degradation in hepatocellular carcinoma (Matsushima-Nishiwaki et al., 2001). Quack and Carlberg (2000) using limited protease digestion and gel shift clipping experiments demonstrated that binding of RXR to VDR not only induces conformational changes to VDR but also the conformational changes induced by ligand binding stabilized VDR/ RXR dimers (Carlberg et al., 2001). Feige and co workers (2005) using FRET to study PPAR- RXR interaction showed that PPAR- RXR

dimerization occurred prior to ligand binding or DNA binding, however heterodimer binding to DNA was only observed to be stable *in vivo* after ligand had bound (Tyagi et al., 2000). Increasing evidence indicates that RXR does not play a passive role as a heterodimeric partner but impacts the responses of its nuclear receptor (NR) partner, regardless of its permissive, nonpermissive, or conditionally permissive status (Bettoun et al., 2003). Taken together these results including ours demonstrate an important role of RXR in VDR/RXR heterodimer binding to target DNA sequences in living cells.

In summary, we show that in ras-transformed cells, RXR α phosphorylation at serine 260 affected VDR, RXR α subcellular localization, VDR/ RXR α heterodimer interaction and VDR/ RXR α complex binding to DNA. These studies suggest that blocking phosphorylation either by the use of a MEK inhibitor or using a non-phosphorylatable RXR α mutant might be effective in the treatment of cancers with a Ras signature.

Proposed model for restoration of vitamin D sensitivity in ras-transformed keratinocytes

A model proposed on how RXR α phosphorylation at serine 260 could affect VDR and RXR interaction and nucleoplasmic trafficking is shown (Fig. 2.8). (A) In normal cells, it is subject to debate whether VDR and RXR move independently or as a complex from the cytoplasm to the nucleus. However, the nuclear import of their mutual heterodimer is controlled predominantly by RXR and regulated by $1\alpha,25(\text{OH})_2\text{D}_3$. Pruffer and coworkers (2000) proposed that in the absence of $1\alpha,25(\text{OH})_2\text{D}_3$ RXR controls the movement of the VDR/RXR complex from the

cytoplasm to nucleus. And in the presence of $1\alpha,25(\text{OH})_2\text{D}_3$, the VDR controls this process. Once in the nucleus, the VDR/RXR heterodimer can bind to chromatin and carry out gene transcription.

(B) In ras-transformed cells VDR and RXR could still move into the nucleus independently or as a complex. **Phosphorylation of RXR alters the conformation of the RXR, which indirectly prevents the mobilization of a large proportion of the mutual heterodimer from entering the nuclear compartment leading to a decrease in localization and binding to chromatin.**

Acknowledgments

We thank Dr. J. White for providing the human vitamin D receptor expression plasmid and Dr. Stephan Laporte for the GFP expression plasmids. Furthermore, we thank Dr. Benoit Ochiatti for the work on subcloning the GFP-tagged plasmids. Lastly, we thank Dr. Min Fu for her assistance with the LSM780 confocal microscopy.

Figure 2.1. Effects of 1,25(OH)₂D₃ and UO126 on cell growth (A,B) and viability (C,D). (A) HPK1A and (B) HPK1Aras cells were seeded at a density of 1x10⁴ cells/well in 24 well plates and grown in DMEM medium containing 10% FBS. At 40% confluency medium was changed and cells were treated with increasing concentrations of 1,25(OH)₂D₃ in the absence or presence of UO126 (10⁻⁶ M). After 72 hours, cells were collected and cells were counted using a coulter counter. HPK1A (C) and HPK1Aras (D) cells were seeded at a density of 5x10³ cells/well in 96 well plates. Twenty four hours later, cells were treated with vehicle, 1,25(OH)₂D₃ alone or a combination of UO126 and 1,25(OH)₂D₃ for 72 hrs. Alamar Blue metabolism was used to assess cell viability. Values are expressed as a percentage of vehicle- treated cells. All values represent means ± SE (bars) of at least three separate experiments conducted in triplicate. Open circles (o) indicate a significant growth inhibition as compared to vehicle-treated cells. Asterisks (*) indicate a significant difference between vehicle treated and treated cells. A p value of P < 0.05 was considered significant.

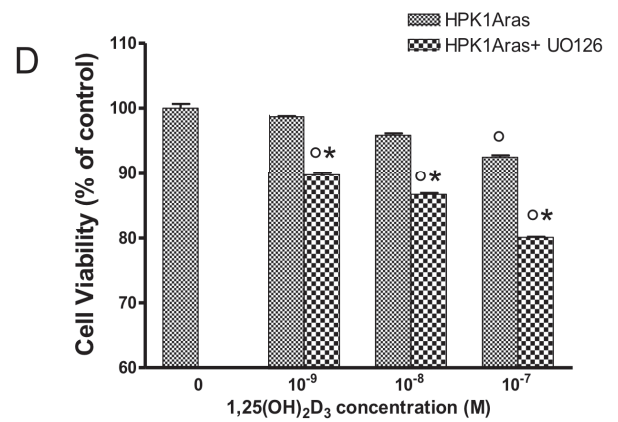
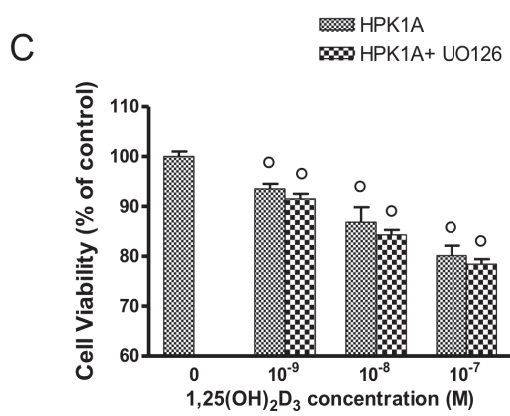
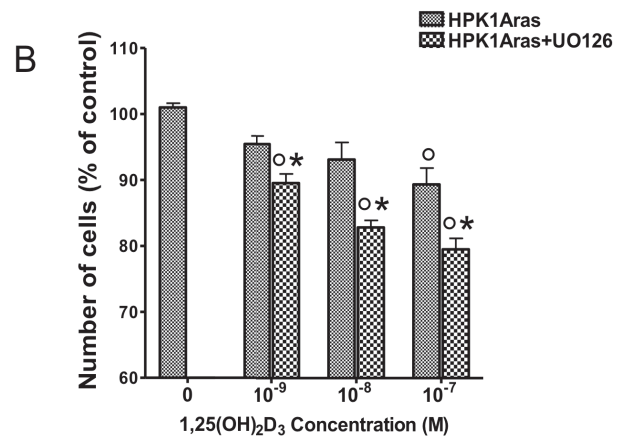
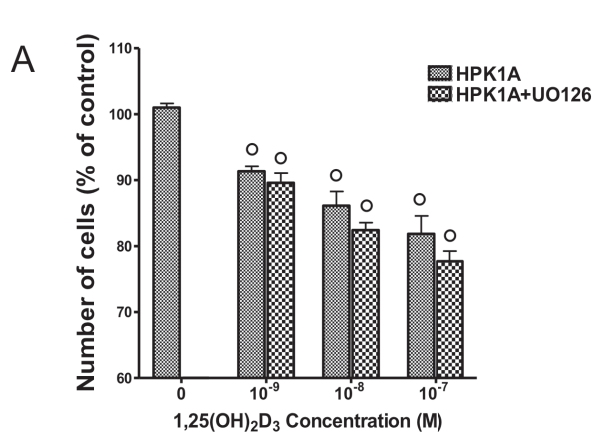
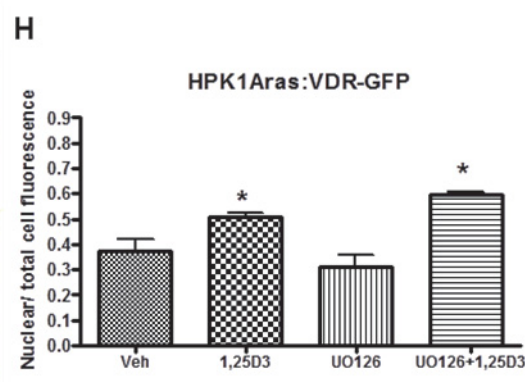
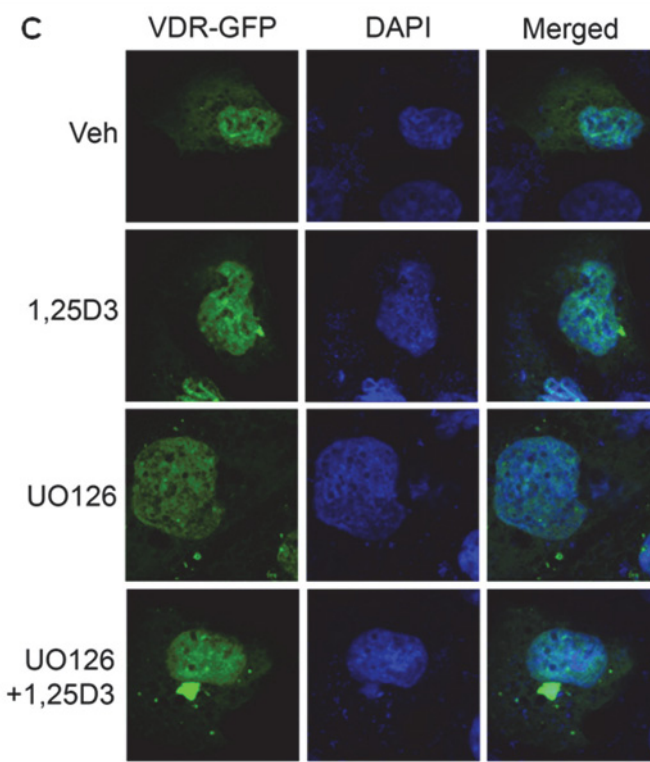
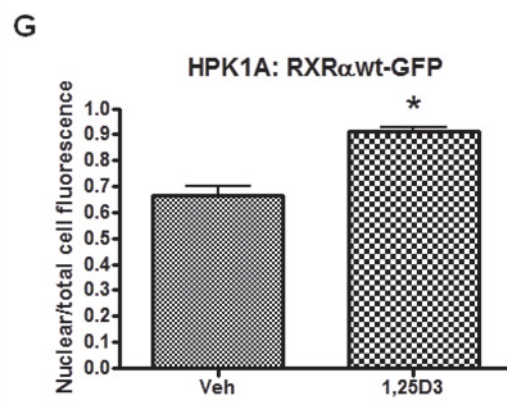
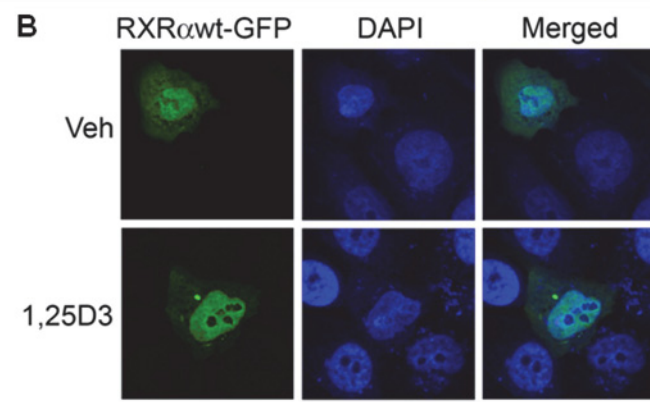
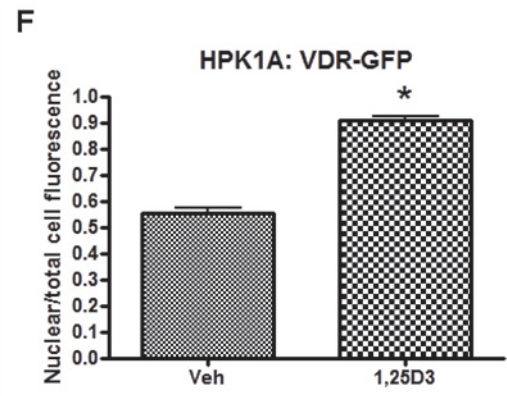
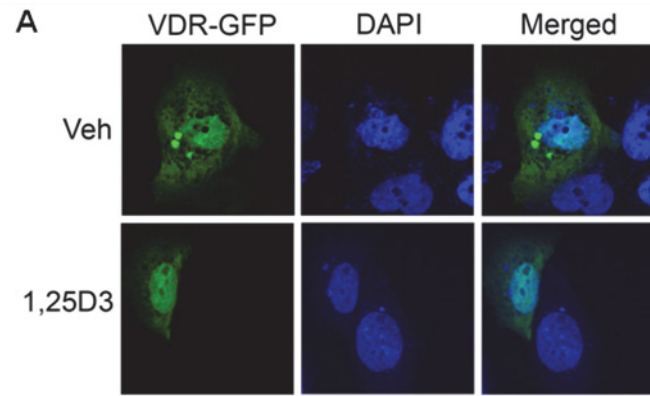


Table 2.1: Cell cycle analysis of HPK1A and HPK1A_{ras} cells following treatment with 1,25(OH)₂D₃ in the absence or presence of UO126. After 24 hr of serum starvation (5 % FBS) cells were treated with 1,25(OH)₂D₃ at 10⁻⁷M with or without UO126. Cells were trypsinized after 72 hrs and cell cycle analyzed by flow cytometry as described under “Materials and Methods”. Results are expressed as percentage of cells in Go/G1 and G2/M phases of cell cycle. Asterisks (*) indicate a significant growth inhibition as compared to vehicle-treated control. Open circles (o) indicates a significant difference between 1,25(OH)₂D₃ treatment alone and combined treatment of UO126 and 1,25(OH)₂D₃. A triangle (Δ) represents significant difference between UO126 treatment alone and combined treatment of UO126 and 1,25(OH)₂D₃. A p value compared to control was considered significant when p < 0.05.

| Percentage of cells in G0/G1 cell cycle phase | | |
|--|----------------|----------------|
| Treatment | HPK1A | HPK1Aras |
| Vehicle | 70.66 ± 1.86 | 64.88 ± 1.13 |
| 1,25 (OH) ₂ D ₃ (10 ⁻⁷ M) | 79.50 ± 2.07* | 69.23 ± 0.93* |
| UO126 | 80.92 ± 1.76 * | 74.71 ± 0.7* |
| UO126 + 1,25 (OH) ₂ D ₃ (10 ⁻⁷ M) | 81.20 ± 2.2* | 81.03 ± 1.9*oΔ |

Figure 2.2: Effects of $1,25(\text{OH})_2\text{D}_3$ with or without UO126 treatment on nuclear localization of VDR and RXR α in HPK1A and HPK1Aras cells. HPK1A cells were transfected with VDR-GFP (A) or RXR α -wt-GFP (B) followed by treatment with either vehicle (veh) or $1,25(\text{OH})_2\text{D}_3$. Similarly, HPK1Aras cells were transfected with either VDR-GFP (C), RXR α -wt-GFP (D) or RXR α -mut-GFP (E) followed by treatment with either vehicle, $1,25(\text{OH})_2\text{D}_3$, UO126 alone or a combination of UO126 and $1,25(\text{OH})_2\text{D}_3$. Nuclear localization was assessed as in the methods. Bar graphs, (2F, G, H, I, J) shows the quantitation of fluorescence of nuclear receptors normalized to total cell fluorescence. Values represent mean \pm SE of at least 10 different cells. Asterisks (*) indicate a significant difference in nuclear localization between $1,25(\text{OH})_2\text{D}_3$ treatment alone or combined UO126 and $1,25(\text{OH})_2\text{D}_3$ treatment compared to vehicle-treated control. A p value of $P < 0.05$ was considered significant.



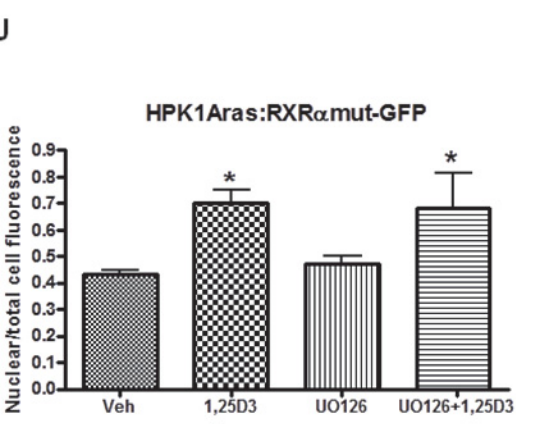
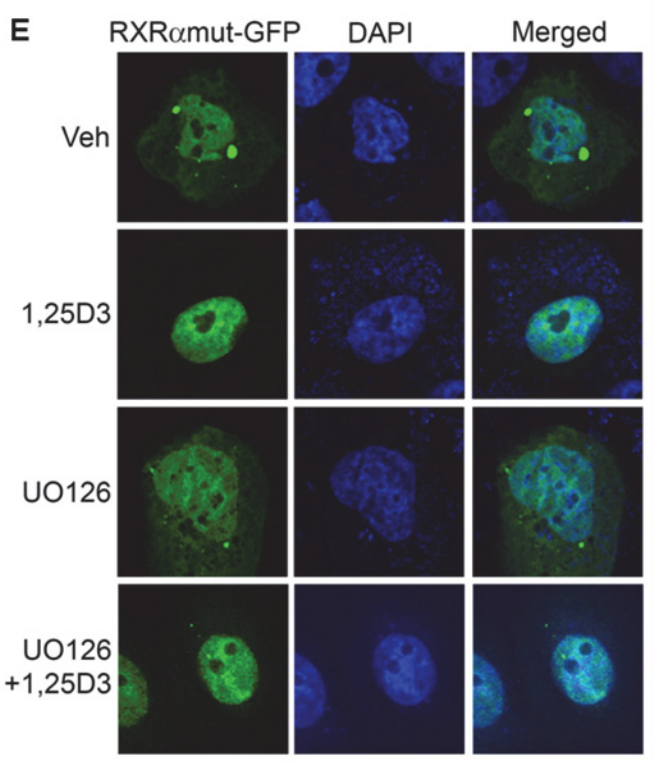
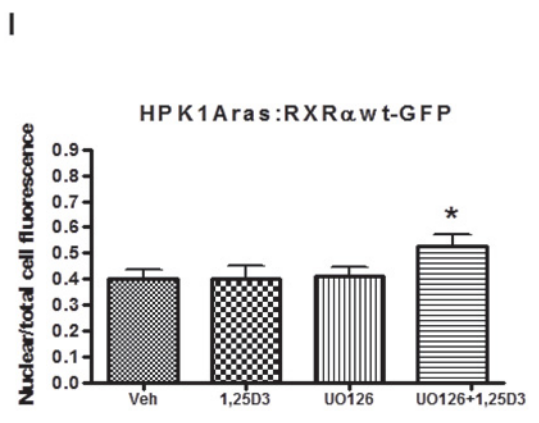
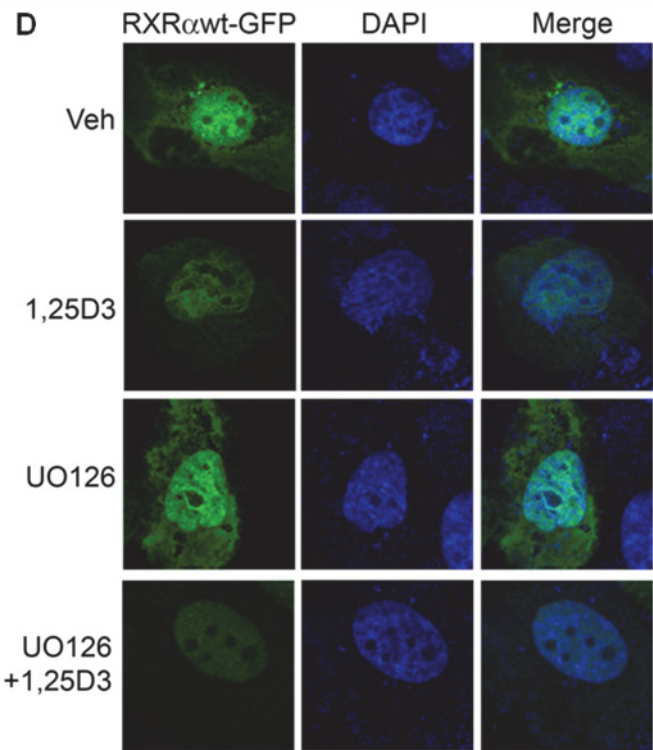
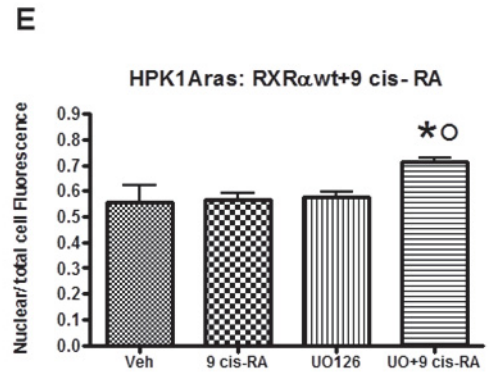
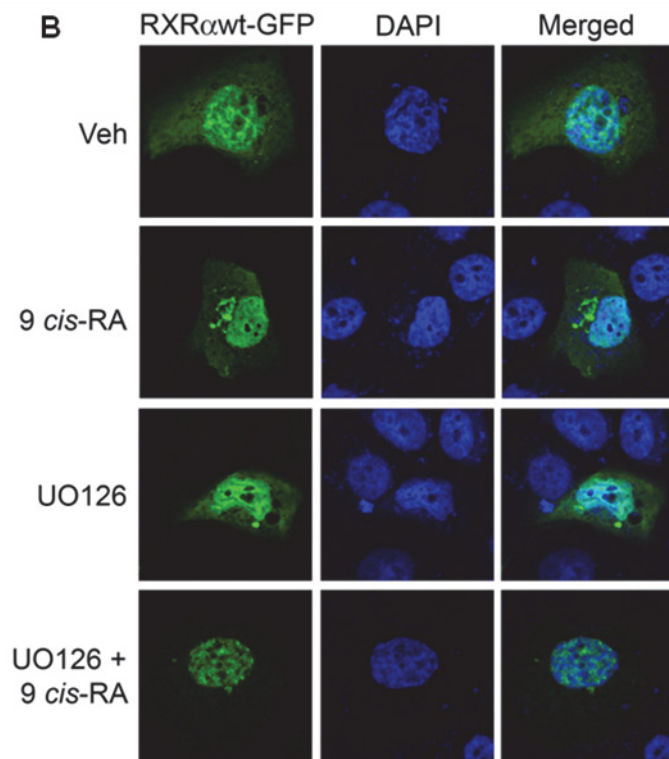
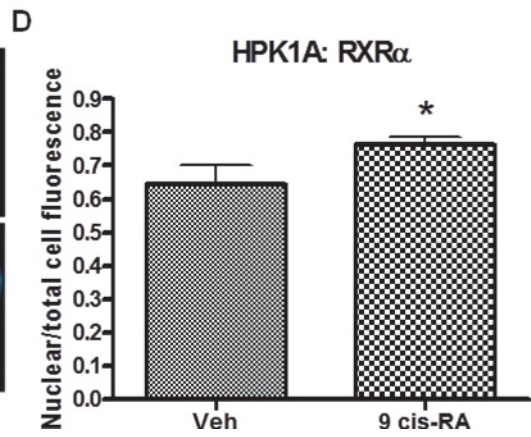
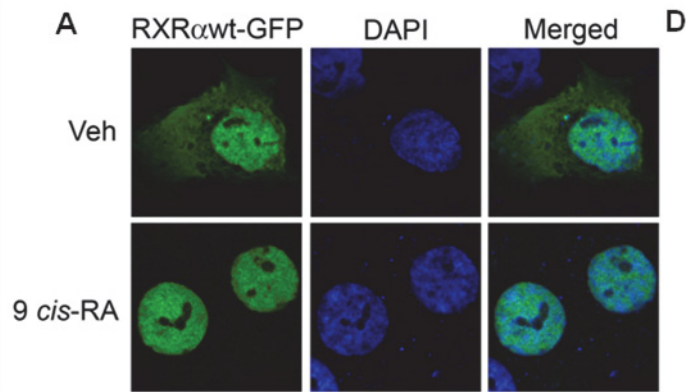


Figure 2.3: Effects of 9 cis-Retinoic Acid on RXR α subcellular localization in HPK1A and HPK1A_{ras} cells. HPK1A cells were transfected with (RXR α -wt-GFP (A and D) followed by treatment with either vehicle (Veh) or 9 cis-RA for four hours. Similarly, HPK1A_{ras} cells were transfected with either RXR α -wt-GFP (B and E) or RXR α -mut-GFP (C and F) followed by treatment with either vehicle, 9 cis-RA, UO126 alone or a combination of UO126 and 9 cis-RA. Nuclear localization was assessed as in the methods. Bar graphs, (2F, G, H, I, J) shows the quantitation of fluorescence of nuclear receptors normalized to total cell fluorescence. Values represent mean \pm SE of at least 10 different cells. Asterisks (*) indicate a significant difference in nuclear localization between 9 cis-RA treatment alone or combined UO126 and 9 cis-RA treatment compared to vehicle-treated control. Open circle (o) indicates a significant difference in nuclear localization of receptors in combined UO126 and 9 cis-RA treatment compared to 9 cis-RA treated cells alone. A p value of $P < 0.05$ was considered significant.



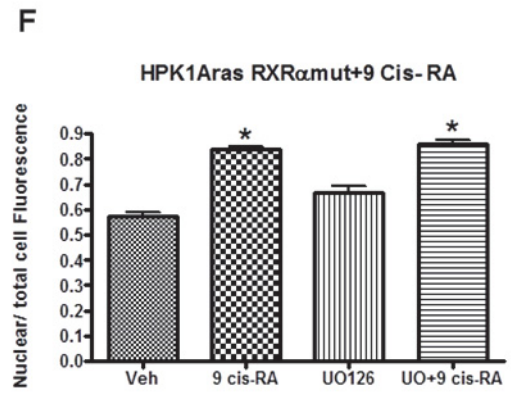
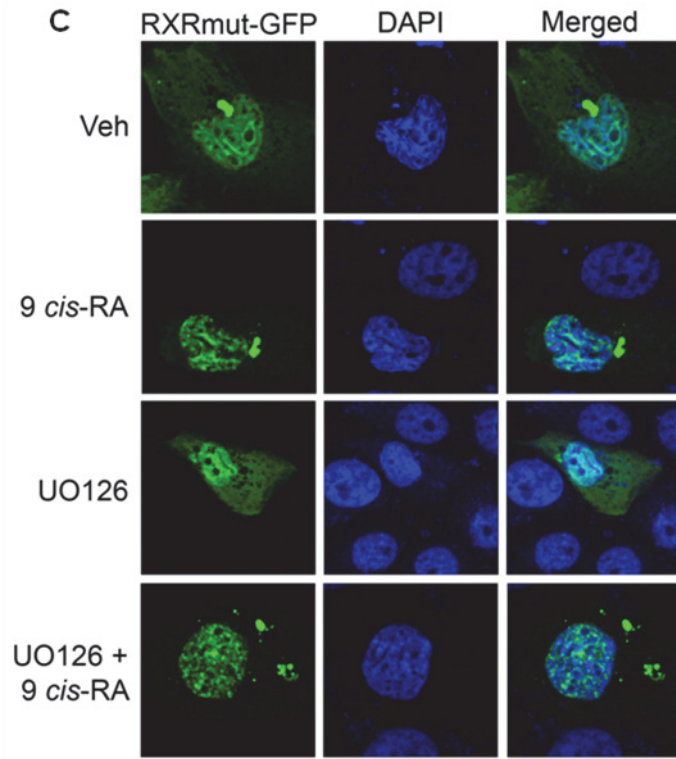


Figure 2.4: Effects of RXR α phosphorylation on VDR/hRXR α co-trafficking (colocalization) in HPK1A and HPK1Aras cells. Cells were co-transfected with either VDR-mCherry/RXR α wt-GFP or VDR-mCherry/RXR α mut-GFP. Following transfection, cells were treated with either vehicle, 1,25(OH) $_2$ D $_3$, UO126 alone or a combination of UO126 and 1,25(OH) $_2$ D $_3$. Bar graph shows colocalization measurement using Pearson correlation coefficient of HPK1A cells co-transfected with VDR-mCherry/RXR α wt-GFP (B) or HPK1Aras cells co-transfected with either VDR-mCherry/RXR α wt-GFP (C) or with or VDR-mCherry/RXR α mut-GFP (D). Values are mean \pm SE of at least 10 cells per treatment condition. Asterisks (*) indicate a significant difference in co-trafficking between 1,25(OH) $_2$ D $_3$, UO126 treatment alone or combined UO126 and 1,25(OH) $_2$ D $_3$ treatment compared to vehicle-treated control. Open circle (O) indicates a significant difference in co-trafficking between combined UO126 and 1,25(OH) $_2$ D $_3$ treatment compared to 1,25(OH) $_2$ D $_3$ treated cells alone. A p value of P < 0.05 was considered significant.

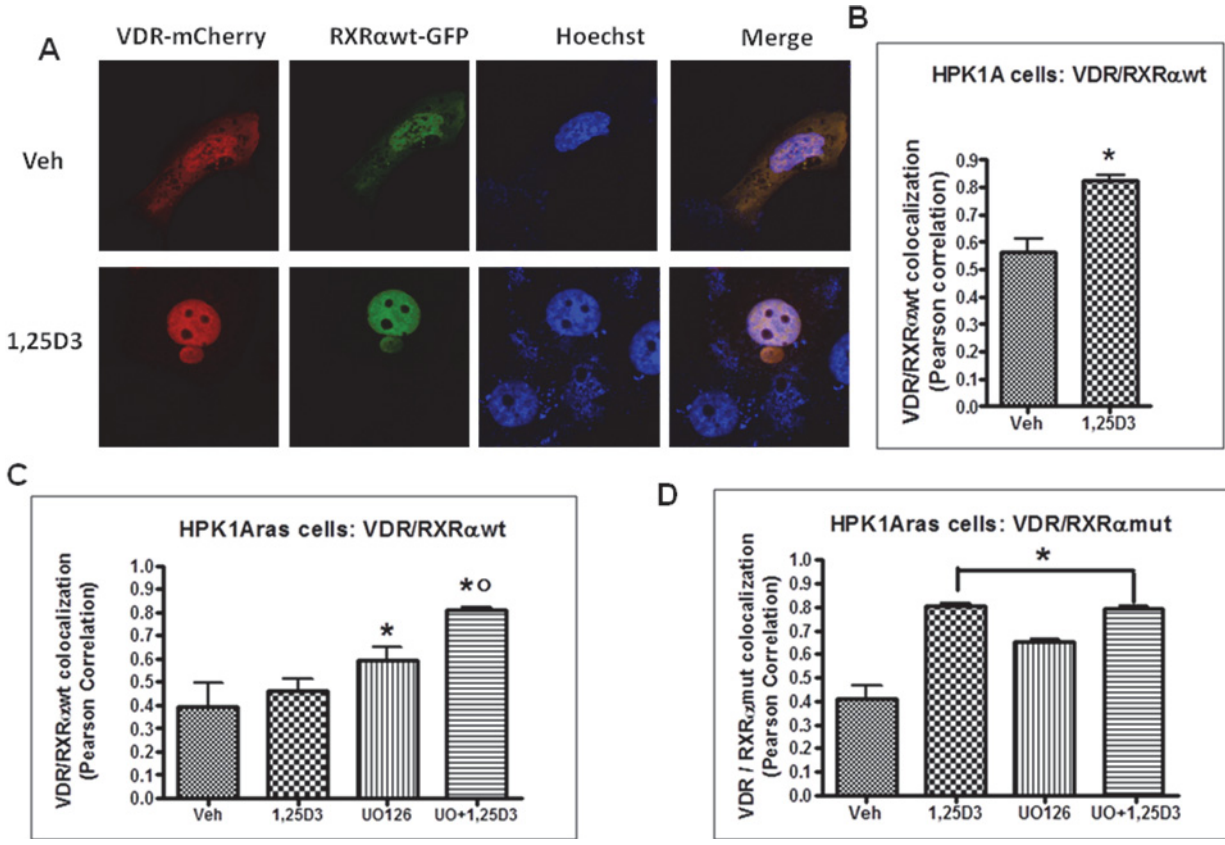


Figure 2.5: Effects of RXR α phosphorylation on VDR and RXR interaction in HPK1A and HPK1A_{ras} cells. Fluorescent Resonance Energy Transfer (FRET) (A) was measured by acceptor photobleaching as described in methods. Cells were co-transfected with either VDR-CFP/RXR α wt-YFP or VDR-CFP/RXR α mut-YFP. Following transfection, cells were treated with either vehicle, 1,25(OH) $_2$ D $_3$, UO126 alone or a combination of UO126 and 1,25(OH) $_2$ D $_3$. Bar graph shows FRET measurement of HPK1A cells co-transfected with VDR-CFP/RXR α wt-YFP (B) or HPK1A_{ras} cells co-transfected with either VDR-CFP/RXR α wt-YFP (C) or with VDR-CFP/RXR α mut-YFP (D). Values are mean percentage dequenching \pm SE of at least 10 cells per treatment condition. Asterisks (*) indicates a significant difference in interaction between 1,25(OH) $_2$ D $_3$ treatment alone or combined UO126 and 1,25(OH) $_2$ D $_3$ treatment compared to vehicle-treated control. Open circle (O) indicates a significant difference in interaction between combined UO126 and 1,25(OH) $_2$ D $_3$ treatment compared to 1,25(OH) $_2$ D $_3$ treated cells alone. A p value of P < 0.05 was considered significant.

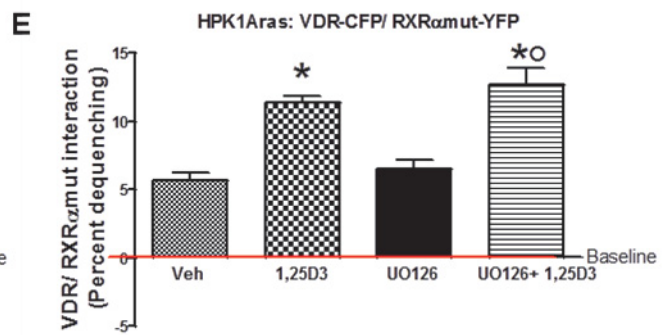
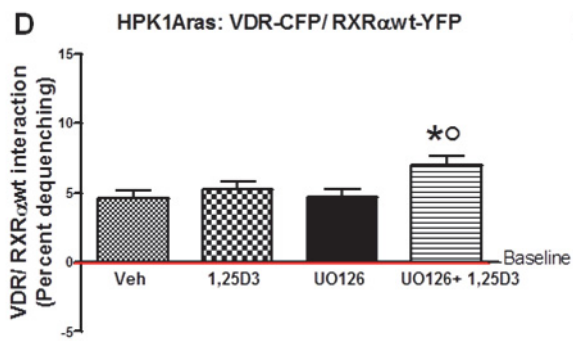
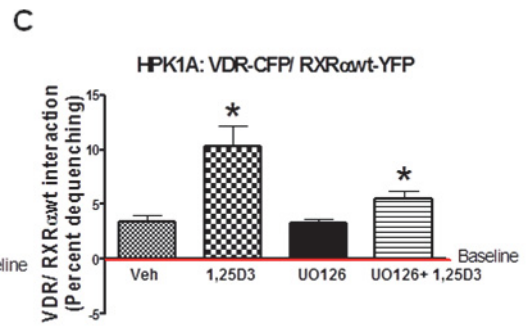
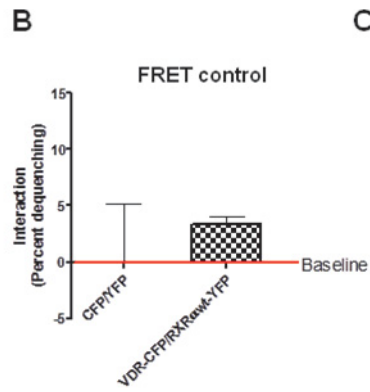
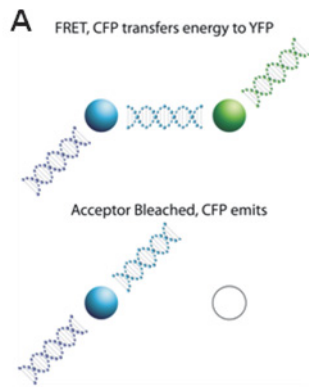


Figure 2.6: Effects of RXR α phosphorylation on nucleocytoplasmic kinetics of RXR α in HPK1A and HPK1A_{ras} cells. Fluorescent Loss in Photobleaching (FLIP) methodology was used to assess nucleocytoplasmic kinetics. HPK1A cells (A-E) were transfected with either RXR α wt-GFP. Following transfection, live cells were treated with either vehicle (Veh) or 1,25(OH) $_2$ D $_3$ and nucleocytoplasmic trafficking was measured using confocal microscopy (see methods). Nuclear area was selected and photobleached (A), other regions of interests measured but not photobleached (B1-3). In (C) time course showing and unbleached nucleus of a neighbouring cell (i) and a cell with a bleached nucleus (ii). The normalized fluorescent intensity of the unbleached and bleached nuclei above is shown in (D). The dissociation curve of vehicle and 1,25(OH) $_2$ D $_3$ treated cells are shown in (E). The bound fraction of HPK1A cells transfected with RXR α wt-GFP (F) or HPK1A_{ras} cells transfected with either RXR α wt-GFP (G) or RXR α mut-GFP (H) are similarly shown. Values are mean \pm SE of at least 10 cells per treatment. Asterisks (*) indicate a significant difference in bound fraction between 1,25(OH) $_2$ D $_3$, UO126 treatment alone or combined UO126 and 1,25(OH) $_2$ D $_3$ treatment compared to vehicle treated. Open circle (O) indicates a significant difference in combined UO126 and 1,25(OH) $_2$ D $_3$ treatment compared to 1,25(OH) $_2$ D $_3$ treated cells. A p value < 0.05 was considered significant.

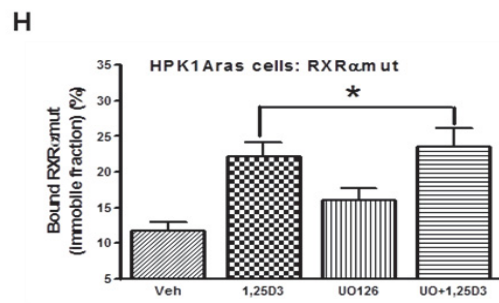
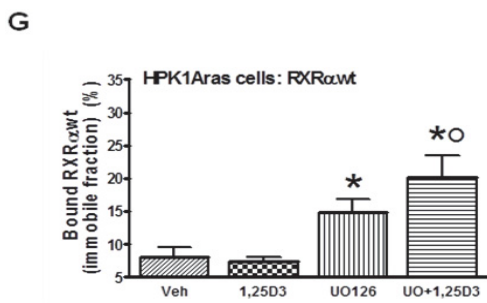
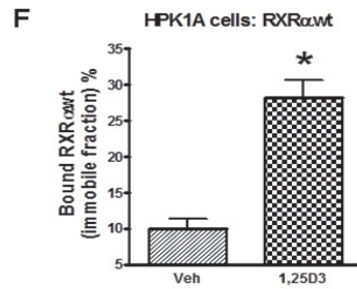
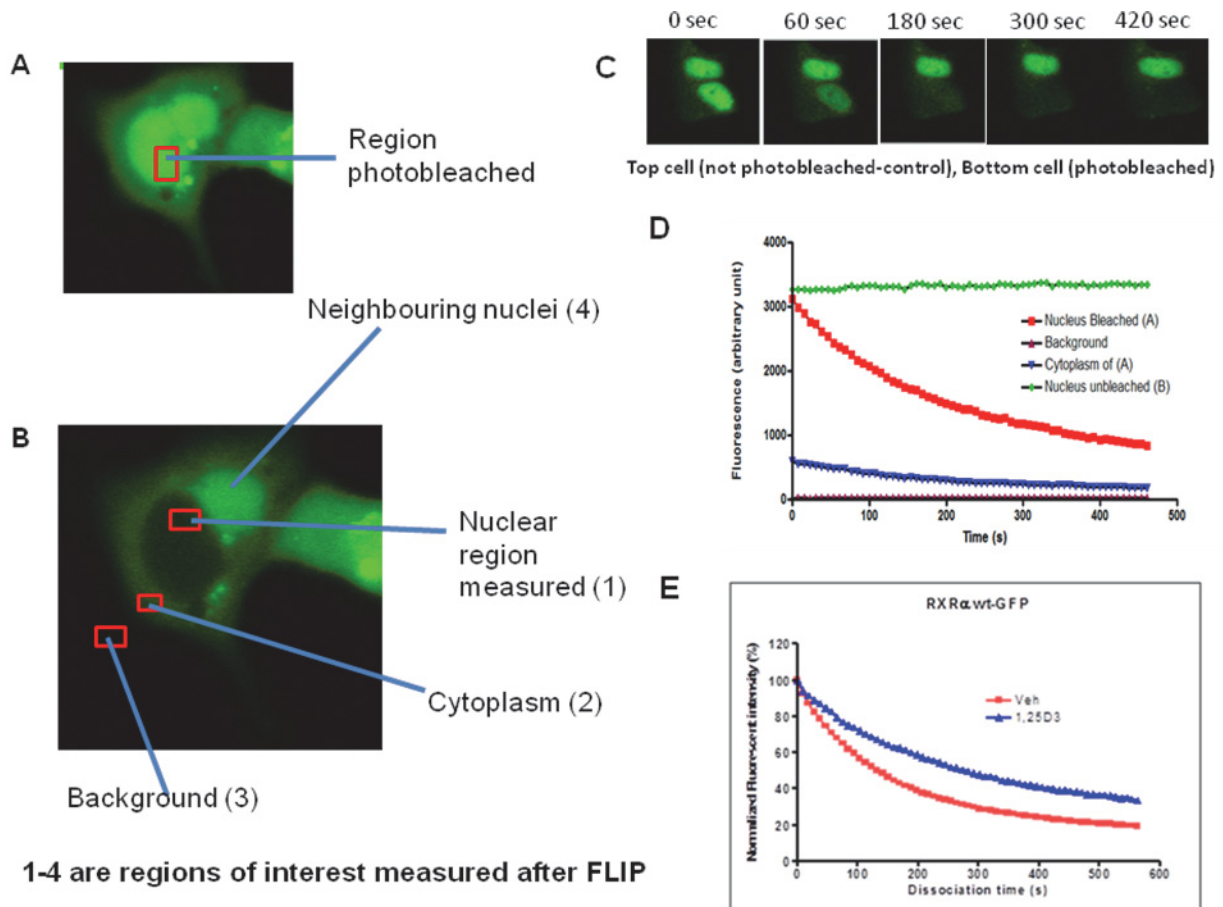
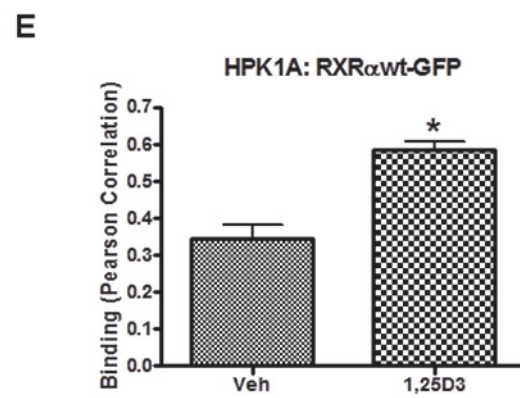
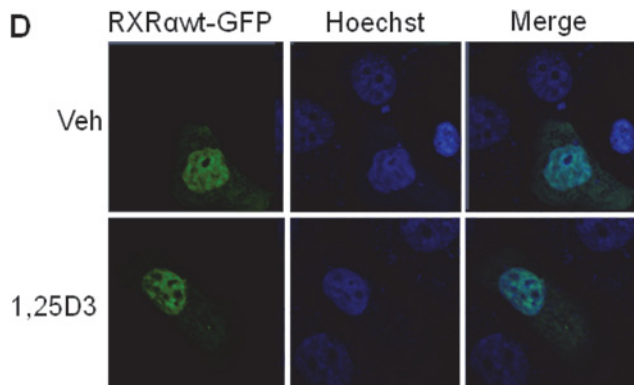
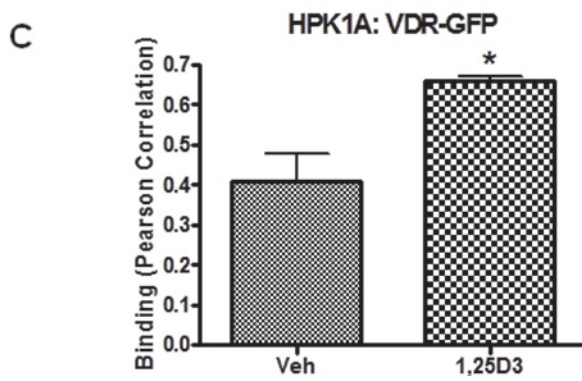
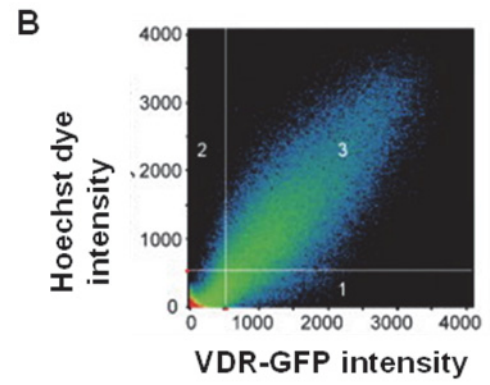
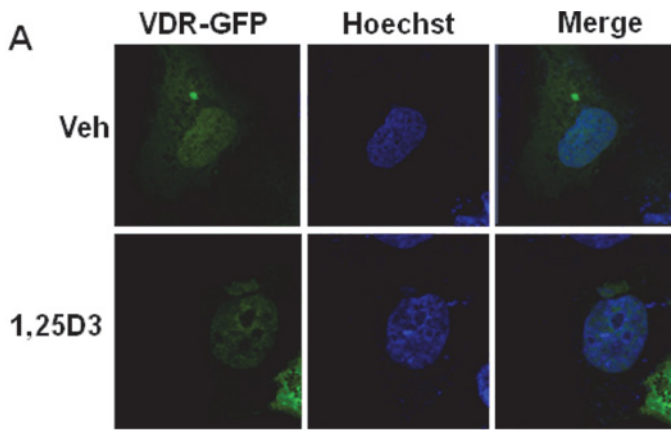
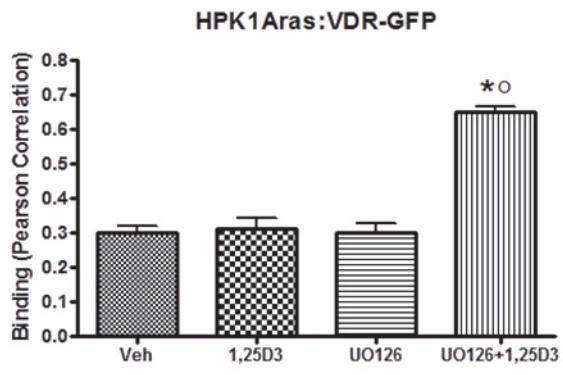


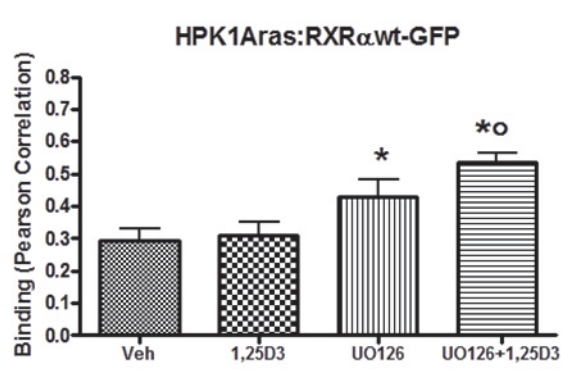
Figure 2.7: Determination of Receptor -DNA interaction. HPK1A cells transfected with VDR-GFP (green) and treated with either vehicle or 1,25(H)₂D₃ post transfection were stained with Hoechst dye (blue, A). Quantitation of binding between DNA (Hoechst) and VDR (GFP) was assessed using confocal microscopy and Pearson correlation (B). Similarly, cells were transfected with RXR α wt-GFP (C) and binding assessed following treatment as above (D). Next, HPK1A_{ras} cells were transfected with either VDR-GFP (E), RXR α wt -GFP (F) or RXR α mut-GFP (G) and binding assessed following treatment with either vehicle (veh), 1,25(H)₂D₃, UO126 alone or a combination of UO126 and 1,25(H)₂D₃. Values are mean \pm SE of at least 10 cells per treatment. Asterisks (*) indicate a significant increase in DNA/receptor interaction in 1,25(H)₂D₃ treatment or combined UO126 and 1,25(OH)₂D₃ treatment compared to vehicle treated cells. Open circle (O) indicates a significant difference in combined UO126 and 1,25(OH)₂D₃ treatment compared to 1,25(OH)₂D₃ treated cells. A p value of P < 0.05 was considered significant.



F



G



H

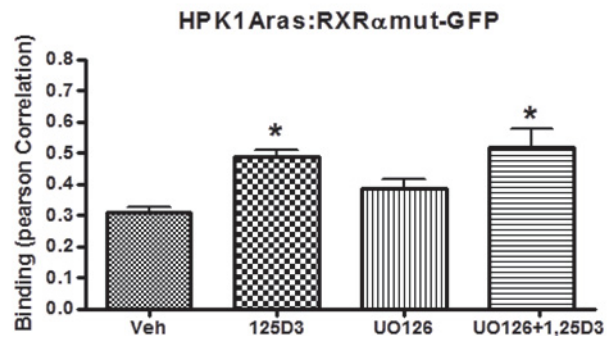
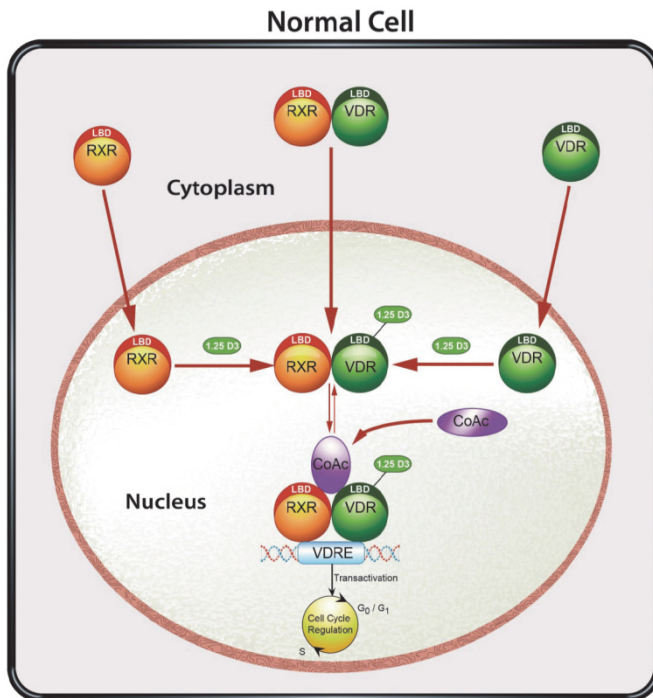


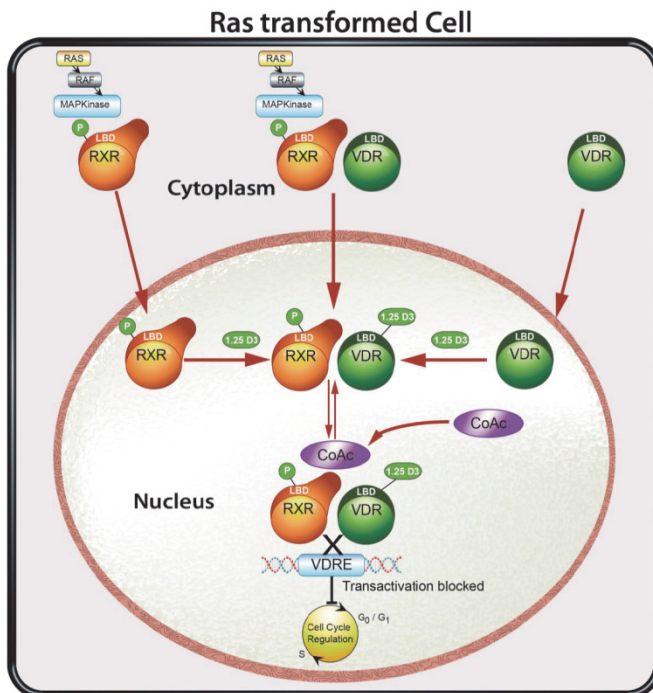
Figure 2.8: Proposed model for nuclear import of VDR, RXR and VDR:RXR interaction and DNA binding in non-transformed and ras-transformed cells. In normal cells (A), the nuclear import of VDR and RXR is mediated by their respective ligands. Once in the nucleus, $1,25(\text{OH})_2\text{D}_3$ binding to VDR is critical for the VDR-RXR heterodimer interaction and binding to the hormone response elements (VDRE), recruitment of co-factors (CoAc) and effects on $1,25(\text{OH})_2\text{D}_3$ signaling. In the ras-transformed keratinocyte (B) phosphorylation of RXR prevents the nuclear translocation of RXR and binding of the VDR/RXR complex to the hormone response element (VDRE). The recruitment of co-factors are impaired thus preventing $1,25(\text{OH})_2\text{D}_3$ signaling. By using either the MEK inhibitor UO126 or a non-phosphorylatable RXR mutant, we can restore the cells nuclear input of RXR, VDR/RXR as well as interaction with DNA and $1,25(\text{OH})_2\text{D}_3$ and VDR signaling.

A



Intranuclear receptor trafficking and binding to DNA is unimpaired

B



Intranuclear receptor trafficking and binding to DNA is impaired

CHAPTER 3

Examination of VDR/RXR/DRIP205 Interaction, Intranuclear Kinetic and DNA Binding in Ras-transformed Keratinocytes and Its Implication for Designing Optimal Vitamin D Therapy in Cancer

Sylvester Jusu¹, John F. Presley² and Richard Kremer¹

¹Department of Medicine and Calcium Research Laboratory, McGill University Health Center, 1001 Decarie Boulevard, Montreal, Quebec H4A 3S1

²Department of Anatomy and Cell Biology, McGill University, 3640 Rue University Montreal, Quebec H3A 0C7

To whom correspondence should be addressed: Richard Kremer, Department of Medicine and Calcium Research Laboratory, McGill University Health Center, 687 Pine Avenue W. Montreal, Quebec H3A 1A1. Canada Tel.: (1)-514 784-2770; Fax (1-514-933-8784). E-mail: richard.kremer@mcgill.ca

The contents of this chapter will be submitted to the Journal of Biological Chemistry

Abstract

We previously reported that the malignant HPK1Aras cell line is resistant to the growth inhibitory action of 1, 25(OH)₂D₃, compared to its normal counterpart immortalized HPK1A cells. We showed this resistance was due to phosphorylation of the vitamin D receptor (VDR) heterodimeric partner, human retinoid X receptor alpha (hRXR α) on a critical amino acid, serine 260 located in close spatial proximity to regions of coactivators and corepressors interactions. We next demonstrated that hRXR α subcellular localization was impaired in HPK1Aras cells but could be restored using either the MAPKK inhibitor UO126 or a non-phosphorylatable mutant of hRXR α (hRXR α S260A). In the current study, we used advanced live and fixed cells imaging techniques to examine further hRXR α intranuclear kinetics, VDR/RXR and DRIP205 interactions and binding of the VDR/ hRXR α /DRIP205 complex to chromatin. Our results showed that VDR/DRIP205, hRXR α /DRIP205 nuclear localization, interaction and VDR/ hRXR α /DRIP205 complex binding to chromatin are impaired in the HPK1Aras when compared to the normal HPK1A cells. However, transfection with the non-phosphorylatable hRXR α mutant or treatment with the MAPK inhibitor UO126 rescued their nuclear localization, interaction and binding of the complex to chromatin in the HPK1Aras cells. In summary we have demonstrated using highly specific intra-cellular tagging methods in live and fixed cells important alterations of the vitamin D signaling system in cancer cells in which the ras-raf-MAP kinase system is activated suggesting that specific inhibition of this commonly activated pathway could be targeted therapeutically to enhance vitamin D efficacy.

Introduction

The biologically active form of vitamin D₃, 1 α ,25-dihydroxyvitamin D₃ (1 α ,25(OH)₂D₃), is a pleiotropic nuclear hormone involved in a broad range of physiological effects. Primarily recognized for the regulation of calcium homeostasis (DeLuca et al., 1990) 1 α ,25(OH)₂D₃ is now known to have widespread effects on immune function, as well as cellular growth, differentiation and apoptosis (Walters, 1992). It blocks cell proliferation in several cancers models including melanoma, myeloid leukemia and carcinomas of the prostate, breast, colon and head and neck (Jones et al., 1998; Bikle, 2012, 2014, Molnar 2014). The genomic effects of 1 α ,25(OH)₂D₃ are mediated through the nuclear vitamin D receptor (VDR) which belongs to a transcription factor superfamily (Mangelsdorf et al., 1995). Active VDR binds preferentially as a heterodimer with the retinoid X receptor (RXR) to hexameric repeats on specific DNA sequences referred to as vitamin D response elements (VDREs) (Haussler et al., 2011) in the promoter regions of 1 α ,25(OH)₂D₃ target genes such as osteocalcin, osteopontin, calbindin-D28K, calbindin-D9K, p21WAF1/CIP1, TGF- β 2 and vitamin D 24-hydroxylase. Simple VDREs typically consist of two hexameric consensus sequence PuG(G/T)TCA which are commonly arranged as direct repeats spaced by three nucleotides (DR3-type VDREs) (Carlberg, 1995). As with other nuclear receptors, the binding of 1 α ,25(OH)₂D₃ to the RXR/VDR heterodimer functions to recruit additional cofactors that play an essential role in transcription (Rachez et al., 2000). A wide range of nuclear receptor cofactors have been identified which perform distinct functions at target promoters, including chromatin modification and remodeling and recruitment of the RNA polymerase II holoenzyme (Baretino et al., 1994).

VDR is able to recruit the vitamin D receptor interacting protein (DRIP) complex which consists of a group of some 10–13 proteins (Rachez et al., 1999). Among these proteins is DRIP205 which has been recognized as the single protein that mediate direct interaction with the VDR (Rachez and Freedman, 2000). VDR is also known to interact with members of the p160 class of coactivators including SRC1, TIF2/GRIP1, and ACTR/AIB1/pCIP which can act directly to catalyze selective acetylation of histones and indirectly to recruit additional regulatory molecules such as histone acetyltransferases capable of eliciting related changes in chromatin structure (Rachez and Freedman, 2000). The interaction of the VDR with comodulators such as DRIP205 as well as SRC1, TIF2/GRIP1 is mediated through NR interaction domains (NID) containing LXXLL motifs that associate directly within the AF-2 region of nuclear receptors (McInerney et al., 1998; Perissi et al., 1999). Recent crystallographic studies have defined the interaction between the LXXLL motif and the AF-2 cleft of the nuclear receptors created upon ligand-binding (Brzozowski et al., 1997; Gampe et al., 2000). Structural studies have demonstrated that a hydrophobic channel (AF2) is exposed on the surface of the LBD as a consequence of ligand binding (Rochel et al., 1997, 2000; Shiau et al., 1998; Gampe et al., 2000). This channel accommodates the LXXLL α -helix, which is held in place by hydrophobic interactions and a charged clamp involving two amino acids (lysine and glutamate) that are conserved throughout the NR family (McInerney et al., 1998, Shiau et al., 1998, Nolte et al., 1998). Different cofactors have been shown to have variable numbers of functional LXXLL motifs. The minimal sequence that can bind the AF2 surface (the LXXLL core motif) is contained within 8 amino acids (–1 to +7) (Heery et al., 2001).

Ras activating mutations are some of the most frequent somatic mutations in human cancers (Cox et al., 2014). Ras activation leads to the stimulation of the Mitogen Activated Protein Kinase (MAPK) pathway and contributes to cancer progression and development (Adjei , 2001; Cox et al., 2014). Several groups including ours have reported that MAPK activation modulates the transcriptional activity of $1,25(\text{OH})_2\text{D}_3$ (Solomon et al., 1999; Narayanan et al., 2004). We previously reported that overexpression of H-ras in human keratinocytes activates the MAPK pathway resulting in the inhibition of transactivation of known vitamin D target genes and resistance to the growth inhibitory action of $1, 25(\text{OH})_2\text{D}_3$ (Sebag et al., 1992). Our lab also demonstrated that this resistance was due to phosphorylation of the vitamin D receptor (VDR) heterodimeric partner, human retinoid X receptor alpha (hRXR α) on a critical amino acid serine 260 located in close spatial proximity to regions of coactivators and corepressors interactions. Furthermore, we have shown that hRXR α phosphorylation interferes with DRIP205 coactivator recruitment and binding (Macorrito et al., 2008).

In the present study, we used fluorescence imaging techniques to examine interactions between the hVDR-hRXR α -DRIP205-DNA complex and to determine the mechanism by which constitutive MAPK activation alters coactivator recruitment and hVDR-hRXR α -DRIP205 complex binding to DNA. Our specific goals were: to understand (i) how hRXR α phosphorylation at serine 260 affects the functional and intranuclear dynamics of the VDR-RXR α complex, (ii) whether blocking phosphorylation by the use of a MAPK inhibitor or a non-phosphorylatable mutant would restore DRIP205 coactivator interaction and recruitment to VDR- RXR α thereby stabilizing the complex in the ras-transformed keratinocytes, (iii) how phosphorylation affects VDR/ hRXR α /DRIP205 complex

binding to DNA and (iv) propose a model for the restoration of RXR α function in the ras-transformed keratinocytes. We hypothesized that RXR α phosphorylation within the omega loop would alter the conformational ensemble of hRXR α and that the dynamics would further lead to defects in coactivator interaction, recruitment and Vitamin D signaling.

EXPERIMENTAL PROCEDURES

Reagents

1 α ,25(OH) $_2$ D $_3$ was purchased from Sigma Aldrich (St. Louis, MO, USA) and stock solutions were prepared in ethanol. The mitogen-activated and extracellular regulated kinase kinase (MEK1/2) inhibitor UO126 (1,4-diamino-2,3-dicyano-1,4-bis[2-aminophenylthio] butadiene) was purchased from Promega (Madison, WI, USA) and stock solutions were prepared in DMSO. Human vitamin D receptor (hVDR) (C-20) and human retinoid X receptor α (hRXR α) (D-20) antibodies were obtained from Santa Cruz Biotechnology (Santa Cruz, CA, USA).

Cell lines and Culture

The HPK1A cell line was previously established by stably transfecting normal human keratinocytes with human papillomavirus type 16 (Sebag et al., 1992). In culture, these cells have an indefinite life span but retain differentiation properties characteristic of normal keratinocytes and are non-tumorigenic when injected into nude mice. These immortalized cells were then transformed into the malignant HPK1A $_{ras}$ cell line after transfection with a plasmid carrying an activated Ha-ras oncogene. HPK1A $_{ras}$ are malignant cells which form colonies in soft agar and also

produce invasive tumors when transplanted into nude mice. The cells were grown in Dulbecco's Modified Eagle's medium (DMEM) (Gibco, Buffalo, NY, USA) supplemented with 2 mM of glutamine, 100 IU/ml of penicillin, 100 µg/ml of streptomycin and 10% of fetal bovine serum (FBS) and passaged twice weekly in six, twenty four or nine six well Falcon plates (Corning, NY, USA).

Cloning of fluorescent (plasmids) tagged constructs.

Subcloning of VDR plasmids

VDR/pSG5 was a kind gift from Dr. John White's laboratory (McGill University, Montreal, Canada). The expression vector was originally constructed by inserting a 2.1-kilobase EcoRI fragment containing the entire coding region of the human VDR into the EcoRI site of pSG5 (34). VDR-CFP, VDR-GFP, VDR-YFP and VDR-mCherry plasmids were constructed by PCR amplification of hVDR sequence using hVDRpSG5 as a template and forward GGTTAC CTCGAG ATG GAG GCA ATG GCG GCC AGC ACT TCC CTG and reverse GTTAC CCG CGG AGA GGA GAT CTC ATT GCC AAA CAC TTC G primers were designed with an XhoI and SacII restriction sites. The hVDR PCR product was ligated to the GFP variants a generous gift from Dr. Stephan Laporte (McGill University, Montreal, Canada) and mCherry (Clontech, (Mountain View, CA, USA).

Subcloning of RXR α plasmids

The h RXR α wild type (WT) and ala260 h RXR α mutant were a kind gift from Dr. Evans (30) The hRXR α wt and the hRXR α ser260 ala (hRXR α S260A) mutant fluorescent GFP variants (ie GFP, CFP, YFP and mCherry) were constructed by

PCR amplification of hRXR α wt and the hRXR α ser260 ala mutant sequences using hRXR α wt and the hRXR α ser260 ala mutant as templates and forward GGTTAC CTCGAG ATG GAC ACC AAA CAT TTC CTG C and reverse GTTAC CCG CGG AGA AGT CAT TTG GTG CGG CGC CTC CAG C primers were designed to create new XhoI and SacII restriction sites. The resulting amplified PCR products were ligated to mCherry and the GFP variants respectively.

Subcloning of DRIP205 plasmids

pcDNA3-DRIP205 expression plasmid was kindly provided by Dr. Michael Degarabedian's laboratory (New York University Medical Center, NY, USA). The DRIP205 fluorescent GFP variants (ie GFP, CFP, YFP and mCherry) were constructed by PCR amplification of DRIP205 as templates using (forward) 5'- GA CAT AAC CGG TTT GTA ATT CCC AAT CAG GGC CAC ATC -3' and (reverse) 5'- GA CAT AAC CGG TTT GTA ATT CCC AAT CAG GGC CAC ATC -3' primers. The resulting amplified PCR products were digested with KpnI and AgeI and ligated to mCherry and the GFP variants respectively.

Subcloning of LXXLL plasmids

LXXLL-GFP motif was kindly provided by Dr. Sylvie Mader (University of Montreal, Montreal, Canada). The LXXLL fluorescent GFP variants (ie GFP, CFP, YFP and mCherry) were constructed by PCR amplification of LXXLL as templates using (forward) 5'- GA CAT AAC CGG TTT GTA ATT CCC AAT CAG GGC CAC ATC -3' and (reverse) 5'- GA CAT AAC CGG TTT GTA ATT CCC AAT CAG GGC CAC ATC -3' primers. The resulting amplified PCR

products were digested with Kpn and Age1 and ligated to mCherry and the GFP variants respectively.

Transfection

HPK1A and HPK1Aras cells were maintained in DMEM containing 10% FBS. For experimentations, cells were plated overnight in six well plates on # 1 coverslips (Fisher Scientific, Pittsburgh, PA) for fixed cell or 35 mm MatTek glass bottom dishes (MatTek Corporation, Ashland, MA, USA) for live cell experiments. Cells were plated at 10×10^4 cells/ well (HPK1A) and 8×10^4 cells/ well (HPK1Aras) in DMEM containing 10% FBS. The next day the medium was changed to serum free DMEM for an hour prior to initiating the experiment. Transfection was carried out in serum free DMEM FuGENE HD at a Fugene HD/ DNA transfection ratio of 6 ul:2 ug DNA. (Roche Applied Science, Indianapolis, IN). The cells were transfected with vectors encoding constructs of hRXR α -GFP, hRXR α -mCherry (2.0 ug) or hVDR-GFP, hVDR-mCherry (2.0 ug), DRIP205-GFP, DRIP205-mCherry, LXXLL-GFP (2.0 ug). In co-transfection studies, a total of 2 ug of the co-transfected vectors was used per well. After 4 hr of incubation, the medium was supplemented with 10 % FBS (by adding 200 ul of FBS/well). Following a 30 hr incubation medium was changed to DMEN containing 5 % FBS and incubated overnight. The next day cells were treated with vehicle (Ethanol+ DMSO 0.1 % v/v) or 1,25(OH) $_2$ D $_3$ (10^{-7} M), UO126 (10^{-6} M) alone or a combination of UO126 and with 1,25 (OH) $_2$ D $_3$ for 4 hr. For real time live cell microscopy the transfected cells were first transferred on to a heated stage at 37 °C for drug treatments and data acquisition. For fixed cell experiments, the cells were washed with PBS after the treatment and fixed for 15 mins in 4 %

paraformaldehyde at 37 °C. Following fixation, cells were re-washed in PBS and mounted using Shandon immu-Mount mounting medium (Fisher Scientific, Pittsburgh, PA, USA). For subcellular localization studies, following fixation and re-washing cells, were stained with either DAPI or Hoechst 33342 dye (Invitrogen, Grand Island, NY, USA) for 10 minutes, washed one more time and then mounted using Shandon immu-Mount mounting medium (Fisher Scientific, Pittsburgh, PA, USA). Imaging was carried out the next day using a Zeiss LSM 780 confocal microscope (Jena, Germany).

Fluorescence Microscopy, Time-Lapse Imaging, and Image Processing

HPK1A and HPK1Aras cells were grown on 35-mm glass-bottom dishes (MatTek Corporation, Ashland, MA, USA) (live cells) or 22 mm no.1 glass slides (fixed cells). Time lapse imaging was performed using a confocal laser scanning microscope (model LSM 510, Carl Zeiss, Inc., Jena, Germany) equipped with a motorized triple line Kr/Ar laser, a 100× 1.4 NA Planapochromat oil immersion objective, a 63× 1.3 NA Planapochromat oil immersion objective, a 40× 1.3 NA Neofluar oil immersion objective, a 25× 0.8 NA Neofluar immersion corrected objective and a temperature and CO₂ controlled stage. Time-lapse sequences were recorded using the time-series function of the Zeiss LSM software.

Receptor expression and Subcellular distribution using Confocal Microscopy

GFP vector alone, hVDR-GFP, hRXR α wt-GFP and hRXR α mut-GFP expression vectors were monitored by viewing and counting fluorescing cells using a Plan-Neofluar 63 x/ 1.3 oil objective, 488 nm excitation and 515-565 nm emission filters (Carl Zeiss Inc.). To monitor subcellular distribution of the receptors ten

healthy cells were observed at random from at least 10 fields. Repeated experiments were done using the same parameters. Z-stacks of double-labeled images were collected to account for total cellular fluorescence.

Morphometric Analysis of Subcellular localization

For evaluation of nuclear/cytoplasmic signal distribution, confocal images were taken of each fluorescing cell. A single optical slice was taken of each cell with focus set to maximize the circumference of the nucleus. At least 10 cells were evaluated for each experimental condition. Cells that showed clear morphological changes due to protein overexpression were excluded from statistical analysis. Image analysis was performed using the ImageJ 1.41 public domain software (U.S. National Institutes of Health, Bethesda, MD, USA) to determine the nuclear (Fn) cytoplasmic (Fc) and background (Fb) fluorescence. Briefly, a mean density measurement of pixel numbers was made on a nonsaturated region of interest (ROI) consisting of the total nucleus, the whole cell (nucleus and cytoplasmic compartments combined) and a background region outside of the cell. The ratio of nuclear to cytoplasmic fluorescence (Fn/c) was then determined according to the formula $Fn/c = (Fn - Fb)/(Fc - Fb)$. Data are presented as mean \pm S.E.

Fixed Cell Imaging and Fluorescence Resonance Energy Transfer (FRET)

Microscopy

HPK1A and HPK1A_{ras} cells were grown on 22mm no.1 coverslips and cotransfected with either VDR-mCherry/DRIP205-GFP, hRXR α wt-mCherry/DRIP205-GFP or hRXR α mut-mCherry/DRIP205-GFP respectively. Transfected cells were next treated with either vehicle control (ethanol or DMSO

0.1 % v/v), 1,25(OH)₂D₃ (10⁻⁷ M) alone or in combination with UO126 (10⁻⁶ M) and 1,25(OH)₂D₃. Treatments were carried out for 4 hr before fixing, mounting and FRET data acquisition using a Zeiss LSM 780 confocal microscope with a Zeiss 63 × NA 1.4 Neofluar oil objective and a chamber to maintain a temperature of 37 °C and 5% CO₂. To assay dequenching of donor after photobleach, a series of eight images of the mCherry and GFP channels were taken. mCherry within the nucleus was bleached after image 4 by scanning with the 561 nm laser line at maximum intensity. GFP intensities inside the nucleus were compared between the immediately prebleach image (image 4) and the postbleach image (image 5). Dequenching was defined as nuclear GFP intensity in image 4 divided by nuclear GFP intensity in image 5. The remainder of the image sequence served as a control for focus stability. At least ten cells per treatment were photobleached for each experiment. Experiments were repeated twice.

To calculate FRET percentage, the fluorescence intensities of three regions of interests (ROIs) –a region exterior to the cell (background), a region in the nucleus that was photobleached (bleached region) and a region of the nucleus that was not bleached (unbleached region) was selected and data acquired for both mCherry and GFP. The fluorescent intensities of GFP immediately before the bleach and immediately after the bleach were next background corrected by subtracting fluorescence intensity of the background region in the GFP channel of the same image. The prebleach and postbleach GFP corrected intensities were then used to calculate the percent dequenching, which is a measure of FRET in this experimental design. A total of ten images were analyzed per experimental condition. Percent dequenching was calculated as follows: Dequenching % =

(GFP_{corrected} postbleach / GFP_{corrected} prebleach) X 100. In this measure, 100% represents a baseline with no change in fluorescence, indicative of no significant FRET, while values greater than 100% are consistent with FRET prior to dequenching.

Live cell imaging using Fluorescent Recovery After Photobleaching (FRAP)

Microscopy

FRAP was used to assess real-time intranuclear mobility of hRXR α -tagged GFP in the presence or absence of 1,25(OH)₂D₃. HPK1A and HPK1A_{ras} cells were transfected with GFP tagged hRXR α wt or hRXR α mut respectively. After 30 hr transfection, the media was changed to one containing 5 % charcoal stripped FBS and the cells were treated with vehicle control (ethanol + DMSO 0.1%v/v) or 1,25(OH)₂D₃ (10⁻⁷M). All photobleached image series were obtained on a 37 °C heated stage using a 40 \times /1.3 NA oil immersion lens. Fluorescence spanning the width of the whole nucleus was bleached using repeated (50-200) scans of 488 nm illumination with 100 % laser transmission. Bleaching alternated with image acquisition at 5% laser transmission. Cells were scanned 0.8 to 3 sec per image with two –to- eight line averaging. Fluorescence intensity in an ROI on the opposite side of the nucleus and outside of the bleach ROI was quantitated at each time point and normalized to the fluorescence intensity before bleaching. Cells were photobleached from 0- 10 minutes respectively followed by fluorescence intensity measurement. A neighboring unbleached cell served as a control for focus drift and photobleaching during image acquisition. Normalization was done to the prebleach data point. At least ten cells were collected per treatment condition.

Analysis of FRAP Data

The Zeiss LSM software package was used to define regions of interests (ROIs) collect mean fluorescent intensities of the background, whole nucleus and the whole cell for each data set measured under the same experimental condition. Images were background subtracted and data normalized and exported into Microsoft Excel before quantitation and processing. The analyzed data were used to plot curves, calculate mobile fraction, diffusion constants and half time of recovery. The mobile fraction M_f was calculated using the equation: $M_f = (F_\infty - F_0)/(F - F_0)$ (Lippincott-Schwartz *et al.*, 2001; Snapp et al, 2003,) where F_∞ is the average fluorescence in the ROI after full recovery, F_0 is the fluorescence immediately after the bleach and F is the average fluorescence before bleaching. The half- life of recovery was calculated to compare relative recovery rates between treatments. The half-life of fluorescence recovery ($t_{1/2}$) is the time required for the fluorescent intensity in the bleach ROI to recover 50 % of the asymptote or plateau intensity (Snapp et al, 2003). The half-life of fluorescence recovery ($t_{1/2}$) was determined by curve fitting of experimental data using a mathematical model of fluorescence recovery by diffusion. The equation of a one phase exponential curve for incomplete bleach is given as: $N(t) = A1 * [1 - e^{(-rt)}] + A2 * e^{(-rt)}$ where $N(t)$ represents the nuclear fluorescence as a function of time, $A1$ is the plateau and $A2$ accounts for incomplete bleach, r is the rate constant K and is the sum of nuclear import rate constant K_{in} and nuclear export rate constant K_{out} (Presley, Methods, 2006). To directly visualize and determine the half-life of fluorescence recovery, the fluorescence intensity data was transformed to a 0 % to 100 % scale. At least ten cells were used per treatment condition.

Binding of Receptor to DNA (Hoechst dye)

HPK1A and HPK1A_{ras} cells were seeded on 22 mm glass slides (Fisher Scientific, Pittsburgh, PA) at a concentration of 1×10^5 cells/ well for 24 hrs in DMEM containing 10 % FBS. The next day, the cells were transfected with hVDR-GFP, hRXR α wt-GFP or hRXR α mut-GFP using Fugene HD at a DNA/Fugene ratio of 2 μ g:6 μ l as described in transfection protocol above and cells treated for 2hr prior to fixation. The cells were next washed with PBS, and fixed in 4 % paraformaldehyde for 15 minutes. Cells were re-washed with PBS and stained with Hoechst 33342 dye (1 μ g/ml) for ten minutes at room temperature. Finally, cells were re-washed with PBS and slides mounted with Shandon immu-mount mounting medium. Imaging was carried out the next day using both the 488 nm and 405 nm lasers to compare colocalization of the GFP and Hoechst dye in the cells. Image analysis was carried out by selecting the nuclei in the images and determining the mean fluorescence intensity of all the GFP and Hoechst dye pixels selected using the Zeiss LSM 780 Image examiner. Pearson's correlation coefficient was used to compare colocalization of Hoechst dye (a DNA marker) to GFP within the nucleus.

Statistical Analysis

We used analysis of variance (ANOVA) and t-test in Graphpad prism software. Results are presented as mean \pm standard error of at least eight independent measurements. Data was analyzed statistically by one-way analysis of variance followed by a post- hoc test and student t-test. Means were considered significantly different when P values were at least below 0.05

Results:

Inhibition of MAP kinase activity enhances intra-nuclear mobility and binding in ras-transformed HPK1Aras cells in response to $1\alpha,25(\text{OH})_2\text{D}_3$ as shown by (FRAP)

In Chapter 2, we used real time FLIP to investigate intranuclear mobility and whether the hRXR α could be immobilized by binding to DNA. In the current study we used FRAP to also assess real-time intranuclear mobility of hRXR α -tagged GFP in the presence or absence of $1,25(\text{OH})_2\text{D}_3$. FRAP which measures association between hRXR α with the nuclear components is complementary to FLIP which measures dissociation of hRXR α from the nuclear components. Since both methods are complementary, we expect the results to be similar.

Effects on Mobility, Residence time and Intra-nuclear binding.

Results show that in cells transfected with RXR α wt-GFP or RXR α mut-GFP, two kinetic pools of the receptors were present in each cell line; a faster mobile pool accounting for 65 % (and independent of ligand treatment) and a slower or less mobile pool. Secondly, in HPK1A cells transfected with RXR α wt-GFP and treated with $1\alpha,25(\text{OH})_2\text{D}_3$ showed a significant increase in residence time of the receptor when compared to vehicle (Fig. 3.1A, $p < 0.05$). In contrast, HPK1Aras cells transfected with RXR α wt-GFP and treated with $1\alpha,25(\text{OH})_2\text{D}_3$ showed no significant increase in residence time of the receptor when compared to vehicle or UO126 treatment alone (Fig. 3.1C, $p > 0.05$). However, pretreatment with UO126 significantly increased the residence time when compared to $1\alpha,25(\text{OH})_2\text{D}_3$, vehicle or UO126 or treatment alone (Fig. 3.1C, $p < 0.05$). In HPK1Aras cells transfected

with RXR α mut-GFP, treatment with 1 α ,25(OH) $_2$ D $_3$ alone or combined treatment with UO126 and 1 α ,25(OH) $_2$ D $_3$ significantly increased the residence time of the receptor when compared to vehicle or UO126 treatment alone (Fig. 3.1E, p<0.05). Regarding the effects RXR α phosphorylation on hRXR α intra-nuclear binding, HPK1A cells transfected with hRXR α wt-GFP, treatment with 1 α ,25(OH) $_2$ D $_3$ increased the percentage of hRXR α wt-GFP bound fraction (28.0 \pm 2.5 %) when compared to vehicle (10.0 \pm 1.3 %, Fig. 3.1B p<0.0001). In HPK1A cells transfected with hRXR α wt-GFP, there was no significant difference in binding between 1,25(OH) $_2$ D $_3$ treatment (7.32 \pm 0.76 %) and vehicle (8.06 \pm 1.5 %, Fig. 3.1D, p>0.05). However, pre-treatment with the MEK inhibitor UO126 followed by treatment with 1,25(OH) $_2$ D $_3$ significantly increased the bound fraction when compared to either 1,25(OH) $_2$ D $_3$ treatment alone or vehicle (20.17 \pm 3.3 %, Fig. 3.1D p<0.05). Furthermore when HPK1A cells transfected with hRXR α mut-GFP, the bound fraction of cells treated with 1,25(OH) $_2$ D $_3$ (22.12 \pm 2.0 %) or combined treatment of UO126 and 1,25(OH) $_2$ D $_3$ (23.46 \pm 2.7 %) significantly increased when compared to control respectively (11.74 \pm 1.2 %, Fig. 3.1F p<0.0001).

RXR α phosphorylation on serine 260 affects VDR/ DRIP205 co-trafficking and nuclear-colocalization in ras-transformed HPK1A cells

We previously used the Pearson correlation coefficient to compare VDR/ RXR α colocalization in the nuclear compartment of the non-transformed and ras-transformed cells (Jusu et al., 2013, ASBMR proceedings). We showed that nuclear colocalization of VDR/ RXR α was impaired in the ras-transformed cells when compared to the non-transformed cells. However, transfection of the

HPK1Aras cells with RXR α mut-GFP or treatment with the MEK inhibitor UO126 significantly increased the nuclear colocalization of VDR/RXR (Jusu, Presley and Kremer submitted). To further understand VDR/RXR and DRIP205 interaction, we also used Pearson correlation coefficient as above to assess VDR/DRIP205 colocalization in the nuclear compartment of the non-transformed HPK1A and ras-transformed HPK1Aras cells. In HPK1A cells co-transfected with VDR-mCherry/DRIP205-GFP, treatment with 1 α ,25(OH) $_2$ D $_3$ (0.59 ± 0.02) significantly increased nuclear VDR/DRIP205 colocalization when compared to vehicle (0.27 ± 0.03 , Fig. 3.2A and 3.2B, $p < 0.0001$). In HPK1Aras cells co-transfected with VDR-mCherry/DRIP205-GFP, treatment with 1 α ,25(OH) $_2$ D $_3$ alone (0.26 ± 0.02) did not increase VDR/DRIP205 colocalization when compared to vehicle (0.21 ± 0.03 , Fig. 3.2C, $p > 0.05$,). However, treatment with UO126 alone (0.35 ± 0.01) or a combination of UO126 and 1 α ,25(OH) $_2$ D $_3$ (0.57 ± 0.01) significantly increased VDR-mCherry/DRIP205-GFP nuclear colocalization when compared to vehicle (control) (Fig. 3.2C, $p < 0.05$).

RXR α phosphorylation on serine 260 affects RXR α / DRIP205 co-trafficking and nuclear-colocalization in ras-transformed HPK1Aras cells

It has been suggested that the transcriptional regulation of 1 α ,25(OH) $_2$ D $_3$ does not only involve VDR but also RXR α binding to DRIP205 (Rachez et al., 2000; Haussler et al., 2011; Bikle 2014; Bikle et al., 2015). This process first involves VDR binding to RXR α as a heterodimer in the presence of 1 α ,25(OH) $_2$ D $_3$ on a VDRE. This is followed by DRIP205 binding to both VDR and RXR via their AF-2 domain (Rachez et al., 2000). The binding of the VDR/RXR heterodimer to DRIP205 results in the dissociation of corepressors and association of other coactivators necessary for transcription of the vitamin D target gene. As above, we

compared RXR α /DRIP205 colocalization in the nuclear compartment of the non-transformed HPK1A and ras-transformed HPK1Aras cells pixel-by-pixel. We tested the significance of the data obtained by using Pearson correlation coefficient. In HPK1A cells co-transfected with RXR α wt-mCherry/DRIP205-GFP, treatment with 1 α ,25(OH) $_2$ D $_3$ (0.56 ± 0.03) significantly increased nuclear RXR α wt/DRIP205 nuclear colocalization when compared to vehicle (0.21 ± 0.02 , Fig. 3.3A and 3.3B, $p < 0.0001$).

In HPK1Aras cells co-transfected with RXR α wt-mCherry /DRIP205-GFP, treatment with 1 α ,25(OH) $_2$ D $_3$ alone (0.21 ± 0.02) did not increase nuclear colocalization when compared to vehicle (0.19 ± 0.02 , Fig. 3.3C, $p > 0.05$,). However, treatment with UO126 alone (0.35 ± 0.04) or a combination of UO126 and 1 α ,25(OH) $_2$ D $_3$ (0.52 ± 0.02) significantly increased nuclear colocalization when compared to control (Fig. 3.3C, $p < 0.05$). In HPK1Aras cells co-transfected with RXR α mut-mCherry /DRIP205-GFP, treatment with 1 α ,25(OH) $_2$ D $_3$ (0.48 ± 0.04), UO126 alone (0.36 ± 0.02) or a combination of UO126 and 1 α ,25(OH) $_2$ D $_3$ (0.52 ± 0.02) significantly increased RXR α mut-mCherry /DRIP205-GFP nuclear colocalization when compared to control (0.21 ± 0.04 , Fig. 3.3D, $p < 0.05$).

Effects of RXR α phosphorylation on VDR and DRIP205 interaction in HPK1A and HPK1Aras using FRET

We used Fluorescence Resonance Energy Transfer (FRET) to investigate interaction between VDR and DRIP205 after ligand addition in both cell lines. The rationale was that while the statistical data obtained using Pearson correlation coefficient could suggest VDR and DRIP205 colocalization, it couldn't itself show

interaction. First we used the FRET pairs of our GFP- tagged proteins and compared it with GFP/mCherry FRET probes (Fig. 3.4A and 3.4B). As expected our results showed VDR/DRIP205 heterodimeric interaction indicating that our FRET pairs were competent to form heterodimers. No FRET signal was observed with the negative control GFP/mCherry probes in both cell lines (data not shown). Next, we tested for VDR and DRIP205 interaction in both cell lines using the VDR-mCherry and DRIP205-GFP FRET pairs. A percentage dequenching baseline of 100 % was set for FRET interaction. This means that any FRET value below 100 % was considered as no interaction. In HPK1A cells co-transfected with VDR-mCherry/DRIP205-GFP, treatment with $1\alpha,25(\text{OH})_2\text{D}_3$ (110.0 ± 2.6 %) significantly increased VDR/DRIP205 interaction when compared to vehicle (99.0 ± 1.2 %, Fig. 3.4C , $p < 0.0005$).

In HPK1A cells co-transfected with VDR-mCherry/DRIP205-GFP, treatment with $1\alpha,25(\text{OH})_2\text{D}_3$ alone (104.1 ± 0.9 %) or combination of UO126 and $1\alpha,25(\text{OH})_2\text{D}_3$ (110.3 ± 2.0 %) significantly increased VDR/DRIP205 interaction when compared to vehicle (95.74 ± 1.9) or UO126 treatment alone (95.87 ± 2.8 %, Fig. 3.4D $p < 0.05$).

Effects of RXR α phosphorylation on VDR/ LXXLL motif interaction in HPK1A and HPK1A cells

It has been shown that binding and interaction of DRIP205 coactivator to either VDR or RXR occurs through short sequences known nuclear interaction domains (NID) or LXXLL motifs (Rachez et al., 2000; Haussler et al., 2011; Bikle 2014; Bikle et al., 2015). The motif on the coactivator binds to the AF2- on the receptor

creating a charge clamp that stabilizes the complex. We therefore used FRET to assess VDR/DRIP205 LXXLL motif interaction in both cell lines. In HPK1A cells co-transfected with VDR-mCherry/LXXLL-GFP, treatment with $1\alpha,25(\text{OH})_2\text{D}_3$ ($110.0 \pm 4.4 \%$) significantly increased VDR/DRIP205 interaction when compared to vehicle ($94.0 \pm 1.4 \%$, $p < 0.0005$, Fig. 3.4E). In HPK1Aras cells co-transfected with VDR-mCherry/LXXLL-GFP, treatment with $1\alpha,25(\text{OH})_2\text{D}_3$ alone ($105.2 \pm 1.1 \%$) or combination of UO126 and $1\alpha,25(\text{OH})_2\text{D}_3$ ($107.1 \pm 0.9 \%$) significantly increased VDR/DRIP205 interaction when compared to vehicle (97.28 ± 2.9 $p < 0.05$) or UO126 treatment alone ($99.93 \pm 1.9 \%$, Fig. 3.4F, $p < 0.05$). This result suggests that *RXR α phosphorylation does not affect VDR/DRIP205 or VDR/LXXLL motif interaction in the ras-transformed cells.*

Effects of RXR α phosphorylation on RXR α and DRIP205 interaction in HPK1A and HPK1Aras using FRET

We next assessed interaction between RXR α and DRIP205 using the same FRET methodology. In HPK1A cells co-transfected with RXR α wt-mCherry/DRIP205-GFP, treatment with $1\alpha,25(\text{OH})_2\text{D}_3$ ($104.2 \pm 2.3 \%$) significantly increased RXR α wt/DRIP205 interaction when compared to vehicle ($89.6 \pm 1.4 \%$, Fig. 3.5A, $p < 0.05$). In HPK1Aras cells co-transfected with RXR α wt-mCherry/DRIP205-GFP, treatment with $1\alpha,25(\text{OH})_2\text{D}_3$ ($100.1 \pm 1.2 \%$) did not increase RXR α wt/DRIP205 interaction when compared to vehicle ($85.15 \pm 2.4 \%$) or UO126 treatment alone ($99.97 \pm 2.4 \%$, Fig. 3.5C, $p > 0.05$). However, a combination of UO126 and $1\alpha,25(\text{OH})_2\text{D}_3$ ($103.8 \pm 3.8 \%$) significantly increased interaction between RXR α and DRIP205 when compared to vehicle or UO126 or $1\alpha,25(\text{OH})_2\text{D}_3$ treatment

alone (Fig. 3.5C, $p < 0.05$). In HPK1Aras cells co-transfected with RXR α mut-mCherry/ DRIP205-GFP, treatment with $1\alpha,25(\text{OH})_2\text{D}_3$ alone ($104.2 \pm 2.5 \%$) or in combination with UO126 and $1\alpha,25(\text{OH})_2\text{D}_3$ treatment ($108.8 \pm 2.1 \%$) significantly increased interaction when compared to vehicle ($85.6 \pm 2.4 \%$) or UO126 treatment alone ($97.4 \pm 2.1 \%$, Fig. 3.5E $p < 0.05$)

RXR α phosphorylation affects on RXR α / LXXLL motif interaction in HPK1Aras cells

We next assessed RXR α /LXXLL interaction in both cell lines. In HPK1A cells co-transfected with RXR α wt-mCherry/LXXLL-GFP, treatment with $1\alpha,25(\text{OH})_2\text{D}_3$ ($104.5 \pm 3.6 \%$) significantly increased RXR α wt/LXXLL interaction when compared to vehicle ($92.59 \pm 2.2 \%$, Fig. 3.5B $p < 0.05$). In HPK1Aras cells co-transfected with RXR α wt-mCherry /LXXLL-GFP, treatment with $1\alpha,25(\text{OH})_2\text{D}_3$ alone ($100.0 \pm 0.4 \%$) did not increase FRET interaction when compared to vehicle ($98.98 \pm 0.7 \%$) or UO126 ($99.27 \pm 1.9 \%$, Fig. 3.5D, $p > 0.05$) alone. Interaction was considered as non-existent. However, the combination of UO126 and $1\alpha,25(\text{OH})_2\text{D}_3$ ($103.5 \pm 1.3 \%$) significantly increased RXR α /LXXLL interaction when compared to vehicle or UO126 treatment alone (Fig. 3.5D, $p < 0.05$). Similarly, HPK1Aras cells co-transfected with RXR α wt-mCherry/LXXLL-GFP and treated with either $1\alpha,25(\text{OH})_2\text{D}_3$ ($105.1 \pm 1.1 \%$) alone a combination of UO126 and $1\alpha,25(\text{OH})_2\text{D}_3$ ($106.0 \pm 0.5 \%$) showed a significant increase in RXR α /LXXLL interaction when compared to vehicle ($98.45 \pm 2.6 \%$) or UO126 ($98.96 \pm 1.1 \%$) alone (Fig. 3.5F, $p > 0.05$). This result shows

that *RXRα phosphorylation affects RXRα/DRIP205 or RXRα/LXXLL motif interaction in the ras-transformed cells.*

Effects of *RXRα* phosphorylation on VDR/DRIP205 complex binding to DNA in non-transformed HPK1A and ras –transformed HPK1A_{ras} cells

We previously showed in ras-transformed cells that were singly transfected with either VDR-GFP or *RXRα* -GFP that *RXRα* phosphorylation on serine 260 affected both VDR and *RXR* binding to DNA and chromatin (Jusu, Presley and Kremer, submitted for publication). In the current study we cotransfected cells with VDR-mCherry /DRIP205-GFP. Following treatment as above, cells were fixed and stained with Hoechst 33342, a widely used DNA-specific dye, which emit blue fluorescence under ultraviolet (UV) illumination when bound to DNA. Hoechst has a preference to bind to A/T-rich DNA sequences and highlights a subset of the genome. We measured binding (colocalization) of DRIP205 to DNA (Hoechst dye) (Fig 3.6 A and B) and then evaluated the statistical significance of the data obtained using Pearson correlation coefficient. In HPK1A cells co-transfected with VDR-mCherry /DRIP205-GFP we found a direct correlation between VDR and DRIP205 both binding to DNA (data not shown). Treatment of cells with $1\alpha,25(\text{OH})_2\text{D}_3$ significantly increased VDR/DRIP205 complex binding to DNA ($31.0 \pm 2.5 \%$) when compared to vehicle ($6.9 \pm 1.9 \%$, Fig. 3.6 C, $p < 0.05$).

In HPK1A_{ras} cells co-transfected with VDR-mCherry /DRIP205-GFP, treatment of cells with $1\alpha,25(\text{OH})_2\text{D}_3$ did not increased VDR/DRIP205 complex binding to DNA ($7.2 \pm 1.3 \%$) when compared to vehicle ($6.4 \pm 1.4 \%$, Fig. 3.6 D, $p > 0.05$). However, treatment with UO126 alone ($16.8 \pm 3.2 \%$) or in combination with

$1\alpha,25(\text{OH})_2\text{D}_3$ significantly increased VDR/DRIP205 complex binding to DNA ($32.0 \pm 1.8 \%$, Fig. 3.6 D, $p < 0.05$)

Effects of RXR α phosphorylation on RXR α /DRIP205 complex binding to DNA in non-transformed HPK1A and ras-transformed HPK1A_{ras} cells

We next assessed RXR/DRIP205 complex binding to DNA in cells cotransfected with either RXR α wt-mCherry /DRIP205-GFP or RXR α mut-mCherry /DRIP205-GFP. Following treatment as above, cells were fixed and stained with Hoechst 33342. Pearson's correlation coefficient was used to compare binding (colocalization) of DRIP205 to DNA (Hoechst). In HPK1A cells co-transfected with RXR α wt-mCherry /DRIP205-GFP we found a direct correlation between RXR α and DRIP205 both binding to DNA. Treatment of cells with $1\alpha,25(\text{OH})_2\text{D}_3$ significantly increased RXR α wt /DRIP205 complex binding to DNA ($30.0 \pm 3.1 \%$) when compared to vehicle ($5.5 \pm 1.6 \%$ Fig. 3.7A, 3.7B and 3.7B $p < 0.05$). In HPK1A_{ras} cells co-transfected with RXR α wt-mCherry /DRIP205-GFP, treatment with $1\alpha,25(\text{OH})_2\text{D}_3$ ($5.8 \pm 1.6 \%$) did not increase RXR α wt /DRIP205 complex binding to DNA when compared to vehicle ($5.2 \pm 1.0 \%$). However, treatment with UO126 alone ($14.3 \pm 2.3 \%$) or a combination of UO126 and $1\alpha,25(\text{OH})_2\text{D}_3$ ($32.00 \pm 1.8 \%$, Fig. 3.7D $p > 0.05$) significantly increased RXR α wt /DRIP205 complex binding to DNA ($P < 0.0001$). Similarly, in cells co-transfected with RXR α mut-mCherry /DRIP205-GFP treatment with $1\alpha,25(\text{OH})_2\text{D}_3$ alone ($24.9 \pm 3.0 \%$) or combination of UO126 and $1\alpha,25(\text{OH})_2\text{D}_3$ ($28.80 \pm 1.7 \%$) significantly increased binding when compared to vehicle ($5.6 \pm 2.0 \%$) or UO126 alone ($12.40 \pm 1.6 \%$, Fig. 3.7E $P < 0.0001$). There was also a direct correlation between RXR α and DRIP205 both binding to DNA.

Discussion

This study expands on our previous work on the mechanism of action of $1\alpha,25(\text{OH})_2\text{D}_3$ in ras-transformed keratinocytes (Maccorito, et al, 2008; Jusu et al., 2013 ASBMR proceedings). In previous studies, we had demonstrated that RXR α phosphorylation on serine 260 resulted in relative resistance to the growth inhibitory action of $1\alpha,25(\text{OH})_2\text{D}_3$ in ras-transformed cells (Solomon et al., 1998, 1999, 2001; Maccorito et al., 2008). We further hypothesized that phosphorylation at serine 260 interfered with VDR and RXR nuclear localization, VDR/RXR heterodimer interaction, binding of the heterodimer complex to DNA and transcriptional activation of VDR. Also, we speculated that blocking RXR α phosphorylation by the use of a MAPK inhibitor UO126 or a non-phosphorylatable RXR α mutant can reverse the effect by sensitizing ras-keratinocytes to $1\alpha,25(\text{OH})_2\text{D}_3$ signaling. By comparing subcellular localization, VDR/RXR interaction and DNA binding in both non-transformed and ras-transformed cells, we have confirmed part of the hypothesis. We showed that VDR/RXR heterodimer interaction and binding to DNA are both impaired in the ras-transformed cells.

In the current work we investigated further the association of VDR, RXR with the DRIP205 coactivator. We first used FRAP to assess intra-nuclear kinetics of RXR. We demonstrated that inhibition of MAPK activity increased the residence time and bound fraction of RXR α in the ras-transformed keratinocyte. The FRAP data confirmed our previous FLIP results (Jusu, Presley and Kremer, ASBMR Proceedings 2013) furthermore suggesting that vitamin D signaling can be restored following the blocking of RXR phosphorylation. Next, we determined the role of DRIP205 in interacting with VDR and RXR and the VDR/RXR complex binding to chromatin. We previously reported that HPK1A and HPK1Aras cells express

DRIP205 and RIP140 at high levels whereas SRC1 and GRIP1 (SRC2/TIF2) could not be detected (Macorrito et al., 2008), we therefore decided to first investigate the nuclear colocalization of DRIP205 with either VDR or RXR. This was important as it is well documented that coactivator interaction with the VDR/RXR heterodimer complex precedes the transcriptional activation of VDR (Rachez et al., 2000). We confirmed that VDR colocalizes with DRIP205 in both non-transformed and ras-transformed cells treated with $1,25(\text{OH})_2\text{D}_3$ suggesting that the effect observed was independent of RXR phosphorylation in the ras-transformed cells. Also, we demonstrated that in both the non-transformed and ras-transformed cell lines, VDR interacted with DRIP205 coactivator and its signature LXXLL motif in a ligand dependent manner furthermore suggesting that RXR phosphorylation on serine 260 does not directly affect association of VDR with DRIP205 in the ras-transformed cell line. Our findings are supported by several other reports showing that VDR interacts with DRIP205 through its LXXLL motif (Nolte et al., 1998; Shiau et al., 1998; Rachez et al., 2000; Pogenberg et al., 2005). While most of the works were done in a cell free system, we have demonstrated it *in vivo* in live cells.

However, the results for RXR and DRIP205 nuclear colocalization were different from those of VDR/DRIP205 colocalization in the ras-transformed cells. Our results showed that RXR phosphorylation on serine 260 reduced RXR and DRIP205 colocalization. Furthermore, when phosphorylated, we recorded very weak to no interaction between RXR with DRIP205 and its signature LXXLL motif. Interestingly, transfection of the ras-transformed cells with a non-phosphorylatable RXR α mutant or pre-treatment with UO126 restored RXR/DRIP205 nuclear colocalization and interaction.

Rachez and coworkers (2000) using a cell free system showed that DRIP205 is the single protein that mediates direct interaction with both VDR and RXR. The interaction of the VDR with coactivators such as DRIP205 as well as SRC-1 and GRIP is mediated through LXXLL motifs that associate directly within the AF-2 region of NRs (Pathrose et al., 2002). DRIP205 contains two LXXLL motifs (Zhu et al., 1997; Rachez et al., 1999), a signature motif that is shared by a variety of cofactors (including SRC family members, PGC-1 family members, p300/CBP and RIP140) and employed for their binding to NRs (Heery et al., 1997). Studies with isolated wild type and reconstituted DRIP complexes containing mutations in DRIP205 LXXLL motifs have shown that these motifs are essential both for strong ligand-dependent interactions with nuclear receptors and for optimal nuclear receptor-mediated transcription *in vitro* (Malik et al., 2004; Ge et al., 2008) and *in vivo* (Bukarov et al., 2000; Jiang et al., 2010). Rachez and coworkers (2000) demonstrated that a mutation in the second LXXLL motif (also called NR2 motif) of DRIP205 abolished its ability to bind the VDR/RXR heterodimer and form a complex in the presence of $1\alpha,25(\text{OH})_2\text{D}_3$. Structural studies for many nuclear receptors including DRIP205 have shown that the AF2-containing LBDs bear a similar three-layered α -helical sandwich structure with a central ligand-binding site in which the ligand is buried. In the unliganded (apo) state, the H12 helix of the AF2 motif extends away from the LBD core however, upon ligand binding (holo state), is folded against the LBD, with two conserved hydrophilic residues (glutamine and lysine) forming a charged clamp that mediates interactions with the α -helix LXXLL motif of coactivators (Poggenberg et al., 2005).

Macorrito and coworkers (2008) using a mouse osteopontin (moP) VDRE and CHIP assay to examine the effects of inactivating MAPKK activity on DRIP205 coactivator recruitment to the VDR/RXR complex in HPK1A and HPK1Aras cells reported that $1\alpha,25(\text{OH})_2\text{D}_3$ significantly increased DRIP205 binding to the VDR/RXR complex in both HPK1A and HPK1Aras cells compared to control. Interestingly in HPK1Aras cells, pre-treatment with UO126 followed by $1\alpha,25(\text{OH})_2\text{D}_3$ addition resulted in a 3-4 fold increase in recruitment compared to $1\alpha,25(\text{OH})_2\text{D}_3$ treatment alone. Furthermore, using a biotinylated mOP VDRE pulldown assay to characterize DRIP205 recruitment and also measure the strength of the interaction, they showed that while $1\alpha,25(\text{OH})_2\text{D}_3$ addition resulted in increased DRIP205 interaction in both HPK1Aras and HPK1A cells, recruitment was less intense in the HPK1Aras cells. However, DRIP205 coactivator recruitment was significantly increased in HPK1Aras cells and also comparable to the non-transformed HPK1A following transfection with a non-phosphorylatable RXR mutant or pre-treatment with UO126. This suggests that RXR phosphorylation perturbs DRIP205 coactivator recruitment to the VDR.RXR complex.

Our results therefore suggest that in addition to the requirement for DRIP205 binding to VDR/RXR, there is also a contribution from both VDR and RXR binding to the LXXLL motif of DRIP205 in the presence of the ligand suggesting the LXXLL motif contacts each subunit of the VDR/RXR heterodimer (Rachez et al., 2000). The data therefore reinforces the key role of DRIP205 recruitment of the DRIP complex to the functional VDR/RXR heterodimer in response to $1\alpha,25(\text{OH})_2\text{D}_3$.

Furthermore, we showed through cotransfection studies and fluorescence microscopy of VDR/DRIP205 and RXR α /DRIP205 tagged chimeras that binding of the complex to DNA was also impaired in the ras -transformed cells. There was a direct correlation of the VDR/RXR heterodimer complex binding to either DRIP205 or VDR/RXR/DRIP205 binding to DNA. Our results demonstrated that even though VDR colocalized and interacted with DRIP205 through its LXXLL motif, it did not increase binding in the ras –transformed cells. Binding of VDR/RXR complex to DNA was only increased following the blocking of RXR phosphorylation at serine 260. The current work thus lend additional support to our previous results using single transfection of VDR or RXR α tagged chimeras also showing impaired binding of both VDR and RXR α to DNA in the ras transformed cells when compared to the non-transformed cells. However, we also found that binding could be restored and increased by using either the MEK inhibitor UO126 or transfection with a non-phosphorylatable RXR α mutant, which blocks MAPK phosphorylation (Jusu, et al., 2013 ASBMR proceedings).

RXR is believed to participate directly as a necessary heterodimeric partner in VDR mediated transactivation (Sone et al., 1991a, b; Yu et al., 1991; Mangelsdorf et al., 1995; Whitfield et al., 1995; Cheskis and Freedman, 1996; Thompson et al., 2001; Pike et al., 2003). Thus mutations in the activation domain of RXR or RXR phosphorylation at serine 260 as observed in the ras-transformed cells could also blunt the ability of VDR to activate transcription. (Pike et al., 2003). These findings indicate that both receptors likely participate in commulator interaction essential to transactivation and DNA binding.

In summary, our findings provide new insights into the mechanisms involved in the partial response to the growth inhibitory action of 1,25(OH)₂D₃ in ras-transformed keratinocytes. We provide additional evidence that RXR α phosphorylation at serine 260 not only reduces VDR/RXR α heterodimer interaction but also blocks the interaction of the VDR/RXR α heterodimer to DRIP205 coactivator resulting in reduced or absent binding of the VDR/RXR α /DRIP205 complex to DNA. These findings provide the basis for future studies on designing optimal vitamin D therapy in cancer. We think that blocking MAPK phosphorylation of the RXR would increase the sensitivity of cell bearing ras oncogene to vitamin D.

Acknowledgments

We thank Dr. Michael Garabedian for providing the DRIP205 expression plasmid. We also thank Dr. John White for the human vitamin D receptor expression plasmid and Dr. Stephan Laporte for the GFP expression plasmids. Lastly, we thank Dr. Min Fu for her assistance with the LSM780 confocal microscopy.

Figure 3.1: Effects of RXR α phosphorylation on intranuclear mobility and binding of RXR α . HPK1A cells were transfected with RXR α -wt-GFP (B) followed by treatment with either vehicle (veh), 1,25(OH) $_2$ D $_3$, UO126 alone or a combination of UO126 and 1,25(OH) $_2$ D $_3$. Similarly, HPK1Aras cells were transfected with either RXR α -wt-GFP (D) or RXR α -mut-GFP (F) followed by treatment as above. Residence time (s) and binding of RXR α was measured in both HPK1A (A and B) or HPK1Aras (C-F). Values represent mean \pm SE of at least 10 different cells. Asterisks (*) indicate a significant difference between 1,25(OH) $_2$ D $_3$ treatment or combined UO126 and 1,25(OH) $_2$ D $_3$ treatment compared to vehicle-treated control. Double asterisks (**) indicate a significant difference between combined UO126 and 1,25(OH) $_2$ D $_3$ compared to 1,25(OH) $_2$ D $_3$ treated cells alone. A p value of P < 0.05 was considered significant.

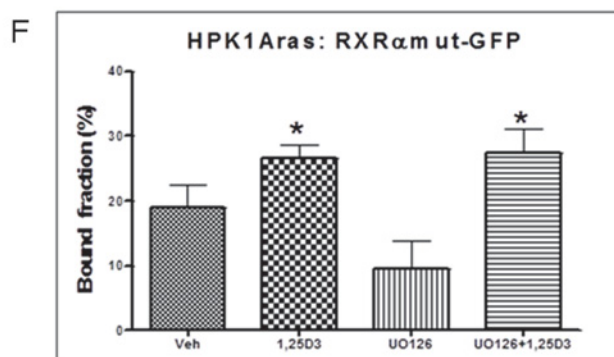
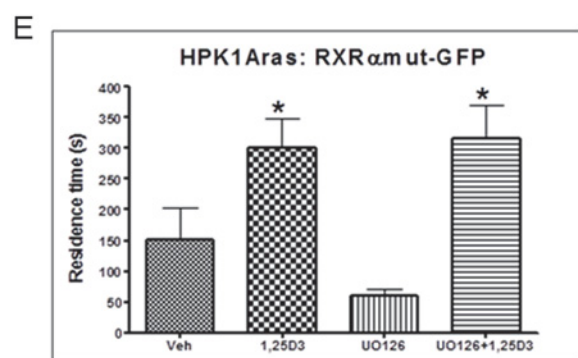
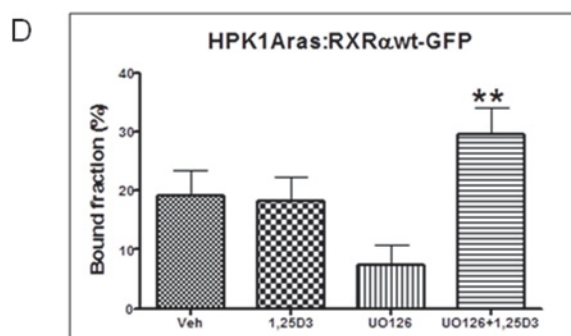
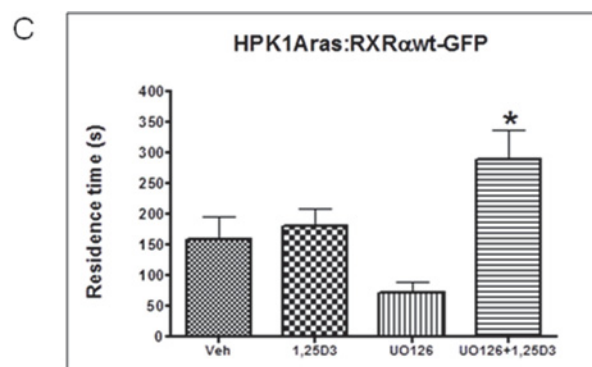
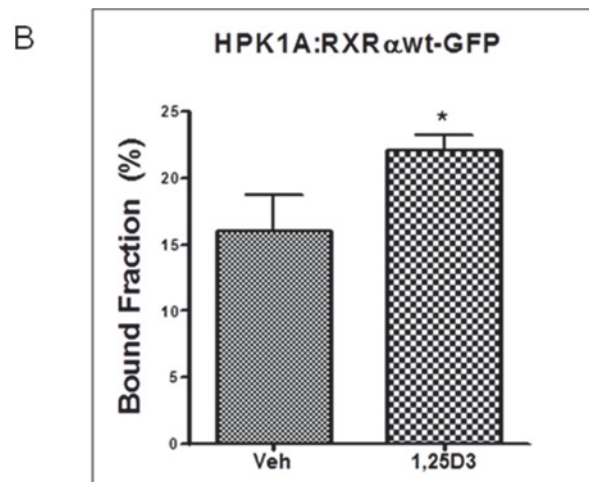
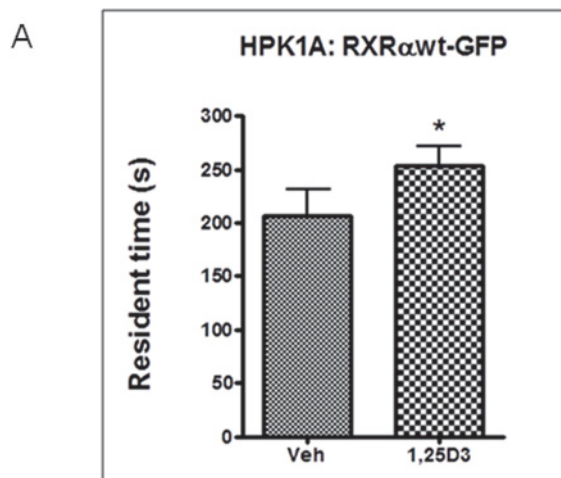


Figure 3.2: Effects of RXR α phosphorylation on VDR and DRIP205 intranuclear colocalization. HPK1A and HPK1Aras cells were co-transfected with VDR-GFP and DRIP205-mCherry re followed by treatment with either vehicle (veh), 1,25(OH) $_2$ D $_3$, UO126 alone or a combination of UO126 and 1,25(OH) $_2$ D $_3$. Pearson coefficient correlation was used to measure intranuclear VDR/DRIP205 colocalization in both HPK1A (A and B) and HPK1Aras (C). Values represent mean \pm SE of at least 10 different cells. Asterisks (*) indicate a significant difference between 1,25(OH) $_2$ D $_3$, UO126 treatment alone or combined UO126 and 1,25(OH) $_2$ D $_3$ treatment compared to vehicle-treated control. Double asterisks (**) indicate a significant difference between combined UO126 and 1,25(OH) $_2$ D $_3$ compared to 1,25(OH) $_2$ D $_3$ treated cells alone. A p value of P < 0.05 was considered significant.

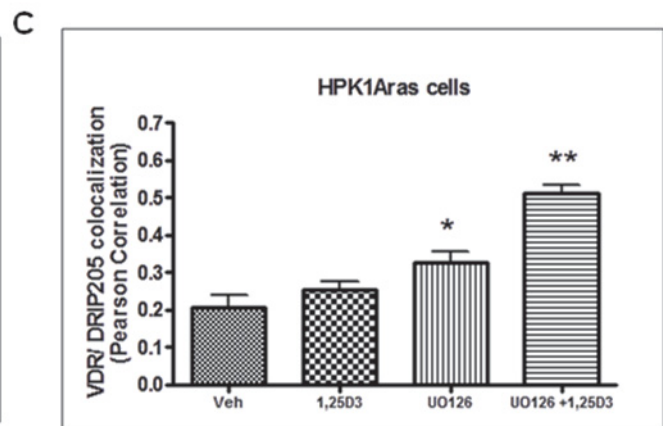
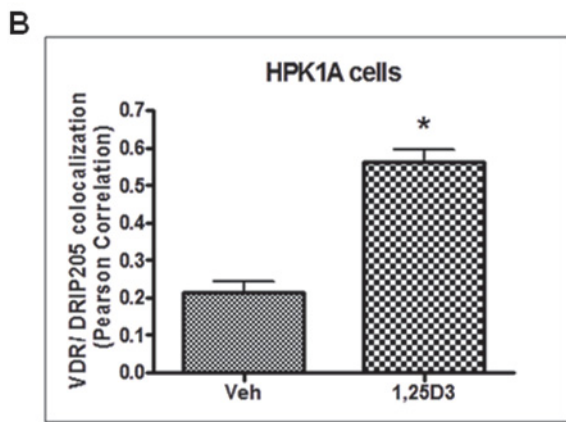
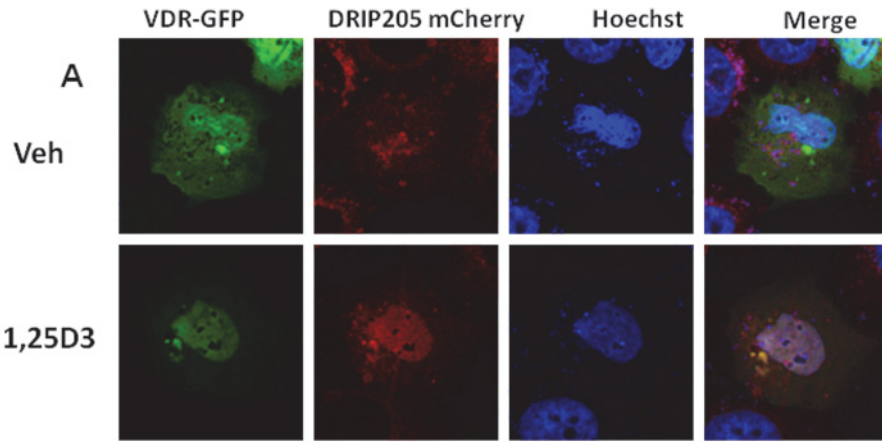


Figure 3.3: Effects of RXR α phosphorylation on RXR α and DRIP205 intranuclear colocalization. HPK1A and HPK1Aras cells were co-transfected with RXR α -GFP/ DRIP205-mCherry or RXR α mut-GFP/ DRIP205-mCherry followed by treatment with either vehicle (veh), 1,25(OH) $_2$ D $_3$, UO126 alone or a combination of UO126 and 1,25(OH) $_2$ D $_3$. Pearson correlation coefficient was used to measure intranuclear RXR α /DRIP205 colocalization in both HPK1A (A and B) and HPK1Aras (C and D). Values represent mean \pm SE of at least 10 different cells. Asterisks (*) indicate a significant difference between 1,25(OH) $_2$ D $_3$, UO126 treatment alone or combined UO126 and 1,25(OH) $_2$ D $_3$ treatment compared to vehicle-treated control. Double asterisks (**) indicate a significant difference between combined UO126 and 1,25(OH) $_2$ D $_3$ compared to 1,25(OH) $_2$ D $_3$ treated cells alone. A p value of P < 0.05 was considered significant.

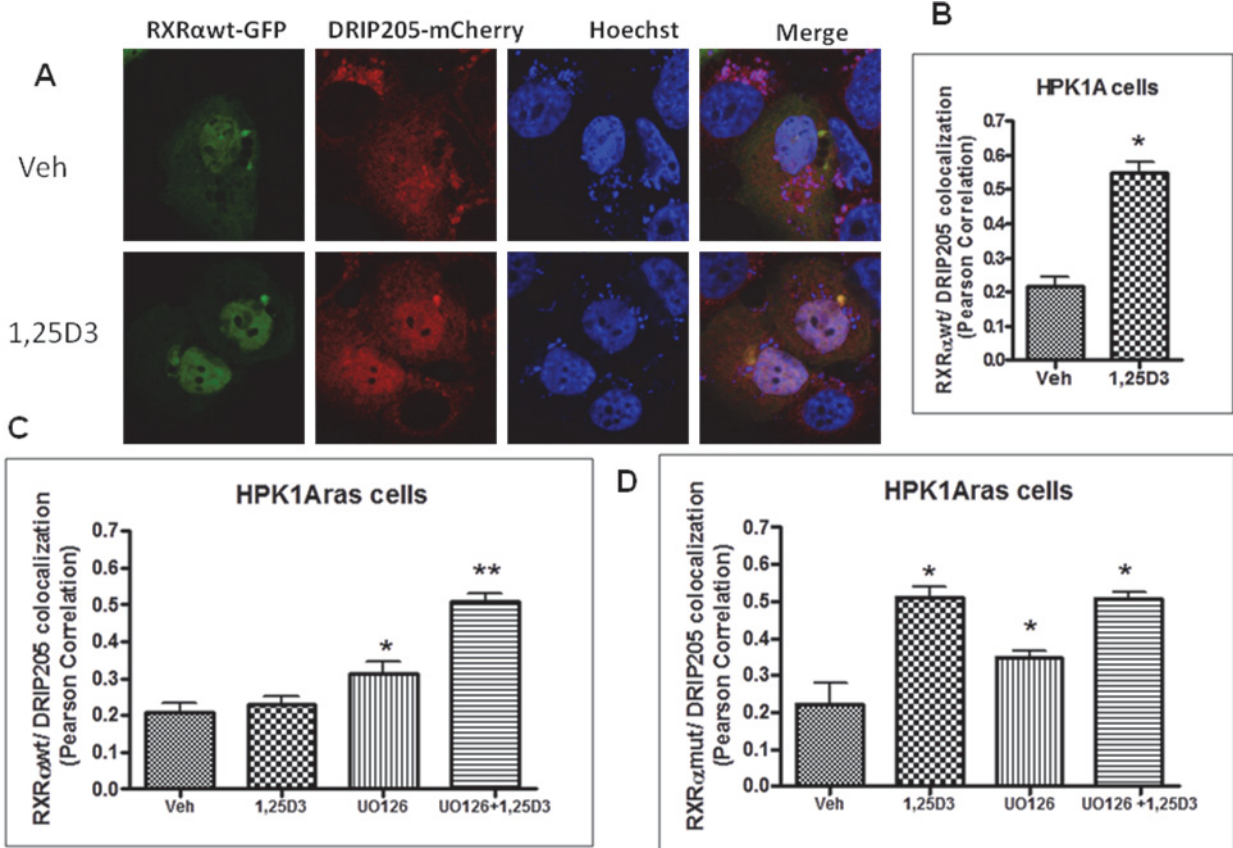


Figure 3.4: Effects of RXR α phosphorylation on VDR/DRIP205 and VDR/LXXLL motif interaction in HPK1A and HPK1Aras cells. Fluorescent Resonance Energy Transfer (FRET) (A and B) was measured by acceptor photobleaching as described in methods. Cells were co-transfected with either VDR-GFP/DRIP205-mCherry or VDR-GFP/LXXLL-mCherry respectively. Following transfection, cells were treated with either vehicle, 1,25(OH) $_2$ D $_3$, UO126 alone or a combination of UO126 and 1,25(OH) $_2$ D $_3$. Bar graph shows FRET measurement by percent dequenching in HPK1A cells co-transfected with VDR-CFP/DRIP205-mCherry (C) or VDR-GFP/LXXLL-mCherry (E). Similarly measurement was done in HPK1Aras cells co-transfected with VDR-GFP/DRIP205-mCherry (D) or VDR-GFP/LXXLL-mCherry (F) respectively. Values are mean percentage dequenching \pm SE of at least 10 cells per treatment condition. Asterisks (*) indicate a significant difference between 1,25(OH) $_2$ D $_3$ treatment alone or combined UO126 and 1,25(OH) $_2$ D $_3$ treatment compared to vehicle-treated control. Double asterisks (**) indicate a significant difference between combined UO126 and 1,25(OH) $_2$ D $_3$ compared to 1,25(OH) $_2$ D $_3$ treated cells alone. A p value of P < 0.05 was considered significant.

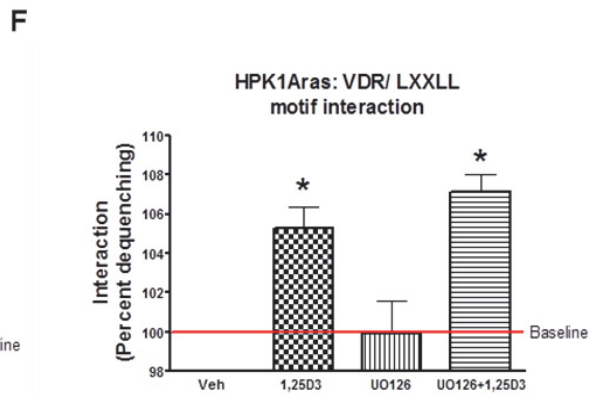
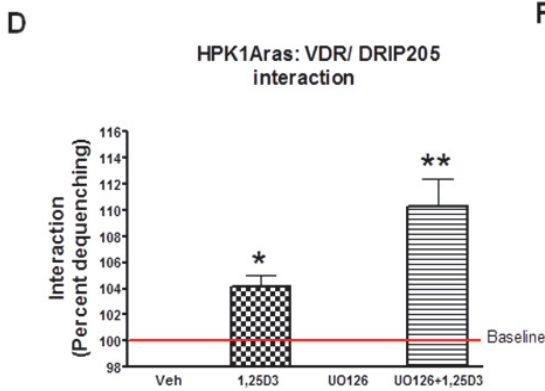
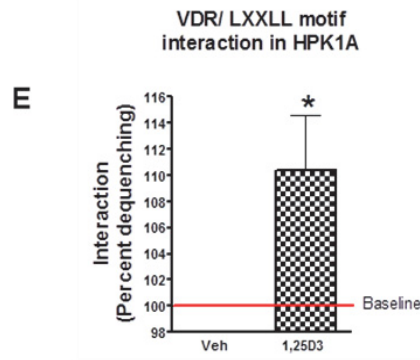
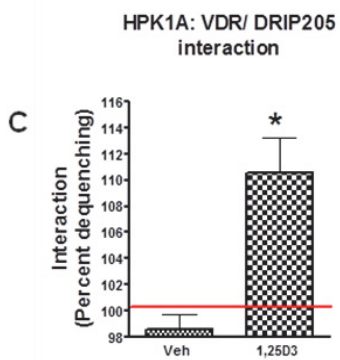
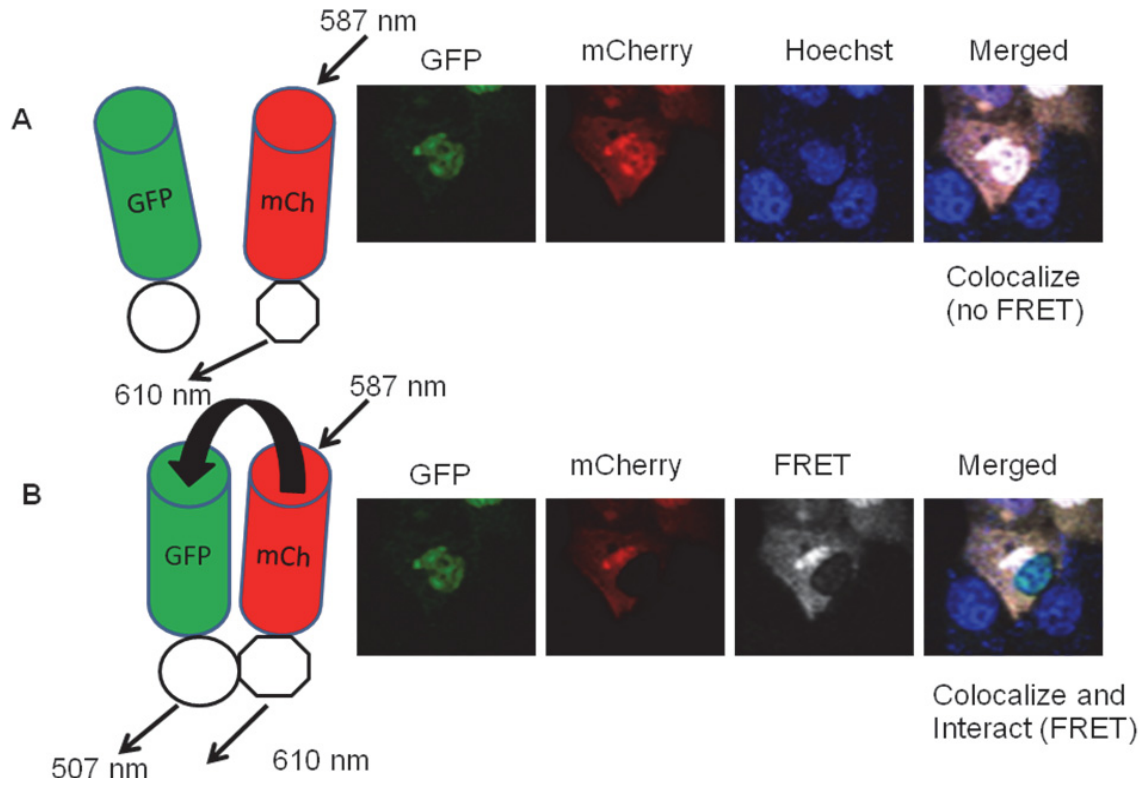


Figure 3.5: Effects of RXR α phosphorylation on RXR α /DRIP205 and RXR α /LXXLL motif interaction in HPK1A and HPK1Aras cells. Fluorescent Resonance Energy Transfer (FRET) was measured by acceptor photobleaching as described in methods. Cells were co-transfected with either RXR α -GFP/DRIP205-mCherry, RXR α mut-GFP/DRIP205-mCherry, RXR α -GFP/LXXLL-mCherry or RXR α mut-GFP/LXXLL-mCherry respectively. Following transfection, cells were treated with either vehicle, 1,25(OH) $_2$ D $_3$, UO126 alone or a combination of UO126 and 1,25(OH) $_2$ D $_3$. Bar graph shows FRET measurement by percent dequenching in HPK1A cells co-transfected with RXR α -GFP /DRIP205-mCherry (A) or RXR α -GFP /LXXLL-mCherry (B). Similarly measurement was done in HPK1Aras cells co-transfected with RXR α -GFP /DRIP205-mCherry (C), RXR α mut-GFP /DRIP205-mCherry (E), RXR α -GFP /LXXLL-mCherry (D), RXR α mut-GFP /LXXLL-mCherry (F) respectively. Values are mean percentage dequenching \pm SE of at least 10 cells per treatment condition. Asterisks (*) indicate a significant difference between 1,25(OH) $_2$ D $_3$ treatment alone or combined UO126 and 1,25(OH) $_2$ D $_3$ treatment compared to vehicle-treated control. Double asterisks (**) indicate a significant difference between combined UO126 and 1,25(OH) $_2$ D $_3$ compared to 1,25(OH) $_2$ D $_3$ treated cells alone.. A p value of P < 0.05 was considered significant.

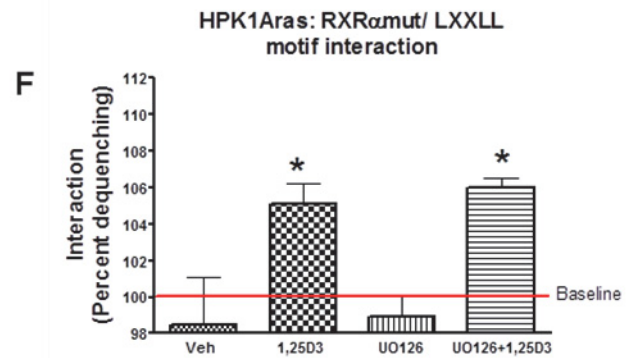
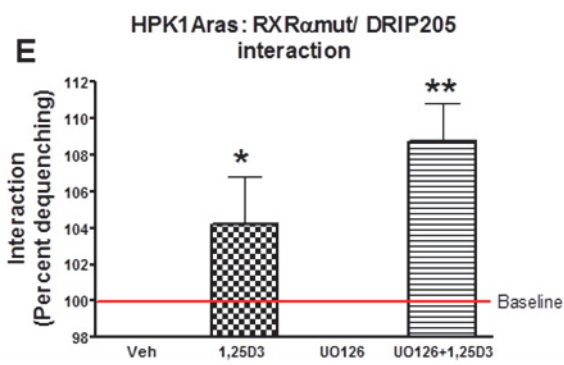
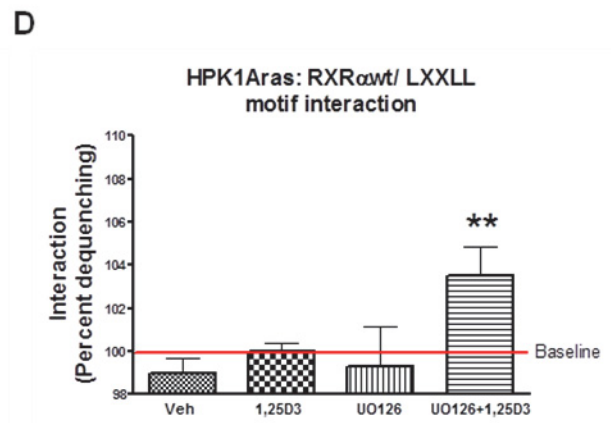
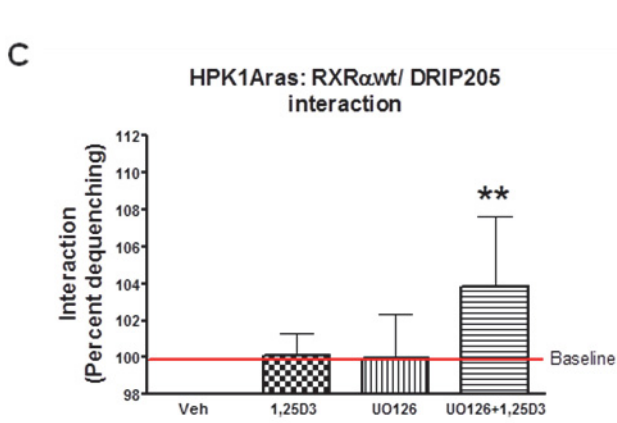
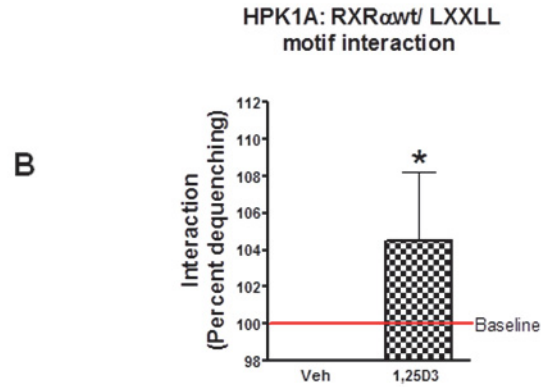
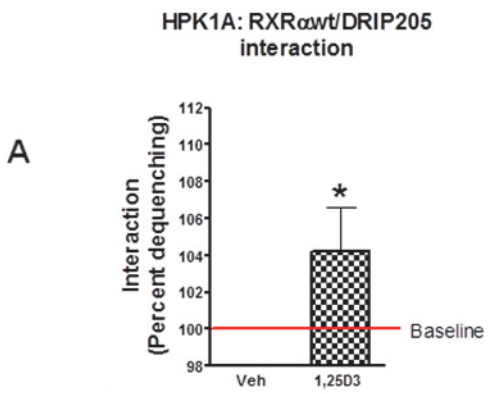
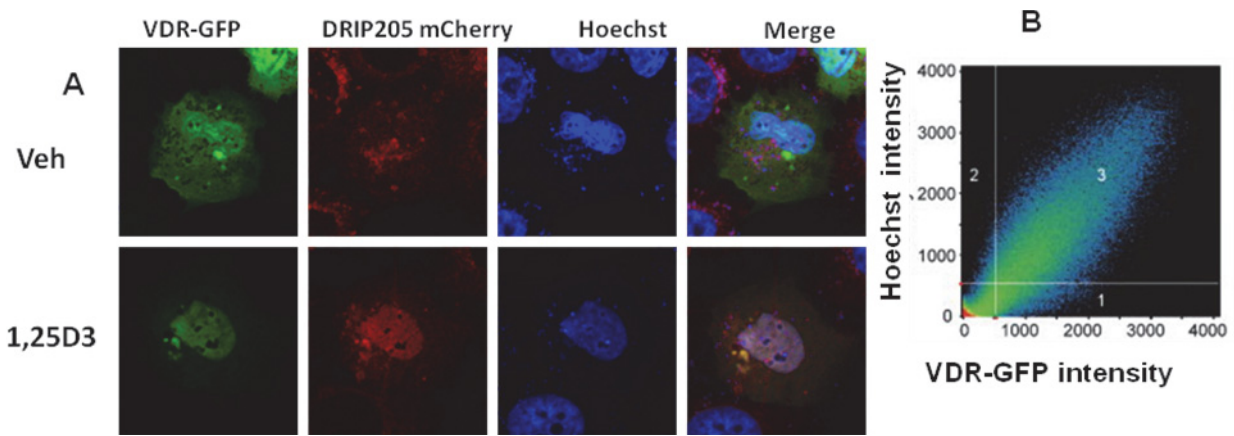
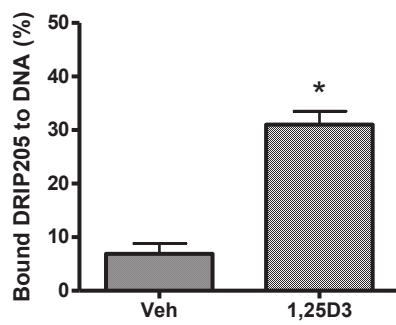


Fig 3.6: Effect of RXR phosphorylation on VDR/DRIP205 complex binding to DNA in non transformed and ras-transformed cells. HPK1A and HPK1Aras cells were cotransfected with VDR-GFP/DRIP205-mCherry and treated with either vehicle, 1,25(OH)₂D₃, UO126 alone or a combination of UO126 and 1,25(OH)₂D₃ for 2 hrs. Cells were stained with Hoechst dye (blue, A) post transfection. Quantitation of binding between DNA (Hoechst) and DRIP205 (mCherry) was assessed using confocal microscopy and Pearson correlation coefficient (B). Values are mean ± SE of at least 10 cells per treatment. Asterisks (*) indicate a significant increase in DNA/receptor interaction in 1,25(OH)₂D₃, UO126 treatment alone or combined UO126 and 1,25(OH)₂D₃ treatment compared to vehicle-treated control. Double asterisks (**) indicates a significant difference in interaction between combined UO126 and 1,25(OH)₂D₃ treatment compared to 1,25(OH)₂D₃ treated cells alone. A p value of P < 0.05 was considered significant.



C HPK1A: VDR-GFP/DRIP205-mCherry/Hoechst



D HPK1A_{ras}: VDR-GFP/DRIP205-mCherry/Hoechst

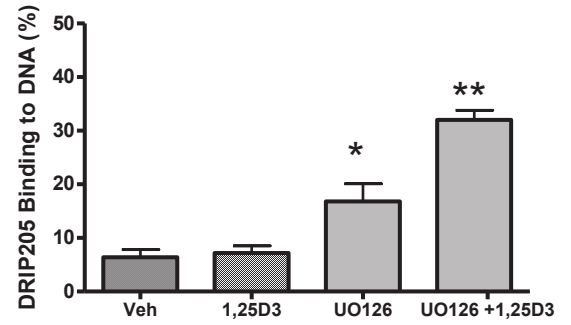
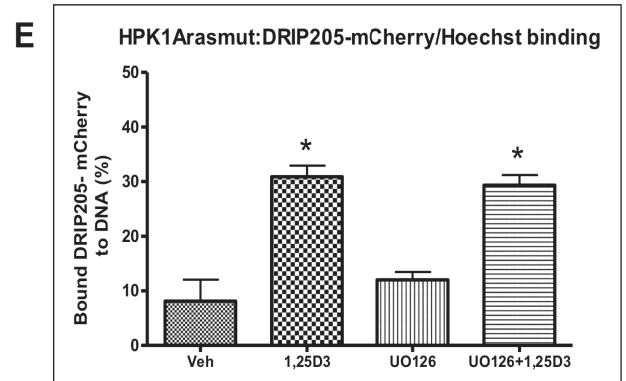
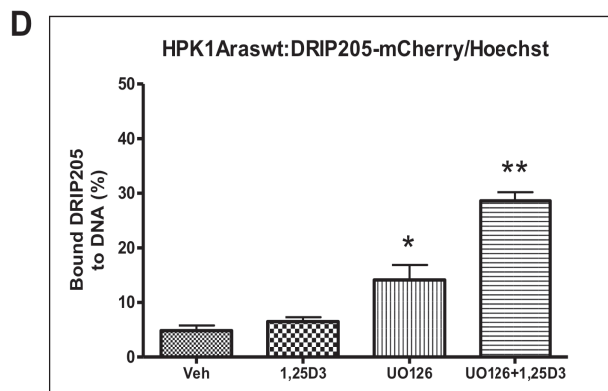
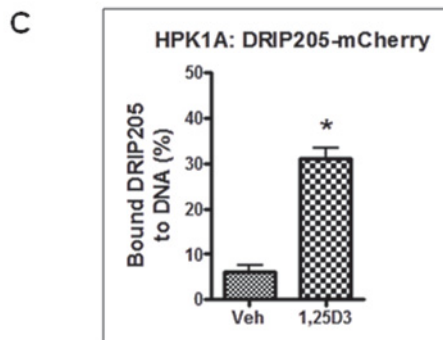
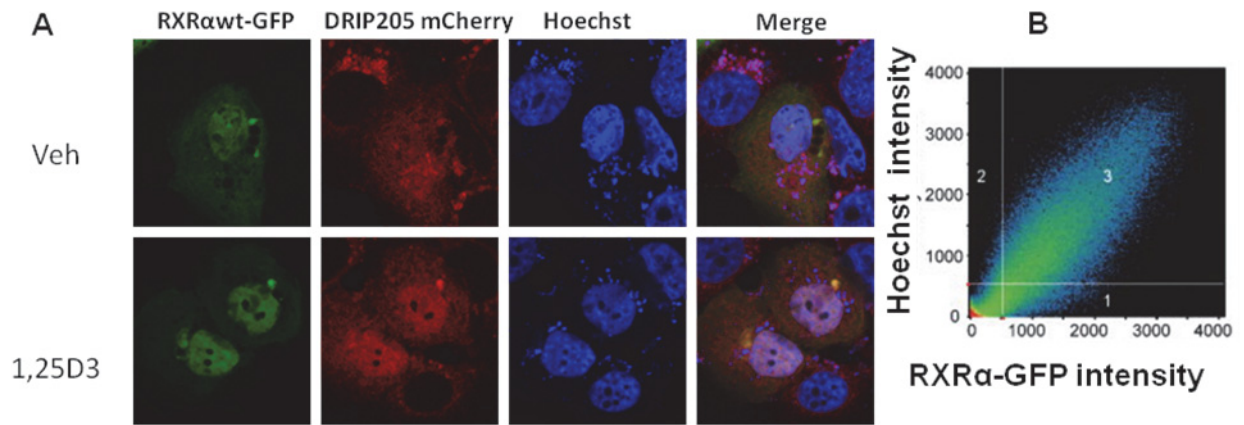


Fig 3.7: Effect of RXR phosphorylation on RXR α /DRIP205 complex binding to DNA in non transformed and ras-transformed cells. HPK1A and HPK1A_{ras} cells were cotransfected with RXR α -GFP/DRIP205-mCherry or RXR α mut-GFP/DRIP205-mCherry and treated with either vehicle, 1,25(OH) $_2$ D $_3$, UO126 alone or a combination of UO126 and 1,25(OH) $_2$ D $_3$ for 2 hrs. Cells were stained with Hoechst dye (blue, A) post transfection. Quantitation of binding between DNA (Hoechst) and DRIP205 (mCherry) was assessed using confocal microscopy and Pearson correlation coefficient (B). Values are mean \pm SE of at least 10 cells per treatment. Asterisks (*) indicate a significant increase in DNA/receptor interaction in 1,25(OH) $_2$ D $_3$,UO126 treatment alone or combined UO126 and 1,25(OH) $_2$ D $_3$ treatment compared to vehicle-treated control. Double asterisks (**) indicate a significant difference in DNA/receptor interaction between combined UO126 and 1,25(OH) $_2$ D $_3$ treatment compared to 1,25(OH) $_2$ D $_3$ treated cells alone. A p value of P < 0.05 was considered significant.



CHAPTER 4 General Discussion

4.1 Mechanisms of 1,25(OH)₂D₃ Resistance through RXR

The vitamin D system is central to the control of bone and calcium homeostasis (DeLuca 2004; Holick 2004; Norman, 2006; Bouillon et al., 2008). Numerous research have indicated that 1,25(OH)₂D₃ (calcitrol) the active and circulating form of vitamin D is tightly regulated and acts through VDR to mediate its genomic actions on target genes (Holick 2004; De Luca 2004; Bouillon et al., 2008; Bikle et al., 2015). Furthermore, researchers have shown that vitamin D plays an important role in other metabolic pathways. Thus alterations in the vitamin D pathway may result in diseases like cancer, diabetes, immune disorders and cardiovascular diseases (Haussler et al., 2008; Bikle, 2014; Bikle et al., 2015). Within this context, understanding the mechanisms responsible for vitamin D resistance will not only provide new evidence on the role of RXR α and VDR/RXR α heterodimer in vitamin D signaling but will also help to identify areas where greater therapeutic targeting can be achieved.

The primary goal of this thesis was thus to examine the mechanisms of 1,25(OH)₂D₃ resistance in cancer cells and the consequences of RXR α phosphorylation at serine 260 on 1,25(OH)₂D₃ mechanism of action using novel fluorescence imaging techniques in both fixed and live cells. This approach allowed us to specifically ask the following questions:

1. Does RXR α phosphorylation affect the nuclear localization or accumulation of RXR α , VDR or of the VDR/RXR α heterodimer?
2. What is the effect of RXR α phosphorylation on VDR/RXR α heterodimer interaction?

3. Does RXR α phosphorylation affect RXR α intra-nuclear mobility and binding?
4. Does RXR phosphorylation affect VDR/DRIP205 or RXR α /DRIP205 nuclear colocalization and interaction?
5. What is the effect of RXR α phosphorylation on VDR/RXR α or VDR/RXR α /DRIP205 complex binding to DNA?

Since 1,25(OH) $_2$ D $_3$ signaling involves receptor trafficking and localization, heterodimer interaction, coactivator recruitment and DNA binding, we hypothesized that investigating the above five questions would shed more light on the mechanisms of resistance.

We first decided to investigate the consequences of RXR α phosphorylation on serine 260 on VDR and RXR α subcellular localization. By using GFP tagged VDR and RXR α transfected into the cell lines and fluorescence microscopy to assess the subcellular localization of both receptors, we found decreased nuclear localization of both VDR and RXR α in the ras-transformed cells treated with 1,25(OH) $_2$ D $_3$. We found that blocking phosphorylation by the use of a pharmacological approach (MEK inhibitor, UO126) or a genetic approach (a non-phosphorylatable RXR α -mutant) reversed the effects observed ie. It increased their nuclear localization. Furthermore, co-localization studies using co-transfection of labeled VDR and RXR α extended our findings by demonstrating impaired nuclear accumulation of the VDR/RXR α complex in the ras-transformed cells.

The next logical step was then to investigate the interaction between the phosphorylated and the non-phosphorylated RXR α with VDR in both cell lines.

We co-transfected the cells with CFP and YFP tagged VDR and RXR α to demonstrate the interaction between the receptors using an acceptor photobleaching method called FRET based on non-radiative energy transfer between the receptors. We used either VDR-CFP / RXR α -wildtype-YFP or VDR-CFP/ RXR α -mutant-YFP cotransfected complexes and subsequently analyzed the interaction using FRET imaging of fixed cells to assess VDR/RXR α interaction. Our results demonstrated impaired interaction of the VDR-CFP/RXR α wt-YFP in the ras-transformed cells. The significance of these findings is that RXR α phosphorylation not only reduces the nuclear colocalization of both VDR and RXR α , but also significantly impairs heterodimer interaction.

We next used live cell imaging employing FRAP and FLIP methodologies to examine whether RXR α phosphorylation affected its intranuclear kinetics. The conventional view so far has been that nuclear receptors including VDR and RXR remain stably bound to their hormone response elements (HREs) and that transcription initiation is static. However, recent FRAP and FLIP measurements have revealed the dynamic and cyclic nature of gene expression controlled by nuclear receptors (McNally et al., 2000; Hager et al., 2004; Nagaich et al., 2004). Also, FRAP and FLIP resolves events in the seconds range (McNally et al., 2000). Following transfection with a GFP tagged RXR α -wildtype or RXR α -mutant, cells were treated with 1,25(OH) $_2$ D $_3$ or vehicle and repeatedly photobleached. The purpose is to remove the GFP fluorescent signal of both the VDR and RXR α in a defined area of the nucleus. This enables real-time, single live-cell imaging and measurement of the dynamic association or dissociation of the fluorescently tagged receptors moving back into the photobleached area. Nuclear receptors have been reported to be highly mobile in the nucleus with rapid exchange of receptor

molecules on DNA (McNally et al., 2000). Our results showed that the half time of dissociation or association and binding of the receptors to subcellular components of the nuclear compartments increased in the non-transformed HPK1A cells but not in the ras-transformed HPK1Aras cells after 1,25(OH)₂D₃ addition. Treatment with UO126 or transfection with the non-phosphorylatable RXR α -mutant in HPK1Aras cells in the presence of 1,25(OH)₂D₃ significantly increased both the half times of dissociation, association and the binding of the RXR α receptor to subcellular nuclear components (Fig. 2.6 A-G and Fig. 3.1 A-F).

FRET has the advantage of examining directly the interaction between VDR and RXR α in an intact cellular environment without disrupting its various nuclear components from the rest of the cell as opposed to our previous studies using nuclear extracts and electromobility gel shift assays (Pruffer et al., 2000; Solomon et al., 2001; Barsony and Pruffer 2002; Macorrito et al., 2008). Our studies in live cells using FRAP and FLIP shed further light on the underlying mechanism of resistance by linking RXR α phosphorylation to dynamic changes in receptor shuttling with intranuclear components. We hypothesised that the major site of this dynamic interaction is with DNA.

The experiment using Hoechst labeled DNA further demonstrated that RXR α binding to DNA could only occur in the presence of VDR since RXR α phosphorylation prevented VDR binding to DNA.

In summary, FRET experiments demonstrated altered interaction between VDR and RXR α in intact cells. Both FRAP and FLIP techniques in live cells were used to assess RXR α intra-nuclear kinetics demonstrating reduced interaction and binding of phosphorylated RXR α to the subcellular nuclear components in the ras-

transformed cells. Finally we demonstrated that RXR α phosphorylation disrupts VDR/RXR α complex interaction with DNA in intact cells.

In chapter 3, we assessed the effects of RXR α phosphorylation on VDR/ DRIP205 nuclear colocalization, RXR α /DRIP205 nuclear colocalization and VDR/DRIP205 and RXR α /DRIP205 interaction. Our results showed that 1,25(OH) $_2$ D $_3$ treatment alone did not increase nuclear colocalization of VDR/DRIP205 or RXR/DRIP205 in the ras-transformed cells when compared to the non-transformed cells. However, we found that DRIP205 and DRIP205 LXXLL motif can interact with VDR in the ras-transformed cells. In contrast, there was no interaction of DRIP205 or its DRIP205 LXXLL motif with phosphorylated RXR α . We further demonstrated that blocking RXR α phosphorylation increased VDR/DRIP205 nuclear colocalization following 1,25(OH) $_2$ D $_3$ treatment. Furthermore, VDR/DRIP205 interaction increased even further in response to 1,25(OH) $_2$ D $_3$ treatment suggesting this enhanced interaction was secondary to the increase in VDR/ DRIP205 nuclear colocalization. When we examined RXR α /DRIP205 colocalization following inhibition of phosphorylation, we could demonstrate that this process was now enhanced in response to 1,25(OH) $_2$ D $_3$ and that the interaction between RXR α /DRIP205 could be clearly demonstrated. This was noteworthy as it suggested that RXR α phosphorylation was to a large extent responsible for the effects observed. Though Rachez and coworkers (2000) have reported DRIP205 interaction with both VDR and RXR AF-2 domains in cell free systems, other groups had only shown DRIP205 interaction with VDR but did not examine DRIP205 interaction with RXR (Bukarov et al., 2000; Panthose et al., 2002; Zella et al., 2007). This interaction was shown to take place between the NR2 domain of DRIP205 and the VDR and between both the NR1 and NR2 domains of DRIP205

and the VDR/RXR complex although the NR2 interaction appeared to be much stronger. Our findings in non-transformed HPK1A cells also showed stronger interaction of VDR/DRIP205 than RXR/DRIP205 interaction supporting findings from Rachez et al., (2000). Using Chromatin –immunoprecipitation assay Kim et al., (2004) previously reported that in intact osteoblasts (MC3T3-E1 cells), 1,25(OH)₂D₃ treatment induces VDR/RXR binding to the osteopontin (Opn) and CYP24 promoters and that this was accompanied by the recruitment of DRIP205 coactivator.

We are the first to report RXR α interaction with DRIP205 in intact keratinocytes. We further demonstrated that in the ras-transformed HPK1A_{ras} cells, RXR α phosphorylation at serine 260 abolished this interaction but did not abolish VDR/DRIP205 interaction. This finding is very significant as it demonstrates that VDR/DRIP205 interaction could still take place despite the absence of a functional VDR/RXR α complex in the ras-transformed cells.

Finally, we used cotransfection studies of VDR/ DRIP205, RXR α /DRIP205 and Hoechst staining to assess VDR/RXR α /DRIP205 complex binding to DNA. Similar to the binding results obtained for single receptor transfection and live cell imaging to assess intra-nuclear kinetics (Fig. 2.6 A-H and 2.7 A-H), our results showed attenuation of VDR/RXR α /DRIP205 complex binding to DNA in the ras transformed cells. Treatment with UO126 or transfection with the non-phosphorylatable RXR α mutant significantly increased binding of the complex to DNA.

To sum up, this work not only brings to light new evidence on the mechanisms of resistance in the ras-transformed keratinocytes, it also opens new avenues for the therapeutic targeting of MAP kinase signaling pathway in other cancer models.

4.2 Nucleocytoplasmic transport of VDR and RXR

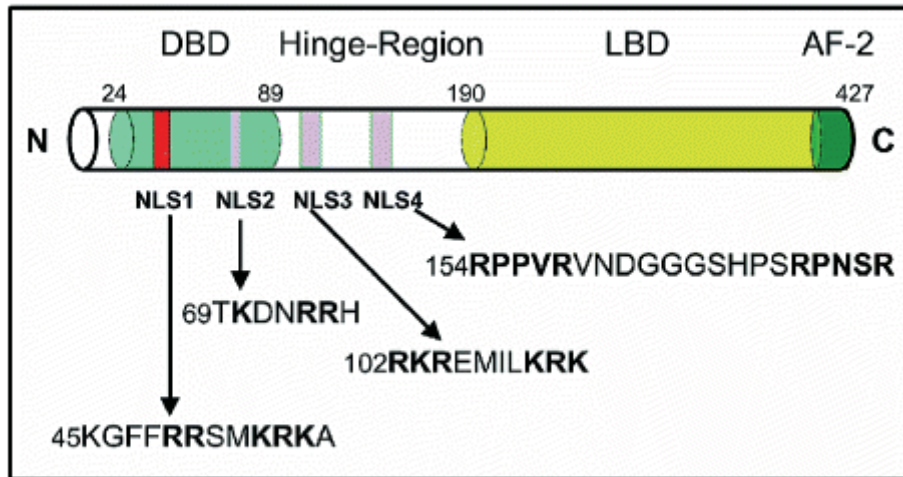
Nucleocytoplasmic transport plays a pivotal role in eukaryotic function (Barsony, 2010). We have used photobleaching techniques such as FRET, FRAP, FLIP and confocal imaging to investigate nuclear localization of VDR and RXR and intra-nuclear kinetics of RXR. In earlier studies Barsony and Pruffer (2002) demonstrated that both VDR and RXR shuttle between the cytoplasm and nucleus and that $1,25(\text{OH})_2\text{D}_3$ increases their nuclear localization in normal cells (Pruffer and Barsony 2002). However, the precise mechanisms by which these proteins shuttle between the cellular compartments have not been completely elucidated. According to Barsony and Pruffer (2002), VDR and RXR shuttle through the nuclear pore complex (NPC) by interaction with the nuclear import and export machinery and other components of the transport pathway. It has been suggested that nuclear receptors including VDR and RXR possess nuclear localization signals (NLSs) and nuclear export signals (NESs) which are recognized by adaptor proteins importins and exportins (Barsony 2010). The NLSs and NESs direct proteins to enter or leave the nucleus. Nuclear transport processes mostly involves the use of a set of cytoplasmic receptors that are members of the importin β (karyopherin β) nuclear transport receptor family. The receptors are regulated by the binding of a small GTPase known as Ran. Inside the nucleus where its GDP-GTP exchange factor RCC1 (regulator of chromosome condensation 1) resides,

Ran exists predominantly in its GTP form. In the cytoplasm Ran exists in the GDP form. Within the cytoplasm is found the GTPase activating protein called RanGAP (Weiss et al., 1996b; Heger et al., 2001; Kaku et al., 2008).

In the cytoplasm, adaptor proteins like importin α recognize the NLS on the cargo. The complex is stabilized by binding of the import receptor importin β which interacts with the importin β - binding domain. (IBB) of the cargo loaded importin α . The triple complex formed next docks to the cytoplasmic side of the NPC via importin α and moves to the nuclear side of the NPC. The next step is the binding of Ran-GTP which terminates translocation leading to the displacement of importin α –cargo protein from the import complex. This is followed by a formation of an importin β /Ran-GTP complex (Weiss et al., 1996b; Barsony, 2010).

In the export process, the C-terminal importin β -binding domain of the now cargo –free importin α binds to the export receptor, cellular apoptosis susceptibility factor (CAS) cooperatively with Ran-GTP and is then recycled back into the cytoplasm. Translocation of the Ran-GTP-bound importin β into the cytoplasm can either occur alone or with new cargoes that bind to it. GTP hydrolysis occurs due to the activities of Ran-binding protein (RanBP1) and Ran-specific GTPase activating protein 1 (Ran-Gap). This results to the disassembly of the export complex. CAS is then recycled back to the nucleus by passing through the nuclear pore complex. Three export factors that likely play significant roles in the export process include calreticulin, exportin-7 and chromosomal region 1 protein (Crm-1). Cargoes for Crm-1 are either proteins that carry a leucine-rich NES or RNAs. Calreticulin and exportin-7 mediated exports have been reported to influence the transcriptional activities of GR (Zilliacus, J et al., 2001)

a VDR NLS Segments



b RXR NLS Segments

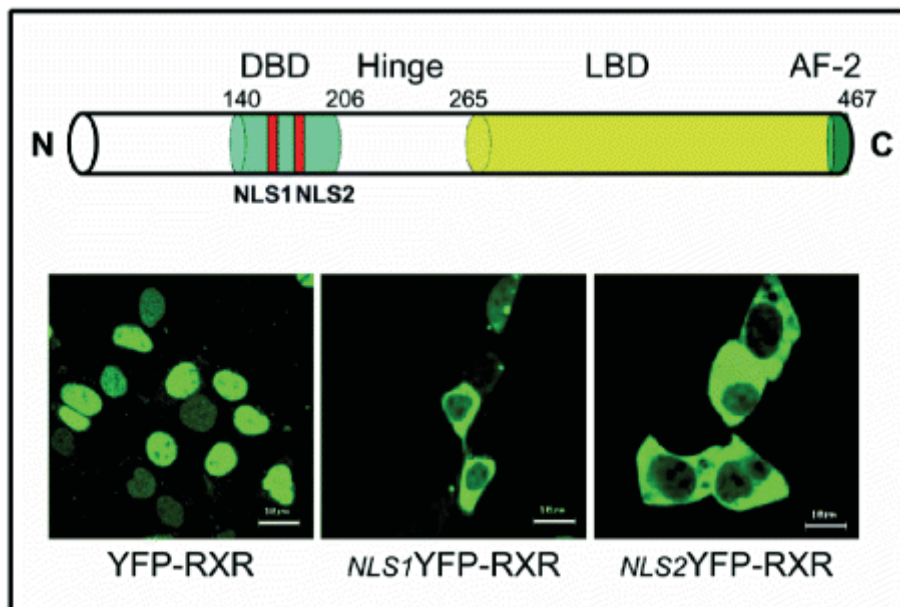


Fig.4.1. Schematic representation of VDR and RXR nuclear import domains. Colored bars, flanked by the bordering amino acid numbers on top, depict VDR and RXR functional domains: DNA-binding domain (DBD), hinge region, and ligand-binding domain (LBD). (a) Amino acids representing the putative nuclear

localization sequences (NLSs) of VDR are shown in bold letters. In living cells only the NLS1 mutations caused cytoplasmic retention of receptors

(b) Two NLSs within the DNA-binding domain of RXR are indicated with the red bars. Images are shown of live HEK293 cells stably expressing wild-type YFP-RXR or its mutants. The NLS1 mutations were K160Q, R161G, and R164G, and the NLS2 mutations were R182E and R184E. Mutations caused cytoplasmic retention. Images were taken using a Zeiss LSM410 confocal microscope. Bars, 10 μ m. (Adapted from Barsony, 2010)

The transport efficiencies of the nuclear receptors are governed by the affinities for the transport receptors and this may play an important role in altering the nuclear receptor abundance in the cytoplasm or nucleus (Heger et al., 2001). Post-transcriptional modifications in the secondary and tertiary structures of the NLS and NES domains may also allow cyclical and timely responses to cellular states (Katagiri et al., 2000; Heger et al., 2001; Mostaqul et al., 2006; Amazit et al., 2007). Mutations of the basic amino acids of the NLS and NES have increased our understanding regarding the functional significance in the transport process (Barsony, 2010). Pruffer and Barsony (2002) found that mutations within the DBD decreased nuclear export of VDR and RXR.

Future studies may be conducted in our model to examine whether RXR phosphorylation has any influence of VDR and RXR shuttling between the cytoplasm and the nucleus.

4.3 RXR as Target for MAPK, Chemoprevention and Cancer Treatment

In previous studies, our group showed that phosphorylation of hRXR α on serine 260 led to a disruption of the VDR/RXR-VDRE complex formation as well as reduced coactivator recruitment in cell free systems (Solomon et al., 1999; Macorrito et al., 2008).

Solomon and coworkers (1999, 2001) reported that in human keratinocytes, RXR α was phosphorylated at serine 260, a critical site located in the Omega loop of the LBD and in close proximity with coactivators. This phosphorylation results in the attenuation of ligand-dependent transactivation by the RXR α /VDR complex, thus resulting in uncontrolled cell growth. The phosphorylation of RXR α at serine 260 is also associated with retinoid resistance (Matsushima-Nishiwaki et al., 2001; Yoshimura et al., 2007). These findings indicate that RXR α phosphorylation, occurs at specific residues located in the Omega loop of the LBD between helices H1 and H3. This region according to structural studies, is also very flexible and dynamic and moves substantially during the conformational rearrangement that accompanies ligand binding to the LBD (Egea et al., 2000). It has therefore been proposed that phosphorylation of the residues in this loop might alter the dynamics of this region and create conformational changes within the LBD, thus disrupting the interactions with coactivators and therefore inhibiting the activation of RXR and RA-responsive genes (Bruck et al., 2005; Macorrito et al., 2008).

In the present study, we extended these findings by demonstrating that VDR and RXR α nuclear accumulation are diminished in ras-transformed cells treated with either VDR specific ligand 1,25(OH) $_2$ D $_3$ or the RXR specific ligand 9-cis-RA.

Given the fact that many nuclear receptors function as either homo or heterodimers with RXR, the implications of our results could be broad. In contrast to

homodimers, heterodimerization of the nuclear receptors with RXR in the presence of their ligands results in the refining of their action (Gronemeyer et al., 2004). Our findings thus show that RXR could be a target for therapeutic enhancement in cancer where MAP kinase signaling is activated such as cancers bearing a ras signature. Reports from Solomon and coworkers (1999) and Macorrito et al., (2008) that phosphorylation of hRXR α on serine 260 led to a disruption of the VDR/RXR-VDRE complex formation and resistance to the growth inhibitory action of multiple RXR ligands similar to that observed in 1,25(OH) $_2$ D $_3$ signaling further supports using RXR as a target for MAP kinase signaling.

Other groups working with several cell types have also reported the MAPK induced phosphorylation of RXR. Lattuada et al., (2006) using myometrium and leiomyoma cells and Narayanan et al., (2004) showed that in MC3T3-E1 cell, phosphorylation of RXR α by ERK led to a reduction in VDR activity and blocking phosphorylation by the use of the MEK inhibitor UO126, in a manner similar to ours increased VDR transcriptional activity.

In contrast to studies in human cells, in which MAP kinase induced phosphorylation of human RXR α at serine 260, Adam-Stitah et al., (1999) reported that phosphorylation of the murine (m) RXR at serine 265 (equivalent to human serine 260) by overexpression of the stress-activated kinases c-Jun NH $_2$ -terminal kinase 1 and 2 (JNK1 and JNK2) had no effect on the transactivation activity RXR/RXR or RXR/RAR. However, Bruck et al., (2005) using an F9 RXR α -null background mice cells that expressed either (knock-in) RXR α wt or a mutant RXR α S265A showed that in cells expressing the RXR α wt, activation of JNK resulted in a decreased activation of the reported genes containing a DR5 RARE.

In contrast, cells expressing the mutant RXR α S265A had a normal transactivation response to anisomycin (an inhibitor of protein synthesis) suggesting that phosphorylation inhibited the transactivation of the RXR α /RAR complex. Finally, Zimmerman et al., (2006) reported that interleukin-1 beta activation of JNKs resulted in RXR phosphorylation at serine 260 in HepG2 cells. The overall effect is an inhibition of its (RXR) transcriptional activity.

4.3.1 RXR/RAR as a Target

Previous studies found that RXR α protein was phosphorylated anomalously in human hepatocellular carcinoma tissues (HCC) as well as HCC cell lines (Matsushima-Nishiwaki et al., 2001, 2003). RXR α phosphorylation at serine 260 also resulted in impairment of its function and resistance to the growth inhibitory effects of all-trans retinoic acid (Matsushima-Nishiwaki et al., 2001). In addition, Adachi et al., (2002) from the same group reported that in hepatocellular carcinoma, RXR ubiquitination was suppressed due to phosphorylation and reported that the phosphorylated form of RXR α was resistant to ubiquitination and proteasome mediated degradation in both HCC tissues and cell lines. Also, the phosphorylated RXR α loses its transactivation activity suggesting that the phosphorylated RXR α (non-functional) may interfere with the function of a normal RXR α in a dominant negative manner thereby playing a critical role in the development of HCC (Fig. 4.2). However, abrogation of phosphorylation by mitogen-activated protein kinase-specific inhibitors restored the degradation of RXR α in an RXR ligand-dependent manner. Further studies revealed that MAPK and MAPK 4 phosphorylation of RXR inhibits the transactivation of RAR

(Yoshimura et al., 2007). The group similarly reported that phosphorylation of RXR at serine 260 results in loss of RXR β transactivating activity. It was further revealed that overexpression of a phosphomimetic RXR α mutant inhibited transcription activity of the RARE promoter in 293T cells. However, the non-phosphorylated RXR α mutant stimulated the transcriptional activity.

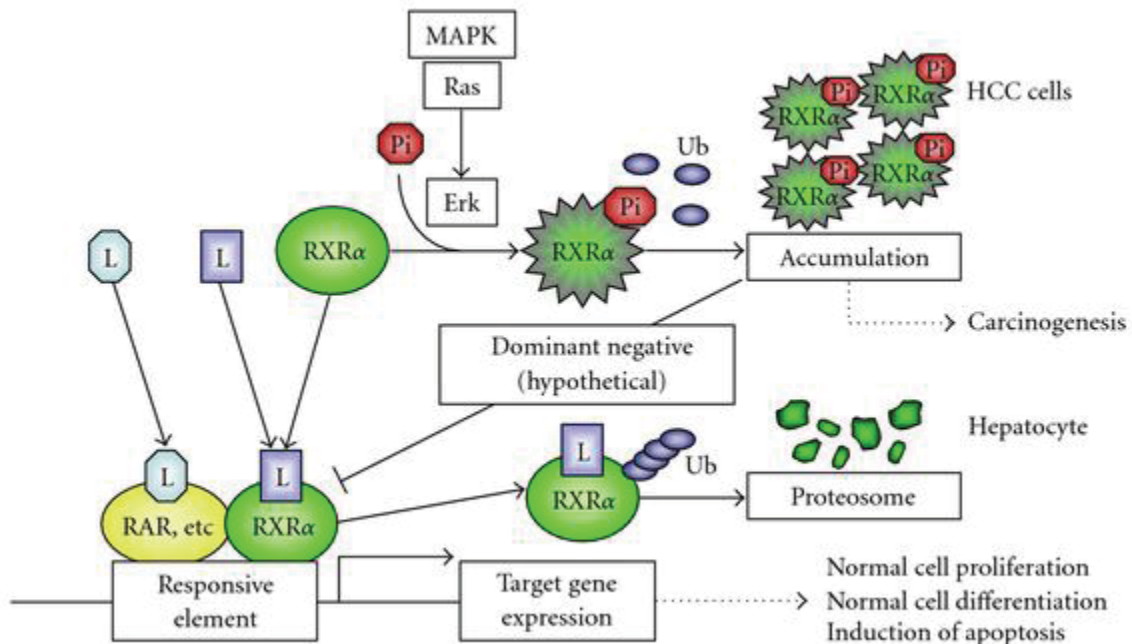


Fig .4.2. A schematic representation of RXR α phosphorylation in HCC cells. In normal hepatocytes, when the ligand (retinoid) binds to and activates RXR α , the receptor becomes able to heterodimerize with other nuclear receptors, including RAR, and then activates the expression of the target genes, which may regulate normal cell proliferation and differentiation, by binding to the specific responsive element. In HCC cells, the Ras/MAPK pathway is highly activated and phosphorylates RXR α at serine residues, thus impairing the functions of the

receptor. Therefore, the accumulated p-RXR α interferes with the remaining normal RXR α , presumably, in a dominant negative manner, thereby playing a critical role in the development of HCC. L: ligand. Ub: ubiquitin (Adapted from Shimitzu and Morkwaki, 2008).

These findings suggest that phosphorylation of RXR α abolishes its ability to form homodimers and heterodimers with RXR and RAR β thus resulting in the loss of cell growth control and the acceleration of cancer development (Yoshimura et al., 2007).

In addition to HCC, phosphorylation of RXR α is also associated with the development of other types of human malignancies. Shimizu et al., (2008) reported that RXR α protein is highly phosphorylated and also accumulates in human colon cancer tissue samples as well as human colon cancer cell lines. While the level of expression of phosphorylated-RXR α is not increased in normal colonic epithelial cells, RXR α protein is phosphorylated in 75% of colorectal cancer tissues when compared with corresponding normal colon epithelial tissues (Yamazaki et al., 2007).

Similar results have also been observed in human pancreatic cancer. Moreover, Kanemura et al., (2008) reported that abnormal phosphorylation of RXR α protein played a role in the enhancement of cell proliferation, while producing an antiapoptotic effect and also acquiring RA-resistance in HL-60R human leukemia cells. In addition to these malignancies, RXR α is highly phosphorylated and accumulates in leiomyoma when compared to myometrial cells and this is associated with a resistance to ligand-mediated ubiquitination and a delay in the receptor proteolytic degradation using 9-cis-Retinoic Acid (Lattuada et al., 2007).

4.3.2 RXR/PPAR as a Target

Other nuclear receptors, including PPARs, also require RXR α as a heterodimeric partner in order to exert their function. *In vitro* and *in vivo* studies have shown that PPAR γ agonist can inhibit the growth of human colon cancer (Sarraf et al., 1998) and the combination of PPAR and RXR α ligand has been shown to be very promising for the treatment of lung cancer, breast cancer and leukemia (Crowde et al., 2004; Konopleva et al., 2004; Avis et al., 2005). Subsequently, Yamazaki et al., (2007) demonstrated that phosphorylated RXR α accumulated in a colon cancer cell line and that inhibition with a MEK inhibitor or transfection with a non-phosphorylatable RXR α mutant and treatment in combination with 9-cis-RA and the PPAR γ agonist ciglitazone had a synergistic effect on growth inhibition and enhanced apoptosis. This suggests that combining inhibition of RXR α phosphorylation and activation of the PPAR γ /RXR complex may be useful in the treatment of colorectal cancer (Fig 4.3).

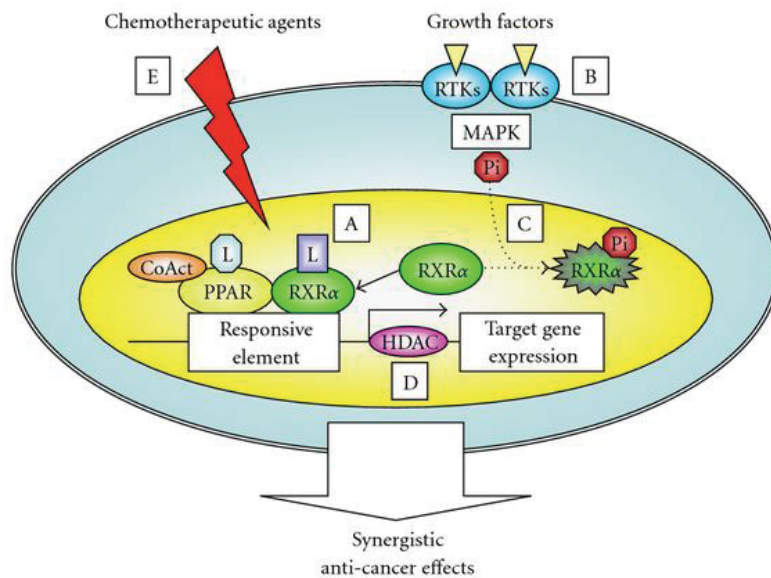


Figure 4.3: A hypothetical schematic representation of the synergistic anticancer effects of the combination of PPAR ligands plus other agents. When PPARs are activated by ligand binding, they are able to heterodimerize with RXR and activate the target gene expression by binding to the PPRE element. Therefore, the retinoids which bind to RXR may be the most preferable partner for the PPAR agonists (A). However, in some types of cancers, the MAPK pathway phosphorylates RXR α , and the accumulated nonfunctional p-RXR α interferes with the function of the remaining normal RXR α , thereby promoting the growth of cancer cells. The activation of RTKs (receptor tyrosine kinases) by their specific ligands (growth factors) can play a critical role in the stimulation of the MAPK pathway. Therefore, the agents which target the activation of RTKs (B) and/or the MAPK pathway (C) restore the function of RXR α as a master regulator of nuclear receptors in cancer cells and this will support the synergistic growth inhibition by PPAR and RXR ligands in cancer cells. The HDACs enforce a tight chromatin structure and thereby repress the transcription of target genes controlled by PPAR/RXR. Therefore, the combination of a PPAR agonist plus an HDAC inhibitor is more efficient to inhibit the growth of cancer cells (D). Finally, the conventional chemotherapeutic agents also cause synergistic or enhancing effects to inhibit cancer cell growth by the combination of PPAR ligands (E). L: ligand (Adapted from Shimizu and Moriwaki, 2008).

4.3.3. Inhibition of Phosphorylation of RXR α with Acyclic Retinoid

The above findings support the possibility that the inhibition of RXR α phosphorylation and the restoration of its physiological function as a master

regulator of nuclear receptors must be an effective strategy for controlling cell growth in various types of human cancers (Shimizu and Moriwaki, 2008; Shimizu et al., 2012).

It has been shown that the new synthetic retinoid, acyclic retinoid (ACR) NIK-333 and Peretinoin (Kowa Pharmaceutical Company Ltd., Tokyo, Japan), which was originally developed as an agonist for both RXR and RAR (Yamada et al., 1994; Araki et al., 1995; Shimizu et al., 2012) can restore the function of RXR α by inactivating the Ras-Erk signaling system and thereby inhibit RXR α phosphorylation (Fig. 4.4, Matsushima-Nishiwaki et al., 2003; Shimizu and Moriwaki 2008). Several *in vitro* and *in vivo* studies have highlighted beneficial effects of ACR. These include inhibition of chemically induced hepatocarcinogenesis in rats as well as spontaneously occurring hepatoma in mice (Muto et al., 1984), inhibition of growth and induction of apoptosis in human HCC-derived cells (Nakamura et al., 1996, Shimizu et al., 2004, 2012). The mechanisms includes activation of the promoter activity of RXRE and RARE and controlling the expression of target genes, including RAR β , p21^{CIP1}, and cyclin D1, which results in induction of apoptosis, cell cycle arrest in G₀–G₁, and growth inhibition in human HCC-derived cells (Shimizu et al., 2012). These findings suggest that the suppression of HCC by ACR is due to at least in part working as a ligand for retinoid receptors and controlling their target genes, especially RAR β and p21^{CIP1} (Shimizu et al., 2012). Similar growth inhibitory effects have also been reported in other types of human cancer cells, such as squamous cell carcinoma or leukemia cells (Tsurumi et al., 1993; Shimizu et al., 2004)

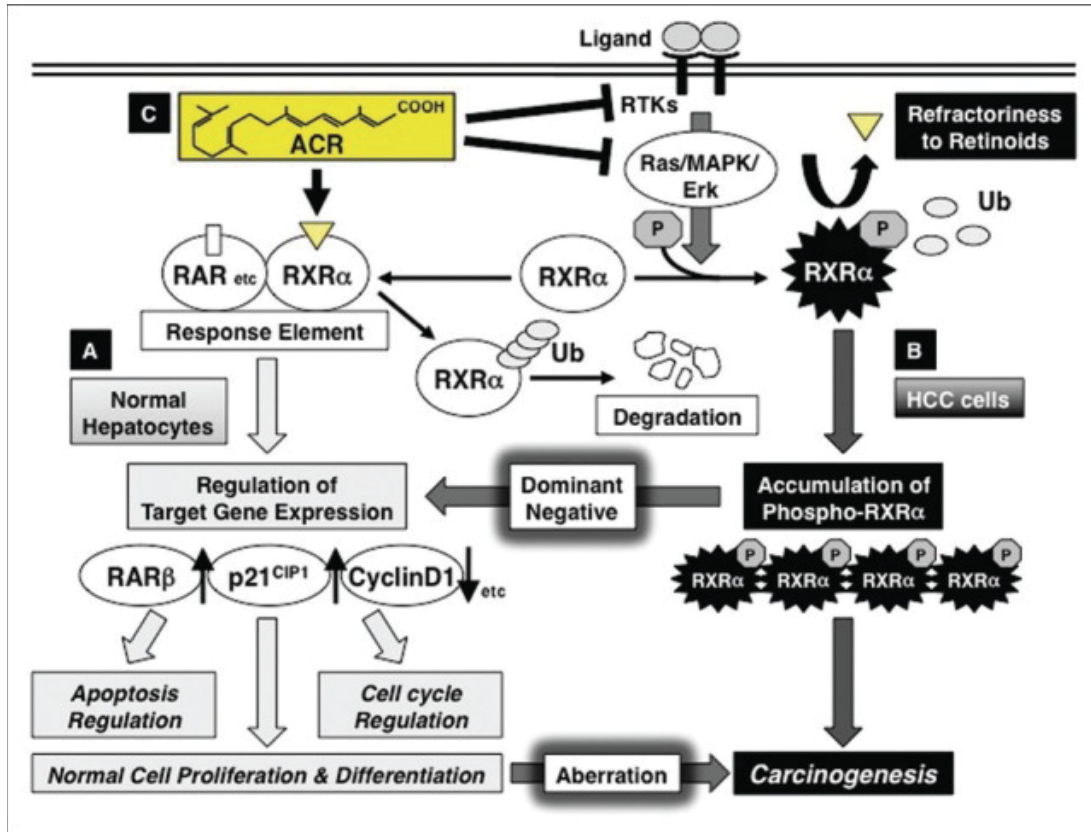


Figure 4.4: Retinoid refractoriness due to phosphorylation of retinoid X receptor alpha (RXR α), and its restoration by acyclic retinoid (ACR) in liver carcinogenesis. (a) In normal hepatocytes, when ACR binds to and activates RXR α , it forms homo- and/or heterodimers with other nuclear receptors, including retinoic acid receptors (RARs). This results in expression of the target genes, such as RAR β , p21^{CIP1}, and cyclin D1, which regulate normal cell proliferation and differentiation, as well as controlling the induction of apoptosis and cell cycle progression. Thereafter, RXR α is rapidly ubiquitinated (Ub) and degraded via the proteasome pathway. (b) In hepatocellular carcinoma (HCC) cells, the Ras–mitogen-activated protein kinase (MAPK) pathway is highly activated and phosphorylates RXR α at serine residues, impairing dimer formation and the

subsequent transactivation functions of the receptor (refractoriness to retinoids). Furthermore, nonfunctional phosphorylated RXR α is sequestered from ubiquitin/proteasome-mediated degradation and accumulates in liver cells. This interferes with the physiologic function of the remaining unphosphorylated (ie, functional) RXR α in a dominant-negative manner, causing a deviation from normal cell proliferation and differentiation, thereby playing a critical role in liver carcinogenesis. (c) ACR is not only a ligand for RXR α , but also a suppressor of the Ras–MAPK signaling pathway; it inhibits RXR α phosphorylation, thereby restoring the function of the receptor and activating the transcriptional activity of the responsive element. ACR also inhibits, directly or indirectly, the ligand (growth factor)-dependent RTK activities, which contribute to the inhibition of ERK and RXR α phosphorylation and suppression of growth in HCC cells (Adapted from Shimizu et al., 2012)

In addition, anticancer effect of ACR in HCC patients was studied in a double-blind placebo controlled study. In this trial, treatment with ACR (administered to 44 patients, 600 mg/day) for 12 months significantly reduced the incidence of recurrent or new HCCs compared with placebo (administered to 45 patients) after a median follow-up period of 38 months; 12 patients (27%) in the ACR group developed HCC compared with 22 patients (49%) in the placebo group ($P = 0.04$). A 62 month follow up study also found improvement in both recurrence-free survival ($P = 0.002$) and overall survival ($P = 0.04$). Furthermore, the estimated 6-year overall survival was 74% in the ACR group and 46% in the placebo group. Computation of the relative risks for the development of secondary HCC and death were 0.31 and 0.33 respectively. Finally, the preventive effects of ACR lasted up to 38 months after completion of the drug or 50 months after randomization. These

results suggest that administration of ACR for only 12 months exerts a long-term effect on the prevention of second primary HCC without causing severe adverse effects from retinoid (Muto et al., 1996, 1999; Takai et al., 2005). Also, it demonstrates that inhibition of RXR phosphorylation has a role in the treatment of human cancers.

Recently, Shimizu and coworkers (2012) proposed a new concept called the concept of “clonal deletion and inhibition” therapy for HCC chemoprevention. It is believed that ACR prevents the development of HCC through implementation of this concept. They reported that in infected cirrhotic patients, though the annual incidence of HCC were approximately 3% in HBV- and 7% in HCV, the frequency of HCC recurrence after curative treatment was very high reaching an annual incidence of 20%–25%. Furthermore, the recurrence rate at 5 years after definitive therapy exceeds 70%. This suggests that once a liver is exposed to a continuous carcinogenic insult such as hepatitis virus infection, the whole liver (at this stage regarded as a precancerous field) will develop multiple as well as independent premalignant or latent malignant clones. The characteristics of such a liver make a curative treatment for HCC difficult once this malignancy has developed. Thus the most promising and practical strategies for HCC treatment is the removal and inhibition of the latent malignant clones from the chronically damaged liver that is in a hypercarcinogenic state before the latent malignant clones expand into a clinically detectable tumor. Muto et al., (1996; 1999) reported that in an early-phase clinical trial, administration of ACR for 12 months significantly reduced the serum levels of lectin-reactive a-fetoprotein factor 3 (AFP-L3) and protein induced by vitamin K absence or antagonist-II (PIVKA-II), both of which indicate the presence of latent (ie, invisible) malignant clones in the remnant liver.

Furthermore, ACR prevented the appearance of serum AFP-L3 in patients whose AFP-L3 levels were negative at trial enrolment whereas the number of patients whose serum AFP-L3 appeared *de novo* was significantly increased in the placebo group and these patients had a significantly higher risk of developing secondary HCC.

According to the “clonal deletion and inhibition” therapy with ACR, administration of ACR first eliminates the AFP-L3- and PIVKA-II-producing premalignant clones from the remnant liver before they expand into clinically detectable tumors (“clonal deletion”). Secondly, the developments of such clones with the potential to become HCC in the liver are inhibited by ACR (“clonal inhibition”). Elimination or inhibition of the malignant clones from the remnant liver by ACR thus resets the *de novo* HCC development in the cirrhotic liver to several years (Fig. 4.5). As demonstrated in an early-phase clinical trial, the short-term administration (12 months) of ACR could exert a long-term (ie, several years) preventive effect on HCC development even after termination of treatment (Shimizu et al., 2012; Takai et al., 2005).

4.3.4 Combination Cancer Chemoprevention with Acyclic Retinoids

More effective strategies including the use of other agents, particularly those that target RXR α phosphorylation and also anticipated potential partners of ACR are now being investigated. For instance, the combination of ACR and interferon- β synergistically inhibits cell growth and induces apoptosis in HCC cells (Obora et al., 2002). The clinical significance of this finding is that interferon exerts a chemopreventive effect against the recurrence of HCC (Miyaki et al., 2010; Shen

et al., 2010). Thus the combination of ACR with other agents provides an opportunity to take advantage of the synergistic effects of ACR on growth inhibition in HCC cells. In addition, ACR acts synergistically with gemcitabine and vitamin K₂ in suppressing growth and inducing apoptosis in human HCC cells, human pancreatic cancer and leukemia cells by inhibiting Ras–MAPK signaling activation and RXR α phosphorylation (Kanamori et al., 2007; Nakagawa et al., 2009; Okita et al., 2010).

Tatebe et al., (2008) using trastuzumab, a humanized monoclonal antibody against HER2, reported that dephosphorylation of RXR α by targeting the Ras–MAPK signaling pathway and its upstream human epidermal growth factor receptor-2 (HER2) also enhances the effect of retinoids including ACR by inhibiting growth and inducing apoptosis in human HCC cells.

Furthermore, the combined treatment of ACR and valproic acid, a histone deacetylase inhibitor, synergistically induced apoptosis and G₀–G₁ cell cycle arrest in HCC cells. The mechanism involved not only the inhibition of RXR α phosphorylation, but also ERK, Akt, and glycogen synthase kinase-3 β proteins (Tatebe et al., 2009)

In summary the inhibition of RXR α phosphorylation and the restoration of its original function as a master regulator of nuclear receptors might therefore be an effective strategy for controlling cancer cell growth in a variety of human malignancies.

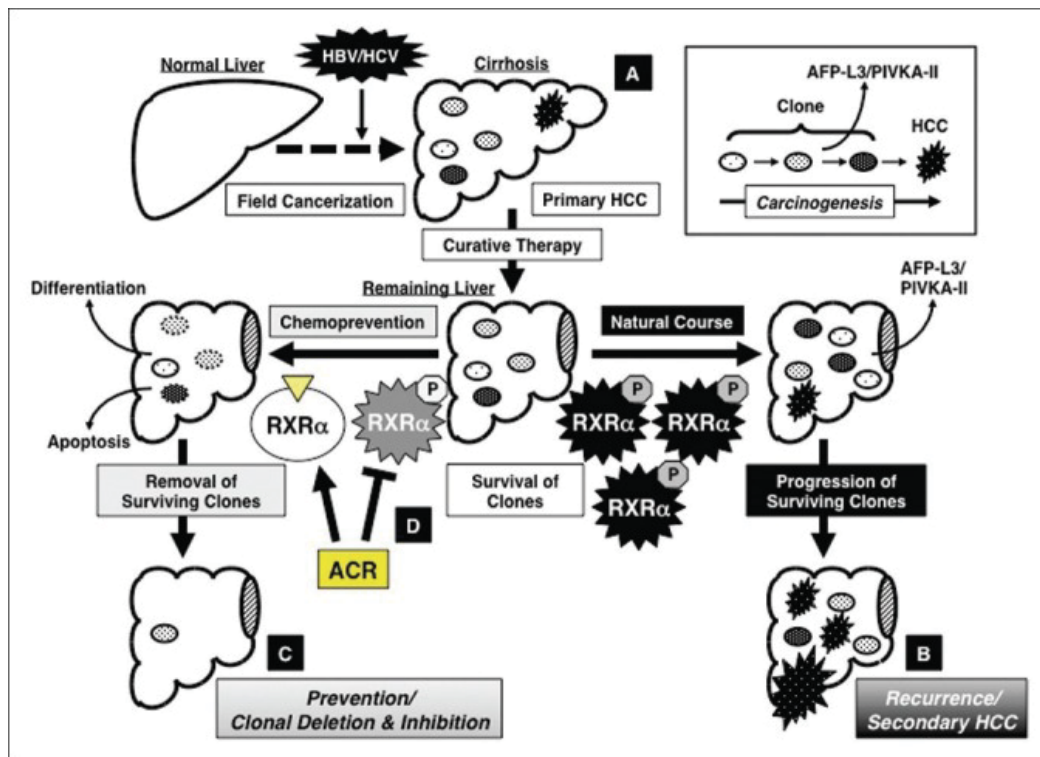


Figure 4.5: Concept of “clonal deletion and inhibition” therapy for hepatocellular carcinoma (HCC) chemoprevention and the effects of acyclic retinoid (ACR) on implementation of this concept. (a) Persistent inflammation caused by hepatitis viral infection transforms the liver into a precancerous field (“field cancerization”) which contains multiple latent malignant clones that can, at some point develop into HCC. (b) Even after early detection and removal of the primary HCC, the remaining clones survive in the remaining liver and grow into secondary HCC lesions (natural course), which is a major cause of the poor prognosis for patients with this malignancy. (c) Therefore, one of the most promising strategies to prevent secondary HCC is the deletion and inhibition of such transformed clones by inducing cell differentiation or apoptosis before the clones expand into clinically detectable tumors. This is the concept of “clonal deletion and inhibition”

therapy for HCC chemoprevention. (d) ACR, which binds to RXR α and inhibits phosphorylation of this nuclear receptor, prevents the recurrence and development of secondary HCC via the mechanism described by this concept (Adapted from Shimizu et al., 2012).

CHAPTER 5 Conclusions

Our study has examined the effects of 1, 25(OH)₂D₃ binding to VDR and RXR α and 9-cis RA binding to RXR α in both the non-transformed HPK1A and ras-transformed HPK1A_{ras} cells. Specifically, we have examined the impact of RXR α phosphorylation at serine 260 on the nuclear localization, intra-nuclear kinetics, VDR/RXR α heterodimer interaction and DRIP205 coactivator recruitment and binding to DNA. We have shown how each of the above named steps is affected in the ras-transformed HPK1A_{ras} cells.

Based on our data, we have reviewed our previously proposed model for the nuclear import of VDR, RXR and VDR-RXR interaction and DNA binding in non-transformed and ras-transformed cells and how it affects 1, 25(OH)₂D₃ signaling (chapter 2, Fig 2.8). The current model for 1, 25(OH)₂D₃ resistance in ras-transformed cells through conformational change of VDR/RXR α and impaired coactivator interaction is shown below (see Fig.5.1A-D below).

In the non-transformed and normal cells, figure 5.1 (A), the nuclear import of VDR and RXR is mediated by their respective ligands. Once in the nucleus, the binding of 1,25(OH)₂D₃ to VDR is critical for the VDR-RXR α heterodimer interaction and binding to the hormone response elements (VDRE), recruitment of co-factors (CoAc) and effect on 1,25(OH)₂D₃ signaling. In (B) the binding of VDR/RXR α to DRIP205 coactivator through its LXXLL motif is especially crucial to 1, 25(OH)₂D₃ sensitivity. This binding further stabilizes the VDR/RXR α /DRIP205 coactivator complex thereby modulating the transcriptional activity.

In the ras-transformed keratinocyte (C) phosphorylation of RXR α prevents the nuclear translocation of RXR α and binding of the VDR/RXR α complex to the hormone response element (VDRE). The recruitment of co-factors are impaired

thus preventing $1,25(\text{OH})_2\text{D}_3$ signaling. In (D) interaction between the VDR heterodimeric partner $\text{RXR}\alpha$ with the LXXLL motif is broken resulting in a conformational change, perhaps the recruitment of other members of the DRIP complex and the overall effect on impaired transcriptional activity.

We have shown that by using either the MEK inhibitor UO126 or a non-phosphorylatable $\text{RXR}\alpha$ mutant we can restore the cells nuclear input of RXR , VDR/ $\text{RXR}\alpha$ as well as interaction with DNA and $1,25(\text{OH})_2\text{D}_3$ and VDR signaling.

Recent structural analysis of the human RXR/VDR nuclear receptor complex with its DR3 target DNA (Rochel et al., 2011; Zhang et al., 2011; Orlov et al., 2012; Molnar, 2014; Rastinejad et al., 2015) shows that the molecular architectures of nuclear receptors is highly ordered with surprisingly complex domain-domain interconnections. Furthermore, the use of more recent methodologies such as small-angle X-ray scattering (SAXS), cryo-electron microscopy (cryo-EM) and hydrogen-deuterium exchange (HDX) provides new insight into how signals can be communicated between domains in an allosteric fashion (Rastinejad et al., 2015).

From a functional and a structural perspective, the crystal structure of VDR (Fig. 5.2) confirms the conserved contact or anchoring points for its interaction with the ligand, $1,25(\text{OH})_2\text{D}_3$.

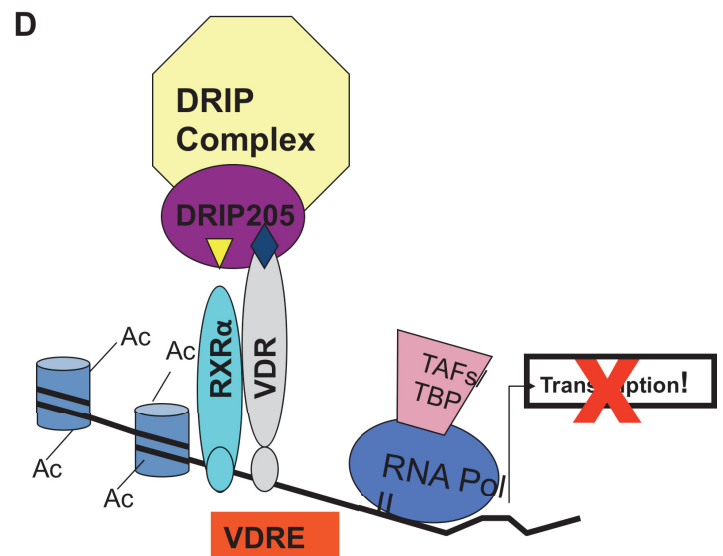
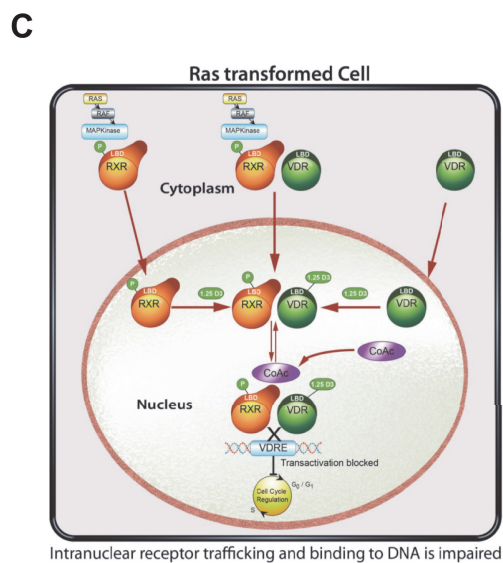
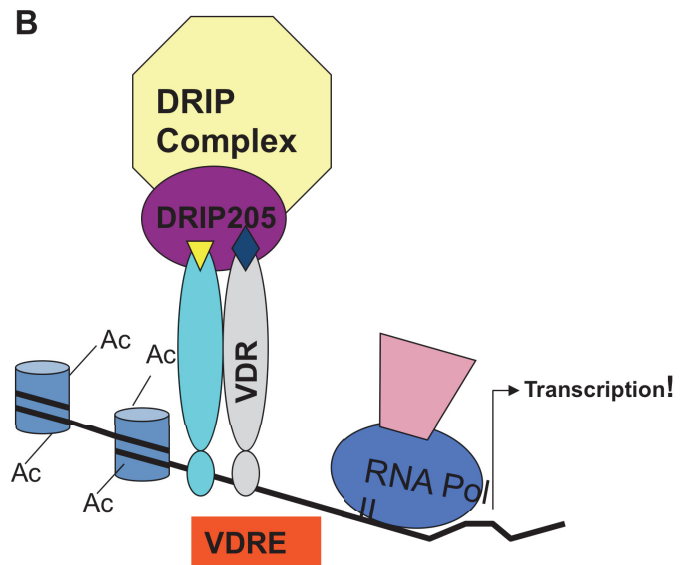
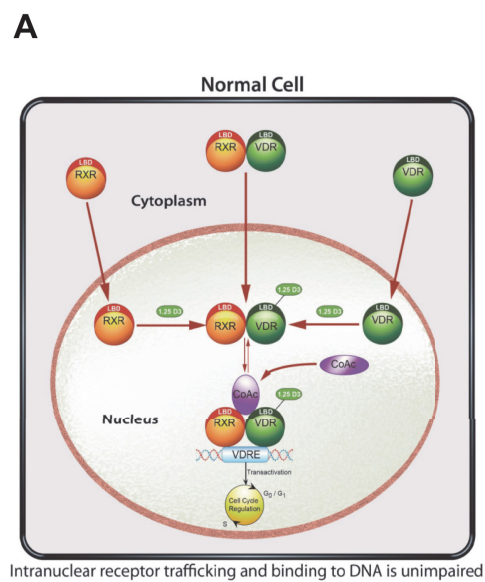


Figure.5.1A-D: The current model for 1, 25(OH)₂D₃ resistance in ras-transformed cells through conformational change of VDR/RXRα and impaired coactivator

interaction, DNA binding (see text for explanation). In non-transformed or normal cells, the previous model (A, chapter 2, figure 2.8A) has been reviewed further in (Fig.5.1B). Similarly, in the ras-transformed cells, the previous model (C, chapter 2, figure 2.8B) has been reviewed further to the current in (Fig.5.1D).

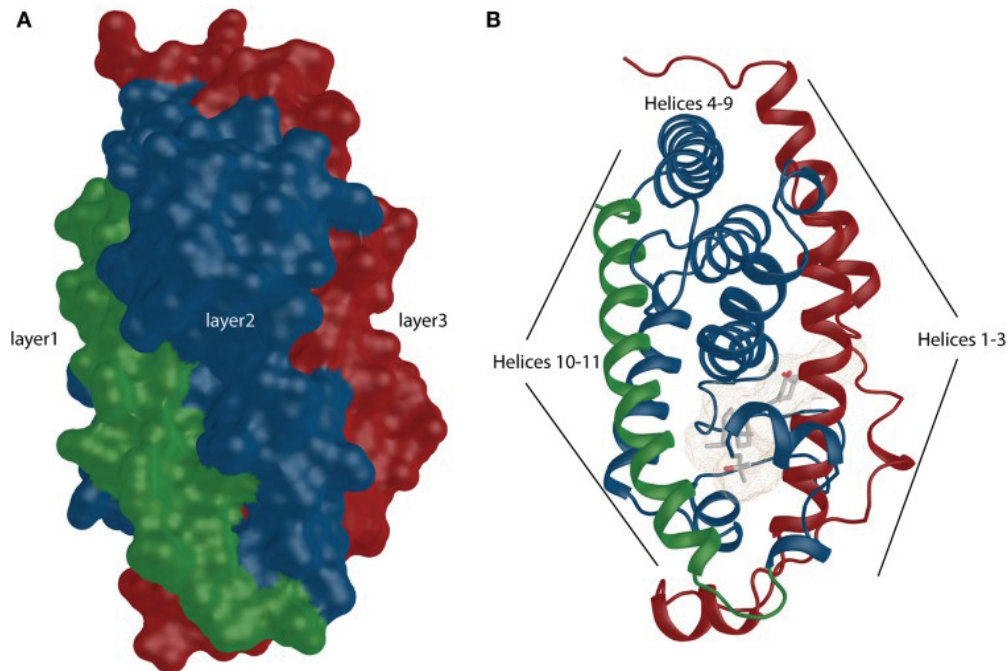


Figure 5.2. VDR shows similarity to canonical NR structural organization. **(A)** The overall surface depiction of the VDR showing the three layers sandwich-like molecule where the layers are highlighted in green, blue and red. **(B)** Numbered helices belonging to different layers are shown and they are highlighted similarly as in surface representation (Adapted from Molnar, 2014).

Disruption of these anchoring points decreases the activation potential of the ligand (Molnar, 2014). Structural analysis of the conserved core of VDR shows two zinc fingers where one contains four cysteine residues per atom of zinc (Fig. 5.3).

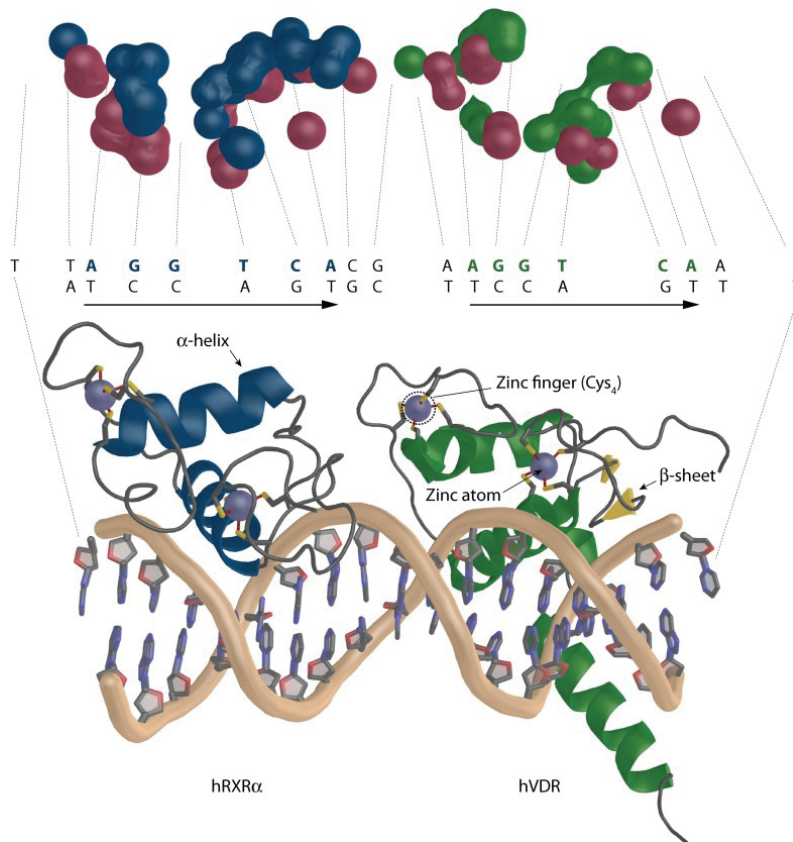


Figure 5.3. The overall architecture of the DBD complex of RXR-VDR on canonical DR3 element (PDBID: 1YNW). The two zinc atoms (light blue spheres) with the respective cysteins are shown (bottom). RXR is shown in blue and VDR in green. The coiled protein regions are in gray and β-sheets in yellow. The surface representation of the contact atoms interacting between DNA and the heterodimer is shown (top). The proteins and DNA are visualized in different color DNA (red), RXR (blue), and VDR (green) (Adapted from Molnar, 2014)

The advantage of this feature is that it allows effective recognition and binding to VDREs which are typically made up of hexameric half-sites most commonly arranged in a direct repeat with three neutral base pairs separating the half sites (DR3). According to Carlsberg (1993), the unliganded VDR can occupy its response elements as a homodimer. However, ligand binding allows VDR to form heterodimeric complex with RXR. This complex binds to VDREs with 5'-prime bound RXR.

The effective functioning of VDR as a transcription factor involves its inevitable interaction with RXR and various protein partners (Molnar, 2014). The DRIP complex has been identified as an important complex that is recruited to VDR in a completely ligand-dependent manner (Rachez et al., 2000). Majority of these protein partners have been implicated in cellular processes such as cell cycle regulation, DNA repair, tumor suppression, transcriptional regulation (Molnar, 2014). New structural data obtained from short interacting peptides from steroid receptor coactivator 1 (SRC1/) with zVDR and mediator subunit 1 (MED1/DRIP205) with rVDR have shown that the LXXLL motifs of both peptides interact with VDR in a similar fashion (Fig. 5.4; Molnar, 2014).

Furthermore, the α -helix of the peptide is oriented with its N-terminus toward helix 12. Most of the interaction is contributed from hydrophobic contacts of coactivator's leucine residues with the hydrophobic core from VDR helices 3, 4, and 12. The short α -helix anchoring points are based on the interaction with the "charge clamp". This consists of the conserved glutamate in helix 12 and lysine in helix 3, and the backbone amides of the coactivator peptide (Fig.5.3; Molnar, 2014). The similarity of the LXXLL motifs however raises the question on how specificity is achieved in the interaction.

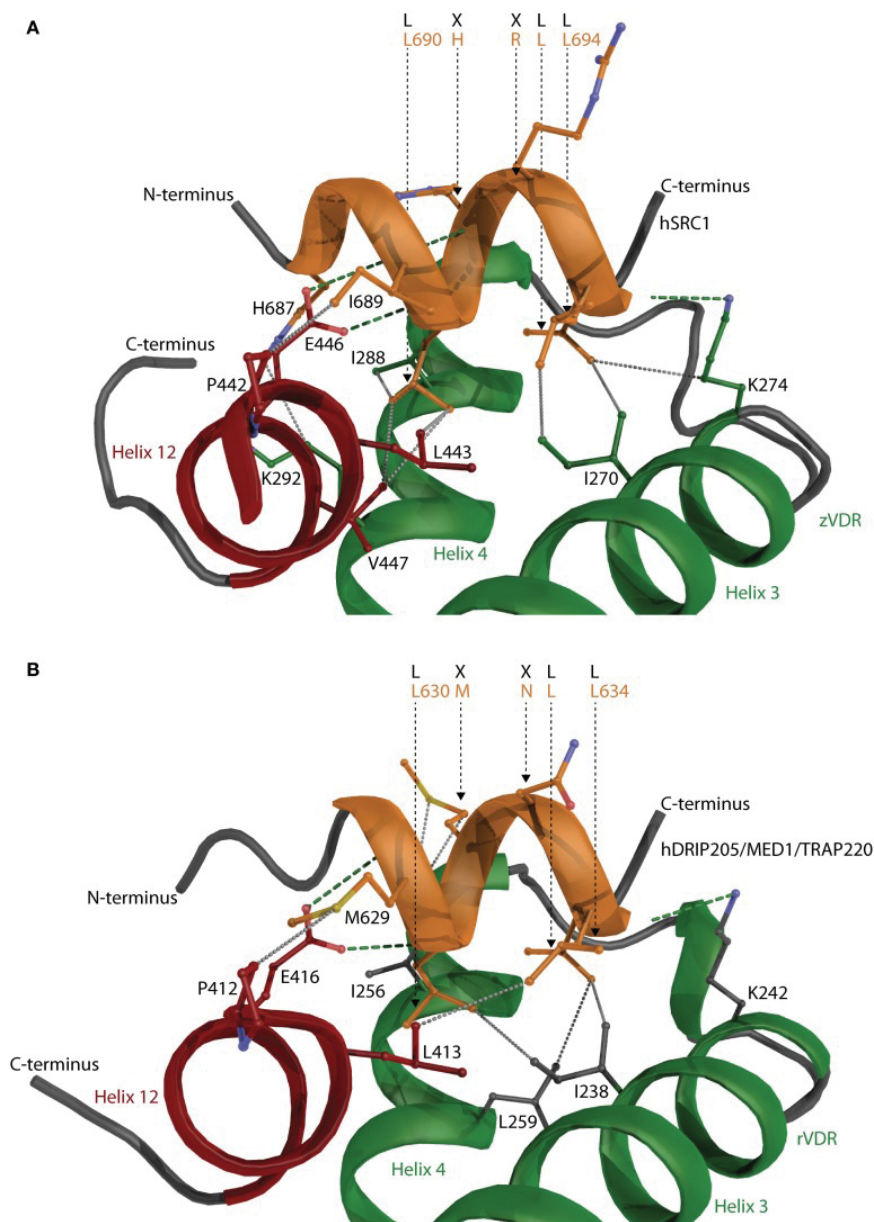


Figure 5.4. The interaction of coactivator peptides with VDR. Peptides derived from **(A)** steroid receptor coactivator 1 (SRC1) with zVDR and **(B)** mediator complex subunit 1 (MED1/DRIP205) with rVDR shown. SRC1 and MED1 is shown in orange and VDR in green. Helix 12 is highlighted in red. The hydrogen bonds and hydrophobic interactions are visualized with green and gray dashed

lines, respectively. The important residues such as the conserved “charge clamp” glutamate from helix 12 and lysine in helix 3 contributing to the CoA-VDR interaction are also shown (Adapted from Molnar, 2014).

Studies with with full length VDR-RXR α complexes and DNA from osteocalcin VDRE in solution using SAXS, cryo-EM, HDX have showed a more comprehensive organization and possible function of the VDR-RXR α -cofactor complex (Molnar, 2014). Derived SAXS data have showed that following binding to DNA from osteocalcin VDRE, RXR-VDR assumes an elongated asymmetric open conformation with separate DBDs and LBDs and a well structured VDR hinge with VDR located downstream and RXR on upstream half sites (Fig. 5.5B; Rochel et al., 2011). However, the coiled structure of the RXR hinge allows it to adapt to different REs. Thus the hinges not only play a very important role in conformational organization, in this case an open conformation but also a fundamental role in the dynamic nature of the VDR-RXR complex (Molnar, 2014).

It has been suggested that the binding of the DBD to DR3 results in a 90° rotation of the LBD dimers with respect to the DNA (Fig. 5.5A). Furthermore, it has been shown that both DRIP205 and SRC1 have higher affinity to VDR compared to RXR. The study however, shows the binding of only one molecule of coactivator through VDR and not binding of one LXXLL motif to VDR and the other to RXR (Rochel et al., 2011; Molnar, 2014)

Ren et al., (2000) using mutants showed that the second LXXLL motif of DRIP205 preferentially bound stronger to VDR compared to a weak recruitment of the first LXXLL motif to RXR. We have also reported in our study that DRIP205 and its

LXXLL motif binds more to VDR than RXR in the non-transformed cells. However, both motifs are crucial for the effectiveness of the NR activation complex *in vivo* (Malik et al., 2004). RXR may play a role in coactivator recruitment as well by associating with some other factors. Other data suggest that coactivator interacts simultaneously with both VDR/RXR co-receptors (Zhang et al., 2011).

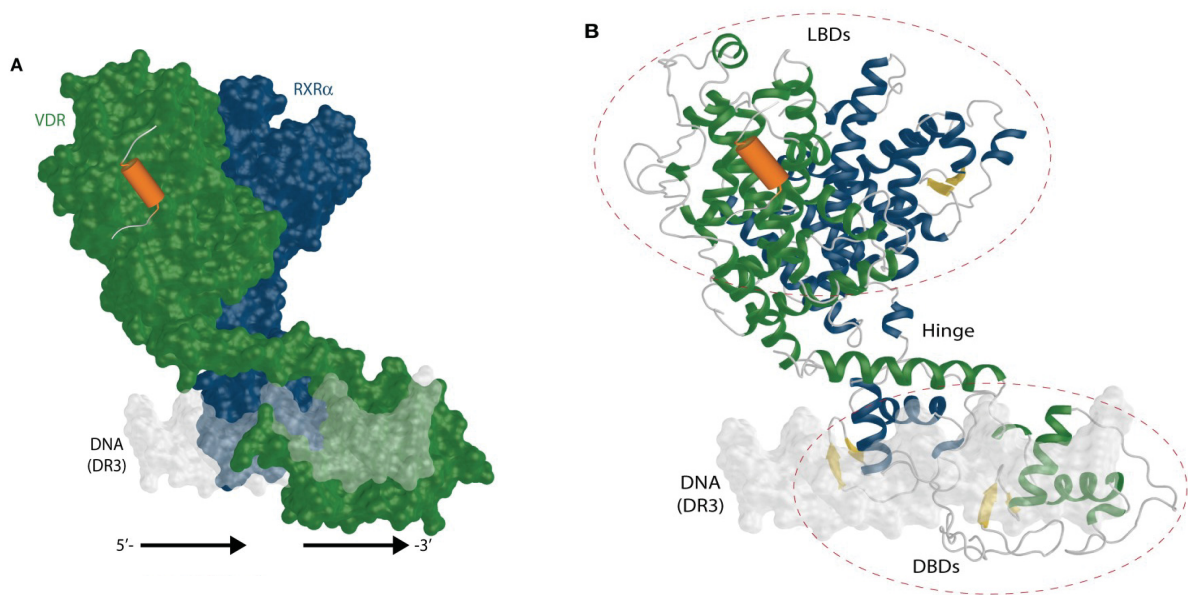


Figure 5.5. The full length RXR-VDR structural model derived from SAXS and cryo-EM experiments. **(A)** A surface representation of the RXR(blue)-VDR(green) heterodimer is shown on DR3 VDRE. The possible location of the coactivator peptide (orange) is highlighted as well. The 5'- and 3'-prime orientation of the DR3 is annotated. **(B)** Ribbon representation of the same complex shows the relative organization and fold of LBD, DBD and the connective hinge between them. The β -sheets are shown in yellow color (Adapted from Molnar, 2014).

Both cryo-EM and SAXS studies have also shown that the VDR/RXR heterodimer assumes an L-shape form on the DR3 with a proper orientation of RXR on the upstream and VDR on the downstream half site thus supporting an asymmetrically open architecture (Fig. 5.5; Molnar, 2014).

Zhang et al., (2011) using the HDX to address the dynamic properties of the RXR-VDR-SRC1 complex reported that the addition of RXR to VDR stabilizes the region with helices 6–7. The effect observed was similar to the binding of some agonist to VDR. Binding of $1,25(\text{OH})_2\text{D}_3$ to the VDR LBD stabilized the helices 1, 3, 5–7, and 11 (the actual region that forms the LBP) however, the binding efficiency of RXR to VDR was not enhanced.

For RXR, stabilization (increase of the heterodimerization) was observed in helices 7 and 10. There was also an allosteric communication in helix 3. In general, *9-cis* RA binding stabilized RXR. However, it also increased the fluctuation in helix 12 a contrasting effect considering the crystal structure. This suggested that the energy conformation for the complex is much more dynamic than the minimized conformation assumed for the crystal structure (Molnar, 2014).

Furthermore, Zhang and co-workers (2011) reported that the loop between helices 10 and 11 in RXR plays an important role in the formation of the hydrophobic groove needed in facilitating coactivator recruitment. Lastly, RXR contains an “aromatic clamp” that is different from the classical charge clamp. This clamp consists of residues in helices 3 and 12 that is also important for coactivator binding.

These findings thus support our view that in the ras-transformed cells, RXR α phosphorylation at serine 260 creates a conformation change within the RXR α omega loop. This prevents the complex binding to coactivators as well as to DNA. We suggest that this affects, 1,25(OH) $_2$ D $_3$ signaling in the ras-transformed cells.

CHAPTER 6 Claims and Originality

Claims and originality

1. In ras-transformed cells, MAPK phosphorylation reduces the nuclear accumulation of both VDR and RXR α .
2. In ras-transformed cells, MAPK phosphorylation of RXR reduces binding of RXR α to nuclear components as shown by live cell imaging using both FLIP and FRAP methods.
3. In non-transformed-cells both VDR and RXR α directly interacts with DRIP205 in intact cells.
4. In ras-transformed cells, MAPK phosphorylation of RXR interferes with DRIP205 coactivator interaction with RXR α as shown by FRET.
5. Inhibition of MAPK phosphorylation of RXR increases DRIP205 coactivator interaction with both VDR and RXR α in intact cells.
6. In ras-transformed cells, MAPK phosphorylation of RXR interferes with binding of VDR/RXR α /DRIP205 complex to DNA.
7. Inhibition of MAPK phosphorylation increases VDR/RXR α /DRIP205 binding to DNA in intact cells.

References

- Adachi S, Okuno M, Matsushima-Nishiwaki R, Takano Y, Kojima S, Friedman SL, Moriwaki H, Okano Y (2002). Phosphorylation of retinoid X receptor suppresses its ubiquitination in human hepatocellular carcinoma. *Hepatology*. 35: 332–340.
- Adams JM, Cory S (2007). The Bcl-2 apoptotic switch in cancer development and therapy. *Oncogene*. 26:1324.
- Adjei AA (2001). Blocking oncogenic Ras signaling for cancer therapy. *J Natl Cancer Inst.*;93:1062–1074.
- Adjei AA, Cohen RB, Franklin W, Morris C, Wilson D, Molina JR, Hanson LJ, Gore L, Chow L, Leong S, Maloney L, Gordon G, Simmons H, Marlow A, Litwiler K, Brown S, Poch G, Kane K, Haney J, and Eckhardt SG (2008). Phase I Pharmacokinetic and Pharmacodynamic Study of the Oral, Small-Molecule Mitogen-Activated Protein Kinase Kinase 1/2 Inhibitor AZD6244 (ARRY-142886) in Patients With Advanced Cancers. *J Clin Oncol*. 26(13): 2139–2146.
- Alagbala AA, Moser MT, Johnson CS, Trump DL, Foster BA (2007). Characterization of Vitamin D insensitive prostate cancer cells. *J Steroid Biochem Mol Biol*;103: 712–716.
- Alberts SR, Schroeder M, Erlichman C, et al., (2004). Gemcitabine and ISIS-2503 for patients with locally advanced or metastatic pancreatic adenocarcinoma: a north central cancer treatment group phase II trial. *J Clin Oncol*. 24:2944–50.
- Alderton WK, Cooper CE, Knowles RG (2001). Nitric oxide synthases: structure, function and inhibition. *Biochem J*. 357:593–615.

Arnaud J, Constans J (1993). Affinity differences for vitamin D metabolites associated with the genetic isoforms of the human serum carrier protein (DBP). *Hum Genet.* 92(2):183-8.

Arnold SF, Obourn JO, Jaffe H, Notides AC (1994). Serine 167 is the major estradiol-induced phosphorylation site on the human estrogen receptor. *Mol. Endocrinol.* 8:1208-1214.

Arnold SF, Obourn JD, Jaffe H, Notides AC (1995). Phosphorylation of the human estrogen receptor on tyrosine 537 in vivo and by src family tyrosine kinases in vitro. *Mol Endocrinol.* 9(1):24-33

Arnold SF, Obourn JD, Jaffe H, Notides AC (1995). Phosphorylation of the human estrogen receptor by mitogen-activated protein kinase and casein kinase II: consequence on DNA binding. *J Steroid Biochem Mol Biol.* 55(2):163-72.

Arita K, Nanda A, Wessagowit V, Akiyama M, Alsaleh QA, McGrath JA (2008). A novel mutation in the VDR gene in hereditary vitamin D-resistant rickets. *Br J Dermatol*;158:168–171.

Arriagada G, et al., (2007). Phosphorylation at serine 208 of the 1 α ,25-dihydroxy Vitamin D₃ receptor modulates the interaction with transcriptional coactivators. *J Steroid Biochem Mol Biol.* 103:425-9

Avruch J, Zhang XF, Kyriakis JM (1994). Raf meets Ras: completing the framework of a signal transduction pathway. *Trends Biochem Sci.*19(7):279-83. Review.

Axelrod D, Koppel DE, Schlessinger J, Elson E, & Webb WW (1976). Mobility measurement by analysis of fluorescence photobleaching recovery kinetics. *Biophys. J.* 16:1055–1069.

Bailleul B, Surani MA, White S, Barton SC, Brown K, Blessing M, Jorcano J, Balmain A (1990). Skin hyperkeratosis and papilloma formation in transgenic mice expressing a ras oncogene from a suprabasal keratin promoter. *Cell*. 62:697-708.

Baker AR, McDonnell DP, Hughes M, Crisp TM, Mangelsdorf DJ, Haussier MR, Pike JW, Shine J, O'Malley BW (1988). Cloning and expression of full-length cDNA encoding human vitamin D receptor. *Proc. Natl. Acad. Sci. USA*. 85:3294-3298.

Balsan S, Garabédian M, Larchet M, Gorski AM, Cournot G, Tau C, Bourdeau A, Silve C, Ricour C (1986). Long-term nocturnal calcium infusions can cure rickets and promote normal mineralization in hereditary resistance to 1,25-dihydroxyvitamin D. *J Clin Invest*. 77(5):1661-7.

Banerjee P, Chatterjee M (2003). Antiproliferative role of vitamin D and its analogs-A brief overview. *Mol Cell Biochem*. 253(1-2):247-54.

Baran DT, Sorensen AM, Shalhoub V, Owen T, Stein G, Lian J (1992). The rapid nongenomic actions of 1 alpha,25-dihydroxyvitamin D₃ modulate the hormone-induced increments in osteocalcin gene transcription in osteoblast-like cells. *J Cell Biochem*. 50(2):124-9.

Barbacid M (1987). ras Genes. *Ann. Rev. Biochem*. 56:779-827.

Barletta F, Freedman LP, Christakos S (2002). Enhancement of VDR-mediated transcription by phosphorylation: correlation with increased interaction between the VDR and DRIP205, a subunit of the VDR-interacting protein coactivator complex. *Mol Endocrinol*. 16(2):301-14.

Barbara D. Boyan, Jiaxuan Chen, Zvi Schwartz (2012). Mechanism of Pdia3-dependent 1 α ,25-dihydroxy vitamin D₃ signaling in musculoskeletal cells. *Steroids*. 77(10):892–896

Barletta F, Dhawan P, Christakos S (2004). Integration of hormone signaling in the regulation of human 25(OH)D3 24-hydroxylase transcription. *Am J Physiol Endocrinol Metab.* 286:E598-608

Bartolome J, et al., (2004). Ribozymes as antiviral agents. *Minerva Med.* 95:11.

Baylis C, Mitruka B, Deng A (1992). Chronic blockade of nitric oxide synthesis in the rat produces systemic hypertension and glomerular damage. *J Clin Invest.* 90:278–81.

Berrabah W, Aumercier P, Lefebvre P, Staels B (2011). Control of nuclear receptor activities in metabolism by post-translational modifications. *FEBS Lett* 585: 1640-1650.

Barsony J, Pike JW, DeLuca HF, Marx SJ (1990). Immunocytology with microwave-fixed fibroblasts shows 1 alpha,25-dihydroxyvitamin D3-dependent rapid and estrogen-dependent slow reorganization of vitamin D receptors. *J Cell Biol.*111:2385–2395.

Barsony J, Renyi I, McKoy W (1997). Subcellular distribution of normal and mutant vitamin D receptors in living cells. *J Biol Chem.* 272:5774–5782.

Barsony J, Carroll J, McKoy W, Renyi I, Gould DL, Htun H, and Hager, GL (1997). Intracellular traffick of glucocorticoid receptors: Studies with green fluorescent protein chimeras in living cells. In "Microscopy and Microanalysis" (G. W. Bailey, R. V. W. Dimlich, J. J. McCarthy, and T. P. Pretlov, Eds.), pp. 131-132. Springer-Verlag, New York.

Bastien J, Adam-Stitah S, Plassat JL, Chambon P, and Rochette-Egly C (2002). *J. Biol. Chem.* 277:28683-28689.

Beck CA, Zhang Y, Altmann M, Weigel NL, Edwards DP (1996). Stoichiometry and site-specific phosphorylation of human progesterone receptor in native target cells and in the baculovirus expression system. *J Biol Chem.* 271(32):19546-55.

Bettoun DJ, Burris TP, Houck KA, Buck DW, Stayrook KR, Khalifa B, Lu J, Chin WW, Nagpal S (2003). Retinoid X receptor is a non-silent major contributor to vitamin d receptor-mediated transcriptional activation. *Mol Endocrinol.* 17: 2320–2328.

Bikle DD, Gee E, Halloran B, Haddad JG (1984). Free 1,25-dihydroxyvitamin D levels in serum from normal subjects, pregnant subjects, and subjects with liver disease. *J Clin Invest.* 74(6): 1966–1971

Bikle DD, Halloran BP, Gee E, Ryzen E, Haddad JG (1986). Free 25-hydroxyvitamin D levels are normal in subjects with liver disease and reduced total 25-hydroxyvitamin D levels.

Bikle DD, Nemanic MK, Gee E, Elias P (1986). 1,25-Dihydroxyvitamin D₃ production by human keratinocytes. Kinetics and regulation. *J Clin Invest.* 78(2): 557–566.

Bikle DD, Gee E, Halloran B, Kowalski MA, Ryzen E, Haddad JG (1986). Assessment of the free fraction of 25-hydroxyvitamin D in serum and its regulation by albumin and the vitamin D-binding protein. *J Clin Endocrinol Metab.* 63(4):954-9.

Bikle, DD (2012b). Vitamin D and the skin: physiology and pathophysiology. *Rev. Endocr. Metab. Disord.* 13, 3–19.

Bikle DD (2014). Vitamin D metabolism, mechanism of action, and clinical applications. *Chem Biol.* 21(3):319-29.

Bikle DD, Oda Y, Tu CL, Jiang Y (2015). Novel mechanisms for the vitamin D receptor (VDR) in the skin and in skin cancer. *J Steroid Biochem Mol Biol.* 148:47-51.

Bikle D, Teichert A, Hawker N, Xie Z, Oda Y (2007). Sequential regulation of keratinocyte differentiation by 1,25(OH)₂D₃, VDR, and its coregulators. *Journal of Steroid Biochem. and Mol. Biol.* 103:396-404

Blumenschein GR, Smit EF, Planchard D, Kim DW, Cadranel J, De Pas T et al., (2013). MEK114653: A randomized, multicenter, phase II study to assess efficacy and safety of trametinib (T) compared with docetaxel (D) in KRAS-mutant advanced non-small cell lung cancer (NSCLC). *J Clin Oncol* 31, (suppl; abstr 8029).

Blutt SE, Allegretto EA, Pike JW, Weigel NL (1997). 1,25-dihydroxyvitamin D₃ and 9-cis-retinoic acid act synergistically to inhibit the growth of LNCaP prostate cells and cause accumulation of cells in G₁. *Endocrinology.* 138(4):1491-7.

Bollag G, McCormick F (1992). GTPase activating proteins. *Semin Cancer Biol.* 3(4):199-208.

Bonjour JP, Chevalley T, Fardellone P (2007). Calcium intake and vitamin D metabolism and action, in healthy conditions and in prostate cancer. *Br J Nutr.* 97(4):611-6. Review.

Bos JL (1989). ras oncogenes in human cancer: a review. *Cancer Res.* 49(17):4682-9.

Bouillon R, van Baelen H, de Moor P (1976). The transport of vitamin D in the serum of primates. *Biochem J.* 159(3):463-6.

Bouillon R, Van Baelen H, DeMoor P (1977). The measurement of vitamin D-binding protein in human serum. *J Clin Endocrinol Metab.* 45(2):225-31.

Bouillon R, Okamura WH, Norman AW (1995). Structure-function relationships in the vitamin D endocrine system. *Endocr Rev.* 16(2):200-57. Review.

Bouillon R, Carmeliet G, Verlinden L, van Etten E, Verstuyf A, Luderer HF, Lieben L, Mathieu C, Demay M (2008). Vitamin D and human health: lessons from vitamin D receptor null mice. *Endocr Rev.* 29(6):726-76.

Bourguet W, Ruff M, Chambon P, Gronemeyer H, Moras D (1995). Crystal structure of the ligand-binding domain of the human nuclear receptor RXR-alpha. *Nature.* 375:377-382.

Bourguet, W., Vivat, V., Wurtz, J. M., Chambon, E, Gronemeyer, H., and Moras, D (2000). Crystal structure of a heterodimeric complex of RAR and RXR ligand-binding domains. *Mol. Cell.* 5:289-298.

Brentjens RJ, Santos E, Nikhamin Y, et al. (2007) Genetically targeted T cells eradicate systemic acute lymphoblastic leukemia xenografts. *Clin Cancer Res.*3:5426-5435.

Brown K, Kemp CJ, Burns PA, Stoler AB, Fowles DJ, Akhurst RJ, Balmain A (1993). Positive and negative growth control in multistage skin carcinogenesis. *Rec. Results. In Cancer Res.* 128:309-321.

Brown TA, DeLuca HF (1991). Sites of phosphorylation and photoaffinity labeling of the 1,25-dihydroxyvitamin D₃ receptor. *Arch Biochem Biophys.* 286(2):466-72.

Brzozowski AM, Pike AC, Dauter Z, Hubbard RE, Bonn T, Engström O, Ohman L, Greene GL, Gustafsson JA, Carlquist M (1997). Molecular basis of agonism and antagonism in the oestrogen receptor. *Nature.* 16;389(6652):753-8.

Burakov D1, Wong CW, Rachez C, Cheskis BJ, Freedman LP (2000). Functional interactions between the estrogen receptor and DRIP205, a subunit of the heteromeric DRIP coactivator complex. *J Biol Chem.* 275(27): 20928-34.

Campbell FC, Xu H, El-Tanani M, Crowe P, Bingham V (2010). The yin and yang of vitamin D receptor (VDR) signaling in neoplastic progression: operational networks and tissue-specific growth control. *Biochem Pharmacol.* 79(1):1-9.

Cantorna MT (2006). Vitamin D and its role in immunology: multiple sclerosis, and inflammatory bowel disease. *Prog Biophys Mol Biol.* 92(1):60-4.

Caponigro F, Casale M, and Bryce M (2003). Farnesyl transferase inhibitors in clinical development. *Expert Opin. Investig. Drugs.* 12: 943–954.

Carlberg C, Quack M, Herdick M, Bury Y, Polly E, and Toell A (2001). Central role of VDR conformations for understanding selective actions of vitamin D(3) analogues. *Steroids.* 66:213-221.

Castelein H, Declercq PE, Baes M (1997). DNA binding preferences of PPAR alpha/RXR alpha heterodimers. *Biochem Biophys Res Commun.* 233(1):91-5.

Chang L, Karin M (2001). Mammalian MAP kinase signalling cascades. *Nature.* 410(6824):37-40.

Cheema C, B F Grant, R Marcus (1989). Effects of estrogen on circulating "free" and total 1,25-dihydroxyvitamin D and on the parathyroid-vitamin D axis in postmenopausal women. *J Clin Invest.* 83(2):537-42.

Chen D, Pace PE, Coombes RC, Ali S (1999). Phosphorylation of human estrogen receptor alpha by protein kinase A regulates dimerization. *Mol Cell Biol.* 19(2):1002-15.

Chen JD, Evans RM (1995). A transcriptional co-repressor that interacts with nuclear hormone receptors. *Nature*. 377:454–457.

Chen L, Davey Smith G, Evans DM, Cox A, Lawlor DA, Donovan J, Yuan W, Day IN, Martin RM, Lane A, Rodriguez S, Davis M, Zuccolo L, Collin S M, Hamdy F, Neal D, Lewis SJ (2009). Genetic variants in the vitamin d receptor are associated with advanced prostate cancer at diagnosis: findings from the prostate testing for cancer and treatment study and a systematic review. *Cancer Epidemiol. Biomarkers Prev*. 18:2874–2881.

Chen M, Cui YK, Huang WH, Man K, Zhang GJ (2013). Phosphorylation of estrogen receptor α at serine 118 is correlated with breast cancer resistance to tamoxifen. *Oncol Lett*. 6(1):118-124.

Chen S, Sims GP, Chen XX, Gu YY, Chen S, Lipsky PE (2007). Modulatory effects of 1,25-dihydroxyvitamin D3 on human B cell differentiation. *J Immunol*. 179(3):1634-47.

Christakos S, Gabrielides C, Rhoten WB (1989). Vitamin D-dependent calcium binding proteins: chemistry, distribution, functional considerations, and molecular biology. *Endocr. Rev*. 10:3-26.

Cockerill FJ, Hawa NS, Yousaf N, Hewison M, O'Riordan JL, Farrow SM (1997). Mutations in the vitamin D receptor gene in three kindreds associated with hereditary vitamin D resistant rickets. *J Clin Endocrinol Metab*. 82:3156–3160.

Cohen-Lahav M1, Shany S, Tobvin D, Chaimovitz C, Douvdevani A (2006). Vitamin D decreases NFkappaB activity by increasing IkappaBalpha levels. *Nephrol Dial Transplant*. 21(4):889-97.

Cole NB, Smith CL, Sciaky N, Terasaki M, Edidin M, Lippincott-Schwartz JC (1996). Diffusional mobility of Golgi proteins in membranes of living cells. *Science*. 273(5276): 797-801.

Colston K, Colston MJ, Feldman D (1981). 1,25-dihydroxyvitamin D₃ and malignant melanoma: the presence of receptors and inhibition of cell growth in culture. *Endocrinology*. 108(3): 1083–1086.

Colston KW, Chander SK, Mackay AG, Coombes RC (1992). Effects of synthetic vitamin D analogues on breast cancer cell proliferation in vivo and in vitro. *Biochem. Pharmacol.* 44:693-702.

Colston KW, Mackay AG, Finlayson C, Wu JC, Maxwell JD (1994). Localisation of vitamin D receptor in normal human duodenum and in patients with coeliac disease. *Gut*. 35(9):1219-25.

Colston KW, James SY, Ofori-Kuragu EA, Binderup L, Grant AG (1997). Vitamin D receptors and antiproliferative effects of vitamin D derivatives in human pancreatic carcinoma cells in vivo and in vitro. *Br J Cancer*. 76(8):1017-1020.

Colston KW, Hansen CM (2002). Mechanisms implicated in the growth regulatory effects of vitamin D in breast cancer (Review). *Endocr Relat Cancer*. 9(1): 45-59.

Conneely OM, O'Malley BW (1994). Orphan receptors: structure and function relationships. In *molecular Biology of SteroidHormone Regulation of Gene Transcription*. O'Malley BW ed. R.O. Landes Company. Texas. pp. 111-133.

Cooke NC, Haddad JO (1997). Vitamin D binding protein. In: *Vitamin D*. Pike JW ed. Academic Press. San Diego. pp. 87-101.

Cox AD, Fesik SW, Kimmelman AC, Luo J, Der CJ (2014). Drugging the undruggable RAS: Mission possible? *Nat Rev Drug Discov*. 13(11):828-51.

Davis, RJ (1993). The mitogen-activated protein kinase signal transduction pathway. *J Biol Chem*. 268:14553-14556.

Dawson MI, and Z Xia (2012). The Retinoid X Receptors and Their Ligands by *Biochim Biophys Acta*. 1821(1): 21–56.

Daya-Grosjean L, Dumaz N, Sarasin A (1995). The specificity of p53 mutation spectra in sunlight induced human cancers. *J Photochem Photobiol B*. 28(2):115-24.

de Fougères A, et al., (2007). Interfering with disease: a progress report on siRNA-based therapeutics. *Nat. Rev. Drug Discov*. 6:443.

Deeb KK, Trump DL, Johnson CS (2007). Vitamin D signalling pathways in cancer: potential for anticancer therapeutics. *Nat Rev Cancer*. (9):684-700.

DeLuca HF (1983). Metabolism and mechanism of action of vitamin D. In: Peck WA. ed. *Bone and Mineral Research: Annual 1*. Excerpta Medica Princeton. pp. 7-73.

DeLuca HF, Schnoes HK (1983). Vitamin D: recent advances. *Annu. Rev. Biochem*. 52:411-439.

De Luca, LM, Darwiche N, Jones CS, and Scita G (1995). Retinoids in differentiation and neoplasia. *Sci. Am. Sci. Med*. 2:28-37.

DeLuca HF, Cantorna MT (2001). Vitamin D: its role and uses in immunology. *FASEB J*. 15(14):2579-85. Review.

DeLuca HF, Krisinger J, Darwish H (1990). The vitamin D system: 1990. *Kidney Int Suppl*. 29:S2-8.

DeLuca HF (2004). Overview of general physiologic features and functions of vitamin D. *Am J Clin Nutr*. 80(6 Suppl):1689S-96S.

di Masi A, Leboffe L, De Marinis E, Pagano F, Cicconi L, Rochette-Egly C, Lo-Coco F, Ascenzi P, Nervi C (2015). Retinoic acid receptors: from molecular mechanisms to cancer therapy. *Mol Aspects Med.* 41:1-115.

Dinsmore CJ, and Bell IM (2003). Inhibitors of farnesyltransferase and geranylgeranyltransferase-I for antitumor therapy: substrate-based design, conformational constraint and biological activity. *Curr. Top. Med. Chem.* 3:1075–1093.

Dong D, and Noy N (1998). Heterodimer formation by retinoid X receptor: Regulation by ligands and by the receptor's self-association properties. *Biochemistry.* 37:10691-10700.

Dou Y, Mizzen CA, Abrams M, Allis CD & Gorovsky MA (1999). Phosphorylation of linker histone H1 regulates gene expression in vivo by mimicking H1 removal. *Mol. Cell.* 4:641–647.

Dudzinski DM, Igarashi J, Greif D, Michel T (2006). The regulation and pharmacology of endothelial nitric oxide synthase. *Annu Rev Pharmacol Toxicol.* 46:235–76.

Dürst M, Gallahan D, Jay G, Rhim JS (1989). Glucocorticoid-enhanced neoplastic transformation of human keratinocytes by human papillomavirus type 16 and an activated ras oncogene. *Virology.* 173(2):767-71.

Egea PF, Mitchler A, Rochel N, Ruff M, Chambon P and Moras D (2000). Crystal structure of the human RXR ligand-binding domain bound to its natural ligand: 9 –cis-retinoic acid. *The EMBO Journal.* 19:2590-2601.

El Abdaimi K, Papavasiliou V, Rabbani SA, Rhim JS, Goltzman D, Kremer R (1999). Reversal of hypercalcemia with the vitamin D analogue EB1089 in a human model of squamous cancer. *Cancer Res.* 59(14):3325-8.

El Abdaimi K, Dion N, Papavasiliou V, Cardinal PE, Binderup L, Goltzman D, Ste-Marie LG, Kremer R (2000). The vitamin D analogue EB 1089 prevents skeletal metastasis and prolongs survival time in nude mice transplanted with human breast cancer cells. *Cancer Res.* 60(16):4412-8.

Elbashir SM, et al., (2001). RNA interference is mediated by 21- and 22-nucleotide RNAs. *Genes Dev.*15:188.

Ellenberg J., Siggia ED, Moreira JE, Smith CF, Presley JF, Worman HJ, *and* Lippincott-Schwartz J (1997). Nuclear membrane dynamics and reassembly in living cells: Targeting of an inner nuclear membrane protein in interphase and mitosis. *J. Cell Biol.* 138:1193-1206.

Esteller, M (2007b). Epigenetics provides a new generation of oncogenes and tumour-suppressor genes. *Br. J. Cancer.* 96: R26–R30.

Evans TRJ, Colston KW, Lofts FJ, Cunningham G, Anthony DA, Gogas H, de Bono JS, Hamberg KJ, Skov T, and Mansi JL (2002). A phase II trial of the vitamin D analogue Seocalcitol (EB1089) in patients with inoperable pancreatic cancer. *Br J Cancer.* 86(5): 680–685

Evans, R M (1988). The steroid and thyroid hormone receptor superfamily. *Science.* 240:889-895.

Evoy D, Hirschowitz EA, Naama HA, et al., (1997). *In vivo* adenoviral-mediated gene transfer in the treatment of pancreatic cancer. *J Surg Res.* 69(1):226–31.

Faivre EJ, Daniel AR, Hillard CJ, Lange CA (2008). Progesterone receptor rapid signaling mediates serine 345 phosphorylation and tethering to specificity protein 1 transcription factors. *Mol Endocrinol.* 22(4):823-37

Farach-Carson MC, Abe J, Nishii Y, Khoury R, Wright G, Nonnan AW (1993). 22oxacalcitriol: dissection of 1,25(OH)2D3 receptor-mediated and Ca²⁺ entry-

stimulating pathways. *Am. J. Physiol. Renal Physiol.* 265: F705-11.

Farla P, Hersmus R, Geverts B, Mari PO, Nigg AL, Dubbink HJ, Trapman J, Houtsmuller AB (2004). The androgen receptor ligand-binding domain stabilizes DNA binding in living cells. *J. Struct. Biol.* 147:50–61.

Feige JN, Gelman L, Tudor C, Engelborghs Y, Wahli W, Desvergne B (2005). Fluorescence imaging reveals the nuclear behavior of peroxisome proliferator-activated receptor/retinoid X receptor heterodimers in the absence and presence of ligand. *J. Biol. Chem.* 280:17880-17890.

Feldman D, Malloy PJ, Miller WL (2013). Genetic disorders of vitamin D synthesis and action. In: Thakker RV, Whyte MP, Eisman JA, Igarashi T (eds). *Genetics of Bone Biology and Skeletal Disease*. Elsevier: San Diego, CA, USA, 537–552.

Feldman D, Malloy PJ (2014). Mutations in the vitamin D receptor and hereditary vitamin D-resistant rickets. *BoneKEY Reports* doi:10.1038/bonekey.2014.5

Ferla S, Aboraia AS, Brancale A, Pepper CJ, Zhu J, Ochalek JT, DeLuca HF, Simons C (2014). Small-molecule inhibitors of 25-hydroxyvitamin D-24-hydroxylase (CYP24A1): synthesis and biological evaluation. *J Med Chem.* 57(18):7702-15.

Ferla S, Goma MS, Brancale A, Zhu J, Ochalek JT, DeLuca HF, Simons C (2014). Novel styryl-indoles as small molecule inhibitors of 25-hydroxyvitamin D-24-hydroxylase (CYP24A1): Synthesis and biological evaluation. *Eur J Med Chem.* 87:39-51.

Ferrara J, McCuaig KA, Hendy GN, Uskokovic M, White JH (1994). Highly potent transcriptional activation by 16-ene derivatives of 1,25-dihydroxyvitamin

D3: lack of modulation by 9-cis retinoic acid of the response to vitamin D3 or its derivatives. *J Biol Chem.* 269:2971–2981.

Fetahu IS, Höbaus J and Kállay E (2014). Vitamin D and the epigenome *Front. Physiol.* 5: 164.

Flaherty KT, Puzanov I, Kim KB, Ribas A, McArthur GA, Sosman JA, O'Dwyer PJ, d J. Lee RA, Grippo JF, Nolop K and Chapman PB (2010). Inhibition of Mutated, Activated BRAF in Metastatic Melanoma. *N Engl J Med.* 363(9): 809–819.

Fleet JC, Eksir F, Hance KW, Wood RJ (2002). Vitamin D-inducible calcium transport and gene expression in three Caco-2 cell lines. *Am J Physiol Gastrointest Liver Physiol.* 283:G618–G625.

Fleet JC, Wood RJ (1994). Identification of calbindin D-9k mRNA and its regulation by 1,25-dihydroxyvitamin D3 in Caco-2 cells. *Arch Biochem Biophys.* 308:171–174.

Fleet JC, Wood RJ (1999). Specific 1,25(OH)₂ D₃-mediated regulation of transcellular calcium transport in Caco-2 cells. *Am J Physiol.* 276:G958–G964.

Fleet, JC (2006). Molecular Regulation of Calcium Metabolism. In: Weaver CM, Heaney RP, editors. *Calcium in Human Health.* Humana Press; Totowa, NJ: pp. 163–190.

Fondell JD, Ge H, Roeder RG (1996). Ligand induction of a transcriptionally active thyroid hormone receptor coactivator complex. *Proc Natl Acad Sci USA.* 93:8329–8333

Forman BM, Samuels HH (1990). Interactions among a subfamily of nuclear hormone receptors: the regulatory zipper model. *Mol. Endocrinol.* 4(9):1293-301.

Forman BM, Umesono K, Chen J, Evans RM (1995). Unique response pathways are established by allosteric interactions among nuclear hormone receptors. *Cell*. 81(4):541-50.

Fujioka T, Hasegawa M, Ishikura K, Matsushita Y, Sato M, Tanji S (1998). Inhibition of tumor growth and angiogenesis by vitamin D3 agents in murine renal cell carcinoma. *J Urol*. 160(1): 247–251.

Fukumura D, Kashiwagi S, Jain RK (2006). The role of nitric oxide in tumour progression. *Nat Rev Cancer*. 6:521–34.

Gampe RT Jr, Montana VG, Lambert MH, Miller AB, Bledsoe RK, Milburn MV, Kliewer SA, Willson TM, Xu HE (2000) Asymmetry in the PPARgamma/RXRalpha crystal structure reveals the molecular basis of heterodimerization among nuclear receptors. *Mol Cell*.;5(3):545-55

Geary RS (2009). Antisense oligonucleotide pharmacokinetics and metabolism. *Expert Opin. Drug Metab. Toxicol*. 5: 381–391

Geary RS, Leeds JM, Henry SP et al., (1997) Antisense oligonucleotide inhibitors for the treatment of cancer: 1. Pharmacokinetic properties of phosphorothioate Oligodeoxynucleotides. *Anticancer Drug Des*. 12:383–93.

Getzenberg RH, Light BW, Lapco PE, Konety BR, Nangia AK, Acierno JS, et al (1997). Vitamin D inhibition of prostate adenocarcinoma growth and metastasis in the Dunning rat prostate model system. *Urology*. 50(6):999–1006.

Giannini CD, Roth WK, Piiper A, Zeuzem S (1999). Enzymatic and antisense effects of a specific anti-Ki-ras ribozyme in vitro and in cell culture. *Nucleic Acids Res*. 27(13):2737-44.

Gibbs JB (1991). Ras C-terminal processing enzymes: new drug targets? *Cell*. 65:1-4.

Giguère V, Hollenberg SM, Rosenfeld MG, Evans RM (1986). Functional domains of the human glucocorticoid receptor. *Cell*. 46(5):645-52.

Glass CK (1994). Differential recognition of target genes by nuclear receptor monomers, dimers and heterodimers. *Endocrine Rev.* 15:391-407.

Glass CK, Rosenfeld MG. (2000). The coregulator exchange in transcriptional functions of nuclear receptors. *Genes Dev* 14: 121–141.

Gniadecki R (1997). Effects of 1,25-dihydroxyvitamin D₃ and its 20-epi analogues (MC 1288, MC 1301, KH 1060), on clonal keratinocyte growth: evidence for differentiation of keratinocyte stem cells and analysis of the modulatory effects of cytokines. *Br J Pharmacol*. March; 120(6): 1119–1127.

Graham MJ, Crooke ST, Monteith DK, Cooper SR, Lemonidis KM, Stecker KK et al., (1998). *In vivo* distribution and metabolism of a phosphorothioate oligonucleotide within rat liver after intravenous administration. *J. Pharmacol. Exp. Ther.* 286: 447–458

Grassi G et al., (2004). Therapeutic potential of hammerhead ribozymes in the treatment of hyper-proliferative diseases. *Curr. Pharm. Biotechnol.*5:369.

Gratton JP, Lin MI, Yu J, Weiss ED, Jiang ZL, Fairchild TA et al., (2003). Selective inhibition of tumor microvascular permeability by cavtratin blocks tumor progression in mice. *Cancer Cell*. 4:31–9.

Green .S, Isserman. I, Sheer E (1988). A versatile *in vivo* and *in vitro* eukaryotic expression vector for protein engineering. *Nucleic Acids Res.*16:369.

Gronemeyer H, Bourguet W (2009). Allosteric effects govern nuclear receptor action: DNA appears as a player. *Sci Signal*. 2(73):pe34.

Guillermet-Guibert J, Davenne L, Pchejetski D et al., (2009) Targeting the sphingolipid metabolism to defeat pancreatic cancer cell resistance to the chemotherapeutic gemcitabine drug. *Mol Cancer Ther*.8(4):809–20

Gulliford T, English J, Colston KW, Menday P, Moller S, Coombes RC (1998). A phase I study of the vitamin D analogue EB 1089 in patients with advanced breast and colorectal cancer. *Br J Cancer*. 78(1):6-13.

Guyton KZ, Kensler TW, Posner GH (2003). Vitamin D and vitamin D analogs as cancer chemopreventive agents. *Nutr Rev*. 61(7):227-38.

Hagan CR, Regan TM, Dressing GE, Lange CA (2011). ck2-dependent phosphorylation of progesterone receptors (PR) on Ser81 regulates PR-B isoform-specific target gene expression in breast cancer cells. *Mol Cell Biol*. 31(12):2439-52.

Hagan CR, Daniel AR, Dressing GE, Lange CA (2012). Role of phosphorylation in progesterone receptor signaling and specificity. *Mol Cell Endocrinol. J*. 357(1-2):43-9.

Hager G1, Kornfehl J, Knerer B, Weigel G, Formanek M (2004). Molecular analysis of p21 promoter activity isolated from squamous carcinoma cell lines of the head and neck under the influence of 1,25(OH)₂ vitamin D₃ and its analogs. *Acta Otolaryngol*. 124(1):90-6.

Hansdottir S, Monick MM, Lovan N, Powers L, Gerke A, and Hunninghake GW (2010). Vitamin D Decreases Respiratory Syncytial Virus Induction of NF-κB–Linked Chemokines and Cytokines in Airway Epithelium While Maintaining the Antiviral State. *J. Immunol*. 184:965-974.

Hatoum A, El-Sabban ME, Khoury J, Yuspa SH, Darwiche N (2001). Overexpression of retinoic acid receptors alpha and gamma into neoplastic epidermal cells causes retinoic acid-induced growth arrest and apoptosis. *Carcinogenesis*. 22:1955-63.

Hatzivassiliou G, Song K, Yen I et al., (2010). RAF inhibitors prime wild-type RAF to activate the MAPK pathway and enhance growth. *Nature*. 464(7287):431–435.

Haussler MR, Jurutka PW, Mizwicki M, Norman AW (2011). Vitamin D receptor (VDR)-mediated actions of $1\alpha,25(\text{OH})_2\text{vitamin D}_3$: genomic and non-genomic mechanisms. *Best Pract Res Clin Endocrinol Metab.* (4):543-59.

Haussler MR, Haussler CA, Jurutka PW, Thompson PD, Hsieh JC, Remus LS, Selznick SH, Whitfield GK (1997). The vitamin D hormone and its nuclear receptor: molecular actions and disease states. *J Endocrinol*. 154 Suppl:S57-73.

Haussler, MR, et al (1998). The nuclear vitamin D receptor: biological and molecular regulatory properties revealed. *J Bone Miner Res*. 13:325-349.

Hedlund, TE, Moffat, KA, Miller, GJ (1996). Vitamin D receptor expression is required for growth modulation by 1-alpha, 25-dihydroxyvitamin D₃ in the human prostatic carcinoma cell line ALVA-31. *J Steroid Biochem Mol Biol*. 58:277-288.

Hendy NH (2005). Calcium –Regulating Hormones in Endocrinology: basic and Clinical principles. Humana Press inc. Totowa.NJ. pages 307-323

Heidorn SJ, Milagre C, Whittaker S, et al., (2010). Kinase-dead BRAF and oncogenic RAS cooperate to drive tumor progression through CRAF. *Cell*. 140(2):209–221.

Hirschberg K, Miller CM, Ellenberg J, Presley JF, Siggia ED, Phair RD, *and* Lippincott-Schwartz J (1998). Kinetic analysis of secretory protein traffic and characterization of Golgi to plasma membrane transport intermediates in living cells. *J. Cell Biol.* 143:1485-1503.

Ho SN, Hunt HD, Horton RM, Pullen JK, Pease LR (1989). Site directed mutagenesis by overlap extension using the polymerase chain reaction. *Gene.* 77:51-59.

Holick MF (2009). Multiple myeloma and cancer: is there a D-lightful connection? *Am J Hematol.* 84(7):393-4.

Hollis BW (1990). 25-Hydroxyvitamin D₃-1 alpha-hydroxylase in porcine hepatic tissue: subcellular localization to both mitochondria and microsomes. *Proc Natl Acad Sci.* 87(16): 6009–6013.

Houle B, Rochette-Egly C, Bradley WE (1993). Tumor-suppressive effect of the retinoic acid receptor beta in human epidermoid lung cancer cells. *Proc Natl Acad Sci USA.* 90:985–9.

Houtsmuller AB, Rademakers S, Nigg AL, Hoogstraten D, Hoeijmakers JH, Vermuelen W (1999). Action of DNA repair endonuclease ERCC1/XFP in living cells. *Science.* 284:958-961.

Hsieh JC et al., (1991) Human vitamin D receptor is selectively phosphorylated by protein kinase C on serine 51, a residue crucial to its trans-activation function. *Proc Natl Acad Sci USA.* 88: 9315-9

Hsieh JC, et al., (2004). Phosphorylation of human vitamin D receptor serine-182 by PKA suppresses 1,25(OH)₂D₃-dependent transactivation. *Biochem Biophys Res Commun.* 324: 801-9

Hsieh JC, Jurutka PW, Nakajima S, Galligan MA, Haussier CA, Shimizu Y, Shimizu N, Whitfield GK, Haussier MR (1993). Phosphorylation of the human vitamin D receptor by protein kinase C. Biochemical and functional evaluation of the serine 51 recognition site. *J. Biol. Chem.* 268: 15118-15126.

Huang J, Powell WC, Khodavirdi AC, Wu J, Makita T, et al. (2002). Prostatic intraepithelial neoplasia in mice with conditional disruption of the retinoid X receptor alpha allele in the prostate epithelium. *Cancer Res.* 62: 4812–4819.

Hwang DY, Cohen JB (1997). A splicing enhancer in the 3'-terminal c-H-ras exon influences mRNA abundance and transforming activity. *J Virol.* 71(9):6416-26.

Infante JR, Somer BG, Park JO, Li CP, Scheulen ME, Kasubhai SM, Oh DY, Liu Y, Redhu S, Stepkowski K, Le N (2014) A randomised, double-blind, placebo-controlled trial of trametinib, an oral MEK inhibitor, in combination with gemcitabine for patients with untreated metastatic adenocarcinoma of the pancreas. *Eur J Cancer.* 50(12):2072-81.

Infante JR, Papadopoulos KP, Bendell JC, Patnaik A, Burris HA, Rasco D, Jones SF, Smith L, Cox DS, Durante M, Bellew KM, Park JJ, Le NT, Tolcher AW (2013) A phase 1b study of trametinib, an oral Mitogen-activated protein kinase kinase (MEK) inhibitor, in combination with gemcitabine in advanced solid tumours. *European Journal of Cancer.* 49(9): 2077–2085

Ingraham BA, Bragdon B, Nohe A (2008). Molecular basis of the potential of vitamin D to prevent cancer. *Curr Med Res Opin.* 24:139–149. 5.

Jakob, F., Gieseler, F., Tresch, A., Hammer, S., Seufert, J., and Schneider, D (1992). Kinetics of nuclear translocation and turnover of the vitamin D receptor in human HL60 leukemia cells and peripheral blood lymphocytes--coincident rise of DNA-relaxing activity in nuclear extracts. *J Steroid Biochem. Mol. Biol.* 42: 11–16.

James GL, Goldstein JL, Brown MS, et al., (1993). Benzodiazepine peptidomimetics: potent inhibitors of Ras farnesylation in animal cells. *Science*. 260(5116):1937–1942.

Johnson LA, Morgan RA, Dudley ME, Cassard L, Yang JC, Hughes MS, Kammula US, Royal RE, Sherry RM, Wunderlich JR, Lee CCR, Restifo NP, Schwarzl SL, Cogdill AP, Bishop RJ, Kim H, Brewer CC, Rudy SF, VanWaes C, Davis JL, Mathur A, Ripley RT, Nathan DA, Laurencot CM and Rosenberg SA (2009). Gene therapy with human and mouse T-cell receptors mediates cancer regression and targets normal tissues expressing cognate antigen. *Blood*: 114 (3) 535-546.

Jones G, Kung M, Kano K (1983). The isolation and identification of two new metabolites of 25-hydroxyvitamin D₃ produced in the kidney. *J Biol. Chem.* 258:12920-12929.

Jones BB, Jurutka PW, Haussler CA, Haussler MR, Whitfield GK (1991). Vitamin D receptor phosphorylation in transfected ROS 17/2.8 cells is localized to the N-terminal region of the hormone-binding domain. *Mol Endocrinol.* 8:1137-46.

Jones G, Calverley MJ. (1993). A dialogue on analogues: newer vitamin D drugs for use in bone disease, psoriasis, and cancer. *Trends Endocrinol Metab.* 4(9):297-303

Jones G, Strugne SA, DeLuca HF (1998). Current Understanding of the Molecular Actions of Vitamin D. *Physio. Rev.* 78: 1193-1230.

Juliano RL, Ming X, Nakagawa O (2012). The chemistry and biology of oligonucleotide conjugates. *Acc. Chem. Res.*45:1067–1076

Jurutka PW, Hsieh JC, MacDonald PN, Terpening CM, Haussler CA, Haussler MR, Whitfield GK (1993). Phosphorylation of serine 208 in the human vitamin D receptor. The predominant amino acid phosphorylated by casein kinase II, in vitro,

and identification as a significant phosphorylation site in intact cells. *J Biol Chem.* 268(9):6791-9.

Jurutka PW, Hsieh JC, Haussier MR (1994). Characterization of a new functional 1,25dihydroxyvitamin D₃ responsive element in the promoter region of the rat 25hydroxyvitamin D₃, 24 hydroxylase gene. *J Bone.Mineral. Res.* 9 (Suppl 1):S 160.

Jurutka PW, Hsieh J-C, Nakajima S, Haussier CA, Whitfield GK, Haussier MR (1996). Human vitamin D receptor phosphorylation by casein kinase II at ser-208 potentiates transcriptional activation. *Proc Natl Acad Sci. USA.* 93:3519-3524.

Jurutka PW, Hsieh JC, MacDonald PN, Terpening CM, Haussler CA, Haussler MR, Whitfield GK (1993). Phosphorylation of serine 208 in the human vitamin D receptor. The predominant amino acid phosphorylated by casein kinase II, in vitro, and identification as a significant phosphorylation site in intact cells. *J Biol Chem.* 268:6791-9

Jusu S, John F. Presley, Loan Nguyen-Yamamoto, Benoit Ochetti and Richard Kremer (2013). Effects of 1 α , 25- Dihydroxyvitamin D₃ on subcellular localization, VDR /RXR α interaction by Fluorescent Resonance Energy Transfer (FRET) and nuclear mobility of RXR α by Fluorescent loss after photobleaching (FLIP). *ASBMR Proceedings, Baltimore MD, USA.*

K Iida, T Shinki, A Yamaguchi, H F DeLuca, K Kurokawa, T Suda (1995). A possible role of vitamin D receptors in regulating vitamin D activation in the kidney. *Proc Natl Acad Sci.* 92(13): 6112–6116.

Kanamori T, Shimizu M, Okuno M, Matsushima-Nishiwaki R, Tsurumi H, Kojima S, et al., (2007). Synergistic growth inhibition by acyclic retinoid and vitamin K₂ in human hepatocellular carcinoma cells. *Cancer Sci.* 98:431–7.

Kane KF, Langman MJS, Williams GR (1996). Antiproliferative responses of two human colon cancer cell lines to vitamin D3 are differentially modified by 9-cis retinoic acid. *Cancer Res.* 56:623–632.

Kang SJ, Xiao-Yan LJ, Duell EA, Voorhees J (1997). The retinoid X receptor agonist 9-cis retinoic acid and the 24-hydroxylase inhibitor ketoconazole increase activity of 1,25dihydroxyvitamin D3 in human skin in vivo. *J Invest. Dermatol.* 108:513-518.

Kelland LR (2003). Farnesyl transferase inhibitors in the treatment of breast cancer. *Expert Opin. Investig. Drugs.* 12: 413–421.

Kelland L (2005). Discontinued drugs in 2005: oncology drugs. *Expert Opin Investig Drugs.* 15(11):1309-18.

Kiehl MG, Ostermann H, Meyer J, Kienast J (1997). Nitric oxide synthase inhibition by L-NAME in leukocytopenic patients with severe septic shock. *Intensive Care Med.* 23(5):561-6.

Kim R1, Emi M, Matsuura K, Tanabe K (2007). Antisense and nonantisense effects of antisense Bcl-2 on multiple roles of Bcl-2 as a chemosensitizer in cancer therapy. *Cancer Gene Ther.*14(1) 1-11

Klasa RJ et al., (2002). Oblimersen Bcl-2 antisense: facilitating apoptosis in anticancer treatment. *Antisense Nucleic Acid Drug Dev.*12:193.

Klopot A, Hance KW, Peleg S, Barsony J, and Fleet JC (2007). Nucleocytoplasmic Cycling of the Vitamin D Receptor in the Enterocyte-Like Cell Line, Caco-2. *J Cell Biochem.* 100:617–628.

Kohl NE, Mosser SO, deSolms J, Giuliani EA, Pompliano DL, Graham SL, Smith RL, Scolnick EM, OlitT A, Gibbs JB (1993). Selective inhibition of ras-dependent transformation by a farnesyltransferase inhibitor. *Science.* 260 (5116):1934-1937.

Kolch W, Heidecker G, Lloyd P, Rapp UR (1991). Raf-1 protein kinase is required for growth of induced NIH/3T3 cells. *Nature*. 31;349(6308):426-8.

Kostner K, Denzer N, Muller CS, Klein R, Tilgen W, Reichrath J (2009). The relevance of vitamin D receptor (VDR) gene polymorphism for cancer: a review of the literature. *Anticancer Res*. 29: 3511–3536.

Kragballe K, Gjertsen BT, DeHoop D, Karlsmark T, Van De Kerkhof PC, Larko O, Nieboer C, Roed-Pet-Ersen J, Strand A, Tikjob G. (1991). Double-blind, right/left comparison of calcipotriol and betamethasone valerate in treatment of psoriasis vulgaris. *Lancet*. 337:193-196.

Krstic MD, Rogatsky I, Yamamoto KR, Garabedian MJ (1997). Mitogen-activated and cyclin-dependent protein kinases selectively and differentially modulate transcriptional enhancement by the glucocorticoid receptor. *Mol Cell Biol*. 17(7):3947-54.

Kumar, V, Chambon, P (1988). The estrogen receptor binds tightly to its responsive element as a ligand-induced homodimer. *Cell*. 55:145–156.

Kuusisto HV, Wagstaff KM, Alvisi G, Roth DM, Jans DA (2012). Global enhancement of nuclear localization-dependent nuclear transport in transformed cells. *FASEB J*. 26:1181-93.

Lala DS, Rice DA, Parker KL (1992). Steroidogenic factor 1, a key regulator of steroidogenic enzyme expression, is the mouse homolog of fushi tarazu-factor I. *Mol. Endocrinol*. 6:1249–1258

Lampson BL, Kendall SD, Ancrile BB, Morrison MM, Shealy MJ, Barrientos KS, Crowe MS, Kashatus DF, White RR, Gurley SB, Cardona DM and Counter CM (2012). Targeting eNOS in Pancreatic Cancer. *Cancer Res*. 72(17):4472–4482.

Lane KT and Beese LS (2006). Thematic review series: Lipid Posttranslational Modifications. Structural biology of protein farnesyltransferase and geranylgeranyltransferase type I. *J. Lipid. Res.* 681-699

Lange CA, Shen T, Horwitz KB (2000). Phosphorylation of human progesterone receptors at serine-294 by mitogen-activated protein kinase signals their degradation by the 26S proteasome. *Proc Natl Acad Sci USA.* 97(3):1032-7.

Larsen SS, I Heiberg, Lykkesfeldt AE (2001). Anti-oestrogen resistant human breast cancer cell lines are more sensitive towards treatment with the vitamin D analogue EB1089 than parent MCF-7 cells. *Br J Cancer.* 84(5):686–690.

le Maire A, Bourguet W, Balaguer P (2010). A structural view of nuclear hormone receptor: endocrine disruptor interactions. *Cell Mol Life Sci.* (8):1219-37.

Leblanc BP, Stunnenberg HG (1995). 9-cis retinoic acid signaling: changing partners causes some excitement. *Genes Dev.* 9:1811-1816.

Lee, MH., I. Reynisdottir, and J. Massague' (1995). Cloning of p57Kip2, a cyclin-dependent kinase inhibitor with unique domain structure and tissue distribution. *Genes & Dev.* 9:639–49.

Lee H, Bai W (2002). Regulation of estrogen receptor nuclear export by ligand-induced and p38-mediated receptor phosphorylation. *Mol Cell Biol.* 22(16):5835-45.

Lee HY, Suh YA, Robinson MJ, Clifford JL, Hong WK, Woodgett JR, *et al.* (2000). Stress pathway activation induces phosphorylation of retinoid X receptor J. *Biol. Chem.*, 275:32193–32199.

Lehmann JM, Ihang X-K, Graupner G, Lee MO, Hermann I, HotTman B, Pfahl M (1993). Formation of retinoid X receptor homodimers leads to repression of T3

response: hormonal cross talk by ligand-induced squelching. *Cell. Biol.* 13:7698-7707.

Leigh DA, Ferguson V, Bentel JM, Miller JO, Smith GJ (1990). Activated Ki-ras proto-oncogene in spontaneously transformed and chemical tumor-derived cell lines related to the mouse lung alveologenic carcinoma. *Mol Carcinog.* 3(6):387-92.

Leigh M, Purkis PE, Jarkey A, Collins P, Neill S, Proby C, Glover M, Lane EB (1993). Keratinocyte alterations in skin tumour development. *Recent Results Cancer Res.* 128:179-91.

Leonetti C, Zupi G. (2007). Targeting different signaling pathways with antisense oligonucleotides combination for cancer therapy. *Curr. Pharm. Des.* 13:463.

Li D, Zimmerman TL, S Thevananther, HY Lee, JM Kurie, SJ Karpen (2002). Interleukin-1 beta-mediated suppression of RXR:RAR transactivation of the Ntcp promoter is JNK-dependent. *The Journal of Biological chemistry.* 277(35):31416-22.

Li D, Li T, Wang F, Tian H, Samuels HH (2002). Functional evidence for retinoid X receptor (RXR) as a nonsilent partner in the thyroid hormone receptor/RXR heterodimer. *Mol Cell Biol.* (16):5782-92.

Li M, Chiba H, Warot X, Messaddeq N, Gerard C, et al., (2001). RXR-alpha ablation in skin keratinocytes results in alopecia and epidermal alterations. *Development.* 128:675-688.

Li M, Indra AK, Warot X, Brocard J, Messaddeq N, Kato S, Metzger D and Chambon P (2000). Skin abnormalities generated by temporally controlled RXR α mutations in mouse epidermis. *Nature.* 407:633-636.

Li YC, Pirro AE, Amling M, Delling G, Baron R, Bronson R et al., (1997). Targeted ablation of the vitamin D receptor: an animal model of vitamin D-dependent rickets type II with alopecia. *Proc Natl Acad Sci USA*. 94:9831–9835.

Li M, Zhang Y, Bharadwaj U, et al., (2009). Down-regulation of ZIP4 by RNA interference inhibits pancreatic cancer growth and increases the survival of nude mice with pancreatic cancer xenografts. *Clin Cancer Res*. 15(19):5993–6001.

Lisiansky V, Naumov I, Shapira S, Kazanov D, Starr A, Arber N, Kraus S (2012). Gene therapy of pancreatic cancer targeting the K-Ras oncogene. *Cancer Gene Ther*. 19(12):862-9

Lianjun Lu, Jianhua Qiu, Shunli Liu, et al., (2008). Vitamin D3 analogue EB1089 inhibits the proliferation of human laryngeal squamous carcinoma cells via p57
Mol Cancer Ther. 7:1268-1274.

Likhite VS, Stossi F, Kim K, Katzenellenbogen BS, Katzenellenbogen JA (2006). Kinase-specific phosphorylation of the estrogen receptor changes receptor interactions with ligand, deoxyribonucleic acid, and coregulators associated with alterations in estrogen and tamoxifen activity. *Mol Endocrinol*. (12):3120-32.

Lim KH, Counter CM (2005). Reduction in the requirement of oncogenic Ras signaling to activation of PI3K/AKT pathway during tumor maintenance. *Cancer Cell*. 8:381–92.

Lim KH, Ancrile BB, Kashatus DF, Counter CM (2008). Tumour maintenance is mediated by eNOS. *Nature*. 452:646–9.

Lippincott-Schwartz, J (2004). Dynamics of Secretory Membrane trafficking. *Ann NY Acad Sci*. 1038:1-10.

Lippincott-Schwartz J, Presley J, Zaal K, Hirschberg K, Miller C, and Ellenberg J (1999). Monitoring the dynamics and mobility of membrane proteins tagged with

green fluorescent protein. In *Green Fluorescent Proteins*, vol. 58 (K.F. Sullivan and S.A. Kay, eds.) pp. 261- 291. Academic Press, San Diego.

Lippincott-Schwartz J, Snapp EL, and Kenworthy A (2001). Studying protein dynamics in living cells. *Nat. Rev. Mol. Cell Biol.* 2:444-456.

Liu M, Lee S, Yaremko B, Chen J, Del J, Nielsen L, et al., (1998). SCH 66336 an orally bioavailable tricyclic farnesyl protein transferase inhibitor, demonstrates broad and potent in vivo antitumor activity [abstract]. *Proc Am Assoc Cancer Res*;39:1843.

Liu P, Cheng H, Roberts TM, Zhao JJ. (2009). Targeting the phosphoinositide 3-kinase pathway in cancer. *Nat Rev Drug Discov.* 8:627–44.

Long MD, Sucheston-Campbell LE, Campbell MJ (2015). Vitamin D receptor and RXR in the post-genomic era. *J Cell Physiol.* 230(4):758-66. D

Lowe LC, Guy M, Mansi JL, Peckitt C, Bliss J, Wilson RG, Colston K W (2005). Plasma 25-hydroxy vitamin D concentrations, vitamin D receptor genotype and breast cancer risk in a UK Caucasian population. *Eur. J. Cancer.* 41:1164–1169.

Lowy DR, Zhang K, DeClue JE, Willumsen BM (1991). Regulation of p21ras activity. *Trends Genet.* 7(11-12):346-51. Review

Lu MJ, Mpoke SS, Dadd CA, & Allis, CD (1995). Phosphorylated and dephosphorylated linker histone H1 reside in distinct chromatin domains in *Tetrahymena* macronuclei. *Mol. Biol. Cell* 6, 1077–1087.

Lu N, Liu J, Liu J, Zhang C, Jiang F, Wu H, Chen L, Zeng W, Cao X, Yan T, Wang G, Zhou H, Lin B, Yan X, Zhang X, Zeng J (2012). Antagonist Effect of Triptolide on AKT Activation by Truncated Retinoid X Receptor-alpha. *PLoS ONE.* 7(4):e35722

Lucas AS, Cohen EE, Cohen RB, Krzyzanowska MK, Chung CH, Murphy BA, Tanvetyanon T, Gilbert J, Moore DT, Hayes DN (2010). Phase II study and tissue correlative studies of AZD6244 (ARRY-142886) in iodine-131 refractory papillary thyroid carcinoma (IRPTC) and papillary thyroid carcinoma (PTC) with follicular elements. *J Clin Oncol.* (ASCO Annual Meeting Abstracts). 28(15S):Abstract 5536.

Macoritto M, Nguyen-Yamamoto L, Huang DC, Samuel S, Yang XF, Wang TT, White JH, Kremer R (2008). Phosphorylation of the Human Retinoid X Receptor α at Serine 260 Impairs Coactivator(s) Recruitment and Induces Hormone Resistance to Multiple Ligands. *J. Biol.Chem.* 283:4943–4956.

Macedo LC, Soardi FC, Ananias N, Belangero VM, Rigatto SZ, De-Mello MP et al., (2008). Mutations in the vitamin D receptor gene in four patients with hereditary 1,25-dihydroxyvitamin D-resistant rickets. *Arq Bras Endocrinol Metabol.* 52:1244–1251.

Malik S, Guermah M, Yuan CX, Wu W, Yamamura S, Roeder RG (2004). Structural and functional organization of TRAP220, the TRAP/mediator subunit that is targeted by nuclear receptors. *Mol. Cell. Biol.* 24: 8244–8254

Malloy PJ, Eccleshall TR, Gross C, Van Maldergem L, Bouillon R, Feldman D (1997). Hereditary vitamin D resistant rickets caused by a novel mutation in the vitamin D receptor that results in decreased affinity for hormone and cellular hyporesponsiveness. *J Clin Invest.* 99:297–304.

Malloy PJ, Feldman D (1998). Molecular defects in the vitamin D receptor associated with hereditary 1,25-dihydroxyvitamin D resistant rickets. In: Holick MF (ed). *Vitamin D: Physiology, Molecular Biology, and Clinical Applications* Humana Press: Totowa, NJ, USA.

Malloy PJ, Feldman D (2011). The role of vitamin D receptor mutations in the development of alopecia. *Mol Cell Endocrinol.* 347:90–96.

Malloy PJ, Zhou Y, Wang J, Hiort O, Feldman D (2011). Hereditary vitamin D-resistant rickets (HVDRR) owing to a heterozygous mutation in the vitamin D receptor. *J Bone Miner Res.* 26:2710–2718.

Malloy PJ, Zhu W, Zhao XY, Pehling GB, Feldman D (2001). A novel inborn error in the ligand-binding domain of the vitamin D receptor causes hereditary vitamin D-resistant rickets. *Mol Genet Metab.* 73:138–148.

Malloy PJ, Xu R, Peng L, Clark PA, Feldman D (2002). A novel mutation in helix 12 of the vitamin D receptor impairs coactivator interaction and causes hereditary 1,25-dihydroxyvitamin D-resistant rickets without alopecia. *Mol Endocrinol.* 16:2538–2546.

Mangelsdorf D, Umesono K, Evans RM (1994). The retinoid receptors. In *The Retinoids: Biology, chemistry and medicine*. Raven Press. New York. pp 319-349.

Mangelsdorf DJ, Thummel C, Beato M, Herrlich P, Schutz G, Umesono K, Blumberg B, Kastner P, Mark M, Chambon P, Evans RM (1995). The nuclear receptor superfamily: the second decade. *Cell.* 83:835-839.

Mangelsdorf DJ, Evans RM (1995b). The RXR heterodimers and orphan receptors. *Cell.* 83:841-850.

Marik, R, Fackler M, Gabrielson E, Zeiger MA, Sukumar S, Stearns V, et al. (2010). DNA methylation-related vitamin D receptor insensitivity in breast cancer. *Cancer Biol. Ther.* 10:44–53.

Markt S, Magnani Z, Ciceri F, et al., (2003). Immunologic potential of donor lymphocytes expressing a suicide gene for early immune reconstitution after hematopoietic T-cell-depleted stem cell transplantation. *Blood.* 101:1290-1298.

Mason SA, Housley PR (1993). Site-directed mutagenesis of the phosphorylation sites in the mouse glucocorticoid receptor. *J Biol Chem.* 268(29):21501-4.

Matsushima-Nishiwaki R, Okuno M, Adachi S, Sano, T, Akita K, Moriwaki H, Friedman, S.L., and Kojima S. (2001). Phosphorylation of Retinoid X Receptor at Serine 260 Impairs Its Metabolism and Function in Human Hepatocellular Carcinoma. *Cancer Res.* 61:7675-7682.

Matsushima-Nishiwaki R, Shidoji Y, Nishiwaki S, Moriwaki H, and Muto Y (1996). Limited degradation of retinoid X receptor by calpain. *Biochem. Biophys. Res. Commun.* 225:946–951.

Matusiak D, Murillo G, Carroll RE, Mehta RG, Benya RV (2005). Expression of vitamin D receptor and 25-hydroxyvitamin D3-1 {alpha}-hydroxylase in normal and malignant human colon. *Cancer Epidemiol. Biomarkers Prev.* 14:2370–2376.

McCullough ML, Bostick RM, Mayo TL (2009). Vitamin D gene pathway polymorphisms and risk of colorectal, breast, and prostate cancer. *Annu. Rev. Nutr.* 29:111–13210.

McNally JG, Muller WG, Walker D, Wolford R, and Hager GL (2000). The glucocorticoid receptor: Rapid exchange with regulatory sites in living cells. *Science.* 287:1262-1265.

Mehta RG, Mehta RR (2002). Vitamin D and cancer. *J Nutr Biochem.* 13(5): 252-264.

Meyer MB, Benkusky NA, and Pike JW (2013). 1, 25-Dihydroxyvitamin D3 induced histone profiles guide discovery of VDR action sites. *J Steroid Biochem Mol Biol.* 144 Pt A:19-21.

McInerney EM, Rose DW, Flynn SE, Westin S, Mullen TM, Kronen A, Inostroza J, Torchia J, Nolte RT, Assa-Munt N, Milburn MV, Glass CK, Rosenfeld MG.

(1998). Determinants of coactivator LXXLL motif specificity in nuclear receptor transcriptional activation. *Genes Dev.* 12(21):3357-68

Michalides R, Griekspoor A, Balkenende A, Verwoerd D, Janssen L, Jalink K, Floore A, Velds A, van't Veer L, Neefjes J (2004). Tamoxifen resistance by a conformational arrest of the estrogen receptor alpha after PKA activation in breast cancer. *Cancer Cell.* 5(6):597-605.

Michigami T, Suga A, Yamazaki M, Shimizu C, Cai G, Okada S, Ozono K (1999). Identification of amino acid sequence in the hinge region of human vitamin D receptor that transfer a cytosolic protein to the nucleus. *J Biol Chem.* 274:33531–33538.

Min Cui, Yan Zhao, Kenneth W. Hance, Andrew Shao, Richard J. Wood, and James C. Fleet (2009). Effects of MAPK Signaling on 1,25 Dihydroxyvitamin D-Mediated CYP24 Gene Expression in the Enterocyte-like Cell Line, Caco-2. *J Cell Physiol.* 219(1): 132–142.

Misteli T, Gunjan A, Hock R, Bustin M, Brown DT (2000). Dynamic binding of histone H1 to chromatin in living cells. *Nature.* 408 (6814):877-81.

Mitsuhashi T, R C Morris, Jr, H E Ives (1991). 1,25-dihydroxyvitamin D₃ modulates growth of vascular smooth muscle cells. *J Clin Invest.* 87(6):1889–1895.

Miyake Y, Takaki A, Iwasaki Y, Yamamoto K (2010). Meta-analysis: Interferon-alpha prevents the recurrence after curative treatment of hepatitis C virus-related hepatocellular carcinoma. *J Viral Hepat.* 17:287–92.

Molnár F (2014). Structural considerations of vitamin D signaling. *Front Physiol.* 5:191.

Monia BP, Sasmor H, Johnston JF, Freier SM, Lesnik EA, Muller M, Geiger T, Altmann KH, Moser H, Fabbro D (1996). Sequence-specific antitumor activity of a phosphorothioate oligodeoxyribonucleotide targeted to human C-raf kinase supports an antisense mechanism of action in vivo. *Proc Natl Acad Sci. USA.* 93(26):15481-15484.

Morgan, DO (1994). Principles of CDK regulation. *Nature.* 374(6518):131-4.

Morgan, DO (1997). Cyclin-dependent kinases: Engines, clocks, and microprocessors. *Annual Review of Cell and Developmental Biology.* 13:261-291.

Morgan MA, Ganser A, and Reuter CW (2003). Therapeutic efficacy of prenylation inhibitors in the treatment of myeloid leukemia. *Leukemia.* 17:1482–1498.

Nagpal S, Chandraratna RA (2000). Recent developments in receptor selective retinoids. *Curr Pharm Des.* 6:919–31.

Nakagawa T, Shimizu M, Shirakami Y, Tatebe H, Yasuda I, Tsurumi H et al., (2009). Synergistic effects of acyclic retinoid and gemcitabine on growth inhibition in pancreatic cancer cells. *Cancer Lett.* 273:250–6.

Nakajima S, Hsieh JC, MacDonald PN, Galligan MA, Haussier CA, Whitfield GK, Haussier MR (1994). The C-terminal region of the vitamin D receptor is essential to form a complex with a receptor auxiliary factor required for high affinity binding to the vitamin D responsive element. *Mol Endocrinol.* 8(2):159-72.

Nakajima S, Yamagata M, Sakai N, Ozono K (2000). Effect of cyclic adenosine 3',5'-monophosphate and protein kinase A on ligand-dependent transactivation via the vitamin D receptor. *Mol Cell Endocrinol.* 159:45-51

Narayanan R, Sepulveda VA, Falzon M, Weigel NL (2004). The functional consequences of cross-talk between the vitamin D receptor and ERK signaling pathways are cell-specific. *J Biol Chem.* 279:47298-310.

Narvaez CJ, Vanweelden K, Byrne I, Welsh J (1996). Characterization of a vitamin D₃-resistant MCF-7 cell line. *Endocrinology.* 137:400-409.

Narvaez CJ, Matthews D, LaPorta E, Simmons KM, Beaudin S, Welsh J (2014). The impact of vitamin D in breast cancer: genomics, pathways, metabolism. *Front Physiol.* 5: 213.

Nemere I, Garbi N, Hammerling G, Korry J. Hintze (2012). Role of the 1,25D₃-MARRS receptor in the 1,25(OH)₂D₃-stimulated uptake of calcium and phosphate in intestinal cells. *Steroids.* 77(10):897–902

Nguyen M, d'Alesio A, Pascussi JM, Kumar R, Griffin MD, Dong X et al., (2006). Vitamin D-resistant rickets and type 1 diabetes in a child with compound heterozygous mutations of the vitamin D receptor (L263R and R391S): dissociated responses of the CYP-24 and rel-B promoters to 1,25-dihydroxyvitamin D₃. *J Bone Miner Res.* 21:886–894.

Norgaard P, Law B, Mays D, Pietenpol JA, Kohl NE, Oliff AI, et al., (1998). Inhibition of cell cycle progression and mitogenic signal transducers in vivo by farnesyltransferase inhibitor [abstract]. *Proc Am Assoc Cancer Res.* 39:1839.

Norman AW, Henry H (1974). 1,25-Dihydroxycholecalciferol--a hormonally active form of vitamin D. *Recent Prog Horm Res.* 30(0):431-80.

Norman AW, Manchand PS, Uskokovic MR, Okamura WH, Takeuchi JA, Bishop JE, Hisatake JI, Koeffler HP, Peleg S (2000). Characterization of a novel analogue of 1 α ,25(OH)₂-vitamin D₃ with two side chains: interaction with its nuclear receptor and cellular actions. *J Med Chem.* 43(14):2719-30.

Norman AW, Bishop JE, Bula CM, Olivera CJ, Mizwicki MT, Zanella LP, Ishida H, Okamura WH (2002). Molecular tools for study of genomic and rapid signal transduction responses initiated by 1 alpha,25(OH)(2)-vitamin D(3). *Steroids*. 67(6):457-66. Review.

Obora A, Shiratori Y, Okuno M, Adachi S, Takano Y, Matsushima-Nishiwaki R, et al., (2002). Synergistic induction of apoptosis by acyclic retinoid and interferon-beta in human hepatocellular carcinoma cells. *Hepatology*. 36:1115–24

Okita K, Matsui O, Kumada H, Tanaka K, Kaneko S, Moriwaki H et al., (2010). Effect of peretinoin on recurrence of hepatocellular carcinoma (HCC): Results of a phase II/III randomized placebo-controlled trial. *J Clin Oncol*. 28(Suppl 15):abstr 4024.

Olmos-Ortiz, Andrea, Euclides Avila, Marta Durand-Carbajal and Lorenza Díaz (2015). Regulation of Calcitriol Biosynthesis and Activity: Focus on Gestational Vitamin D Deficiency and Adverse Pregnancy Outcomes *Nutrients* 7, 443-480.

Oridate N, Esumi N, Lotan D, Hing WK, Rochette-Egly C, Chambon P, and Lotan R (1996). Implication of retinoic acid receptor gamma in squamous differentiation and response to retinoic acid in head and neck SqCC/Y1 squamous carcinoma cells. *Oncogene*. 12:2019–2028.

Orlov I, Natacha Rochel, Dino Moras and Bruno P Klaholz (2012). Structure of the full human RXR/VDR nuclear receptor heterodimer complex with its DR3 target DNA. *The EMBO Journal* . 31:291–300.

Oza AM, Elit L, Swenerton K, Faught W, Ghatage P, Carey M, McIntosh L, Dorr A, Holmlund JT, Eisenhauer E (2003). Phase II study of CGP 69846A (ISIS 5132) in recurrent epithelial ovarian cancer: an NCIC clinical trials group study (NCIC IND.116) *Gynecologic Oncol*. 89:129–133

Palmer DC, Chan CC, Gattinoni L, et al., (2008). Effective tumor treatment targeting a melanoma/melanocyte-associated antigen triggers severe ocular autoimmunity. *Proc Natl Acad Sci. USA.* 105:8061-8066.

Pearson G, Robinson F, Gibson TB, Xu BE, Karandikar M, Berman K, Cobb MH (2001). Mitogen-activated protein (MAP) kinase pathways: Regulation and physiological functions. *Endocrine Reviews.* 22(2):153-183.

Penna-Martinez M, Ramos-Lopez E, Stern J, Hinse N, Hansmann M, Selkinski I, Grünwald F, Vorländer C, Wahl RA, Bechstein WO, Zeuzem S, Holzer K, Badenhop K (2009). Vitamin D receptor polymorphisms in differentiated thyroid carcinoma. *Thyroid.* 19:623–62810.

Perissi V, Rosenfeld MG (2005). Controlling nuclear receptor: the circular logic of cofactor cycles. *Nature Reviews Molecular Cell Biology.* 6:542-54

Perissi V, Jepsen K, Glass CK, Rosenfeld MG (2010). Deconstructing repression: evolving models of co-repressor action. *Nature reviews.* 11:109-23

Perissi V, Staszewski LM, McInerney EM, Kurokawa R, Kronen A, Rose DW, Lambert MH, Milburn MV, Glass CK, Rosenfeld MG (1999). Molecular determinants of nuclear receptor-corepressor interaction. *Genes Dev.* 13(24):3198-208.

Pérez E, Bourguet W, Gronemeyer H, de Lera AR (2012). Modulation of RXR function through ligand design. *Biochim Biophys Acta.*;1821(1):57-69.

Petros A, Bennett D, and Vallance P (1991) “Effect of nitric oxide synthase inhibitors on hypotension in patients with septic shock,” *Lancet.* 338(8782-8783): 1557–1558

PhosphoSitePlus website;

<http://www.phosphosite.org/proteinAction.action?id=5051&showAllSites=true>

Phair RD, and Misteli, T (2000). High mobility of proteins in the mammalian cell nucleus. *Nature*. 404:604-609.

Pike JW, Sleator NM (1985). Hormone-dependent phosphorylation of the 1,25-dihydroxyvitamin D₃ receptor in mouse fibroblasts. *Biochem Biophys Res Commun*. 131(1):378–385.

Pike JW, Meyer MB (2010). The vitamin D receptor: new paradigms for the regulation of gene expression by 1,25-dihydroxyvitamin D(3). *Endocrinol. Metab. Clin. North Am*. 39:255–269.

Poggenberg V, Guichou JF, Vivat-Hannah V, Kammerer S, Pérez E, Germain P, de Lera AR, Gronemeyer H, Royer CA, Bourguet W (2005). Characterization of the interaction between retinoic acid receptor/retinoid X receptor (RAR/RXR) heterodimers and transcriptional coactivators through structural and fluorescence anisotropy studies. *J Biol Chem*. 280(2):1625-33.

Polek TC, Weigel NL (2002). Vitamin D and prostate cancer [review]. *J Androl*. 23(1):9–17.

Popp S, Waltering S, Holtgreve-Grez H, Jauch A, Proby C, Leigh IM, Boukamp P (2000). Genetic characterization of a human skin carcinoma progression model: from primary tumor to metastasis. *J Invest Dermatol*. 115(6):1095-103.

Prufer K, Racz A, Lin GC, Barsony J (2000). Dimerization with retinoid X receptors promotes nuclear localization and subnuclear targeting of vitamin D receptors. *J Biol Chem*. 275: 41114–41123.

Prufer K, Barsony J (2002). Retinoid X receptor dominates the nuclear import and export of the unliganded vitamin D receptor. *Mol Endocrinol*. 16:1738–1751.

Quack M, and Carlberg C. (2000). The impact of functional vitamin D(3) receptor conformations on DNA-dependent vitamin D(3) signaling. *Mol Pharmacol.* 57: 375-384.

Quack M, Carlberg C. (2000b). Ligand-triggered stabilization of vitamin D receptor/retinoid X receptor heterodimer conformations on DR4-type response elements. *J Mol Biol.* 296(3):743-56.

Rachez C, Freedman LP (2001) Mediator complexes and transcription. *Curr. Opin. Cell Biol.* 13(3):2274-280

Rachez C, Gamble M, Chang CPB, Atkins GB, Lazar MA, Freedman LP (2000). The DRIP complex and SRC-1/p160 coactivators share similar nuclear receptor binding determinants but constitute functionally distinct complexes. *Mol Cell Biol.* 20:2718–2726.

Rachez C, Suldan Z, Ward J, Chang CP, Burakov D, Erdjument-Bromage H, Tempst P, Freedman LP (1998). A novel protein complex that interacts with the vitamin D3 receptor in a ligand-dependent manner and enhances VDR transactivation in a cell-free system. *Genes Dev.* 12:1787–1800.

Racz A, Barsony J (1999). Hormone-dependent translocation of vitamin D receptors is linked to transactivation. *J Biol Chem.* 274:19352–19360.

Raimondi S, Johansson H, Maisonneuve P, Gandini S (2009). Review and meta-analysis on vitamin D receptor polymorphism and cancer risk. *Carcinogenesis.* 30: 1170–1180.

Rajakulendran T, Sahmi M, Lefrancois M, Sicheri F, Therrien M (2009). A dimerization-dependent mechanism drives RAF catalytic activation. *Nature.* 461(7263):542–545.

Rasmussen H, DeLuca HF (1963). Calcium homeostasis. *Ergeb Physiol.* 53:108-73.

Rastinejad F, Ollendorff V, Polikarpov I (2015). Nuclear receptor full-length architectures: confronting myth and illusion with high resolution. *Trends Biochem Sci.* 40(1):16-24.

Rasmussen H, Deluca H, Arnauld C, Hawker C, Vonstedingk M. (1963). The relationship between vitamin D and parathyroid hormone. *J Clin Invest.* 42:1940-6.

Redell MS, Tweardy DJ (2005). Targeting transcription factors for cancer therapy. *Curr. Pharm. Des.* 11:2873.

Reichel H, Koemer HP, Norman AW (1989). The role of vitamin D endocrine system in health and disease. *N Engl. J. Med.* 320:980-991.

Reichrath J, Mittmann M, Kamradt J, and Muller SM (1997). Expression of retinoid-X receptors (-alpha, -beta, -gamma) and retinoic acid receptors (-alpha, -beta, -gamma) in normal human skin: An immunohistological evaluation. *Histochem. J.* 29:127-133.

Reits EA, Neefjes JJ. (2001). From fixed to FRAP: measuring protein mobility and activity in living cells. *Nature Cell Biology.* 3:E145 - E147

Ren Y, Behre B, Ren Z, Zhang J, Wang Q, and Fondell JD (2000). Specific Structural Motifs Determine TRAP220 Interactions with Nuclear Hormone Receptors. *Mol Cell Biol.* 20(15):5433–5446.

Repasky GA, Chenette EJ, Der CJ (2004). Renewing the conspiracy theory debate: does Raf function alone to mediate Ras oncogenesis? *Trends Cell Biol.* 14:639–47.

Matsushima-Nishiwaki R, Okuno M, Adachi S, Sano T, Akita K, Moriwaki H, Friedman SL, and Kojima S (2001). Phosphorylation of Retinoid X Receptor {alpha} at Serine 260 Impairs Its Metabolism and Function in Human Hepatocellular Carcinoma *Cancer Res.* 61:7675-7682.

Ren Y, Behre E, Ren Z, Zhang J, Wang Q, Fondell JD (2000). Specific structural motifs determine TRAP220 interactions with nuclear hormone receptors. *Mol. Cell. Biol.* 20:5433–5446

Robbins PF, Dudley ME, Wunderlich J et al., (2004). Cutting edge: persistence of transferred lymphocyte clonotypes correlates with cancer regression in patients receiving cell transfer therapy. *J Immunol.*173:7125-7130.

Rochel N, Wurtz JM, Mitschler A, Klaholz B, Moras D (2000). The crystal structure of the nuclear receptor for vitamin D bound to its natural ligand. *Mol Cell.* 5(1):173-9.

Rochette-Egly C (2003). Nuclear receptors: integration of multiple signalling pathways through phosphorylation. *Cell Signal.* 15(4):355-66.

Rochel N, Ciesielski F, Godet J, Moman E, Roessle M, Peluso-Iltis C, Moulin M, Haertlein M, Callow P, Mély Y, Svergun DI, Moras D (2011). Common architecture of nuclear receptor heterodimers on DNA direct repeat elements with different spacings. *Nat Struct Mol Biol.* 18(5):564-70.

Safadi FF, Hermey DC, Popoff SN, Seifert MF (1999). Skeletal resistance to 1,25-dihydroxyvitamin D₃ in osteopetrotic rats. *Endocrine.*11(3):309-19.

Sadelain M, Riviere I, Brentjens R. (2003). Targeting tumours with genetically enhanced T lymphocytes. *Nat Rev Cancer.* 3:35-45.

Sala E, Mologni L, Truffa S, Gaetano C, Bollag GE, Gambacorti-Passerini C (2008). BRAF silencing by short hairpin RNA or chemical blockade by PLX4032

leads to different responses in melanoma and thyroid carcinoma cells. *Mol Cancer Res.* 6(5):751–759.

Schröder M, Bendik I, Becker-André M, Carlberg C (1993). Interaction between retinoic acid and vitamin D signaling pathways. *J Biol Chem.* 268(24):17830-6.

Sebag M, Henderson J, Rhim J, Kremer R (1992). Relative resistance to 1,25-dihydroxyvitamin D₃ in a keratinocyte model of tumor progression. *J Biol Chem.* 267(17):12162-7.

Sebolt-Leopold JS (2008). Advances in the development of cancer therapeutics directed against the RAS-mitogen-activated protein kinase pathway. *Clin Cancer Res.* (12):3651-6.

Sexton CJ, Proby CM, Banks L, Stables JN, Powell K, Navsaria H, Leigh IM (1993). Characterization of factors involved in human papillomavirus type 16-mediated immortalization of oral keratinocytes. *J Gen Virol.* 74 (Pt 4):755-6.

Shen YC, Hsu C, Chen LT, Cheng CC, Hu FC, Cheng AL (2010). Adjuvant interferon therapy after curative therapy for hepatocellular carcinoma (HCC): A meta-regression approach. *J Hepatol.* 52:889–94.

Shesely EG, Maeda N, Kim HS, Desai KM, Krege JH, Laubach VE, et al. Elevated blood pressures in mice lacking endothelial nitric oxide synthase. *Proc Natl Acad Sci. USA.* 93:13176–81.

Shi H, Yan PS, Chen CM, Rahmatpanah F, Lofton-Day C, Caldwell CW, et al., (2002). Expressed CpG island sequence tag microarray for dual screening of DNA hypermethylation and gene silencing in cancer cells. *Cancer Res.* 62:3214–3220.

Shilkaitis A, Green A, Christov K. (2015). Retinoids induce cellular senescence in breast cancer cells by RAR- β dependent and independent pathways: Potential clinical implications (Review). *Int J Oncol.* 47(1):35-42.

Shimizu M, Takai K, Moriwaki H (2008). Synergistic effects of PPAR γ ligands and retinoids in cancer treatment. *PPAR Res.* 1-10.

Shimizu M, Takai K, Moriwaki H (2008). Strategy and mechanism for the prevention of hepatocellular carcinoma: Phosphorylated retinoid X receptor alpha is a critical target for hepatocellular carcinoma chemoprevention. *Cancer Sci.* 100:369–74

Shimizu Mashahito, Yohei Shirakami, Kenji Imai, Koji Takai, and Hisataka Moriwaki (2012). Acyclic retinoid in chemoprevention of hepatocellular carcinoma: Targeting phosphorylated retinoid X receptor- α for prevention of liver carcinogenesis. *J Carcinog.* 11:11.

Simboli-Campbell M, Narvaez CJ, VanWeelden K, Tenniswood M, Welsh JE (1997). Comparative effects of 1 α ,25(OH) D and EB1089 on cell cycle kinetics and apoptosis in MCF-7 cells. *Breast Cancer Res Treat.* 42:31– 41.

Snapp EL, Altan N, and Lippincott-Schwartz J (2002). Measuring Protein Mobility by Photobleaching GFP Chimeras in Living Cells. *Curr.Prot. Cell Biol.* 21:1-21.

Solomon C, Sebag M, White JH, Rhim J, Kremer R (1998). Disruption of vitamin D receptor-retinoid X receptor heterodimer formation following ras transformation of human keratinocytes. *J Biol Chem.* 273:17573-8.

Solomon C, White JH, Kremer R (1999). Mitogen-activated protein kinase inhibits 1,25-dihydroxyvitamin D₃-dependent signal transduction by phosphorylating human retinoid X receptor α . *J Clin Invest.* 103:1729–1735.

Solomon C, Kremer R, White JH, Rhim JS (2001). Vitamin D resistance in RAS-transformed keratinocytes: mechanism and reversal strategies. *Radiat Res;* 155(1 Pt 2):156–162.

Solomon C, Macoritto M, Gao XL, White JH, Kremer R (2001). The unique tryptophan residue of the vitamin D receptor is critical for ligand binding and transcriptional activation. *J Bone Miner Res.* 16:39-45.

Spinella MJ, Freemantle SJ, Sekula D, Chang JH, Christie AJ, and Dmitrovsky E (1999). Retinoic acid promotes ubiquitination and proteolysis of cyclin D1 during induced tumor cell proliferation. *J. Biol. Chem.* 274:22013–22018.

Stein, CA, Tonkinson JL, Zhang LM, Yakubov L, Gervasoni J, Taub R, and Rotenberg SA (1993). Dynamics of the internalization of phosphodiester oligodeoxynucleotides in HL60 cells. *Biochemistry.* 32:4855 –4861

Stenoien DL, Patel K, Mancini MG, Dutertre M, Smith CL, O'Malley BW, and Mancini MA (2001). FRAP reveals that mobility of oestrogen receptor-alpha is ligand- and proteasome dependent. *Nat. Cell Biol.* 3:15-23.

Straarup EM, Fisker N, Hedtjarn M, Lindholm MW, Rosenbohm C, Aarup V et al., (2010). Short locked nucleic acid antisense oligonucleotides potently reduce apolipoprotein B mRNA and serum cholesterol in mice and non-human primates. *Nucleic Acids Res.* 38:7100–7111

Suda T, Miyaura C, Abe E (1986). Modulation of cell differentiation, immune responses and tumor promotion by vitamin D compounds. In: Peck WA ed. *Bone and Mineral Research.* Vol. 4. New York, NY: Elsevier: 1–48.

Sugawara A, Sanno N, Takahashi N, Osamura RY, and Abe K (1997). Retinoid X receptors in the kidney: Their protein expression and functional significance. *Endocrinol.* 138:3175-3180.

Sullenger BA, Cech TR (1994). Ribozyme-mediated repair of defective mRNA by targeted, trans-splicing. *Nature.* 371:619.

Sun SY, and R Lotan (2002). Retinoids and their receptors in cancer development and chemoprevention. *Crit. Rev. Oncol. Hematol.* 41:41-55.

Taber LT, Lynn S. Adams, and Dorothy Teegarden (2009). Mechanisms of nuclear vitamin D receptor resistance in Harvey-ras-transfected cells. *J Nutr Biochem.* 20(8): 629–637.

Taneja R, Rochette-Egly C, Plassat JL, Penna L, Gaub MP, Chambon P (1997). Phosphorylation of activation functions AF-1 and AF-2 of RAR α and RAR γ is indispensable for differentiation of F9 cells upon retinoic acid and cAMP treatment. *EMBO J.* 16:6452–6465.

Takeyama K, and Kato S (2011). The vitamin D3 1, alpha-hydroxylase gene and its regulation by active vitamin D3. *Biosci. Biotechnol. Biochem.* 75:208–213.

Tanaka Y, DeLuca HF (1981). Measurement of mammalian 25-hydroxyvitamin D3 24R-and 1 alpha-hydroxylase. *Proc Natl Acad Sci. USA.* 78(1):196-9.

Tanaka T, Dancheck BL, Trifiletti LC, Birnkrant RE, Taylor BJ, Garfield SH, Thorgeirsson U, and De Luca LM (2004). Altered Localization of Retinoid X Receptor α Coincides with Loss of Retinoid Responsiveness in Human Breast Cancer MDA-MB-231 Cells. *Mol Cell Biol.* 24:3972–3982.

Tatebe H, Shimizu M, Shirakami Y, Tsurumi H, Moriwaki H (2008). Synergistic growth inhibition by 9-cis-retinoic acid plus trastuzumab in human hepatocellular carcinoma cells. *Clin Cancer Res.* 14:2806–12.

Tatebe H, Shimizu M, Shirakami Y, Sakai H, Yasuda Y, Tsurumi H et al., (2010). Acyclic retinoid synergises with valproic acid to inhibit growth in human hepatocellular carcinoma cells. *Cancer Lett.* 285:210–7.

Tavera-Mendoza L, Wang TT, Lallemand B, Zhang R, Nagai Y, Bourdeau V, Ramiro Calderon, M, Desbarats J, Mader S, and White JH (2006). Convergence of

vitamin D and retinoic acid signaling at a common hormone response element. *EMBO Rep.* 7:180-185.

Tolcher AW (2005). Targeting Bcl-2 protein expression in solid tumors and hematologic malignancies with antisense oligonucleotides. *Clin. Adv. Hematol. Oncol.* 3:635.

Touvier M, Chan DS, Lau R, Aune D, Vieira R, Greenwood DC, Kampman E, Riboli E, Hercberg S, Norat T (2011). Meta-analyses of vitamin D intake, 25-hydroxyvitamin D status, vitamin D receptor polymorphisms, and colorectal cancer risk. *Cancer Epidemiol. Biomarkers Prev.* 20:1003–101610.

Trahey M, McCormick F (1987). A cytoplasmic protein stimulates normal N-ras p21 GTPase but does not affect oncogenic mutants. *Science.* 238:542-545.

Tsai MJ, O'Malley BW (1994). Molecular mechanisms of action of steroid/thyroid receptor superfamily members. *Annu Rev Biochem.* 63:451-86.

Tyagi R, Lavrovsky Y, Ahn SC, Song CS, Chatterjee B, and Roy AK (2000). Dynamics of intracellular movement and nucleocytoplasmic recycling of the ligand-activated androgen receptor in living cells. *Mol. Endocrinol.* 14:1162-1174.

Umesono K, Evans RM (1989). Determinants of target gene specificity for steroid/thyroid hormone receptors. *Cell.* 57(7):1139-46.

Vendrell JA, Bieche I, Desmetz C, Badia E, Tozlu S, Nguyen C, Nicolas JC, Lidereau R, Cohen PA (2005). Molecular changes associated with the agonist activity of hydroxy-tamoxifen and the hyper-response to estradiol in hydroxy-tamoxifen-resistant breast cancer cell lines. *Endocr Relat Cancer.* 12(1):75-92.

Verstuyf A, Carmeliet G, Bouillon R, Mathieu C (2010). Vitamin D: a pleiotropic hormone. *Kidney Int.* 78:140–145.

Vuolo Laura, Carolina Di Somma, Antongiulio Faggiano, and Annamaria Colao (2012). Vitamin D and Cancer. *Front Endocrinol (Lausanne)*. 3: 58.

Wahli W. Martinez E (1991). Superfamily of steroid nuclear receptors: positive and negative regulators of gene expression. *FASEB J*. 7:273-282.

Walters MR (1992). Newly identified actions of the vitamin D endocrine system. *Endocr Rev*. 13(4):719-64.

Wan H, MI Dawson, WK Hong, and R Lotan (1998). Overexpressed activated retinoid X receptors can mediate growth inhibitory effects of retinoids in human carcinoma cells. *J. Biol. Chem*. 273:26915-26922.

Wang HG, Rapp UR, Reed JC (1996). Bcl-2 targets the protein kinase Raf-1 to mitochondria. *Cell*. 15;87(4):629-38.

Ward RD, Weigel NL (2009). Steroid receptor phosphorylation: Assigning function to site-specific phosphorylation. *Biofactors*. 35(6):528.

Watts J. K., Corey D. R. (2012). Silencing disease genes in the laboratory and the clinic. *J. Pathol*. 226:365–379

Weigel, NL (1994). Receptor phosphorylation in molecular biology intelligence unit. In *Mechanism of steroid hormone regulation of gene transcription*. M-J. Tsai, editor. R.G. Landes Co. Austin, Texas. 93–110.

Weigel NL, Bai W, Zhang Y, Beck CA, Edwards DP, Poletti A (1995). Phosphorylation and progesterone receptor function. *J Steroid Biochem. Mol. Biol*. 53:509-514.

Weigel NL, Zhang Y (1998). Ligand-independent activation of steroid hormone receptors. *J Mol Med (Berl)*. 76(7):469-79.

Welsh J (2007). Vitamin D prevention and breast cancer. *Acta Pharmacologica Sinica*. 28:1373–138242.

Westaway D, Papkoff J, Moscovici C, Varmus HE. (1986). Identification of a provirally activated c-Ha-ras oncogene in an avian nephroblastoma via a novel procedure: cDNA cloning of a chimaeric viral-host transcript. *EMBO J*. 5(2):301–309.

Willumsen BM, Norris K, Papageorge AG, Hubbert NL, Lowy DR (1984). Harvey murine sarcoma virus p21 ras protein: biological and biochemical significance of the cysteine nearest the carboxy terminus. *EMBO J*. 3(11):2581-5.

Wilson TE, Paulsen RE, Padgett KA, Millbrandt J (1992). Participation of non-zinc finger residues in DNA binding by two nuclear orphan receptors. *Science*. 256:107-110.

Wu G, Fan RS, Li W, Ko TC and Brattain MG (1997). Modulation of cell cycle control by vitamin D3 and its analogue EB1089 in human breast cancer. *Oncogene* . 15:1555-1563.

www.clinicaltrials.gov (viewed 2/25/15)

Xu XC, Sneige N, Liu X et al., (1997). Progressive decrease in nuclear retinoic acid receptor beta messenger RNA level during breast carcinogenesis. *Cancer Res*. 57:4992–6.

Xu XC, Sozzi G, Lee JS et al., (1997). Suppression of retinoic acid receptor beta in non-small-cell lung cancer in vivo: implications for lung cancer development. *J Natl Cancer Inst*. 89:624–9.

Yamazaki K, Shimizu M, Okuno M, Matsushima-Nishiwaki R, Kanemura N et al., (2007). Synergistic effects of RXR alpha and PPAR gamma ligands to inhibit

growth in human colon cancer cells—phosphorylated RXR alpha is a critical target for colon cancer management. *Gut*. 56:1557–1563.

Yasmin R, Williams RM, Xu M, Noy N (2005). Nuclear import of the retinoid X receptor, the vitamin D receptor, and their mutual heterodimer. *J Biol Chem*. 280:40152–40160.

Yoneda T, Aya S, and Sakuda M (1984). Sodium butyrate (SB) augments the effects of 1,25 dihydroxyvitamin D3 (1,25(OH)2D3) on neoplastic and osteoblastic phenotype in clonal rat osteosarcoma cells. *Biochem. Biophys. Res. Commun*. 121:796–801.

Yoshizawa T, Handa Y, Uematsu Y, Takeda S, Sekine K, Yoshihara Y *et al.* (1997). Mice lacking the vitamin D receptor exhibit impaired bone formation, uterine hypoplasia and growth retardation after weaning. *Nat Genet*. 16:391–396.

Yu J, Papavasiliou V, Rhim J, Goltzman D, Kremer R (1995). Vitamin D analogs: new therapeutic agents for the treatment of squamous cancer and its associated hypercalcemia. *Anticancer Drugs*. 6(1):101–108.

Yu XP, Bellido T, Manolagas SC (1995). Down-regulation of NF-kappa B protein levels in activated human lymphocytes by 1,25-dihydroxyvitamin D3. *Proc Natl Acad Sci. USA* 92: 10990–10994.

Zachos, G, Spandidos GA (1997). Expression of ras proto-oncogenes: regulation and implications in the development of human tumors. *Crit Rev Oncol Hematol*. 26:65-75.

Zassadowski F, Rochette-Egly C, Chomienne C, Cassinat B (2012). Regulation of the transcriptional activity of nuclear receptors by the MEK/ERK1/2 pathway. *Cell Signal*. 24(12):2369-77.

Zhang X, Chen S, Yoo S, Chakrabarti S, Zhang T, Ke T, Oberti C, Yong SL, Fang F, Li L et al., (2008). Mutation in nuclear pore component NUP155 leads to atrial fibrillation and early sudden cardiac death. *Cell*. 135:1017-1027.

Zhang J, Chalmers MJ, Stayrook KR, Burris LL, Wang Y, Busby SA, Pascal BD, Garcia-Ordenez RD, Bruning JB, Istrate MA, Kojetin DJ, Dodge JA, Burris TP, Griffin PR (2011). DNA binding alters coactivator interaction surfaces of the intact VDR-RXR complex. *Nat Struct Mol Biol*. 18(5):556-63.

Zugmaier G, Jager R, Grage B, Gottardis MM, Havemann K, Knabbe C (1996). Growth inhibitory effects of vitamin D analogs and retinoids on human pancreatic cancer cells. *Br J Cancer*. 73(11):1341-6.

Appendix

Abstract: **Effects of 1 α , 25- Dihydroxyvitamin D₃ on subcellular localization, VDR /RXR α interaction by Fluorescent resonance energy transfer (FRET) and nuclear mobility of RXR α by Fluorescent loss in Photobleaching (FLIP)**

Presented at: 1. American Society for Bone and Mineral Research on
 October 4, 2013 in Baltimore, MD.
 2. Journee Phare, University of Sherbrooke, November 21, 2013 Quebec
 3. Endocrine Retreat McGill University May 22, 2014 Montreal

Effects of 1 α , 25- Dihydroxyvitamin D₃ on subcellular localization, VDR /RXR α interaction by Fluorescent resonance energy transfer (FRET) and nuclear mobility of RXR α by Fluorescent loss after photobleaching (FLIP)

Sylvester Jusu¹, John F. Presley², Loan Nguyen-Yamamoto¹, Benoit Ochetti¹ and Richard Kremer¹

¹Department of Medicine and Calcium Research Laboratory, McGill University Health Center, 687 Pine Avenue W. Montreal, Quebec H3A 1A1.

²Department of Anatomy and Cell Biology, McGill University, 3640 rue University Montreal Quebec Canada Montreal, Quebec H3A 0C7

Abstract

Human retinoid X receptor alpha (hRXR α) plays a critical role in DNA binding and transcriptional activity through its heterodimeric association with several members of the nuclear receptor superfamily including the human vitamin D receptor (hVDR). Several cancers cell lines derived from many tissues have been shown to be resistant to the growth inhibitory action of 1,25-dihydroxyvitamin D₃ (1,25(OH)₂D₃), the biologically active metabolite of vitamin D₃. In the malignant ras-transfected human keratinocyte cell line (HPK1 *Aras*) 10-100 fold higher concentrations of 1,25(OH)₂D₃ are required than the non-malignant normal human epidermal keratinocyte cell line (HPK1A) to achieve comparable inhibition of cell growth. We previously demonstrated that hRXR α phosphorylation on serine 260 was responsible for this resistance.

To obtain insight into the effects of hRXR α phosphorylation on the hVDR/ hRXR α complex physiological function in living cells, we studied subcellular localization/ partitioning, hVDR-hRXR α interaction and nuclear mobility of green fluorescent protein (GFP)-tagged hVDR or hRXR α wt and the non-phosphorylatable hRXR α ala260 mutant in the presence of either 1,25(OH)₂D₃, the MEK inhibitor UO126 or a combination of UO126 and 1,25(OH)₂D₃.

We show, through transfection of hVDR and hRXR α tagged constructs, that subcellular localization of both hVDR and hRXR α are localized to the nucleus in 1,25(OH)₂D₃- treated HPK1A cells and HPK1 $Aras$ cells treated with UO126 or following transfection of the non-phosphorylatable hRXR α ala260 mutant. Also, we demonstrate using FRET that hVDR and hRXR α interact in the absence of the ligand in both HPK1A and HPK1 $Aras$ cell lines. However, ligand addition increases their interaction in HPK1A cell but only in HPK1 $Aras$ cells treated with either UO126 or transfected with the non- phosphorylatable hRXR α ala260 mutant. This clearly demonstrates that heterodimerization of the hVDR / hRXR α complex and interaction in HPK1 $Aras$ cells can be improved and possibly reversed with the use of a non-phosphorylatable hRXR α ala260 mutant which completely abolishes hRXR α phosphorylation and restores the function of 1,25(OH)₂D₃.

Lastly, we demonstrate using FLIP that the half time of dissociation of the receptor in the nucleus and residence time of the receptor within the nuclear compartments are significantly increased in HPK1 $Aras$ cells transfected with the non-phosphorylatable hRXR α ala260 mutant

suggesting that binding of the hVDR/ hRXR α complex to chromatin and therefore effective gene transcription or repression can be achieved with HPK1Aras cells transfected with non-phosphorylatable hRXR α ala260 mutant.

Funding

Fond de la Recherche en Sante du Quebec(FRSQ) and Canadian Institutes of Health research (CIHR)

Abstract: Ras/ Mitogen –activated protein kinase (MAPK) phosphorylation, Of the Human Retinoid X Receptor α at serine 260 impairs VDR, RXR interaction, DRIP205 coactivator recruitment of 1α , 25- DD ihydroxyvitamin D3 signaling in ras- transformed Keratinocytes.

Submitted at: 1. Endocrine Society Meeting, March 5, 2015 in San Diego

Ras/ Mitogen –activated protein kinase (MAPK) phosphorylation of the Human Retinoid X Receptor α at serine 260 impairs VDR, RXR α interaction, DRIP205 coactivator recruitment and 1 α , 25-Dihydroxyvitamin D₃ signaling in ras- transformed keratinocytes

Authors

Sylvester Jusu¹, John F. Presley², Loan Nguyen-Yamamoto¹, Benoit Ochetti¹ and Richard Kremer¹

Site Affiliation

¹Departments of Medicine, Royal Victoria Hospital; ²Department of Anatomy & Cell Biology, McGill University, Canada

Body of Abstract

Human Retinoid X receptor alpha (hRXR α) plays a critical role in DNA binding and transcriptional activity through heterodimeric association with several members of the nuclear receptor superfamily including the human vitamin D receptor (hVDR). hVDR/ hRXR α heterodimerization and co-activator recruitment are required for downstream signaling and biological activity. We previously reported that the malignant human keratinocyte HPK1Aras cell line is resistant to the growth inhibitory action of 1,25(OH)₂D₃, and that 10-100 fold higher concentrations of 1,25(OH)₂D₃ are required to achieve inhibition of cell growth compared to the non-malignant normal HPK1A cell line. We showed that phosphorylation of hRXR α on serine 260 was responsible for this resistance. In this study, we first looked at the intra-nuclear mobility of the receptors by Fluorescent Recovery After Photobleaching using GFP-tagged hVDR or hRXR α wt and the non-phosphorylatable hRXR α ala260 mutant transfected into HPK1A and HPK1Aras cell lines and treated with 1,25(OH)₂D₃.

We showed that the residence time and immobile fractions of hRXR α wt in the nucleus of HPK1Aras cells decreased compared to the non-transformed HPK1A cells. In contrast, treatment with UO126 or expression of the non-phosphorylatable hRXR α ala260 mutant reversed the effect on residence time and immobility. This was further confirmed by subcellular partitioning studies of hVDR, hRXR α and hVDR /hRXR α respectively. Next we showed that hVDR/hRXR α complex binding to DNA was impaired in the HPK1Aras cells but could be improved upon pre-treatment with UO126 or transfection of the nonphosphorylatable hRXR α ala260 mutant. Lastly, we showed that in HPK1Aras cells, the vitamin D receptor- interacting protein DRIP205 co-activator recruitment was also impaired.

We conclude that blocking the MAPK phosphorylation of hRXR α in the ras-transformed keratinocytes either by using the MEK inhibitor UO126 or transfection with the nonphosphorylatable hRXR α ala260 mutant could restore the function of 1,25(OH)₂D₃ on VDR/RXR α binding and co-activator recruitment.

Funding Support

Canadian Institutes of Health Research (CIHR)

Abstract: **Effects of 1 α , 25- Dihydroxyvitamin D₃ on subcellular localization, VDR /RXR α interaction by Fluorescent resonance energy transfer (FRET) and nuclear mobility of RXR α by Fluorescent loss in Photobleaching (FLIP)**

Presented at: 1. American Society for Bone and Mineral Research on
 October 9, 2015 in Seattle, WA
 2. Endocrine Retreat McGill, May 21, 2015 Montreal,
 3. Endocrine Retreat McGill University May 19, 2014 Montreal

Examination of VDR/RXR/DRIP205 interaction, intranuclear kinetic and DNA binding in ras-transformed keratinocytes and its implication for designing optimal vitamin D therapy in cancer.

Authors

Sylvester Jusu¹, John F. Presley² and Richard Kremer¹

Site Affiliation

¹Departments of Medicine, Royal Victoria Hospital; ²Department of Anatomy & Cell Biology, McGill University, Canada

We previously reported that the malignant human keratinocyte HPK1Aras cell line is resistant to the growth inhibitory action of 1, 25(OH)₂D₃, compared to its normal counterpart immortalized HPK1A cells. We further demonstrated that this resistance was due to phosphorylation of the vitamin D receptor (VDR) heterodimeric partner, human retinoid X receptor alpha (hRXR α) on a critical amino acid, serine 260 located in close spatial proximity to regions of coactivators and corepressors interactions. We next demonstrated that subcellular localization of the hRXR α was impaired in HPK1Aras cells but could be restored using either the MAPKK inhibitor UO126 or a non-phosphorylatable mutant of hRXR α (hRXR α ala260 mutant). In order to examine further the mechanisms of 1,25(OH)₂D₃ resistance we looked at VDR/RXR and DRIP 205 (a critical coactivator required for downstream signaling of 1,25(OH)₂D₃) interactions, intranuclear kinetic in live cells and DNA binding in fixed cells using FRET (Fluorescent Resonance Energy Transfer), FLIP (Fluorescence Loss In Photobleaching), FRAP (Fluorescence Recovery After Photobleaching) and Hoechst staining. We used VDR-GFP, hRXR α wt-GFP, hRXR α mutant-GFP, VDR-mCherry, hRXR α wt-mCherry, hRXR α mutant-mCherry and DRIP205-GFP fluorescent receptors constructs transfected into either HPK1A or HPK1A ras cells and treated with 1,25(OH)₂D₃, 9-*cis*- Retinoic Acid or vehicle in the presence or absence of UO126. Using FRET we showed that 1, 25(OH)₂D₃ addition increases their interaction in HPK1A cell but only in HPK1Aras cells treated with either UO126 or transfected with the hRXR α mutant. Furthermore, we demonstrated using FLIP that the half time of dissociation of hRXR α in the nucleus and residence time of the receptor within the nuclear compartments are significantly increased in HPK1Aras cells transfected with the non-phosphorylatable hRXR α mutant or treated with the MAPK inhibitor UO126. Finally we demonstrated with Hoechst staining impaired VDR/ hRXR α /DRIP205 complex binding to chromatin in HPK1A-ras cells that was restored with UO126 treatment or transfection of the hRXR α mutant.

In summary we have demonstrated using highly specific intra-cellular tagging methods in live cells important alterations of the vitamin D signaling system in cancer cells in which the ras-raf-MAP kinase system is activated suggesting that specific inhibition of this commonly activated pathway could be targeted therapeutically to enhance vitamin D efficacy.

Funding

Canadian Institutes of Health Research (CIHR)